Seismic Hazard Evaluation Using Apparent Stress Ratio for Mining-Induced Seismic Events

by

Laura Grace Brown

A thesis submitted in partial fulfillment
of the requirements for the degree of
Master of Applied Science (M.A.Sc.) in Natural Resources Engineering

The Faculty of Graduate Studies
Laurentian University
Sudbury, Ontario, Canada

THESIS DEFENCE COMMITTEE/COMITÉ DE SOUTENANCE DE THÈSE
Laurentian Université/Université Laurentienne
Faculty of Graduate Studies/Faculté des études supérieures

Title of Thesis Titre de la thèse	Seismic Hazard Evaluation using Apparent Stress Ratio for Mining-Induced Seismic Events	
Name of Candidate Nom du candidat	Brown, Laura Grace	
Degree Diplôme	Master of Applied Science	
Department/Program Département/Programme	Natural Resources Engineering	Date of Defence August 20, 2015 Date de la soutenance

APPROVED/APPROUVÉ

Thesis Examiners/Examinateurs de thèse:

Dr. Marty Hudyma
(Supervisor/Directeur(trice) de thèse)

Dr. Ming Cai
(Committee member/Membre du comité)

Dr. Eugene Ben-Awuah
(Committee member/Membre du comité)

Dr. Mike Yao
(External Examiner/Examinateur externe)

Approved for the Faculty of Graduate Studies
Approuvé pour la Faculté des études supérieures
Dr. David Lesbarrères
Monsieur David Lesbarrères
Acting Dean, Faculty of Graduate Studies
Doyen intérimaire, Faculté des études supérieures

ACCESSIBILITY CLAUSE AND PERMISSION TO USE

Abstract

This thesis investigates precursory trends in seismic data prior to the occurrence of large and potentially damaging seismic events at Agnico Eagle's LaRonde mine. A variety of sample populations are selected to represent varying degrees of seismic hazard within a large area of interest at LaRonde. The main factor considered for hazard assessment is the local stress conditions within the rock mass, inferred from the apparent stress of seismic events.

An alternative means of analyzing apparent stress measurements using a relative ratio, referred to as Apparent Stress Ratio (ASR), is presented. The use of a ratio eliminates the need for thresholds values to define high and abnormal apparent stress. ASR values are analyzed in reference to varying time frames, allowing for changes in stress conditions over time to be considered. Hazard maps created using ASR and peak ASR values correspond well to areas of elevated seismic hazard previously identified at LaRonde. For an area of interest at LaRonde, ASR as an alarm tool possesses a success rate of 68% with a false alarm ratio of 2:1.

Keywords: Seismicity, Mining, Hazard, Apparent Stress, LaRonde.

Acknowledgments

I would like to thank Dr. Marty Hudyma for the opportunity to undertake this research. Without his much appreciated support and guidance this research would not have been possible.

Financial support for this research was provided by Agnico Eagle's LaRonde mine, the Natural Sciences and Engineering Research Council (NSERC), the Canadian Engineering Memorial Foundation (CEMF) and the Goodman School of Mines.

A special acknowledgment is due to the ACG, specifically the mXrap team, for their much appreciated time and guidance throughout this research.

Table of Contents

List of Tables

List of Figures

List of Appendices

Glossary

AS	Apparent Stress
ASP	Apparent Stress Percentile
ASR	Apparent Stress Ratio
ASRTH	Apparent Stress Ratio Time History
ES:EP	Ratio of S-wave to P-wave Energy

Chapter 1

1 « Introduction »

Deep and high stress mining is the future for many current and developing operations. A main area of concern for these mines is dynamic rock mass failure, also known as mining-induced seismicity. A seismic event is the dynamic stress wave generated by a failure within a rock mass (Hedley, 1992). Small seismic events are a frequent occurrence in most active mines and pose very little risk to the operation. They result primarily from changes in the local stress field caused by mine excavations and in this thesis, will be referred to as mining process events.

When higher stress conditions are encountered (typically at depth), or unfavourable geology is introduced, the rock mass may begin to generate larger seismic events. When failure within a rock mass results in violent and significant damage to an excavation it is referred to as a rockburst (Ortlepp, 1997). Rockbursting is one of the largest hazards present in deep mining environments and poses a significant risk to underground equipment, excavations and personnel.

Seismic hazard is referred to as the likelihood of occurrence of a seismic event of a certain size. The degree of hazard is independent of the damage the event may cause. The possibility and consequence of damage is considered in seismic risk.

Seismic risk refers to both the likelihood of a seismic event of a certain size and the resultant effect on the mine (Heal, 2010). Two of the primary factors required for calculating risk are hazard and exposure. An area of high seismic hazard may be considered low risk if there are no

personnel in the area and therefore no exposure. Seismic monitoring systems are a key tool in understanding the rock mass response to mining and mitigating the associated seismic risk.

Many seismic analysis techniques aim to identify trends in source parameters that may be correlated to increased hazard. Seismic data can provide insight into changes in local geology and stress conditions within the rock mass. Identifying conditions that are prone to generating large seismic events (high hazard) prior to the occurrence of the rock mass failure is key to minimizing risk. The main objectives of seismic monitoring in mines include: indicating the location of potential rockbursts, providing warnings by detecting unexpected changes in the behaviour of seismic parameters and provide information through back analysis (Mendecki et al., 1999).

Many operations such as Agnico Eagle's LaRonde mine are leading the way into the new frontier of deep mining. The objective of this thesis is to identify areas of increased seismic hazard at LaRonde mine based on precursory trends in seismic data.

1.1 « Precursory Trends in Seismic Data »

Previous research has identified the possibility of using precursory trends in seismic data to forecast the occurrence of large and potentially damaging seismic events. A study conducted at Glencore's, formally Xstrata's, Craig mine in Zone 10/11 successfully categorized 30% of very large events as having some microseismic precursory activity (Simser, 2008). The results of this study are summarized in Figure 1.

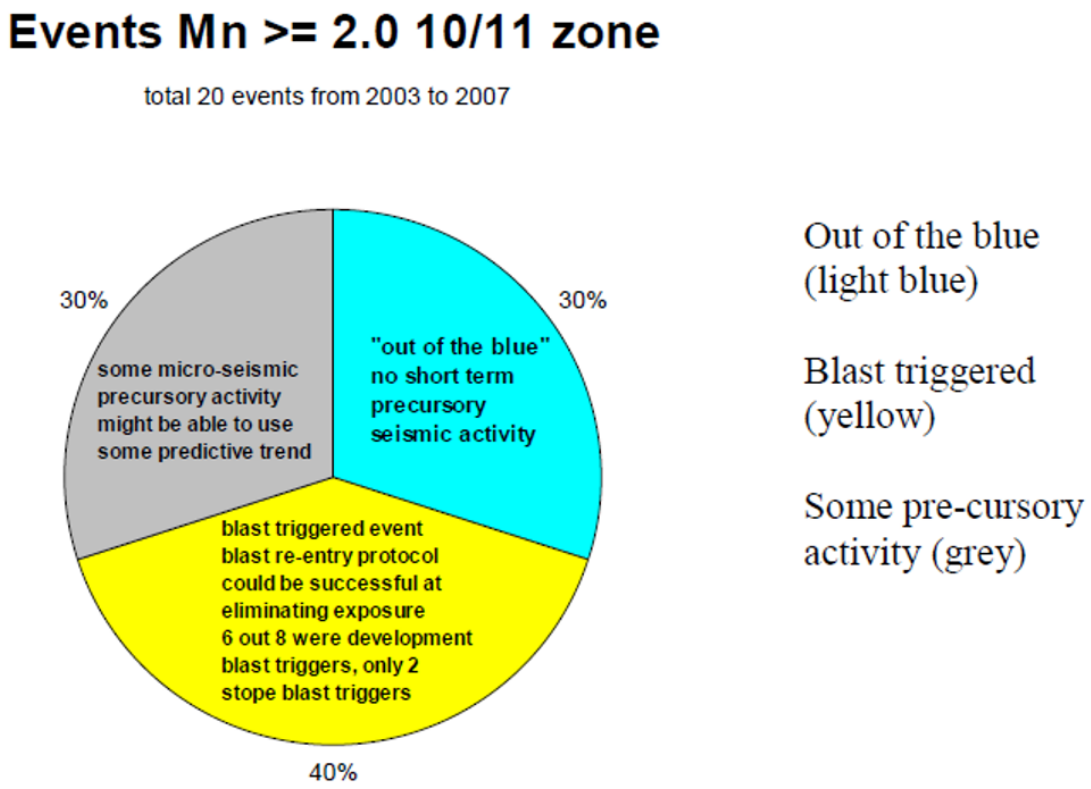

Figure 1: Pie chart showing results from analysis of 20 seismic events over magnitude 2. Some precursory activity was identified prior to the occurrence of 30% of events (Simser, 2008).

In addition to the 30% of large events with precursory microseismic activity, a further 40% were identified as being related to mine blasting. Only 30% of large events occurred “out of the blue”. In these cases, there was no precursory activity associated with the event. Based on these results, an ideal analysis technique utilizing precursory trends in microseismic data, to identify areas of increased seismic hazard, may be able to successfully identify elevated hazard conditions prior to the occurrence of 30% to 70% of large events - excluding the 30% of “out of the blue” events. The nature of these precursory trends in seismic data remains a mystery. Although 30% of events in the Craig mine study had precursory seismic activity, no comment was made on what trend may be used to identify elevated hazard.

1.2 « Research Scope »

This thesis aims to identify a precursory trend in seismic data prior to the occurrence of large and potentially damaging seismic events at Agnico Eagle's LaRonde mine. Analysis focuses on a variety of sample seismic populations of varying seismic hazard level. The main factor considered for hazard assessment is the local stress conditions in the rock mass inferred from seismic events. In this thesis, stress conditions determined from numerical modeling are not considered. The primary objective of this thesis is to develop an analysis technique utilizing only precursory trends in seismic data to identify areas of elevated hazard within a mine. This will serve as an additional tool used to minimize the risk to underground equipment, excavations and personnel from mining-induced seismicity.

1.3 « Research Approach »

This research is primarily an observational study utilizing a natural experimental approach. The complex rock mass at LaRonde mine represents the natural system. A rock mass is not an engineered material and is further subjected to the influence of stress and mining excavations. Due to unknowns and large degrees of uncertainty (in the rock mass and stress conditions), the system cannot be controlled and therefore must be observed.

Seismic data allows for insight to be gained into local rock mass conditions and failure mechanisms. Because the occurrence of seismic events is uncontrolled, data collection cannot be duplicated or repeated. This prevents the application of statistical validation or analysis. This research approach focuses specifically on using seismic data to infer unknowns pertaining to the rock mass. The seismic data can be considered a sample of the seismic response to mining.

1.4 « Thesis Structure »

Chapter 1 outlines the objectives and context of this research.

Chapter 2 provides background information necessary to understand the fundamental concepts presented in this thesis. Insight into stress, seismicity, source mechanism, seismic source parameters and current seismic analysis techniques is provided.

Chapter 3 provides background information on LaRonde mine. All seismic data used in the thesis has been collected at LaRonde mine and analyzed in reference to their specific mining conditions.

Chapter 4 is a general outline of the methodology presented and used in this thesis. It introduces Apparent Stress Ratio (ASR) and provides examples of how it may be used as a precursory trend in seismic data analysis for LaRonde mine.

Chapter 5 presents the results from the application of Apparent Stress Ratio (ASR) to multiple sample seismic populations at LaRonde. Discussions are presented on the selection of sample populations and threshold values.

Chapter 6 highlights the key conclusions and contributions of this thesis. Recommendations for further work are provided.

Chapter 2

2 « Literature Review »

This chapters provides background information necessary to understand the fundamental concepts presented in this thesis. Insight into stress, seismicity, source mechanism, seismic source parameters and current analysis techniques is provided.

2.1 « Terminology »

The following terminology is used throughout this thesis and forms the basis of study for the field of mining-induced seismicity.

2.1.1 « Stress »

Knowledge of local stress conditions is crucial to mine planning and operation. It is one of the driving factors behind seismic activity and a key component of rockbursting. The local stress state surrounding a mine excavation is a result of the in-situ stress and mining-induced stress (Gibowicz and Kijko, 1994). The in-situ stress refers to the natural stress state that exists in the rock mass prior to mining. Mining-induced stress refers to the stress state surrounding an excavation as a result of mining processes.

In-situ stress is largely a result of tectonic forces and the compressive force from the weight of the overlying rock mass (Herget, 1974). When rock is removed as a result of mining, the remaining rock mass must account for the previously supported load. This generates additional stress for the rock mass surrounding the excavation (Herget, 1988) - the mining-induced stress.

The mining-induced stress is not necessarily higher than the original stress state. Based on the geometry and orientation of excavations, areas of increased and decreased stress are created. Stress flows around mining excavations in the same manner water streams flow around obstructions. Figure 2 is a sketch of streamlines obstructed by three bridge pillars (Hoek and Brown, 1980).

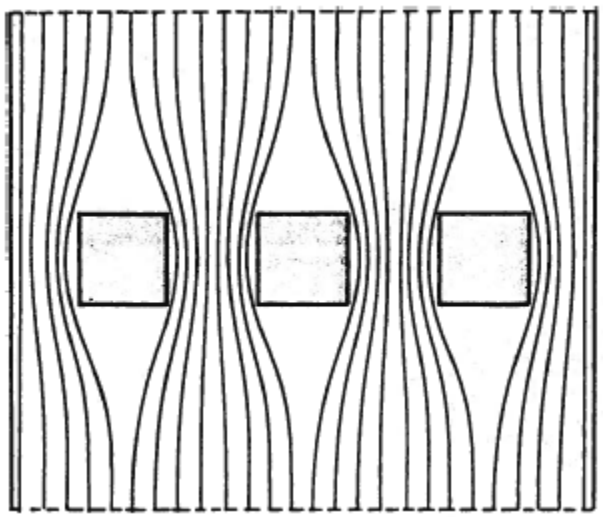

Figure 2: Sketch of streamlines in a smoothly flowing stream obstructed by three bridge pillars (Hoek and Brown, 1980).

As a result of the three bridge pillar obstructions in Figure 2, the streamlines must deviate from the original paths in order to flow around the pillars. This generates areas of increase and decrease in the streamlines. Figure 3 depicts the deflection of stress streamlines around a cylindrical obstruction (Hoek and Brown, 1980).

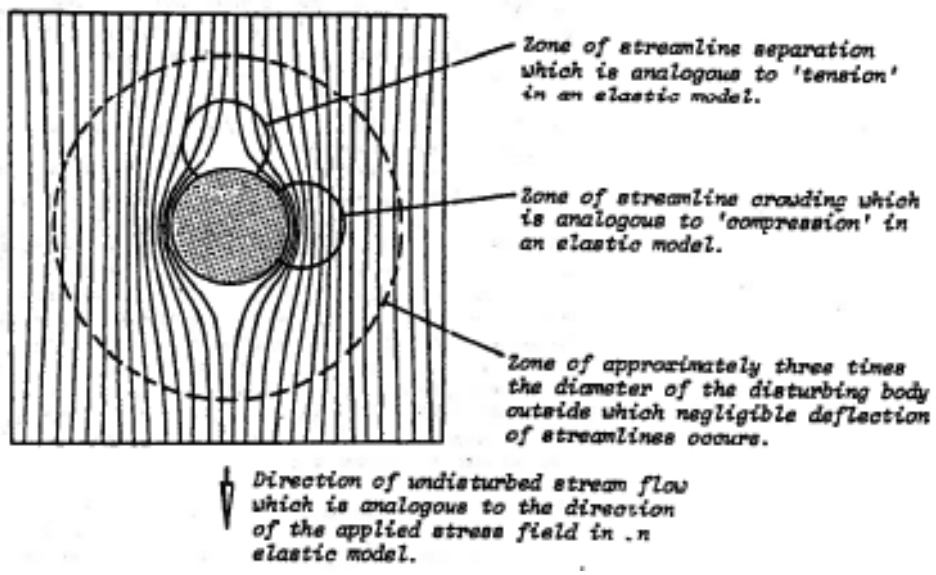

Figure 3: Deflection of stress streamlines around a cylindrical obstruction (Hoek and Brown, 1980).

Just as was seen in Figure 2, areas of increase and decrease are formed in reference to the obstruction or excavation. Stress is forced to concentrate around the sides parallel to the direction of the applied stress field, and are relaxed around the perpendicular sides. In instances where the mining-induced stress exceeds the strength of the rock, failure in the form of rockbursting can occur (Hoek and Brown, 1980).

2.1.2 « Seismicity »

Seismicity is a common occurrence in deep and high stress mining operations. Unlike earthquake seismology, mines commonly experience increased volumes of microseismic events (smaller than Richter magnitude 0) as a result of mining processes. Mining excavations disturb and redistribute local stress fields, generating mining-induced seismic events (Cook, 1976). A seismic event is the dynamic stress wave generated by a failure within a rock mass (Hedley, 1992). The initial wave is referred to as the primary wave (p-wave), followed closely by the secondary wave (s-wave). Figure 4 is an example of a large seismic event with clear p and s-

wave arrivals recorded by a regional seismic network. Due to the difference in travel velocities of the two waves, the degree of separation between their arrivals can be used to determine the distance from the location of the sensor station to the source of the seismic event.

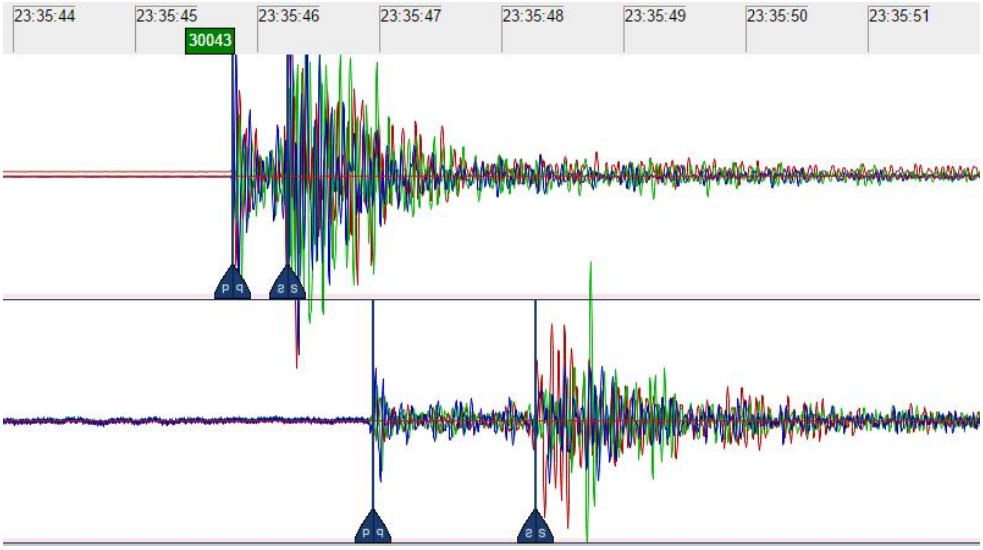

Figure 4: Example waveform for a large event picked up on a regional seismic network with identified p-wave and s-wave arrivals.

Mining-induced seismicity was first observed and documented in deep Canadian mines during the mid 1930's, such as those located in Sudbury and Kirkland Lake (Hedley, 1992). It is a common problem worldwide in a variety of metalliferous, potash, and coal operations (Gibowicz and Kijko, 1994). With the onset of hazardous seismic activity, mining operations install seismic monitoring systems to record and analyze seismic data. These seismic databases can then be back analyzed over time to identify patterns and precursory trends that may help to reduce seismic risk as the operation progresses.

2.1.3 « Seismic Response to Mining »

The seismic response to mining is a function of many factors such as the local stress and geological conditions. Mine excavations affect local stress fields and while seismicity is expected to accompany stress redistribution, there is a normal and abnormal seismic response to mining.

The rock mass failure associated with mining is typically related to stress change induced by mining activities, such as blasting. A normal seismic response to mining is relatively proportional to the scale of mining. Typically, this type of seismicity primarily consists of very small seismic events (typically less than Richter magnitude 0) and is associated with low seismic hazard.

The occurrence of large seismic events (greater than Richter magnitude 0) and seismicity outside of blasting influences is typically an abnormal response to mining. This type of activity indicates more than just small events related to local stress redistributions are occurring in response to mining. This type of response is often associated with unfavourable geology or very high stress conditions. An abnormal seismic response to mining is typically associated with elevated seismic hazard.

2.1.4 « Seismic Source Mechanism »

Seismic source mechanism refers to the failure mode of the rock mass resulting in a seismic event. Understanding source mechanism allows for insight into the stress, geological and mining influences on the local rock mass failure modes. Figure 5 provides depictions of six basic mechanisms driving mining-induced seismic events in Canadian mines (Hasegawa et al., 1989).

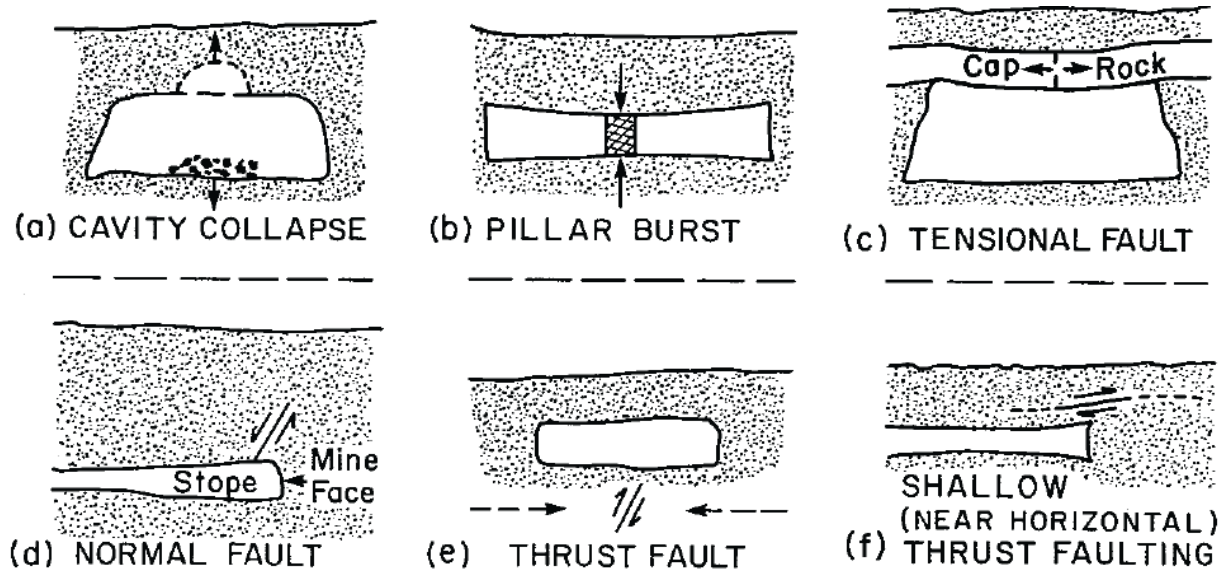

Figure 5: Six basic mechanisms driving mining-induced tremors in Canadian mines (Hasegawa et al., 1989).

Cavity collapse, pillar burst, and tensional fault mechanism events are all subtypes of volumetric and stress fracturing seismic events. These events are usually associated with mining activities such as blasting and typically constitute a normal seismic response. Normal fault, thrust fault, and shallow thrust faulting all contain a shearing component and are sub-types of fault-slip seismic events. Fault-slip events tend to release more energy and are therefore associated with larger magnitudes and are typically an abnormal seismic response. Many analysis techniques provide insight into source mechanism, such as frequency-magnitude and S:P energy ratio charts. The use of these charts for seismic analysis is discussed in detail in 2.4 « Seismic Analysis Techniques ».

2.1.5 « Rockburst »

When a seismic event results in violent and significant damage to an excavation it is referred to as a rockburst (Ortlepp, 1997). Events that may result in significant rock mass damage pose a high risk to the safety of underground personnel, excavations and equipment. A rockburst may be further classified as bulking, ejection, or a seismically-induced fall of ground based on the damage mechanism as shown in Figure 6 (Kaiser et al., 1996).

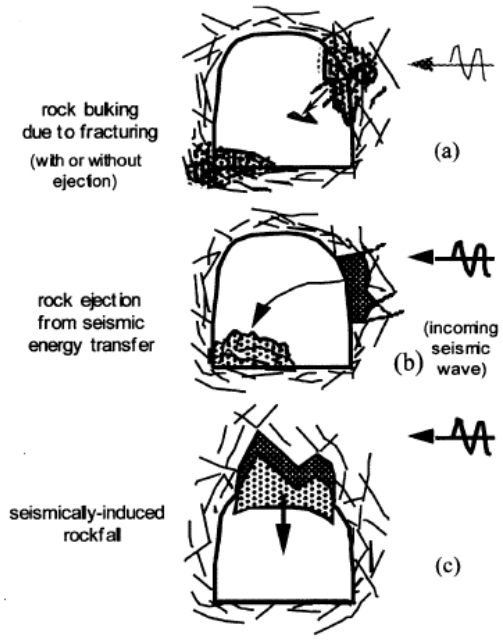

Figure 6: Rockburst classifications (Kaiser et al., 1996); (a) rock bulking due to fracturing; (b) rock ejection from seismic energy transfer; (c) seismically-induced rockfall.

Rock bulking due to fracturing may occur as a result of immediate or remote seismic events and does not have to be accompanied by ejection. When this type of failure occurs rapidly it is typically referred to as a strain burst. This is the most common type of damage observed in Canadian hardrock mines (Kaiser et al., 1996).

Seismically induced falls of ground are gravity-driven failures. When a stable volume of rock is subjected to a seismic wave, it is accelerated with the potential to overcome the capacity of the

ground support. Areas with geological conditions prone to generating blocks/wedges or large spans are more likely to experience damage resulting from this mechanism. This type of damage is the second most commonly observed in Canadian hardrock mines (Kaiser et al., 1996).

Rock ejection from seismic energy transfer is a more violent damage mechanism. It occurs when the energy resulting from the seismic wave is transferred to a block/slab at the boundary of an excavation. The rock is unable to absorb the energy, and the lack of confinement enables it to be ejected into the open area of the excavation. The extent of damage is inversely proportionate to the distance of the excavation boundary from the seismic source. This type of damage is rarely observed in Canadian hardrock mines (Kaiser et al., 1996).

Large seismic events have the potential to be rockbursts. It is for this reason large seismic events are associated with high hazard. Butler (1997) defines seismic events greater than or equal to Richter magnitude 1 as large and potentially damaging. For the purposes of this thesis, reference to large seismic events will indicate a Richter magnitude greater than or equal to 1.

2.2 « Seismic Monitoring Hardware »

Seismic monitoring systems allow for mining operations to record and analyze the seismic response to mining. Though a combination of hardware and software components, ground motion can be recorded as high quality seismic data that can be analyzed and interpreted. The main hardware components of a typical seismic monitoring system include: sensors, communication networks, digitizers and data storage.

2.2.1 « Sensors »

In order to accurately represent a large range of event magnitudes, a variety of seismic sensors must be integrated into a comprehensive system. In Canada, piezoelectric accelerometers are the most common sensors used in microseismic monitoring and typically have an upper frequency limit of 15,000 Hz. They are high frequency sensors with increased sensitivity and the ability to detect very small magnitude events. Accelerometers and pressure transducers convert pressure from ground motion into an electrical signal representing ground acceleration.

Uniaxial sensors are only capable of representing movement in a single direction, limiting the ground motion information that can be inferred from them. Large quantities of uniaxial sensors are typically used to surround the area of interest, to aid in accurate location of seismic events. Triaxial sensors are capable of measuring ground motion in three orthogonal directions simultaneously and can therefore be used to record three dimensional ground motion needed for the calculation of seismic source parameters. A combination of uniaxial and triaxial accelerometers is commonly used in a seismic array in a mine to provide accurate location and source parameters for recorded microseismic events.

Geophones are composed of a mass within a spring. Ground motion from a seismic event induces movement of the mass, which generates an electrical signal proportional to ground velocity. A small quantity of low frequency geophones placed on or near surface at varying distances from a mine site can be used to calculate source parameters for large seismic events.

Different seismic sensors are capable of accurately representing different ranges of ground motion. For a seismic monitoring system, the maximum signal level capable of being recorded in ratio to the noise level when there is no signal, is referred to as the dynamic range (Mendecki et

al., 1999). Dynamic range is expressed in decibels and should be a minimum of 120 dB for a comprehensive seismic monitoring system utilizing a range of sensor (Mendecki et al., 1999). Figure 7 depicts the sensitivity and dynamic range for different sensors commonly used in microseismic monitoring systems.

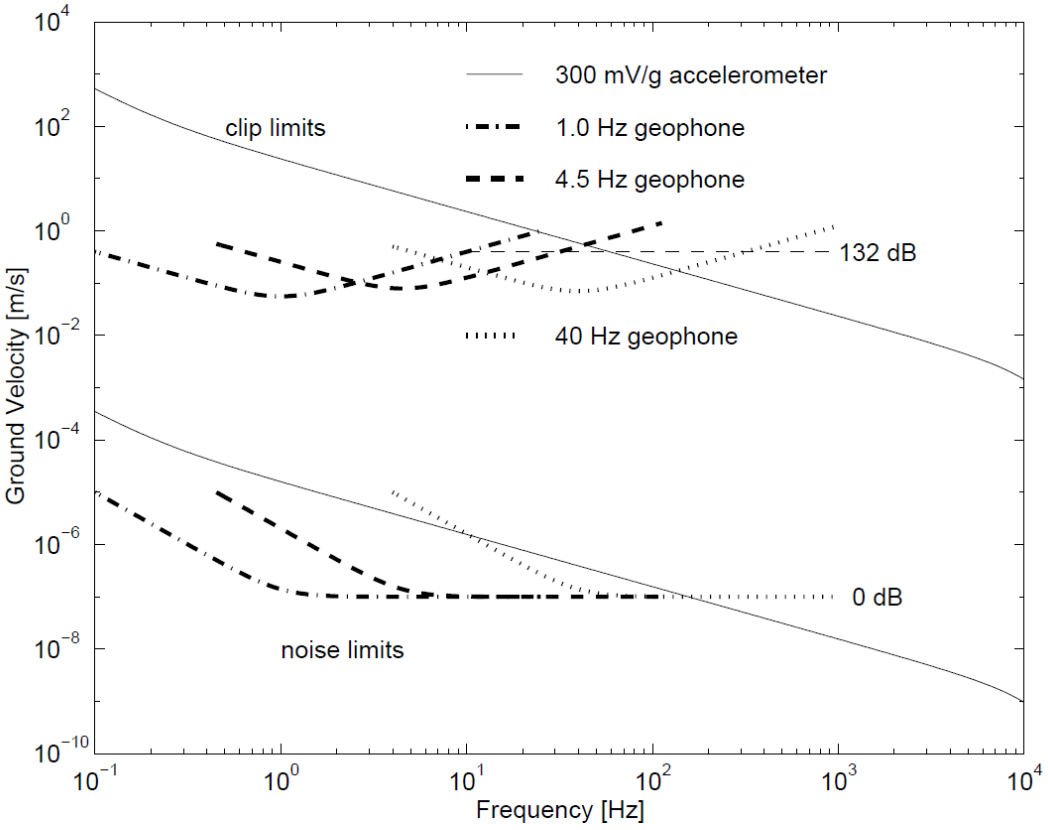

Figure 7: Sensitivity and dynamic range for sensors commonly used in mine seismic systems (Mendecki et al., 1999).

Figure 7 depicts noise (lower) and clip (upper) limits for an accelerometer and a variety of geophones. Clip limits refer to the point at which the amplitude of ground motion exceeds the measuring capacity of a sensor. Noise limits refer to the point at which background noise on a sensor is equal to or greater than the amplitude of the ground motion. When either of these limits is exceeded, the sensor is no longer capable of accurately representing ground motion.

Unlike geophones, accelerometers require a constant electrical input in order to function. As a result, there is a continuous electrical signal on the sensor referred to as noise. Noise affects the sensitivity of a system, dictating the smallest events that can be detected and accurately represented. In order to develop a seismic monitoring system with a dynamic range of 120 dB, a combination of accelerometers and geophones must be used.

Ground motion from low frequency seismic events cannot be accurately represented by close proximity accelerometers, as it falls beyond the clip limits. In order to record and utilize this data, low frequency geophones distant to mine workings must be used. Through a combination of accelerometers and geophones, a seismic system is capable of accurately representing a dynamic range of 0 to 132 dB (Figure 7) - approximately 6 orders of magnitude.

2.2.2 « Microseismic Monitoring Systems »

Microseismic monitoring systems allow for insight into where local rock mass fracturing is occurring within a rock mass in relation to mining activities. When the signal amplitude on an individual sensor exceeds a background threshold value it is considered to be “triggered”. To minimize the number of false events arising from artificial ground motion, such as drills and mobile equipment near sensors, a sufficient quantity of sensors must be “triggered” simultaneously for ground motion to be recorded as a seismic event. As uniaxial sensors are significantly less expensive than triaxial sensors, they commonly form the majority of the seismic monitoring system. For a large seismic array, the number of triaxials required to ensure accurate calculation of seismic source parameters is approximately 6 to 8 sensors (Hudyma and Brummer, 2007).

In a typical ESG (Engineering Seismology Group) microseismic network, sensors record the ground motion radiated by rock mass failure and it is transferred across copper cable to Paladins (digital seismic recorders). The signal is digitized and relayed to computers on surface through a fibre optic network. Figure 8 is an example of a typical ESG microseismic monitoring system (Collins et al., 2014).

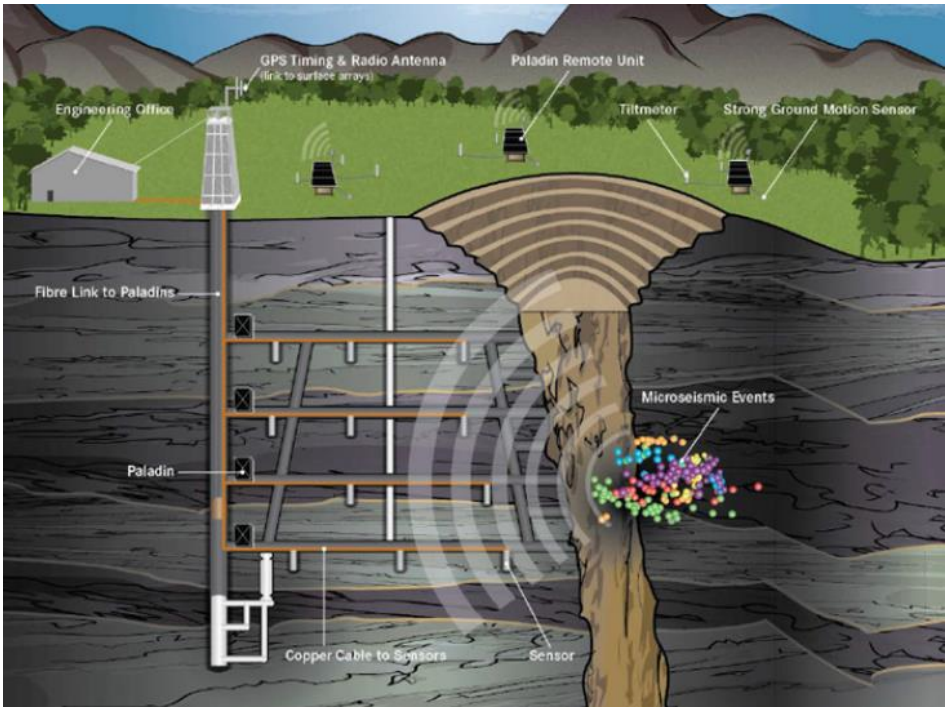

Figure 8: Example of a typical ESG microseismic monitoring system setup (Collins et al., 2014).

The networked seismic data is typically received by an acquisition computer at a central engineering office. Real time results are displayed and analyzed using various components of the ESG software suite. Data storage allows for years of seismic data to be maintained and archived, facilitating back analysis. The strong ground motion sensors shown on surface in Figure 8 represent a macroseismic monitoring system.

2.2.3 « Macroseismic Monitoring Systems »

Macroseismic monitoring systems are also referred to as regional monitoring networks. They work in the same manner as microseismic systems, but with the objective of providing accurate source parameters for large magnitude events. When a very large event occurs underground, the microseismic system may provide an accurate location but may not provide an accurate representation of the ground motion. By placing low frequency sensors, such as 4.5 Hz geophones, near surface, the true ground motion can be recorded and accurate seismic source parameters calculated for large events.

2.3 « Seismic Source Parameters »

Established in earthquake seismology, seismic source parameters are used to quantitatively describe the rock mass conditions associated with a seismic event. In order to provide a meaningful description of a seismic event, the event time, location and two additional independent source parameters are required (Mendecki et al., 1999). Additional independent seismic source parameters include: energy, moment and size. These parameters can be further manipulated to generate secondary source parameters such as magnitude and apparent stress.

2.3.1 « Time »

The time of a seismic event is the absolute time of occurrence of a seismic event. Time is commonly the parameter used to cross reference events recorded by multiple seismic monitoring systems (i.e. complementary micro and macro systems). Event rate frequency and proximity of event times to regular blast times can provide insight into the mechanisms driving seismicity (Cook, 1976). Large seismic events typically show less correlation to blasting than smaller mining process events.

2.3.2 « Location »

Seismic event location is a primary consideration of seismic analysis (Gibowicz and Kijko, 1994). Event location can often give valuable insight into seismic source mechanism by investigating proximity to active mining faces, pillars, or known geological features.

When a seismic related rock mass failure occurs, the distance from the location of the event to each seismic sensor must be determined, as many source parameters are scaled according to distance. The most common methodologies used for calculating location employ a technique to minimize the difference between measured and theoretical wave arrival times (Gibowicz and Kijko, 1994). Theoretical arrival times are calculated based on the velocity model assumed for the mine.

The location of seismic events is critical to determining areas of increased hazard within a rock mass. Concentrations of large events can provide an immediate indicator of areas of elevated hazard. Temporal variations in seismic event location are a primary consideration of analysis in this thesis.

2.3.3 « Event Magnitude »

Event magnitude is used as a measure of size or intensity of a seismic event. Mines commonly employ logarithmic scales such as Richter (Richter, 1935) or Nuttli (Nuttli, 1973), to provide a measure for the size of macroseismic events (Richter magnitude greater than 0). Microseismic events (Richter magnitude less than 0) are commonly measured using a local logarithmic scale. Local scales are typically defined using in mine equipment and may not be calibrated to a recognizable magnitude scale. Table 1 details the observable rock mass response for seismic events of a particular Richter magnitude (Hudyma, 2004).

Table 1: Relation between varying degrees of Richter magnitude and the observable rock mass response (Hudyma, 2004).

RICHTER MAGNITUDE	QUALITATIVE DESCRIPTION
-3.0	-Small bangs or bumps felt nearby. Typically only heard relatively close to the source of the event. -This level of seismic noise is normal following development blasts in stressed ground. -Event may be audible but vibration likely too small to be felt. -Undetectable by a microseismic monitoring system.
-2.0	-Significant ground shaking. -Felt as good thumps or rumbles. May be felt more remote from the source of the event (i.e. more than 100 m away). -May be detectable by microseismic monitoring system.
-1.0	-Often felt by many workers throughout the mine. -Major ground shaking. -Similar vibration to a distant underground secondary blast. -Should be detectable by microseismic monitoring system.
0.0	-Vibration felt and heard throughout the mine. -Bump commonly felt on surface (hundreds of meters away), but may not be audible on surface. -Vibration felt on surface similar to those generated by a development round.
1.0	-Felt and heard clearly on surface. -Vibrations felt on the surface similar to a major production blast. -Can be detected by regional seismological sensors located hundreds of kilometers away.
2.0	-Vibration felt on the surface is greater than large production blasts.
3.0	-The largest mining-induced seismic events recorded in Australia registered about Richter 3 to Richter 4.

2.3.4 « Seismic Energy »

Seismic energy (E) is the total energy radiated from a seismic source and provides a good indication of event size. The total radiated energy is the sum of energy from the primary and secondary waves. The energy for each wave can be calculated as follows (Gibowicz and Kijko, 1994):

$$E = 4\pi pcR^2 \frac{J_c}{Fc^2}$$

where,

E = Radiated Energy (Joules)

ρ = Rock Density (kg/m^3)

c = Velocity of the Wave in Rock (m/s)

R = Distance from the Seismic Source (m)

J_c = Integral of the Square of the Ground Velocity

Fc = Empirical Radiation Pattern Coefficient

2.3.5 « Seismic Moment »

Seismic moment (M_o) is an independent source parameter that provides a widely accepted measure of size for slip-related events. It is the most important parameter used to describe the strength of the source and is related to the local coseismic rock mass deformation (Gibowicz and Kijko 1994). Gibowicz and Kijko (1994) define seismic moment as:

$$Mo = 4\pi\rho c^3 R \frac{\Omega o}{Fc}$$

where,

Mo = Seismic Moment (Nm)

ρ = Rock Density (kg/m^3)

c = Velocity of the Wave in Rock (m/s)

R = Distance from the Seismic Source (m)

Ωo = Low Frequency Plateau of the Frequency Spectrum of a Seismic Waveform (see Figure 9)

Fc = Empirical Radiation Pattern Coefficient

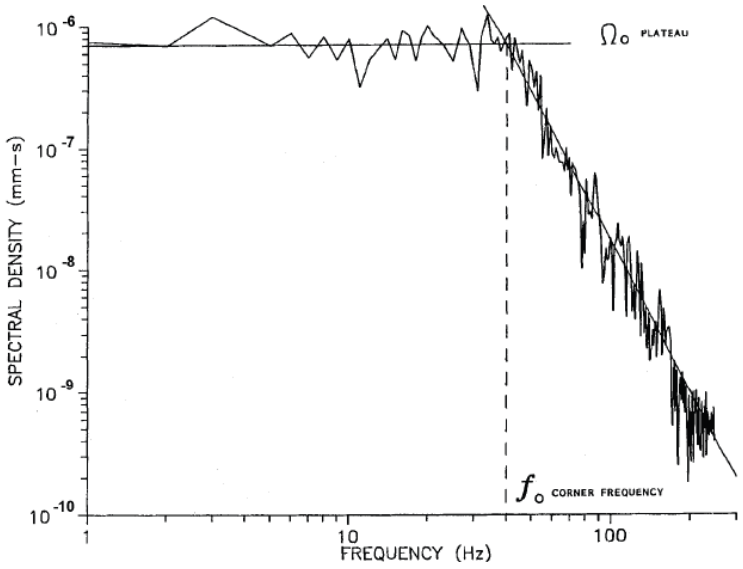

Figure 9: Corner frequency (f_0) and low frequency plateau (Ω_o) for a typical seismic event (Hedley, 1992).

2.3.6 « Apparent Stress »

Apparent stress (σ_a) is a measure of the state of stress at a seismic source. It was originally defined by Wyss and Brune (1968) as:

$\sigma_a = \mu (E/Mo)$

where,

σ_a = Apparent Stress (Pa)

μ = Shear Modulus of Rigidity of the Source Material (N/m^2)

E = Seismic Energy (Joules)

Mo = Seismic Moment (Nm)

Apparent Stress does not depend on any particular failure model and is therefore model independent (Mendecki, 1997). Large variations in apparent stress exist among events with similar magnitudes. Figure 10 shows a series of events with a Local magnitude of 1.0. The events are scaled by apparent stress and show a large spatial variation. This variation is a result of different varying local stresses and geological conditions.

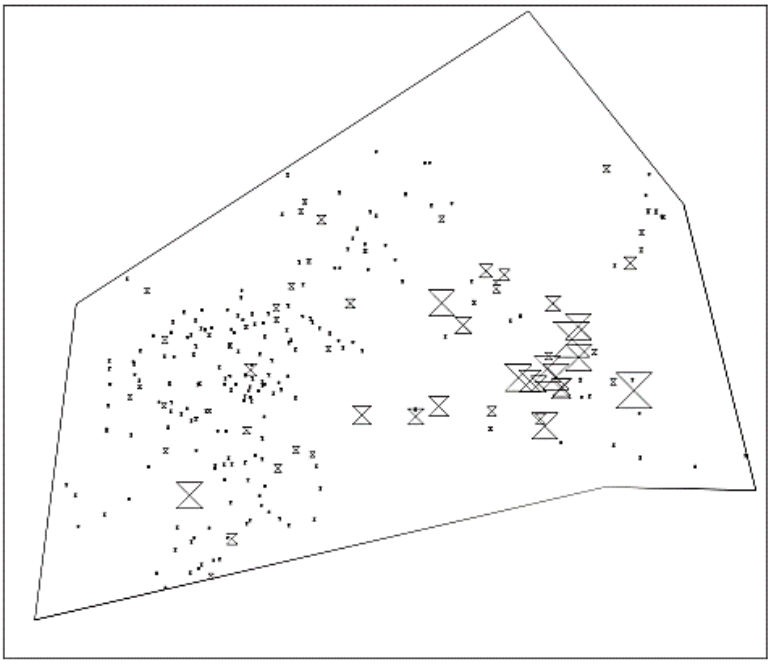

Figure 10: Events of the same Local magnitude scaled by apparent stress in a South African gold mine (Mendecki et al., 1999)

Apparent stress is a function of seismic moment and seismic energy. The presence of geological features, such as fractured or relatively soft rock, enables the source of a seismic event to yield more slowly at a lower stress than an equivalent sized source in strong rock and higher stress (Mendecki et al, 1999). Events occurring in these rock mass conditions have low seismic energy and high seismic moment– generating small apparent stress values. High stress regions release more seismic energy but deformation is limited as a result of high clamping forces (Simser et al.,

2003). Events occurring in these rock mass conditions have large seismic energy and low seismic moment– generating large apparent stress values.

In the past, the majority of seismic analysis utilizing apparent stress was undertaken independent of time, generating images similar to Figure 10. Mining is a dynamic process however, and to gain meaningful insight into the rock mass response to mining, time needs to be incorporated into analysis techniques. Analyzing apparent stress with reference to time is a primary component of this thesis.

2.4 « Seismic Analysis Techniques »

Seismic analysis techniques allow for meaningful observations and conclusions to be drawn from seismic databases or subsets within the data. Various techniques provide insight into data integrity, seismic hazard, stress conditions and the general normal/abnormal rock mass response to mining.

2.4.1 « Gutenberg-Richter Frequency-Magnitude Relation »

One of the most fundamental seismic analysis techniques, the Gutenberg-Richter Frequency-Magnitude Relation provides insight into data quality, source mechanism and seismic hazard. The cumulative number of events (y-axis) greater than or equal to a given magnitude (x-axis) is plotted. Figure 11 represents a large population of seismic data.

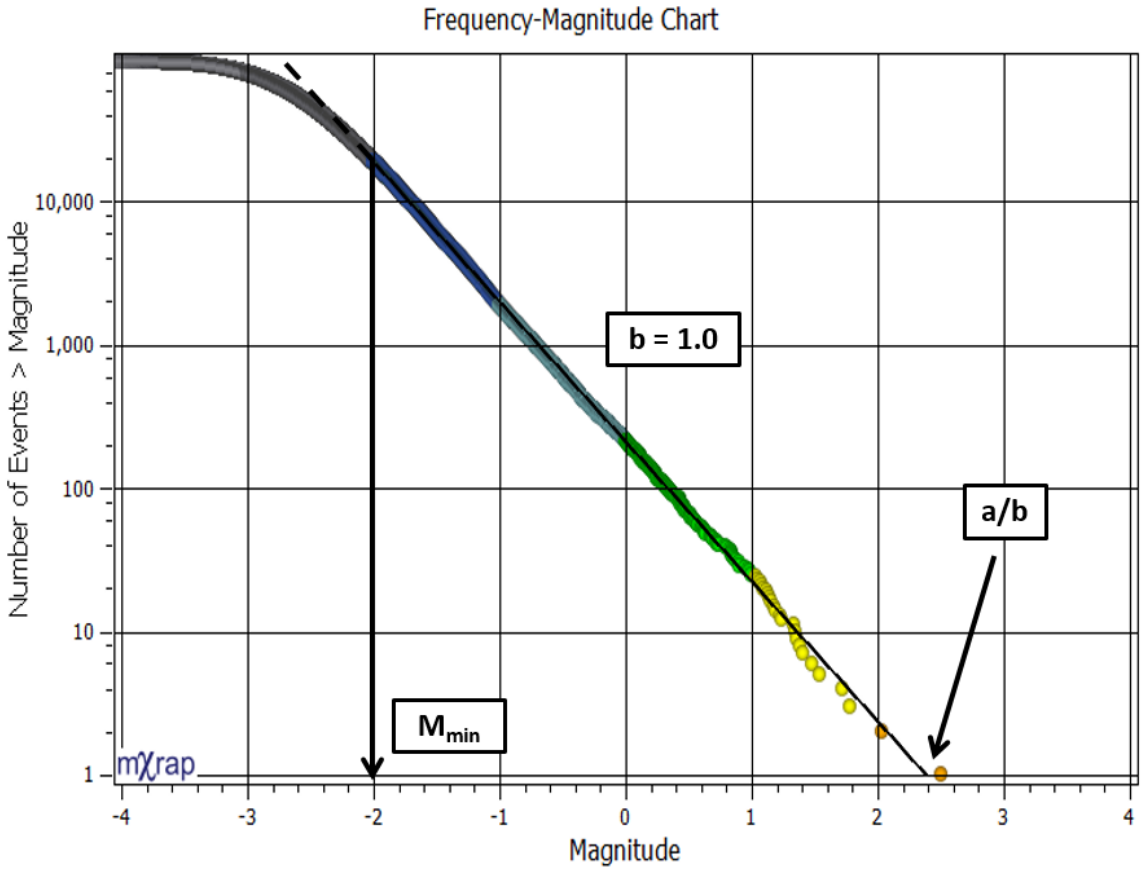

Figure 11: Frequency-Magnitude chart for a large population of seismic data. Colour variations correspond to Local magnitude values.

Many insights into seismic data can be gained from the analysis of a frequency magnitude plot. Gutenberg and Richter (1935) proposed a power law relation between the frequency of seismic events and their magnitude:

$$\log(N) = a - (b)(m)$$

where,

N = Number of seismic events of at least magnitude 'm'

m = Magnitude

a = Constant

b = Constant

Where this relation no longer approximates the real data is referred to as the M_{min} value (Figure 11). It represents the seismic system sensitivity or the completeness of the data record. In other words, the system has reliably recorded all events greater than or equal to this magnitude for the seismic population (M_L = -2.0 in Figure 11). The 'a/b' value, or the intersection of the relation with this x-axis, is an estimation of the largest expected magnitude event. The 'a/b' value for this area is M_L = 2.4, very close to the largest event contained within the population, M_L = 2.5. This value is commonly used as a means of assessing long term seismic hazard.

The slope of the relation (b-value) provides insight in the seismic source mechanism. A low b-value (less than 0.8) is indicative of a fault-slip mechanism driving seismicity, while a high b-value (1.2 – 1.5) is indicative of a primarily volumetric and stress fracturing source mechanism (Hudyma, 2008). For well-behaved populations, a value approximating 1.0 is expected - as seen in Figure 11.

2.4.2 « Magnitude-Time History »

The Magnitude-Time History analysis technique (Hudyma, 2008), allows the user to visually and quantitatively analyze the seismic response to mining over time. Events are plotted in chronological order with date/time on the x-axis and Local magnitude on the primary y-axis. On the secondary y-axis, the cumulative number of seismic events is plotted. A flat line represents no seismicity. A constant slope represents a constant rate of events. A slope that increases over time represents an increasing rate of events. This analysis can provide insight into data integrity and be used to monitor changes and trends in the seismic monitoring system. Figure 12 is a typical Magnitude-Time History chart for a large seismic population.

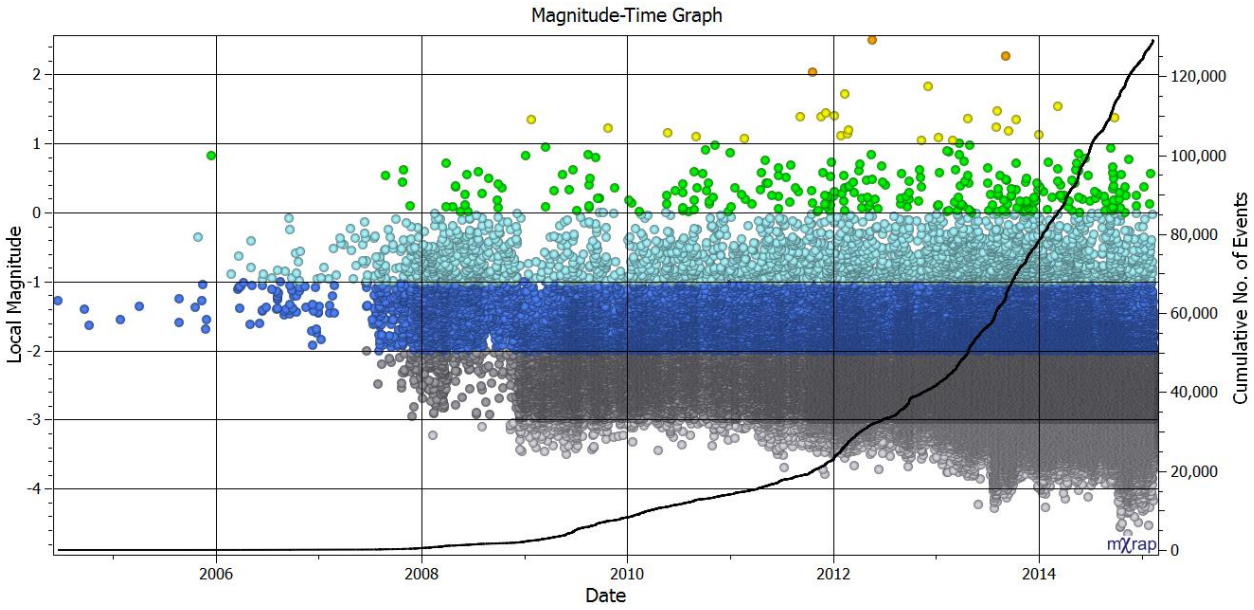

Figure 12: Magnitude-Time History chart for a large population of seismic data. Colour variations correspond to Local magnitude values.

An increase in seismic hazard over time can easily be identified (Figure 12) from the increasing quantity and magnitude of large events. In this case, the slope of the cumulative number of events (secondary y-axis), is largely skewed by changes to the seismic monitoring system. Abrupt changes in system sensitivity (smaller events being recorded), can be seen in mid 2007 and late 2008. Changes in system sensitivity create a bias in the cumulative number of events. This bias can be eliminated by only plotting events greater than or equal to the M_{min} value for the population. Figure 13 is a Magnitude-Time History chart for the same seismic population shown in Figure 12 but using a lower bound of $M_L \geq -1.5$.

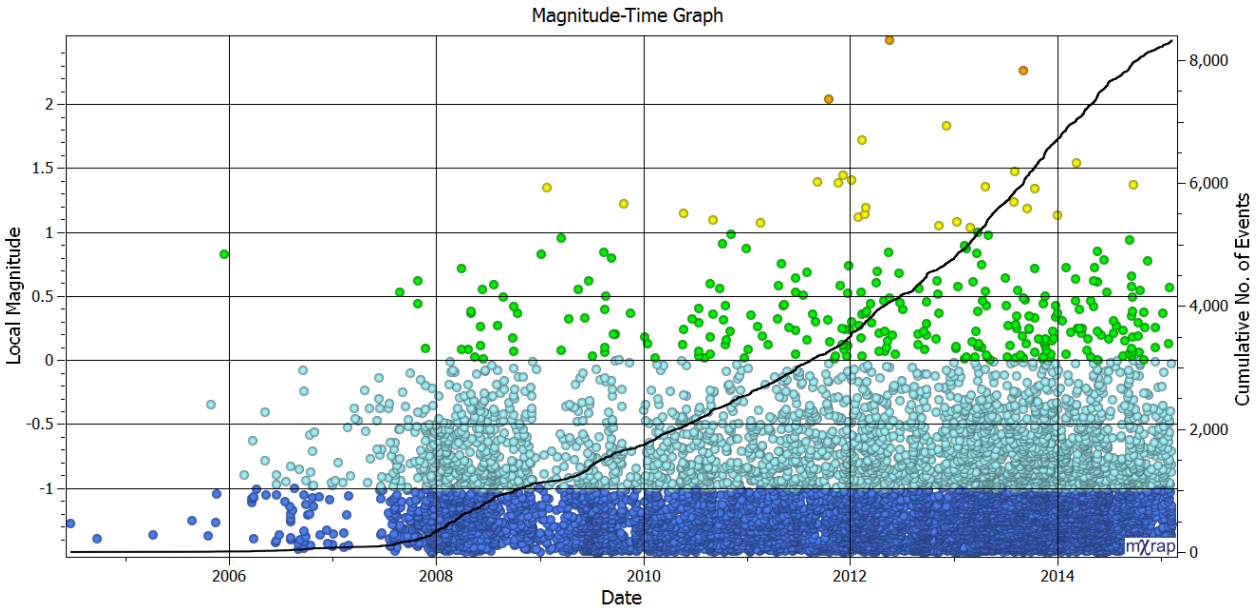

Figure 13: Magnitude-Time History chart for the same seismic data shown in Figure 12 using a magnitude cut off of -1.5. Colour variations correspond to Local magnitude values.

By eliminating all events below the minimum system sensitivity ($M_L \geq -1.5$), trends in the seismic data can be interpreted without bias. The cumulative number of events is no longer skewed by changes in the system sensitivity and a relatively constant trend can be observed from 2009 to 2012. There is a modest increase in event rate from 2012 to mid 2014. The use of this chart with detailed knowledge of the mining history is a powerful seismic analysis tool. It enables the user to identify seismic trends relating to development/production blasting, stope sequencing, etc.

2.4.3 « Energy-Moment Relation »

The relation between total radiated energy and seismic moment for an ideal seismic population is logarithmic. Energy-Moment charts are often displayed with the log of moment and log of energy on the x and y-axis's respectively. Figure 14 is a typical energy-moment relation for a large seismic population. The numbers seen on the axes represent the power of 10 to which the value is raised.

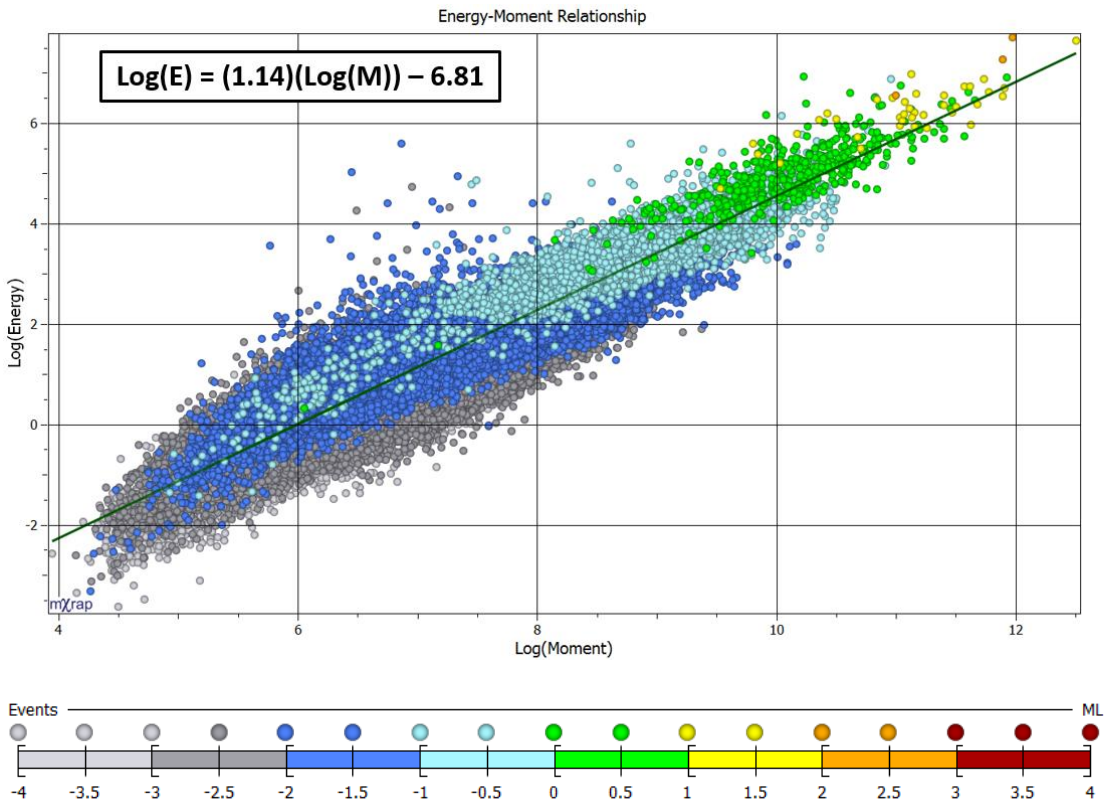

Figure 14: Energy-Moment relation chart for a large seismic population.

Figure 14 depicts a well behaved logarithmic relation between moment and energy for the given seismic population. Variations in seismic energy are largely contained with plus or minus an order of magnitude from the best-fit relation. The line of best fit for such a relation provides insight into the qualities of the associated rock mass (Mendecki and van Aswegen, 2001). The generic equation for the line is:

$$\log(E) = c + (d)(\log(Mo))$$

where,

E = Seismic Energy (Joules)

Mo = Seismic Moment (Nm)

c = A constant related to the stress acting on the rock mass system (Mendecki and van Aswegen, 2001)

d = A constant related to the stiffness of the rock mass system (Mendecki and van Aswegen, 2001)

2.4.4 « S:P Energy Ratio (ES:EP) »

The ratio of energy in the s-wave (ES) to the energy in the p-wave (EP) for a seismic event can be an indicator of seismic source mechanism (Urbancic et al., 1992). By plotting the cumulative number of events (y-axis) greater than or equal to a given S:P energy ratio (x-axis), a visual representation of the ES:EP distribution for a given seismic population can be generated. Figure 15 is a cumulative ES:EP chart for a large seismic population.

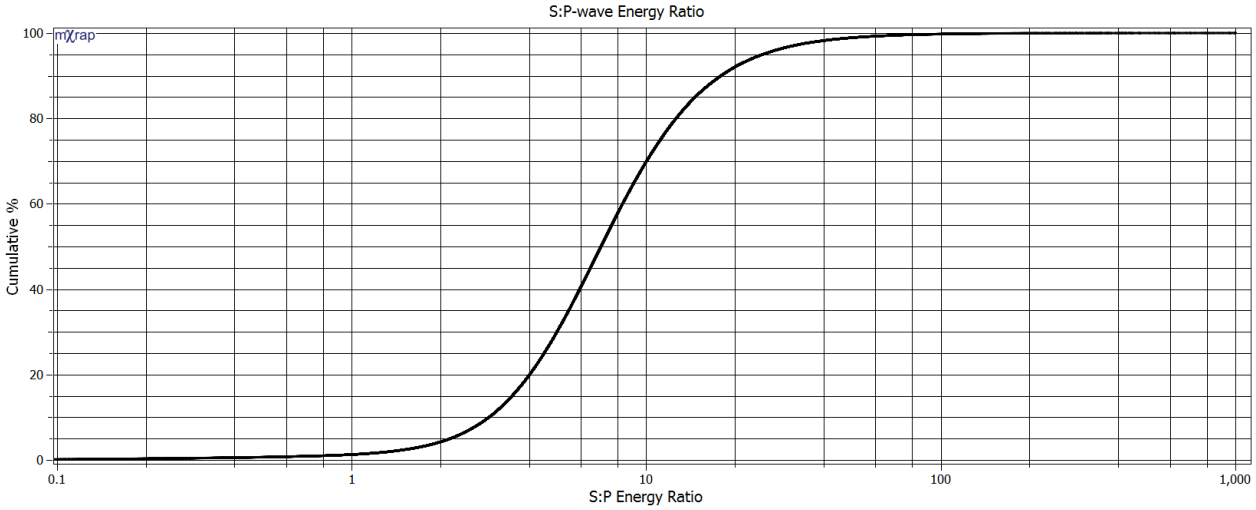

Figure 15: Cumulative ES:EP chart for a large seismic population.

Volumetric and stress fracturing events typically have an ES:EP ranging from 1 to 3 (Urbancic et al., 1992). For the seismic population shown in Figure 15, this value range corresponds to approximately the 10th percentile of the data. Fault-slip mechanism events typically have an ES:EP in excess of 10 (Boatwright and Fletcher, 1984). For this seismic population the 70th

percentile corresponds to an ES:EP value of approximately 10. This data set contains a significant volume of events that can be inferred as having a dominant fault-slip source mechanism.

2.4.5 « Apparent Stress Time History (ASTH) »

Apparent Stress Time History charts (Young, 2012) are a means of displaying and analyzing changes in apparent stress over time for seismic populations. ASTH charts work to identify time periods of elevated apparent stress using a trailing moving average of the number of events with a high apparent stress value. Seismic events are plotted in chronological order along the x-axis with corresponding apparent stress values along the y-axis. The secondary y-axis is used to display the total number of high apparent stress events in the defined time window. In order to utilize this analysis technique, two parameters must be defined: what value or percentile of events corresponds to high apparent stress and what trailing time period provides an accurate representation of the data. Both of these parameters must be determined independently for every dataset analyzed and can generate bias within the analysis. Figure 16 is an ASTH chart for a large seismic population. Apparent stress frequency displayed on the secondary y-axis is measured per day.

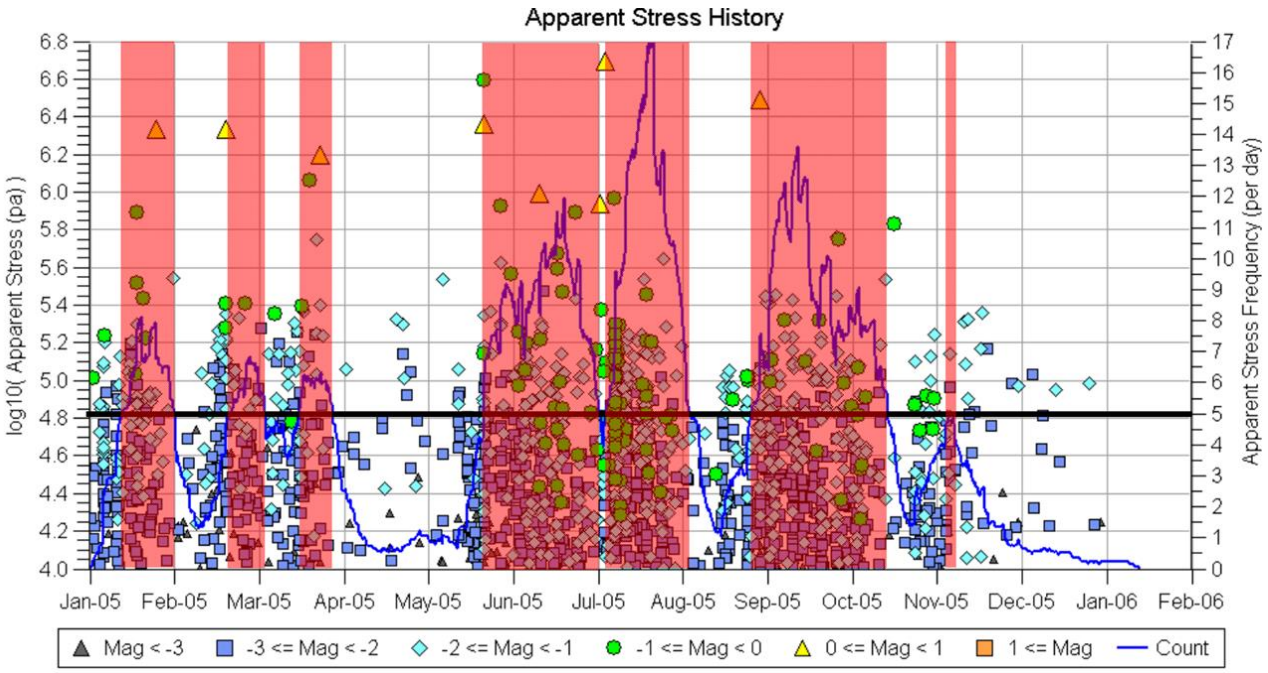

Figure 16: Apparent Stress Time History chart for a large seismic population (Hudyma, 2014).

A clear relation between the frequency of high apparent stress events and the occurrence of large magnitude events is evident in Figure 16. All 8 of the largest events within the population occur during or very close to a period of time where the frequency of high apparent stress events exceeds 5. ASTH charts can be used to identify trends in apparent stress that may be correlated to elevated seismic hazard, but require the selection of parameters that can be difficult to define, or which may vary significantly for various seismic populations.

2.4.6 « Seismic Hazard Mapping »

Spatial variation of seismic source parameters and analysis techniques can be used to create seismic hazard maps. Hazard maps are generated by analyzing seismic populations and assigning attributes from the population to nearby mine excavations. This enables a mine site to visually estimate areas of elevated hazard and mitigate seismic risk accordingly.

Grid-based hazard mapping is a common approach for creating hazard maps. One of the main advantages to using a grid-based approach is the ability to identify anomalous activity without requiring predefined groups of seismic events. Introducing a 3-dimensional grid to a large volume, such as the area incorporating and surrounding mine workings, allows for unbiased generation of seismic populations. A representative seismic parameter can then be assigned to each grid point based on the events contained within a defined proximity or search radius. The grid spacing and search radius must be defined based on the purposes of the analysis and will vary based on the density and quality of seismic data (Wesseloo et al., 2014). Figure 17 is an example of grid-based spatial variation of b-values, obtained from the Gutenberg-Richter frequency-magnitude relation, for an Australian mine (Wesseloo et al., 2014).

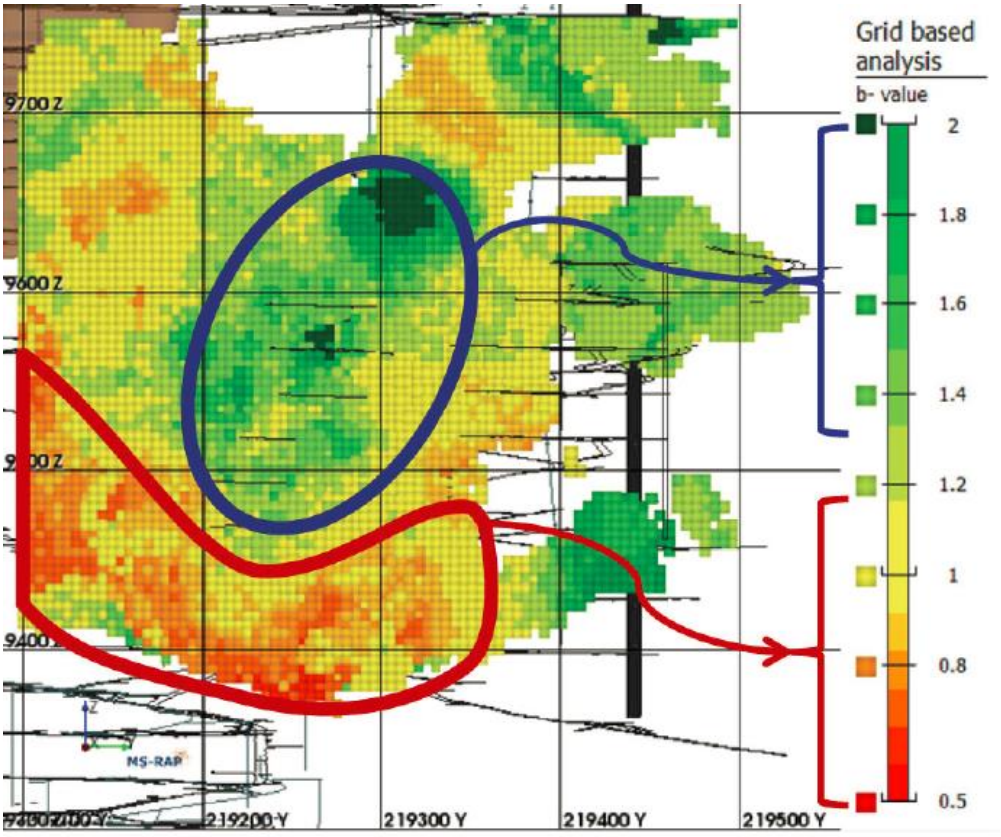

Figure 17: Grid-based interpretation of b-values for a large area within an Australian mine. Blue and red highlighted areas represent stoping and abutment areas respectively (Wesseloo et al., 2014).

Using a grid-based spatial analysis enables the user to visually identify differences in parameters throughout a rock mass. The area highlighted in blue (Figure 17), corresponds to significantly higher b-values than the surrounding areas, and reflects the seismic response to local stoping activity. The area highlighted in red (Figure 17), corresponds to significantly lower b-values than the surrounding areas and is a reflection of the failure mechanisms occurring at the abutment of the mining front. Hazard maps enable a user to visually identify areas with similar characteristics and consequently areas of elevated seismic hazard.

Other hazard mapping methodologies typically require predefined groups or clusters of seismic events. These groups represent individual seismic populations, similar to those generated for each grid point. A disadvantage to these approaches is the potential bias that is introduced by user defined groups. Using a grid-based approach eliminates this bias.

2.5 « Chapter Summary »

Mining-induced seismicity is a hazard to deep and high stress mining operations. Seismic events result from a combination of local stress and geological conditions and can be driven by a variety of failure mechanisms. Large seismic events ($M_R \geq 1$) can lead to rockbursting and pose a significant risk to underground excavations, equipment and personnel.

Seismic monitoring systems enable mining operations to gain insight into the conditions and failure mechanisms of the local rock mass. Seismic source parameters, calculated from triaxial sensors, can be used to quantitatively describe a seismic population. These parameters include: time, location, energy, moment, magnitude and apparent stress. A variety of analysis techniques can be used to identify meaningful trends in seismic source parameters. Trends related to source

mechanism, local stress conditions and event frequency can be used to infer seismic hazard and generate seismic hazard maps.

Chapter 3

3 « LaRonde Mine »

Agnico Eagle's flagship LaRonde mine is a Canadian operation located in northern Quebec, approximately 650 km northwest of Montreal near the town of Preissac (Figure 18). It is a world-class Au-Ag-Cu-Zn massive sulphide lens complex with over 4 million ounces of gold in proven and probable reserves (Turcotte, 2014). Current mining extends more than 2,930 metres below surface, producing approximately 6,300 tonnes per day (Turcotte, 2014). Bulk mining at such depth has resulted in a history of seismic activity at LaRonde that has been recorded since 2003.

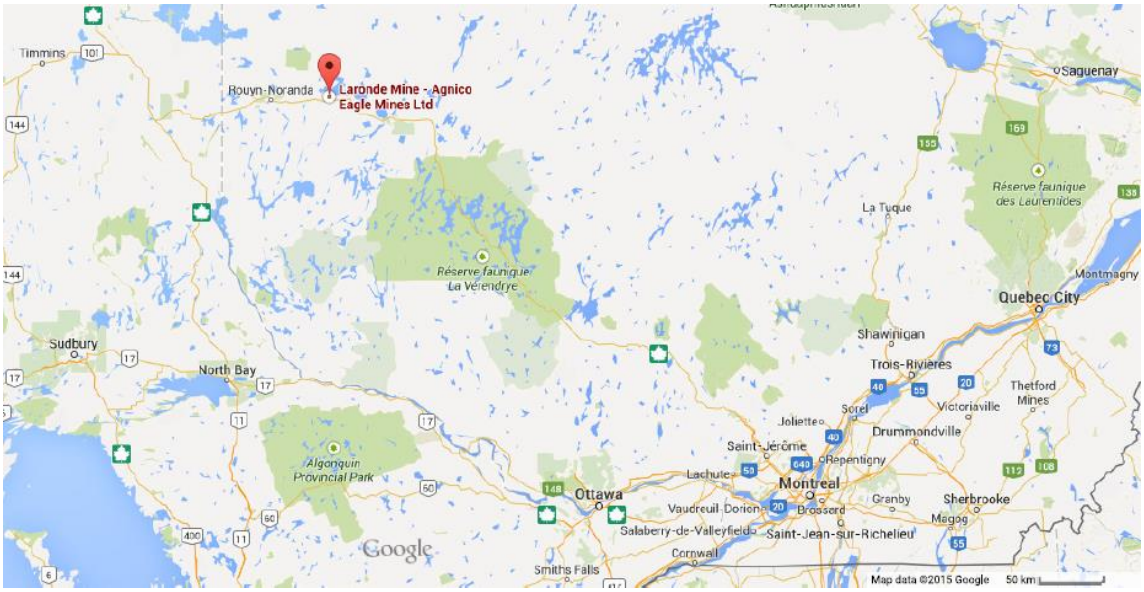

Figure 18: Map of Canada showing parts of Ontario and Quebec with LaRonde mine identified by a red marker (Google Maps, 2015).

3.1 « Mining Method »

LaRonde employs an open stoping bulk mining method to extract ore from three sub parallel sulphide lenses. The majority of production tonnes are extracted from a single lens, referred to as zone 20 (Turcotte, 2014). The other zones (7 and 21), are narrow and discontinuous sulphide lenses ranging from 1 to 5 m in thickness (Mercier-Langevin, 2010). All zones have a combined thickness of 1 to 40 m and a dip of 70-80° towards the South (Mercier-Langevin, 2010). Figure 19 is a long section of LaRonde mine.

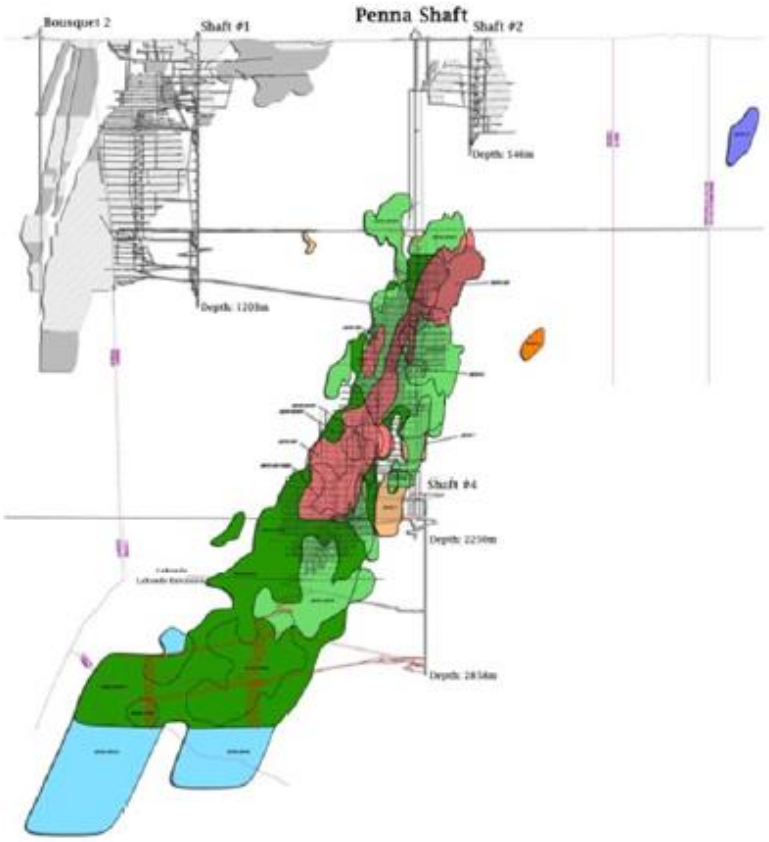

Figure 19: Long section of LaRonde mine (Turcotte, 2014)

3.1.1 « Mining Method Parameters »

The majority of ore is extracted using transverse open stoping with a primary/secondary pyramid mining sequence. Typical stope sizes are 30 m high with widths for primary and secondary stopes of 13.5 m and 16.5 m respectively (Mercier-Langevin, 2010). Stope thickness is equivalent to the width of the orebody (to a maximum of 40 m). Select areas, such as the narrow extremities, are mined using a longitudinal retreat open stoping mining method. Paste fill or cemented rockfill is employed for backfilling of primary stopes, while secondary stopes are backfilled using dry rockfill (Mercier-Langevin, 2010).

The average stope size at LaRonde is approximately 20,000 to 40,000 tonnes. In order to maintain the production rate of 6,300 tonnes per day, an average of 5 stopes must be turned over per month. In order to achieve this highly demanding schedule, both primary and secondary stopes are typically blasted in a single shot. A 30" raise bore is used to generate the initial slot void and the blast is carefully laid out using i-kon^{TM} electronic detonators.

3.1.2 « Mine Sequence »

Traditional mine sequencing at LaRonde consists of stopes taken in a continuous retreating overhand pyramid. This generates sill pillars between pyramids that have been particularly hazardous in the past. In an effort to break through sill pillars as early as possible, the mine sequence was altered to include underhand as well as overhand stopes.

Historically, the majority of seismic activity resulting from production mining has been associated with the extraction of primary stopes. During the mining of primary stopes a high stress failure front is created. The stress failure front is often half or a full stope above the

primary stopes. The secondary stopes yield when the primary stopes are mined. As a result there is no seismicity in the secondary stopes.

3.2 « Geology »

Geological conditions are a critical component to the design and operation of any mine. The local geology governs mining practices while the regional geology dictates characteristics of the orebody and surrounding area. LaRonde mine is located within one of the most productive gold mining belts in Canada.

3.2.1 « Regional Geology »

LaRonde is located within the Blake River Group of the Abitibi Greenstone Belt. This belt spans Ontario and Quebec and is home to many gold rich volcanogenic massive sulphide (VMS) deposits. A gold-rich VMS deposit is defined as a lens of iron, copper, zinc and lead sulphides that contains significant quantities of gold and silver. These deposits are formed by hot springs on or below the sea floor that are located near submarine volcanoes (Dube et al., 2007). Figure 20 is a map of gold deposits along the Abitibi Greenstone Belt.

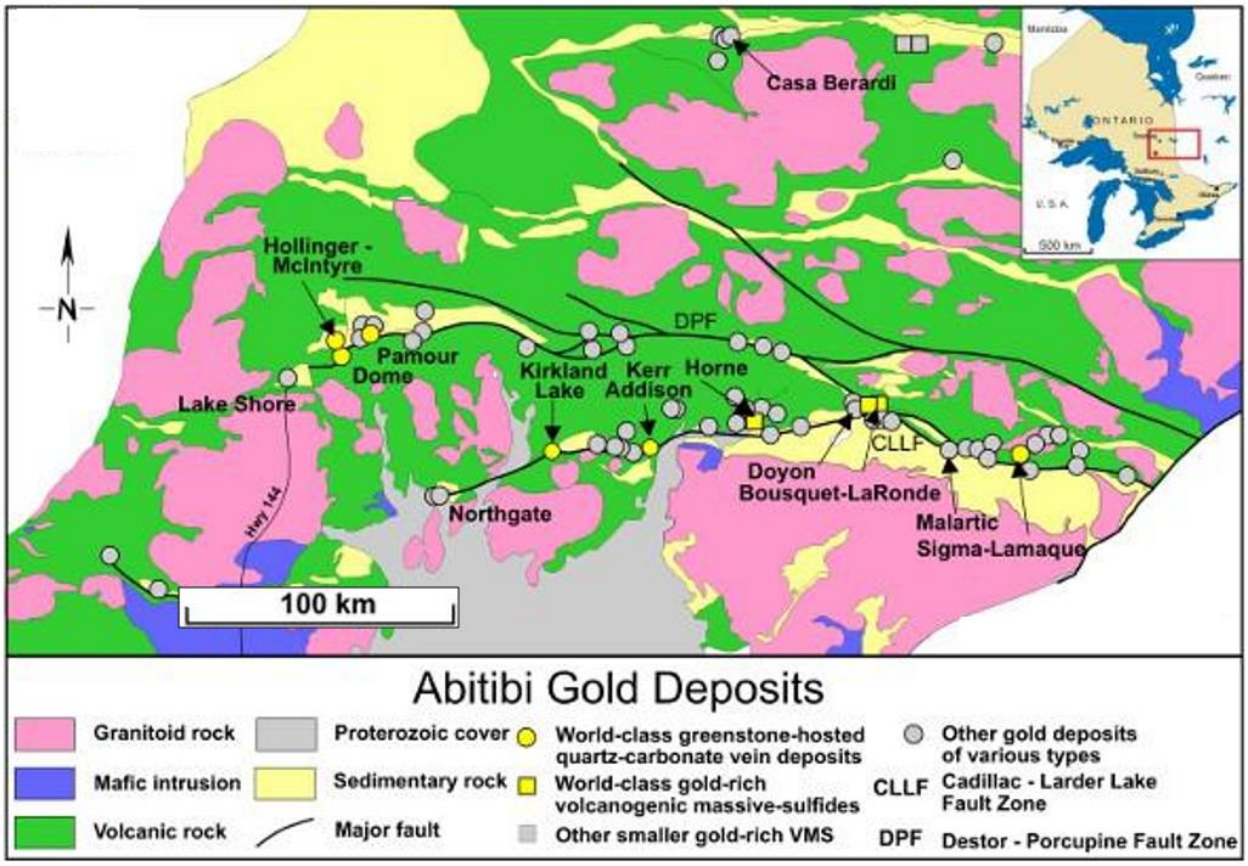

Figure 20: Map showing gold deposits along the Abitibi Greenstone Belt (adapted from Iamgold, 2012).

In addition to LaRonde, the Abitibi Greenstone Belt has been home to many world-class deposits such as Kirkland Lake and Kerr Addison. Other deposits currently being mined in the direct vicinity of LaRonde include Lapa and Westwood.

3.2.2 « Mine Geology »

LaRonde is home to a complex geology that plays a dominate role in the historic and current seismic response to mining activities. The orebody is located approximately 900 to 3000 metres below surface and has a strike length ranging from 240 to 530 metres. The in-situ stress for various depths can be estimated from the equations presented in Table 2:

Table 2: In-situ stress gradients at LaRonde mine (Turcotte, 2014). DBS refers to depth below surface (in metres).

Component	Equation (MPa)	Plunge/Direction
σ_1	8.62 + (0.04 x DBS)	0°/000°
σ_2	5.39 + (0.0262 x DBS)	0°/090°
σ_3	0.0281 x DBS	-90°/000°

The following table indicates the intact rock strength for the common lithological units at LaRonde found at depth (approximately 2900 m below surface).

Table 3: Mechanical properties of intact rock at LaRonde 290 Level (Turcotte, 2014)

Rock Type	UCS (MPa)	E (GPa)
Basalt	100	50
Rhyolite	260	66
Rhyodacite	200	63
Semi-Massive Sulphide	200	70

The basalt host rock is home to much of the permanent infrastructure, with haulage drifts and drawpoints located predominately in the rhyolite and rhyodacite (Turcotte, 2014). The mechanical properties presented in Table 3 are further influenced by the degree of alteration present in the rock mass. The rhyolite and rhyodacite are characterized by localised sericite alteration zones, and tightly spaced (centimetre to decimetre**)** foliation striking parallel to the orebody and dipping south at 75-80° (Turcotte, 2014).

At depth the rock mass is characterized as more silicified with less alteration; contributing to more brittle behaviour (Turcotte, 2014). Figure 21 is an image taken from the 290 Level showing silicification (quartz veining) in ore.

Figure 21: Silicification in ore on 290 Level at LaRonde mine.

Due to the large variations in geological conditions at LaRonde, the seismic response of the rock mass varies greatly - even across individual levels. Seismic response can range from violent ejection to aseismic squeezing depending on the rock mass characteristics (Turcotte, 2010). The majority of large and potentially damaging seismic events are concentrated in the FW and Eastern portion of the orebody, as seen in Figure 22.

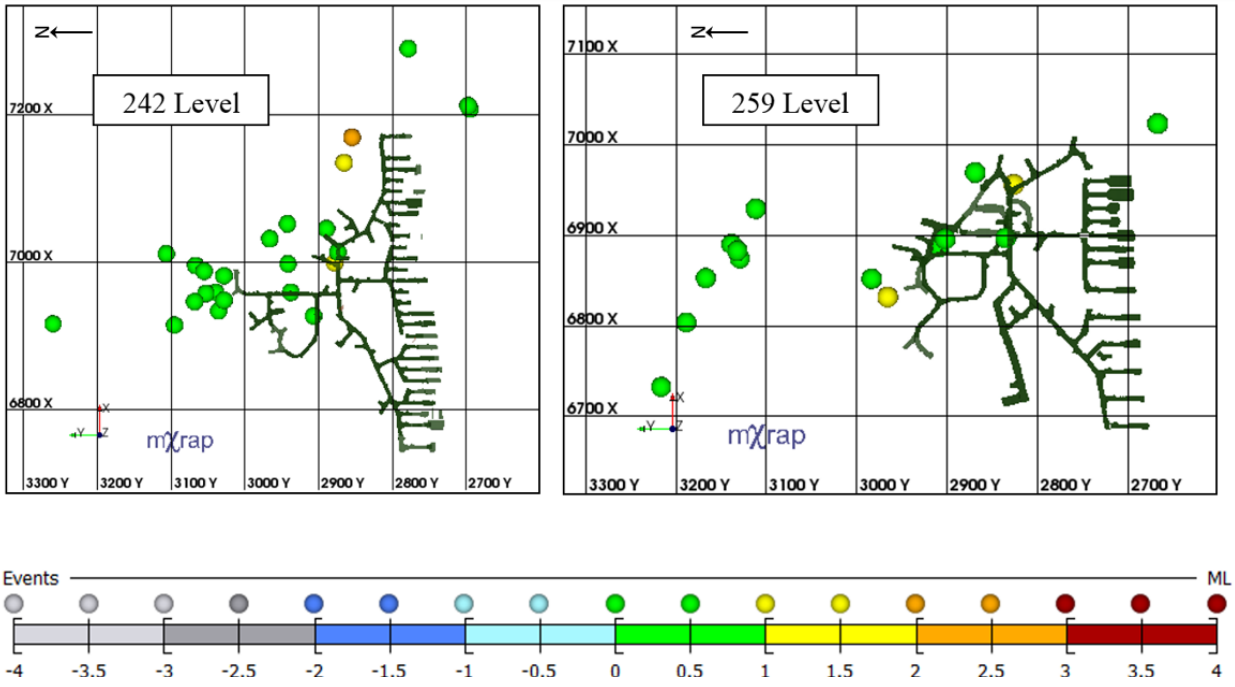

Figure 22: Plan views of 242 and 259 Levels respectively. All seismic events $M_L \geq 0$ are shown.

The concentration of large and potentially damaging seismic events coincides with the hard/brittle rock mass. Figure 23 is an image taken from the 242 Level at LaRonde that exemplifies both the typical squeezing and non-squeezing response to local stress conditions.

Figure 23: Drift on 242 Level at LaRonde mine showing both squeezing (left wall) and non-squeezing ground (right wall) response to stress conditions.

Understanding the variability of seismic response in a mine is essential to identifying regions of elevated seismic hazard. Areas that are prone to large seismic events should correspond to areas of increased seismic risk. Specific to LaRonde, these areas are concentrated in the FW and Eastern portion of the orebody.

3.3 « Rockbursting at LaRonde »

Rockburst type events pose the largest seismic hazard to mining operations. LaRonde mine has a history of rockbursting depicted by Figure 24.

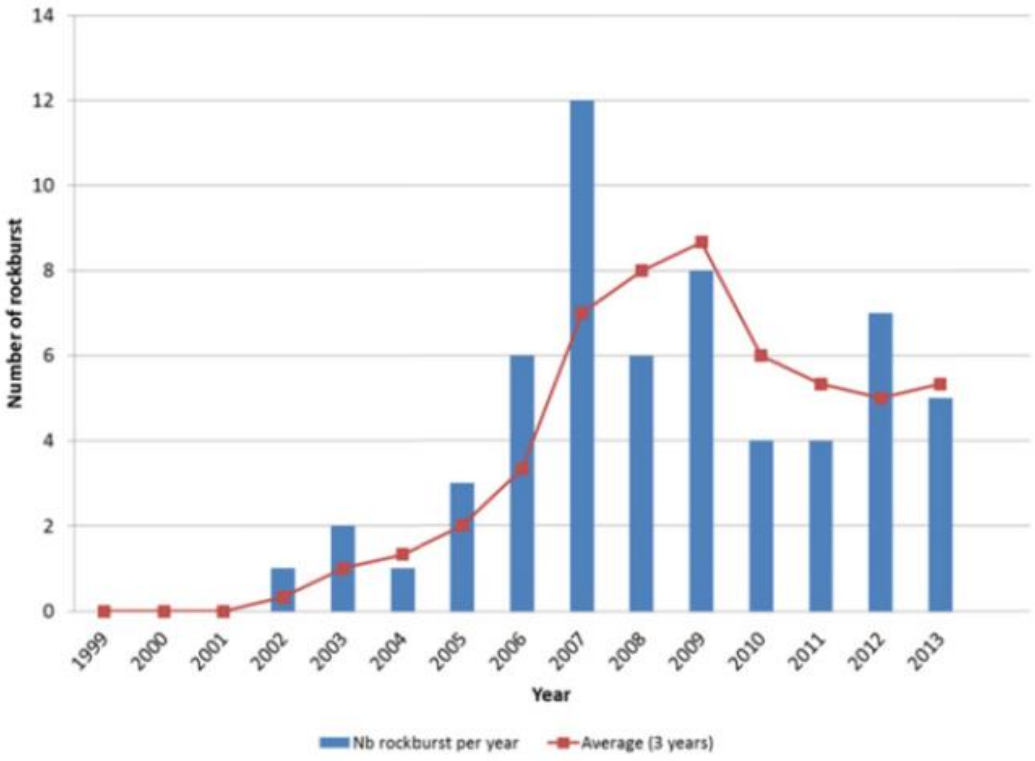

Figure 24: Number of rockbursts recorded at LaRonde since the onset of production in 1999 (Turcotte, 2014).

Sixty-one rockbursts have occurred at LaRonde between 1999 and 2013 (Turcotte, 2014). A clear increase in the number of rockbursts can be seen as time increases and mining progresses deeper. The peak of the 3 year trailing average occurs in 2009, at a value of just less than 9 rockbursts per year. The decrease in the number of rockbursts per year following the peak in 2009 can be attributed to changes in mining and ground control practices implemented as part of a new risk management program (Mercier-Langevin and Hudyma, 2007). Figure 25 depicts typical rockburst damage observed at LaRonde. Damage is commonly found in the bottom corners of drifts, below the lowest row of rockbolts, and in the upper corners of drifts.

Figure 25: Typical rockburst damage to the wall of an excavation and back of an excavation observed at LaRonde respectively (Turcotte, 2014).

Rockbursting at LaRonde constitutes a considerable risk to underground excavations, equipment, and personnel. Although new mitigation techniques have been successful in reducing the frequency of rockbursts, they are still a continuous hazard. By identifying areas in the rock mass that are prone to high stress conditions, the risk posed by rockbursting to the operation can be reduced.

3.4 « Seismic Monitoring at LaRonde »

Seismic monitoring systems in underground mines are commonly used to locate and provide insight into rock mass failure. Varying analysis techniques using seismic data have been discussed in Chapter 2. LaRonde has a detailed seismic database ranging from 2003 to present.

3.4.1 « Seismic Monitoring Systems »

The LaRonde ESG seismic monitoring system has gone through many upgrades since its implementation in 2003. The most influential change being a conversion from a Hyperion to a Paladin based system in late 2008. This change from an analog to a digital system enables greater frequency response and dynamic range, increasing the system sensitivity. The microseismic monitoring system currently covers all active areas of the mine with 84 sensors - a mix of 7 triaxial and 77 uniaxial accelerometers, with a sensitivity of approximately M_L = -2.2.

A macroseismic regional seismic system consisting of a single 4.5 Hz geophone located on surface was implemented in 2006. The purpose of this system is to provide accurate magnitudes for large low frequency events occurring at LaRonde. Additional geophones were integrated into the network in 2012. Magnitudes calculated for events occurring after this date are typically an average of at least two sensors. Currently, the macroseismic monitoring system consists of five surface geophones. The sensors are located at distances of 2 to 15 km from the mine as seen in Figure 26.

Figure 26: Map of area surrounding LaRonde mine. Each red marker corresponds to one of the surface geophones used by the macroseismic monitoring system (Google Maps, 2015).

3.4.2 « Magnitude Scales »

Magnitude scales have a logarithmic basis which allows for a large range of event sizes to be expressed in a short range of numbers. There are three main scales currently used by LaRonde: Nuttli, Richter and Local. Each one of these magnitude scales is generated by an individual seismic monitoring system.

Large events that are recorded by Natural Resources Canada (NRCan) are reported with a Nuttli magnitude. This magnitude scale was developed by Otto Nuttli (1973) specifically for small to moderate sized earthquakes in Eastern Canada. A Nuttli magnitude is 0.3 to 0.6 units higher than a Richter magnitude for the same event (Plouffe, 1992).

Richter magnitudes are reported for large events recorded by the regional macroseismic network near LaRonde. Richter is a commonly recognized scale for reporting seismic event magnitude. It was developed by Charles Richter (1935) for describing the size of earthquakes in California. Magnitude values are calculated using the peak displacement amplitude of the secondary seismic wave and the location of the instrumentation relative to the seismic source.

A Local magnitude value is calculated for all events recorded by the underground ESG microseismic monitoring system. This scale is well suited for analysis as it provides a consistent and accurate representation for the small events and most large mining-induced seismic events recorded. ESG does not provide a relative calibration of the Local magnitude scale.

Based on data recorded at LaRonde, relations for the three magnitude scales are presented in Table 4. They are based on local, Richter and Nuttli magnitudes calculated by the ESG microseismic system, regional macroseismic system, and NRCan respectively. Graphs from

which the relations were drawn can be found in Appendix A. Future reference to event magnitude in this thesis will use LaRonde's Local magnitude.

Table 4: Magnitude conversion relations between Local, Richter and Nuttli magnitude scales for LaRonde.

Magnitude Scales	Relation
RSN Richter & NRCan Nuttli	NRCan Nuttli = RSN Richter + 0.3
ESG Local & NRCan Nuttli	ESG Local = NRCan Nuttli - 1.3
RSN Richter & ESG Local	RSN Richter = ESG Local + 1.0

3.4.3 « Seismic Event Frequency »

As mining at LaRonde progresses deeper, changes in the typical seismic response to mining can be observed. By dividing the seismic history into two separate time frames, Hyperion (approximately 2004 to 2009) and Paladin (approximately 2009 to present), changes in the general trends of the data can be observed. Figure 27 is a Magnitude-Time History chart for all seismic events occurring at LaRonde during the Hyperion time frame.

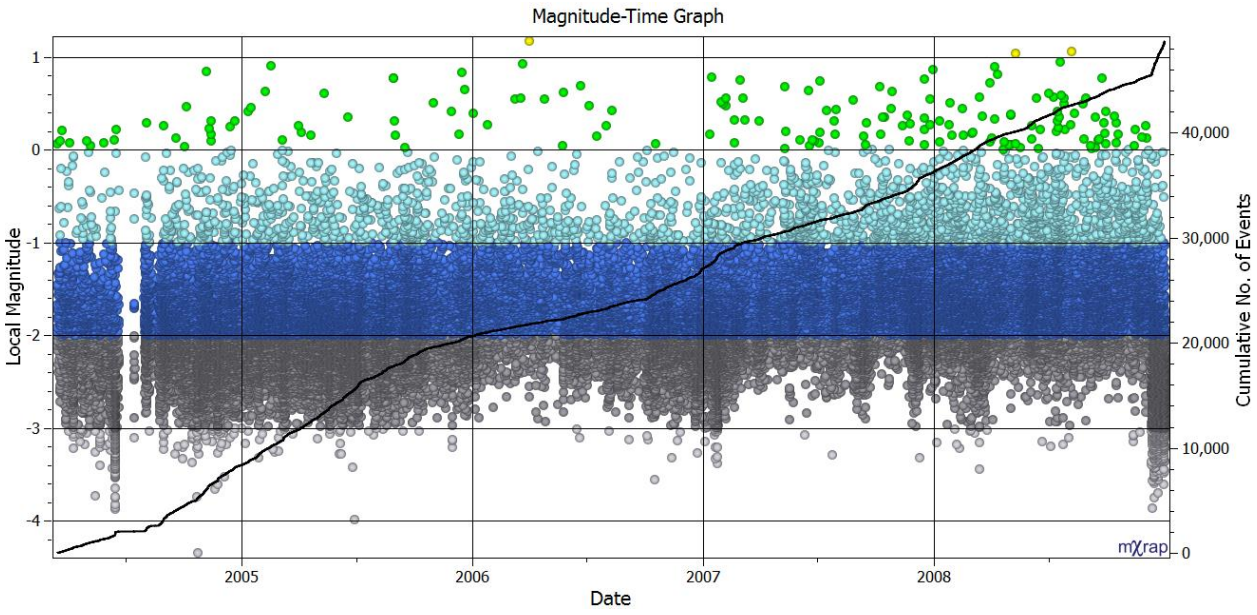

Figure 27: Magnitude-Time History chart for all events occurring at LaRonde between 2004 and 2009. Colour variations correspond to Local magnitude values.

The quality and collection of the data is consistent throughout the time frame with the exception of a small period in approximately July 2004. This corresponds to a period of time where the seismic system was not operational. Changes to the system sensitivity throughout the time period can be observed along with associated variations in the slope of the cumulative number of events (secondary y-axis). While there is a significant population of large magnitude events (168 events $M_L \geq 0$), there are only 3 events greater than Local magnitude 1. The increase to system sensitivity and event frequency seen in late 2008 corresponds to the conversion of the seismic monitoring system from Hyperion to Paladin. Figure 28 is a Magnitude-Time History chart for all seismic events occurring at LaRonde during the Paladin time frame.

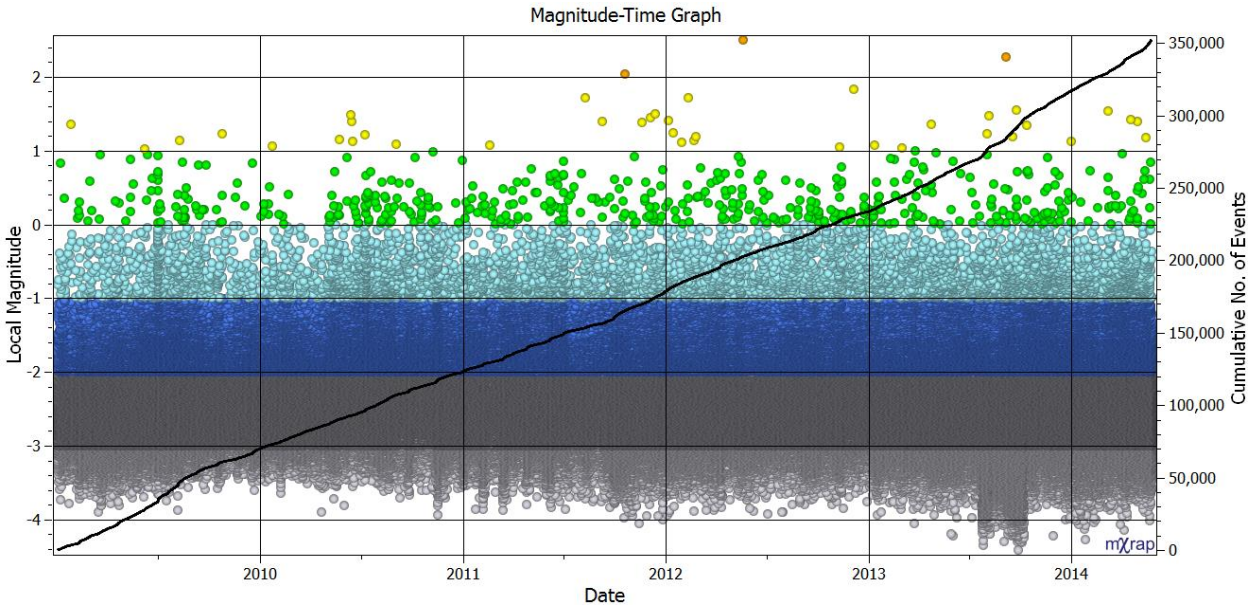

Figure 28: Magnitude-Time History chart for all events occurring at LaRonde between 2009 and approximately 06/2014. Colour variations correspond to Local magnitude values.

The most evident distinction between the time periods is the overall number of recorded events. Approximately 350,000 events were recorded during the Paladin period (approximately 70,000 events per year), versus less than 50,000 events during the Hyperion period (approximately 10,000 events per year). This is due to the increase in system sensitivity paired with an increase

in seismic activity generated from mining at increased depth. The slope of the cumulative number of events is relatively constant throughout the entire Paladin time period. The number of large events ($M_L \geq 0$) recorded after the installation of the paladins is 471, with 38 events greater than Local magnitude 1 and three events greater than Local magnitude 2. This reflects a substantial increase to seismic hazard for the Paladin time period compared to the Hyperion time period.

As previously discussed, frequency-magnitude charts can be used to infer information pertaining to the capabilities of the seismic monitoring system as well as seismic hazard. Figure 29 is a frequency magnitude chart for all seismic events occurring at LaRonde during the Hyperion time frame.

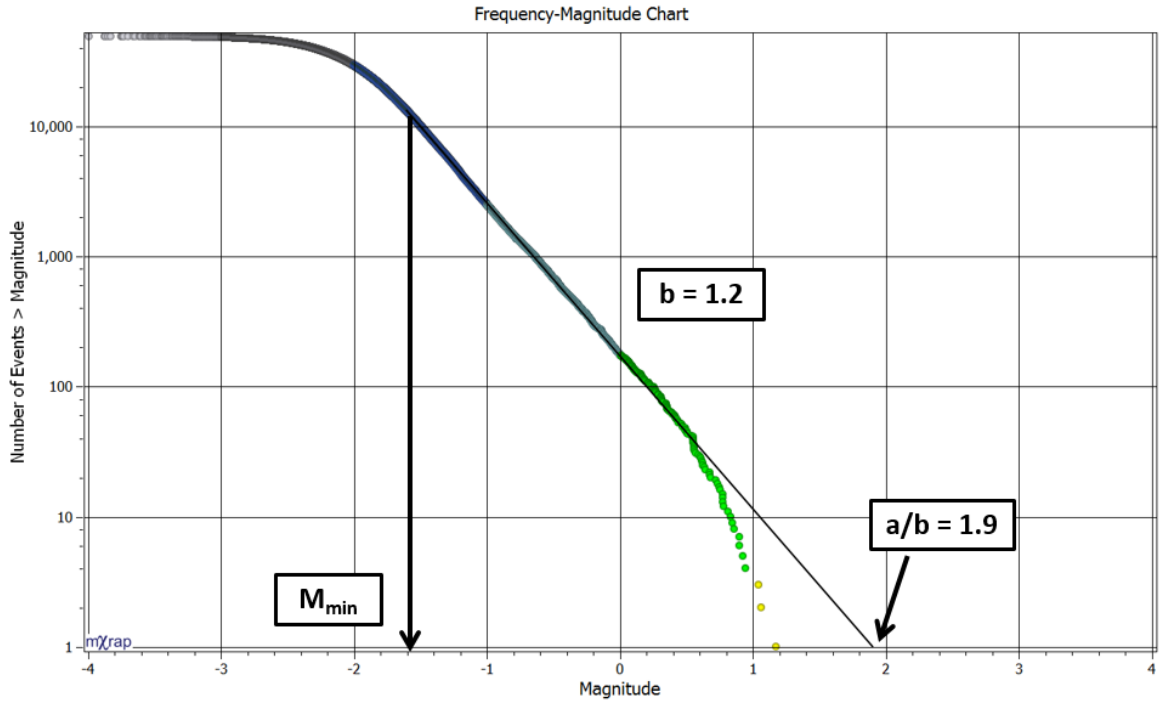

Figure 29: Frequency-Magnitude relation for all seismic events occurring at LaRonde between 2004 and 2009. Colour variations correspond to Local magnitude values.

For the data collected using the Hyperion monitoring system, the system sensitivity is approximately M_L= -1.6. This indicates that all events with a magnitude greater than this value have been reliably recorded since the implementation of the seismic monitoring system. Well behaved seismic data for large populations typically has a slope approaching 1. The slope of the linear portion of the data is slightly larger at approximately 1.2. This indicates that the data is largely dominated by stress fracturing events. The largest expected event for this population is approximately M_L= 1.9. Figure 30 is a frequency magnitude chart for all seismic events occurring at LaRonde during the Paladin time frame.

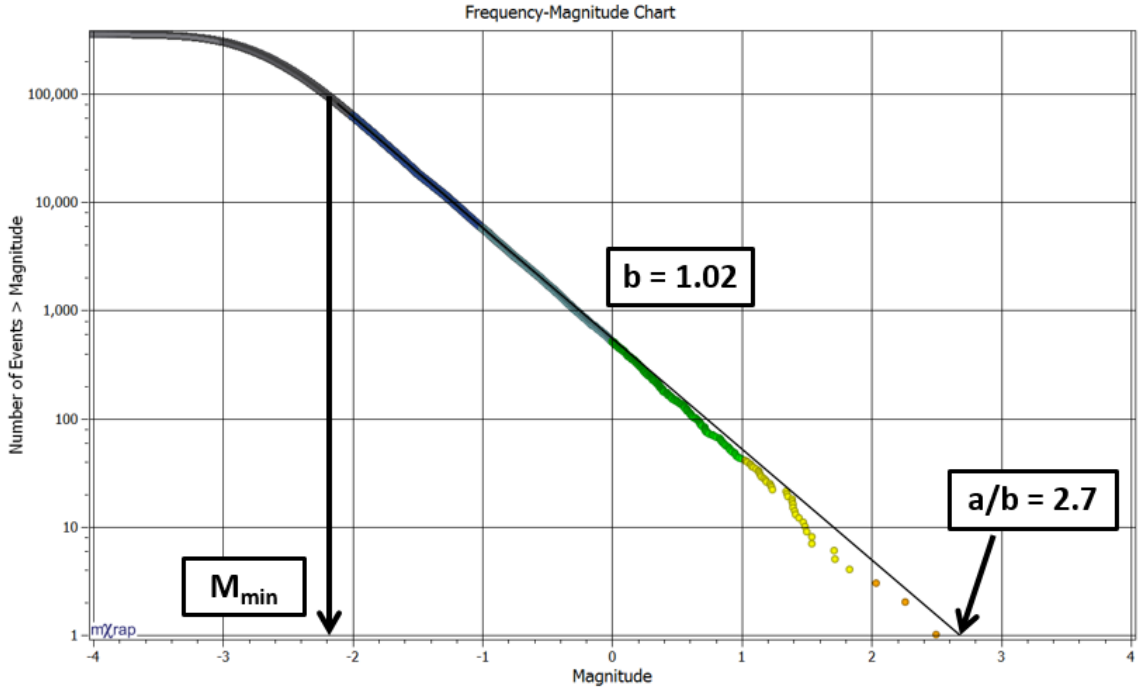

Figure 30: Frequency-Magnitude relation for all seismic events occurring at LaRonde between 2009 and approximately 06/2014. Colour variations correspond to Local magnitude values.

The same differences seen between the Hyperion and Paladin time frames in the Magnitude-Time History graphs are present in the frequency magnitude charts. The system sensitivity has increased from M_L= -1.6 to approximately M_L= -2.2. This is a large contributor to the increase in the number of recorded seismic events. The slope of the linear relation portion of the data for this

time period is approximately 1.02. This indicates the data is well behaved. The largest expected event has increased nearly a complete order of magnitude from M_L= 1.9 to M_L= 2.7 between the two time periods. This is a clear indication of an increase in seismic hazard.

With the upgrade from a Hyperion to a Paladin based monitoring system, the system sensitivity and quality of seismic data recorded has dramatically increased. This paired with the progression of the mining front depicts the increase in seismic hazard associated with mining at depth for LaRonde.

3.4.4 « Normal versus Abnormal Seismic Response at LaRonde »

As previously discussed, a normal seismic response to mining consists primarily of small volumetric fracturing events. These events are typically $M_L \leq$ -1 and are driven by mining processes such as blasting. Figure 31 and Figure 32 depicts a normal seismic response to mining at LaRonde. Each plan view shows successive 1 week periods of seismicity during ramp development at depth.

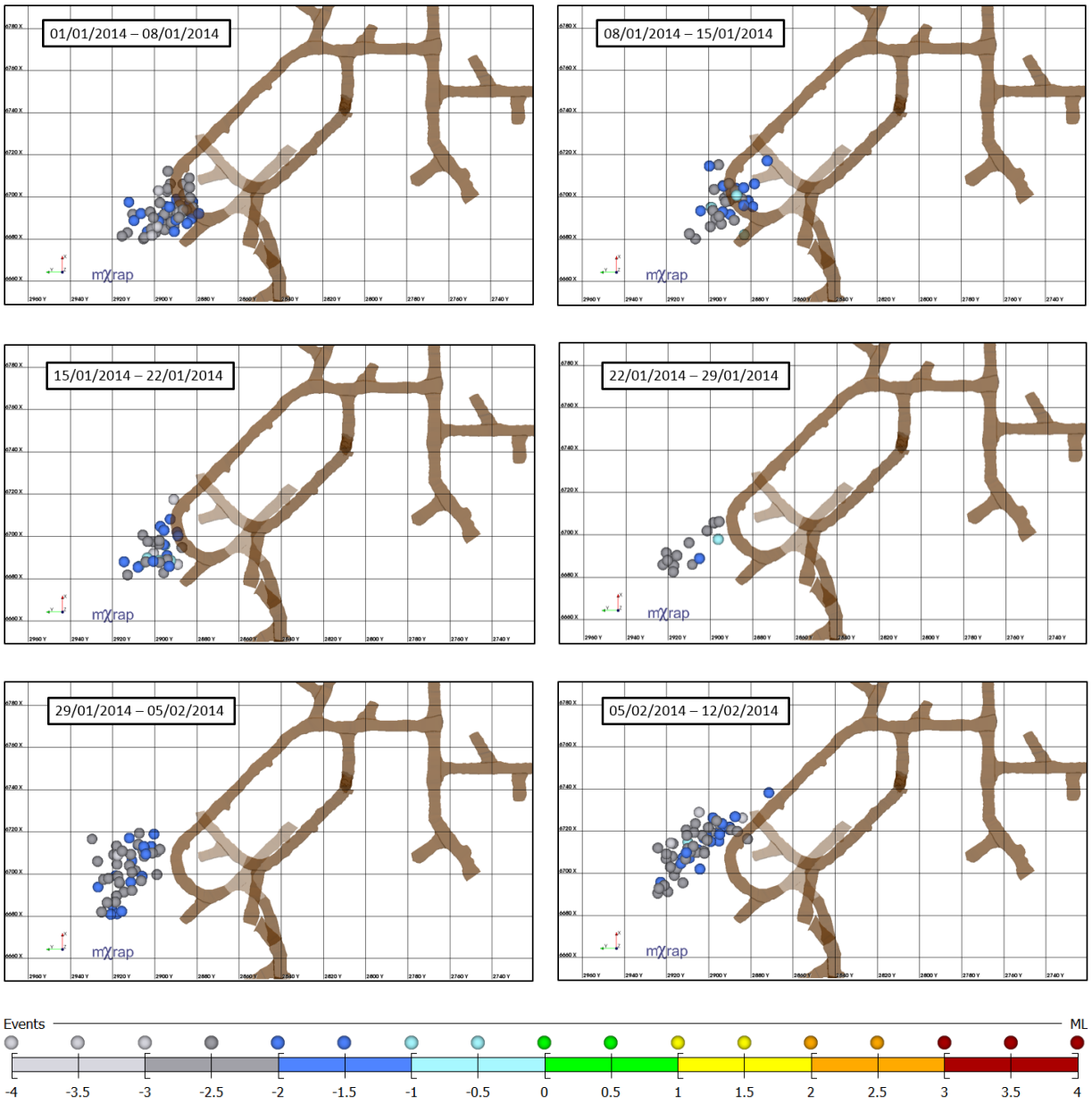

Figure 31: Seismic events plotted weekly during the development of a section of ramp at LaRonde mine.

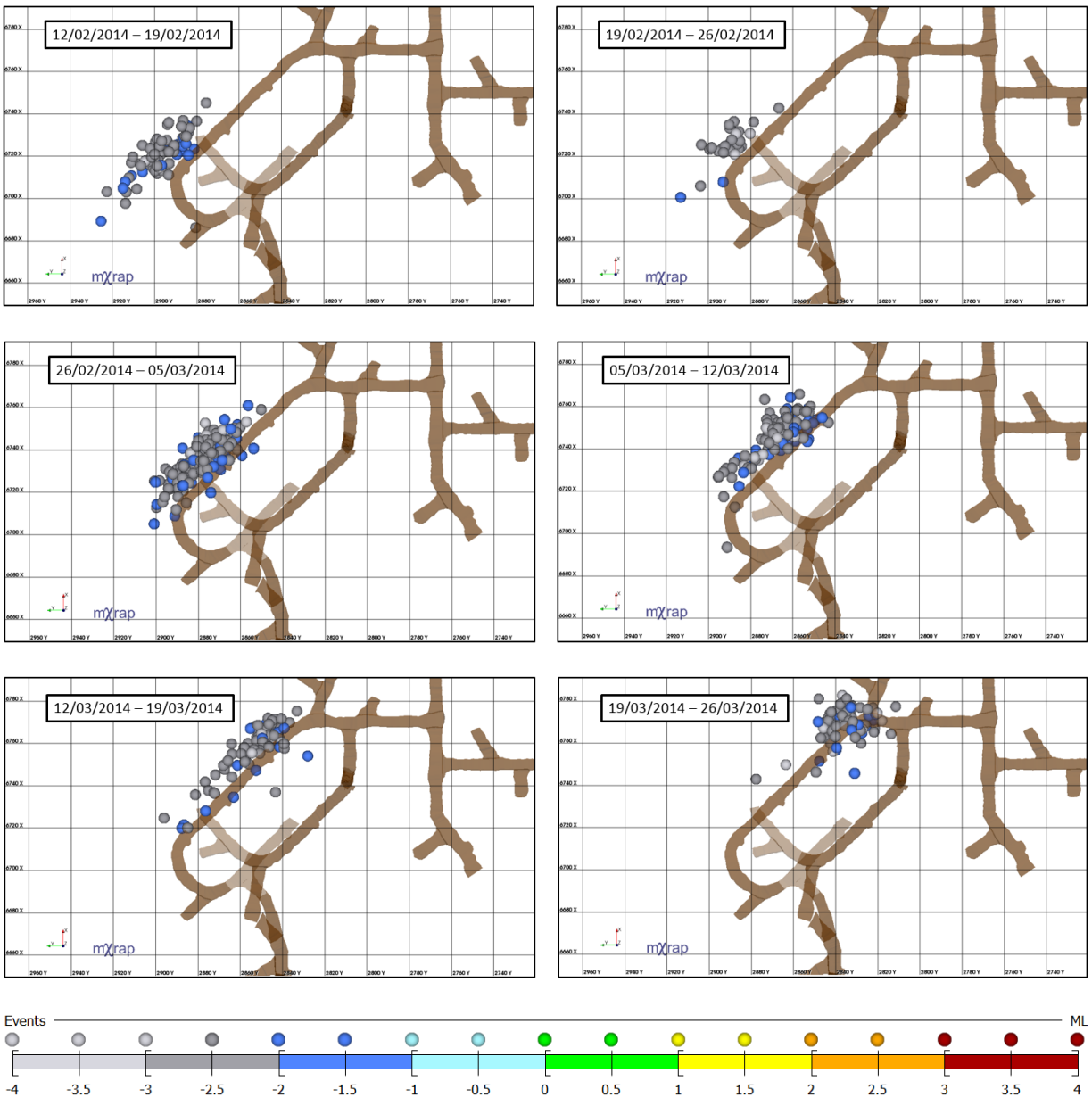

Figure 32: Seismic events plotted weekly during the development of a section of ramp at LaRonde mine.

The progression of seismic events in Figure 31 and Figure 32 coincides with development blasting of the ramp. Events are located in close proximately to the excavation with very few events $M_L > -1$. Figure 34 is a Magnitude-Time History chart for all seismic events shown in Figure 31 and Figure 32. Red icons along the x-axis corespond to local development blasts.

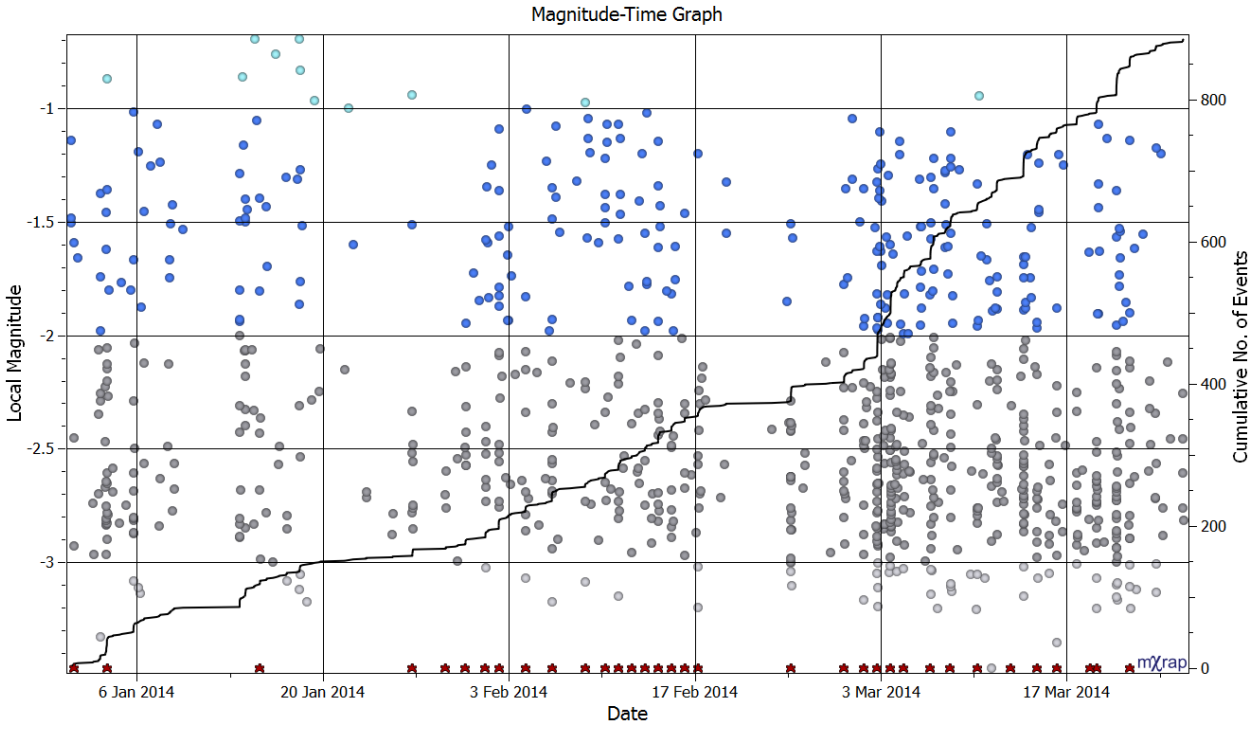

Figure 33: Magnitude-Time History chart for all seismic events shown in Figure 31 and Figure 32. Red icons along the x-axis represent development blasts and event colour variations correspond to Local magnitude values.

No large events ($M_L \geq 0$) occur throughout the development shown in Figure 31 and Figure 32. Periods of reduced seismic activity can be observed between blasts using a Magnitude-Time History chart (Figure 33). The "steps" shown in the cumulative number of events correspond directly to development blasting. Periods of reduced seismic activity between successive development blasts, such as seen from approximately Fed 20 to Feb 25, indicate the occurrence of events is strongly correlated to blasting. Out of the total 885 events recorded during the time period, only 1.2% (11 events), are $M_L > -1$. Figure 34 is a frequency-magnitude chart for the same population of events shown in Figure 33.

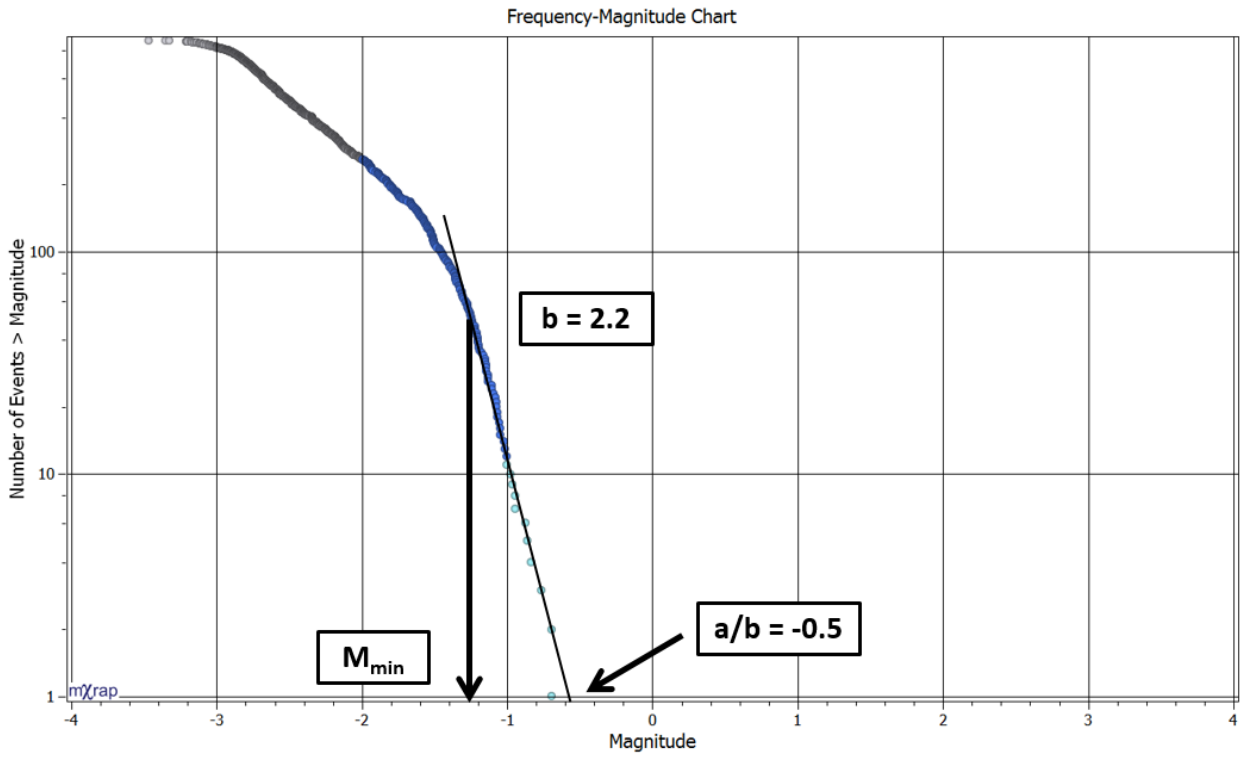

Figure 34: Frequency-Magnitude chart for all seismic events shown in Figure 31 and Figure 32. Colour variations correspond to Local magnitude values.

The large b-value (2.2) in Figure 34 indicates this seismic population consists primarily of volumetric fracturing events. The largest expected event (a/b) for this population is approximately M_L = -0.5. This chart characterizes a relatively low hazard seismic population that is unlikely to generate large seismic events. This is considered a normal response to mining at LaRonde.

An abnormal seismic response to mining is typically characterized by the presence of large seismic events ($M_L \geq 0$) and consequently elevated seismic hazard. Figure 35 is a plan view of 242 Level at LaRonde showing all seismic activity.

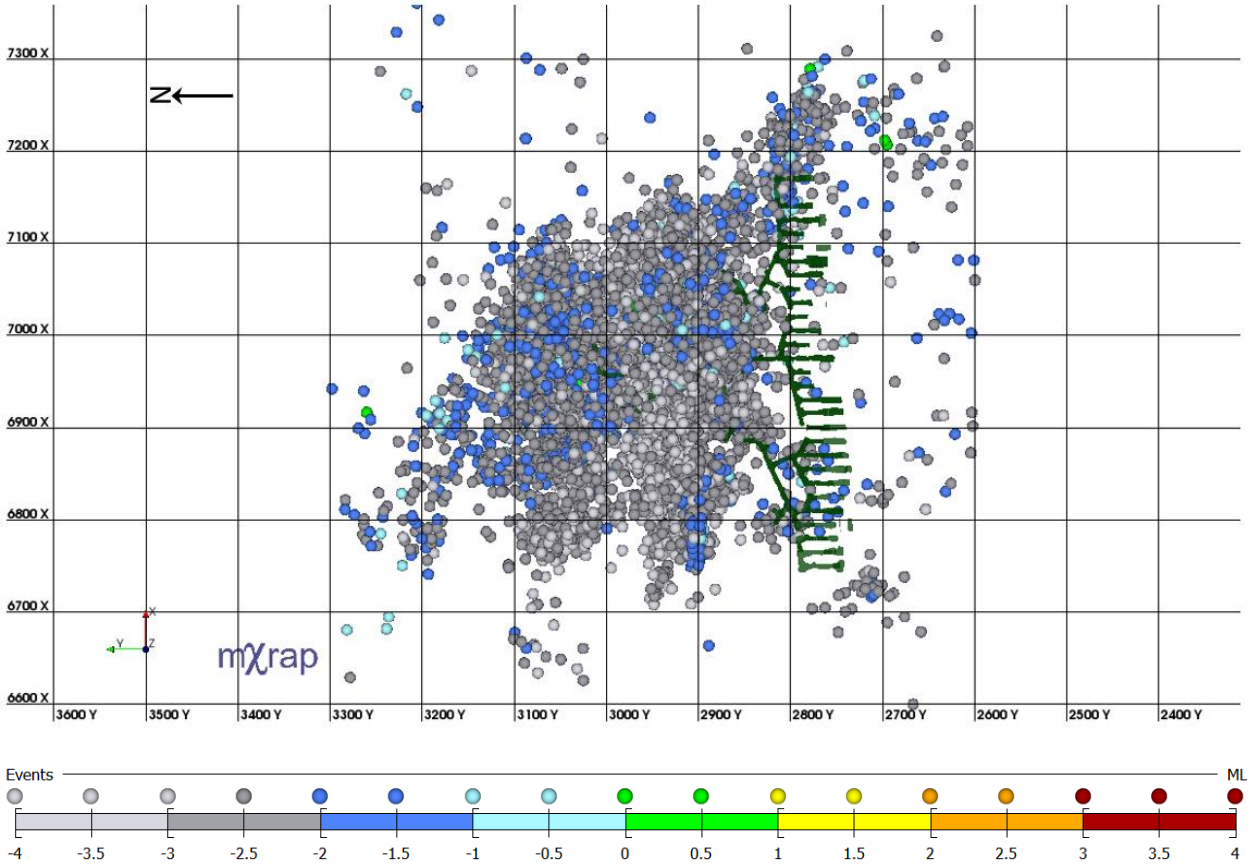

Figure 35: Plan view of a 242 Level at LaRonde mine showing all seismic activity.

A large volume of small events, typically associated with a normal response to mining, can be observed in Figure 35. In addition to these events there is a significant quantity of large events throughout the level. Figure 36 is a plan view of 242 Level at LaRonde showing only large seismic events ($M_L \geq 0$).

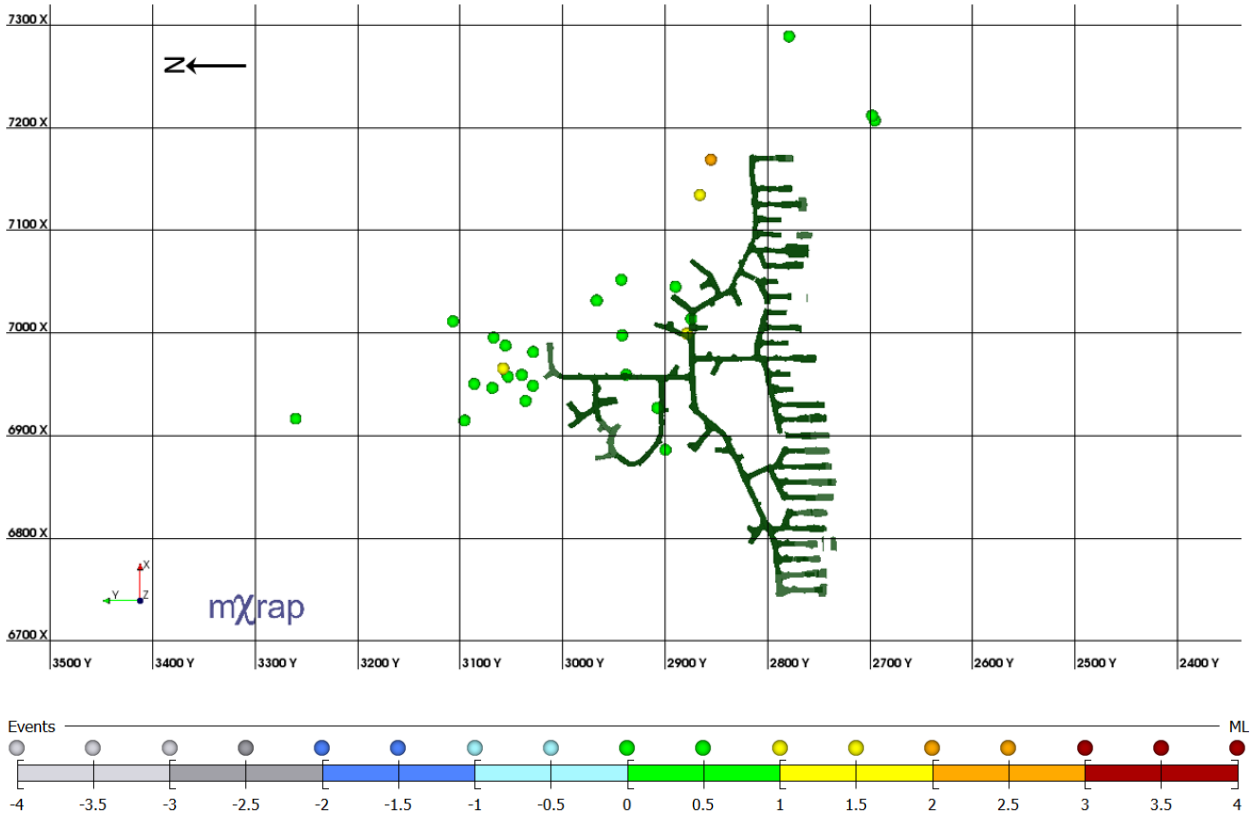

Figure 36: Plan view of 242 Level at LaRonde showing only events $M_L \geq 0$.

The presence of large seismic events on this level indicates an abnormal seismic response to mining. Large events are concentrated in the FW and Eastern portion of the orebody. These regions may correspond to high stress and/or unfavourable geological conditions contributing to elevated seismic hazard. Figure 37 is a Magnitude-Time History chart for all seismic events shown in Figure 35.

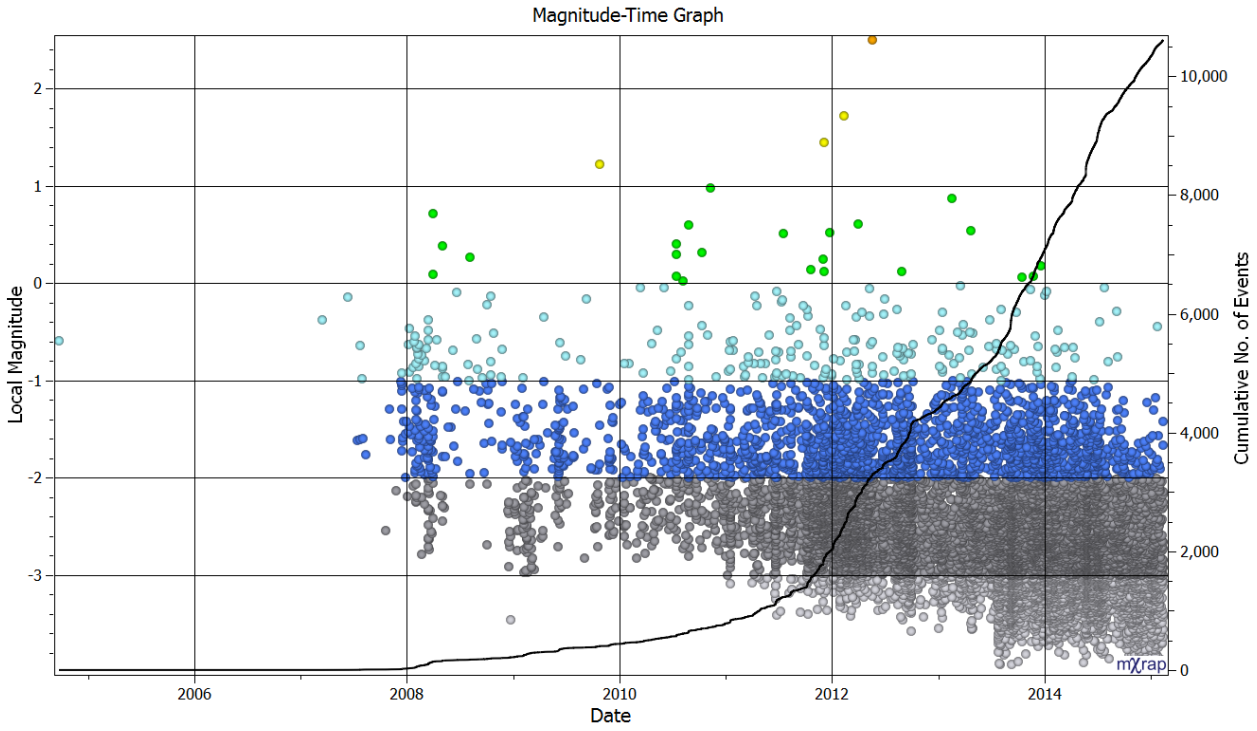

Figure 37: Magnitude-Time History chart for all seismic events shown in Figure 35. Colour variations correspond to Local magnitude values.

A clear contrast exists between the Magnitude-Time History chart for a normal (Figure 33) and an abnormal (Figure 37) response to mining at LaRonde. The abnormal response to mining contains a significant quantity of large events and shows no clear influence from blasting on the cumulative number of events line. This indicates a large portion of seismic activity is being driven by processes and mechanisms not directly related to local blasting. Large seismic events are typically characterized by a fault-slip source mechanism. Figure 38 is a frequency-magnitude chart for all seismic events shown in Figure 37.

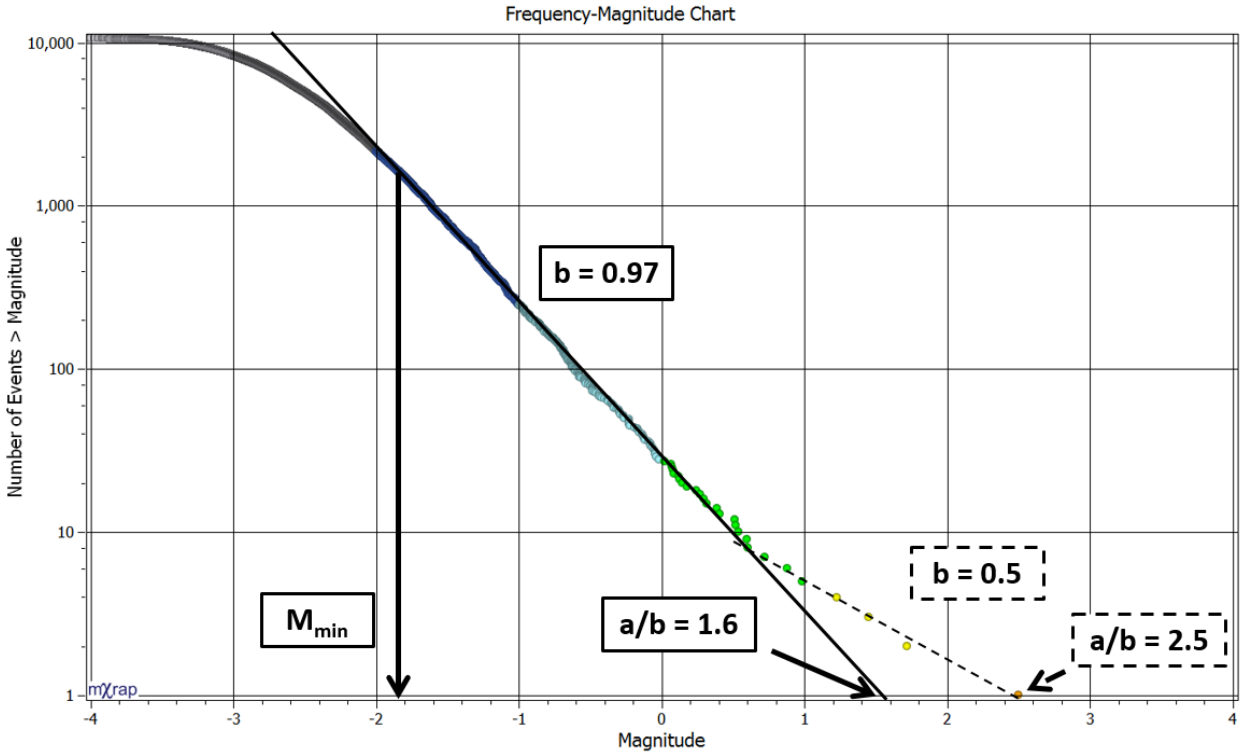

Figure 38: Frequency-Magnitude chart for all seismic events shown in Figure 35. Colour variations correspond to Local magnitude values.

There is a clear differentiation between the normal and abnormal seismic response within the population seen in Figure 38**.** The majority of seismic events represent a normal response to mining – small volumetric fracturing events. These events are contained within the population characterized by the solid black line. The b-value for this line is 0.97, indicating a well behaved seismic population, with a largest expected event of M_L = 1.6. A secondary population, consisting of the largest events, is characterized by the dashed black line. The b-value of this line is 0.5, indicating a fault-slip source mechanism. The largest expected event for this population is M_L = 2.5, which is equivalent to the largest event within the population. This population of events represents a significantly higher seismic hazard and an abnormal response to mining.

A normal seismic response to mining at LaRonde consists of small seismic events (typically $M_L \leq -1$) driven by local mining processes (i.e. blasting). These are predominately volumetric

fracturing events and are commonly associated with low seismic hazard. An abnormal seismic response to mining at LaRonde is characterized by the presence of large seismic events ($M_L \geq 0$). These are usually characterized by a fault-slip source mechanism and are commonly associated with a high seismic hazard.

3.4.5 « Seismicity below 224 Level »

Mining below 224 Level consists primarily of the 245 and 269 pyramids. This region possessed good sensor coverage through development and production mining and is therefore an ideal area of interest for seismic investigation. Figure 39 is a longitudinal projection of 224 to 262 Level of LaRonde mine showing all large ($M_L \geq 0$) seismic events.

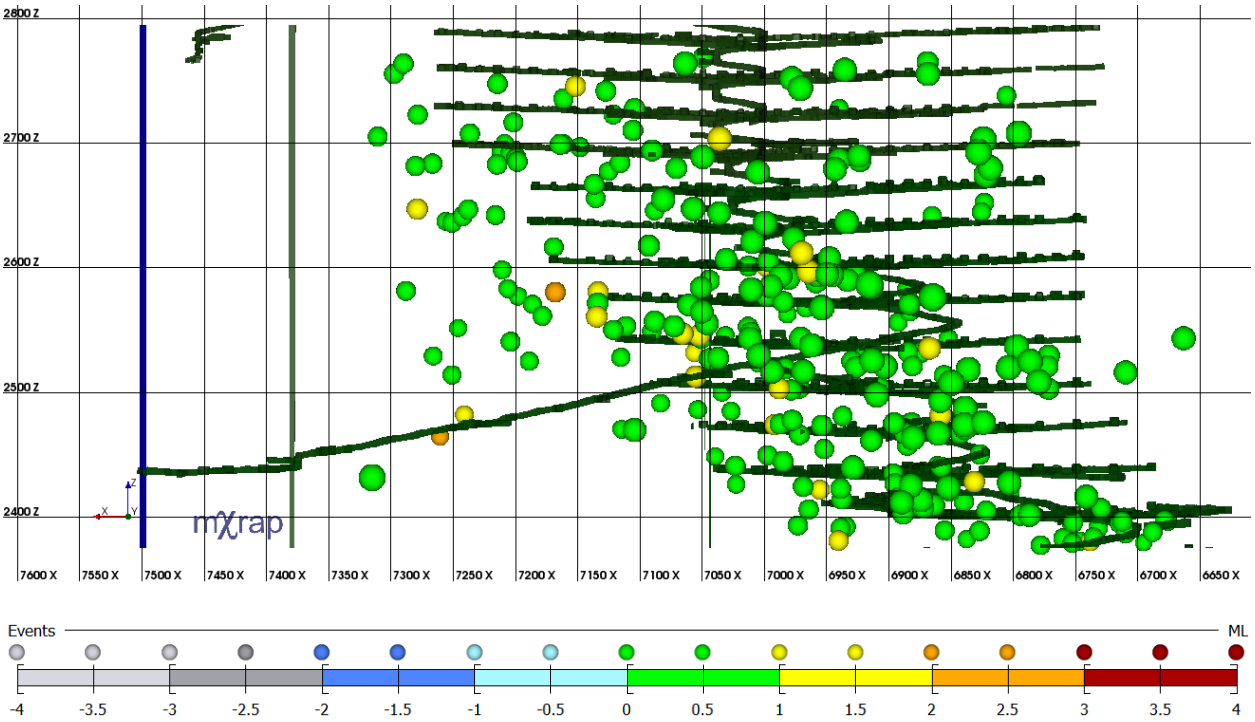

Figure 39: Longitudinal projection of 224 to 262 Level of LaRonde mine showing all large ($M_L \geq 0$) seismic events.

A large quantity of large seismic events have occurred within the area of interest (224 to 262 Level), predominantly in the FW. Figure 40 is a Magnitude-Time History chart for all events

occurring between 224 and 262 Level for LaRonde mine. This is the same chart that was previously analyzed in Section 2.4.2 « Magnitude-Time History ».

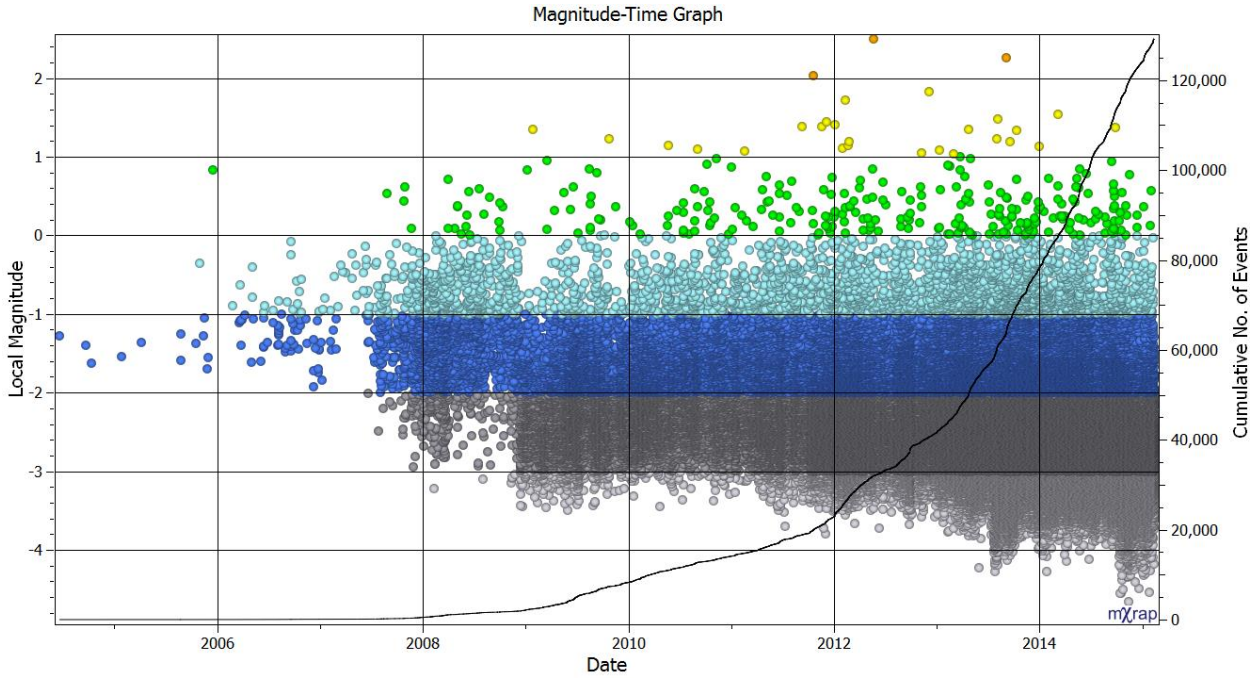

Figure 40: Magnitude-Time History chart for all events between 224 and 262 Level at LaRonde. Colour variations correspond to Local magnitude values.

Due to the change in system sensitivity over time at LaRonde, a lower magnitude bound for events considered in analysis must be determined. This is evident in Figure 40, which shows the smallest recorded event decreasing in magnitude over time. Using a value of M_L = -1.5, eliminates bias introduced from using data collected prior to the paladin installation. Figure 41 is a Magnitude-Time History chart for the same seismic population shown in Figure 40 but using a lower bound of $M_L \geq$ -1.5.

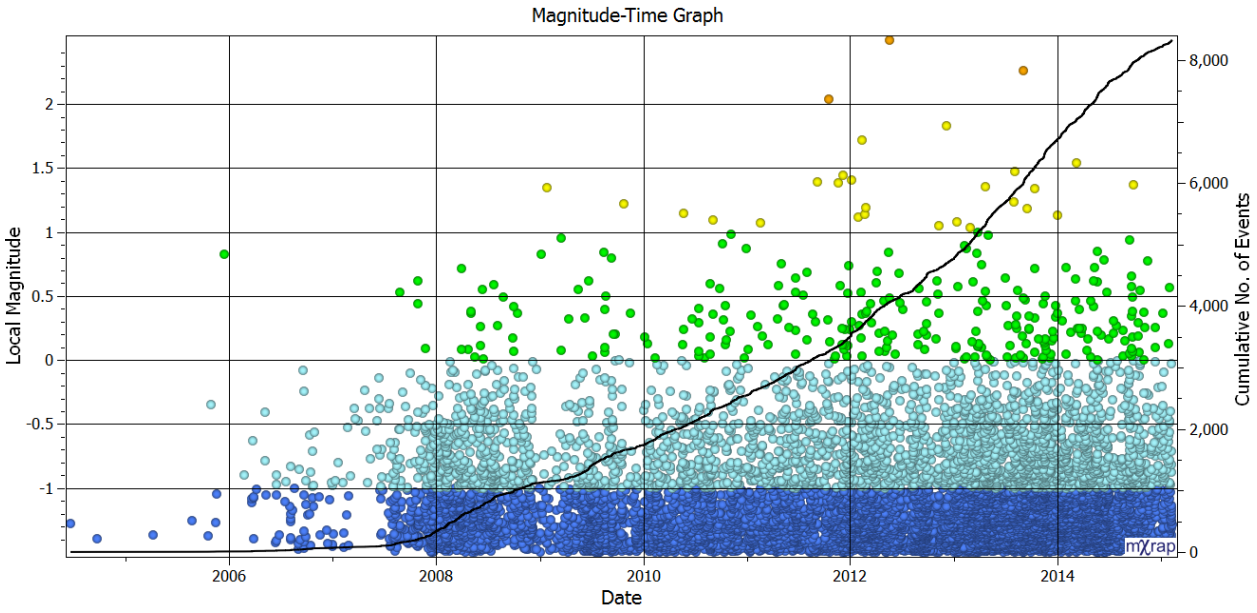

Figure 41: Magnitude-Time History chart for the same seismic data shown in Figure 40 using a magnitude cut off of -1.5. Colour variations correspond to Local magnitude values.

Using a lower bound of $M_L \geq -1.5$ enables trends in event rate and seismic hazard to be analyzed without the bias introduced from the Hyperion to Paladin conversion in late 2008. It also serves to minimize the impact of mining process seismic events (typically $M_L < -1$), while including sufficient data to identify precursory trends. Mining process events comprise the vast majority of the seismic database (in this case more than 90% of all events recorded). They are small events that are a direct product of stress fracturing caused by mining processes (i.e. blasting). Figure 42 is a frequency magnitude chart includes all events $M_L \geq -1.5$ occurring between 224 and 262 Level for LaRonde mine.

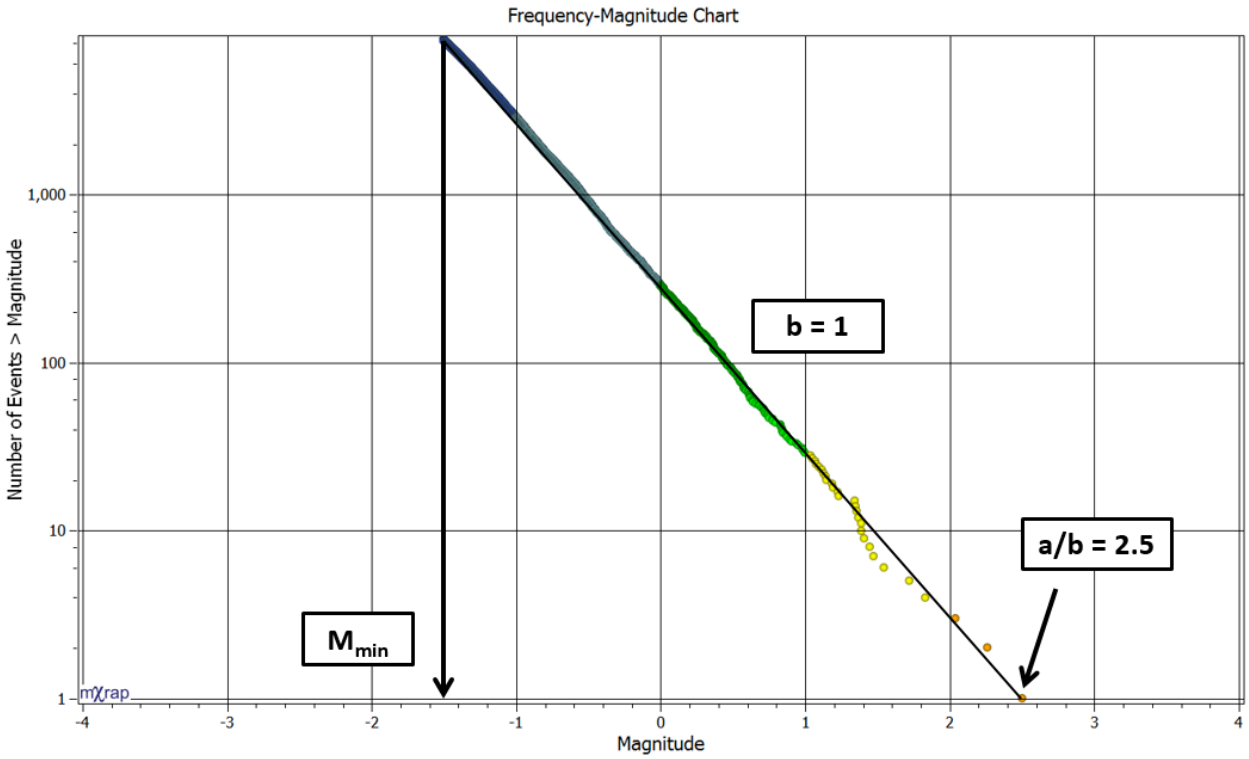

Figure 42: Frequency magnitude chart for all events $M_L \geq -1.5$ between 224 and 262 Level at LaRonde. Colour variations correspond to Local magnitude values.

Figure 42 validates the quality of the seismic population used for analysis based on the b-value of 1 and the linear relation throughout the entire population. This indicates that events of $M_L \geq -1.5$ have been reliably recorded by the seismic monitoring system for this area from the onset of development and through production. This is an essential component of the data quality check and reinforces that conclusions drawn from seismicity in the area of interest are founded on reliable and accurate data.

3.5 « Chapter Summary »

LaRonde mine is a bulk open stoping operation located in the Abitibi Greenstone Belt of Northern Quebec. Current mining extends more than 2,930 metres below surface with a daily production rate of 6,300 tonnes. The combination of complex local geology and high stress conditions results in regions of high seismic hazard with the possibility of rockbursting. Areas of elevated seismic hazard are commonly concentrated in the FW; corresponding to areas of hard/brittle rock and elevated stress resulting from stope sequencing forcing stresses to redistribute to the outskirts of the orebody.

Mining-induced seismicity at LaRonde has been recorded using an ESG microseimsic monitoring system since 2003. Seismicity from 224 to 262 Level is the focus of this thesis. This region has been selected primarily due to good seismic sensor coverage during development and production mining. In order to minimize bias from upgrades in seismic monitoring hardware and the influence of mining process events, a lower bound of $M_L = -1.5$ has been placed on the data. With this lower bound in place, the seismic data is well behaved and reliable for drawing meaningful conclusions.

Chapter 4

4 « Methodology for Hazard Assessment »

The 224 Level to the 262 Level was selected as the area of investigation for this research as it possessed good seismic sensor coverage throughout development and production mining. The objective of this methodology is to proactively forecast seismic hazard using apparent stress measurements for a range of seismic populations possessing varying degrees of hazard (high, moderate and low). For the purposes of this thesis, high seismic hazard is defined as the presence of large and potentially damaging seismic events ($M_L \geq 0$). This is similar to Butler (1997), who noted a greater likelihood of rockburst damage for events with a magnitude greater than Richter 1. Moderate hazard is defined as a lack of potentially damaging events ($M_L \geq 0$), but an abnormal response to mining reflected in the presence of events of magnitude $M_L \geq -0.5$. Low hazard is defined as essentially no large events and no quantifiable abnormal response to mining – only events $M_L < -0.5$. Sample populations were selected to represent both normal and abnormal seismic response in the area of interest. These populations were then assessed for levels of seismic hazard over varying time periods.

This methodology chapter:

- Introduces the 50 test and control populations from LaRonde used for analysis in this thesis.
- Discusses high, medium and low seismic hazard evaluation of the seismic populations.
- Introduces the apparent stress ratio (ASR) methodology.

- Discusses the periods of seismic hazard evaluation in the context of the 50 populations used in this thesis.
- Introduces an apparent stress ratio time history analysis for seismic hazard evaluation.
- Discusses ASR as a potential tool for identifying elevated seismic hazard.

4.1 « Sample Populations »

A total of 50 sample populations were selected to analyze the effectiveness of using apparent stress measurements in assessing seismic hazard. Test and control population were selected in order to analyze areas of varying hazard. Test populations refer to those that contain large seismic events and are consequently considered to reflect high seismic hazard. Within these populations an abnormal seismic response to mining activities is expected. Control populations refer to those that do not contain large seismic events. They represent both moderate and low seismic hazard and often reflect a normal seismic response to mining activities.

Sample populations were generated using a central point and a search radius. For test populations central points were selected from large magnitude events. Central points for control populations were created on an equally spaced grid of 50 m. Sample population consists of all seismic events within the search radius from the central point. A constant search radius of 30 m was used for the generation of both test and control populations. This value (30 m), was selected as it lends itself well to mine wide application, i.e. the methodology could be used to investigate all of the seismicity in the mine. With a sublevel spacing of 25-30 m, using points along current excavations, a 30 m search radius generates populations including all seismicity up to the level above and below. Similar results of hazard assessment are found when the search radius is increased and decreased, as discussed later in this thesis in 5.5 « Discussion of Search

Radius ». The choice of test and control populations was intended to demonstrate that the proposed methodology would be a reliable means of forecasting seismic hazard over varying sizes of seismic populations and intensities of seismic response.

4.1.1 « Test Populations »

Test populations are representative of areas of high seismic hazard. They were specifically chosen as they contain large magnitude seismic events ($M_L \geq 0$) and are relatively close to mine workings. The current ground control program at LaRonde specifies mine workings are only restricted if a protocol event ($M_L \geq -0.8$) occurs within 20 m of the workings. With a 30 m search radius used to generate the sample populations, 50 m is the largest distance a central point can be located away from excavations and still contain a seismic event that produces a seismic hazard related restriction. Test populations were therefore selected from the largest magnitude events located within 50 m of mine excavations. Areas of the rock mass that generate the largest events should represent the areas with the highest seismic hazard, and consequently are the areas of most interest. Large events must also contain a reasonable quantity of preceding seismic events within the 30 m search radius to be considered a valid test population. With insufficient preceding seismicity, it is unreasonable to assume any parameters can be used to forecast seismic hazard from precursory trends. The test population selection process ignores large events that are distant from mine excavations and have a very small number of nearby events. Table 5 summarizes the 25 events selected as central points for the generation of sample test populations.

Table 5: Summary of 25 large seismic events selected as central points for test populations.

ID	Date/Time	Location X	Location Y	Location Z	Local Magnitude	Apparent Stress (Pa)	Moment (N·m)	Energy (J)	S:P
1	2013/09/16 15:06:17	7068	2955	2547	1.79	8.99E+05	9.84E+09	2.23E+05	47.69
2	2013/08/04 10:03:38	7053	2945	2546	1.47	1.62E+06	1.50E+10	6.14E+05	14.68
3	2009/01/24 22:03:58	7153	2886	2746	1.35	2.17E+05	2.95E+11	1.62E+06	3.38
4	2013/10/12 11:12:24	6832	2967	2428	1.34	1.52E+06	3.17E+10	1.21E+06	5.58
5	2013/08/01 10:28:20	6956	2828	2422	1.23	2.27E+06	2.68E+10	1.54E+06	3.26
6	2009/10/23 21:13:40	6999	2880	2601	1.22	1.73E+05	7.77E+11	3.40E+06	0.65
7	2013/12/31 10:07:49	6993	2867	2474	1.13	4.72E+05	1.08E+11	1.28E+06	3.70
8	2012/01/30 01:48:22	6989	2915	2503	1.11	5.94E+05	1.06E+10	1.60E+05	2.50
9	2013/01/10 21:30:39	6739	2867	2381	1.08	3.30E+05	1.08E+11	8.97E+05	10.55
10	2012/11/08 18:33:32	6941	2868	2381	1.05	2.64E+05	3.19E+11	2.13E+06	1.13
11	2013/03/25 16:32:24	6999	2839	2450	0.99	3.60E+05	1.94E+10	1.77E+05	5.86
12	2013/02/08 18:27:13	6708	2880	2373	0.90	1.31E+06	8.68E+09	2.87E+05	13.78
13	2013/02/15 01:54:53	7052	2944	2584	0.87	3.63E+05	6.59E+09	6.03E+04	13.92
14	2014/05/23 00:56:39	6875	2863	2532	0.85	2.68E+05	4.44E+10	3.00E+05	19.13
15	2009/08/13 11:30:36	7291	2854	2764	0.84	6.87E+05	3.53E+10	6.13E+05	6.30
16	2012/05/16 18:17:45	6930	2940	2525	0.84	2.80E+05	7.31E+10	5.17E+05	9.02
17	2013/03/24 02:58:20	6963	2869	2403	0.84	2.67E+05	1.26E+10	8.46E+04	5.47
18	2009/01/05 16:26:37	7215	2850	2748	0.83	1.27E+05	2.08E+11	6.67E+05	2.95
19	2008/04/11 20:43:39	7067	3078	2792	0.81	7.45E+05	2.57E+07	4.91E+02	51.50
20	2009/09/10 22:14:17	7237	2835	2708	0.80	1.99E+05	1.29E+11	6.47E+05	2.78
21	2011/12/27 04:54:00	6986	2924	2573	0.73	1.96E+07	1.68E+10	8.30E+06	10.13
22	2014/02/02 11:27:21	6843	2881	2472	0.72	1.35E+06	1.04E+10	3.53E+05	8.83
23	2013/10/12 01:35:14	6896	2903	2427	0.71	5.93E+05	9.25E+09	1.38E+05	14.43
24	2011/08/03 02:04:45	7279	2839	2723	0.69	5.21E+05	1.02E+10	1.34E+05	6.46
25	2012/06/22 01:50:54	6908	2874	2504	0.68	1.96E+05	2.70E+10	1.33E+05	4.15

The test populations contain 93% (27 out of 29) of the largest events in the area of interest within 50 m of an excavation. The two large events not included contain only a single other event within the 30 m search radius and were therefore deemed as unable to be identified with precursory trends. Between the 224 and 262 Level, 38% (55 out of 146) of all events $M_L \geq 0$ located within 50 m of an excavation are contained in the test populations. Accounting for over a third of all potentially damaging seismic events within 25 test populations reinforces that areas of seismic hazard are concentrated throughout the rock mass and it may be possible to identify trends in seismic hazard.

Figure 43 and Figure 44 provide a visual representation of the locations for test population central events.

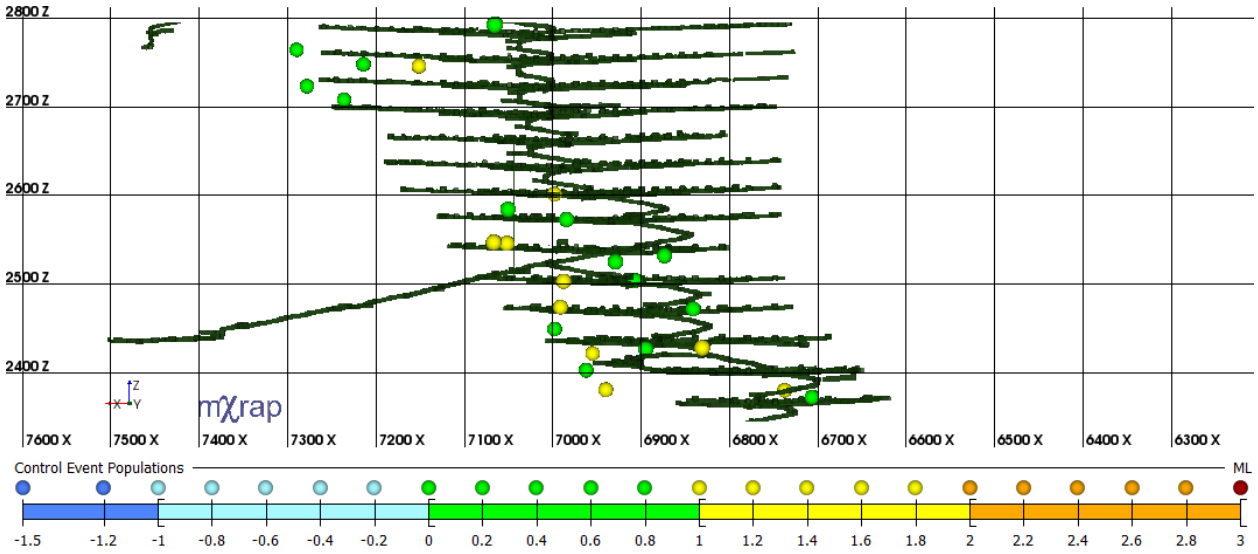

Figure 43: Longitudinal projection looking south of LaRonde showing events selected for test populations - coloured by Local magnitude.

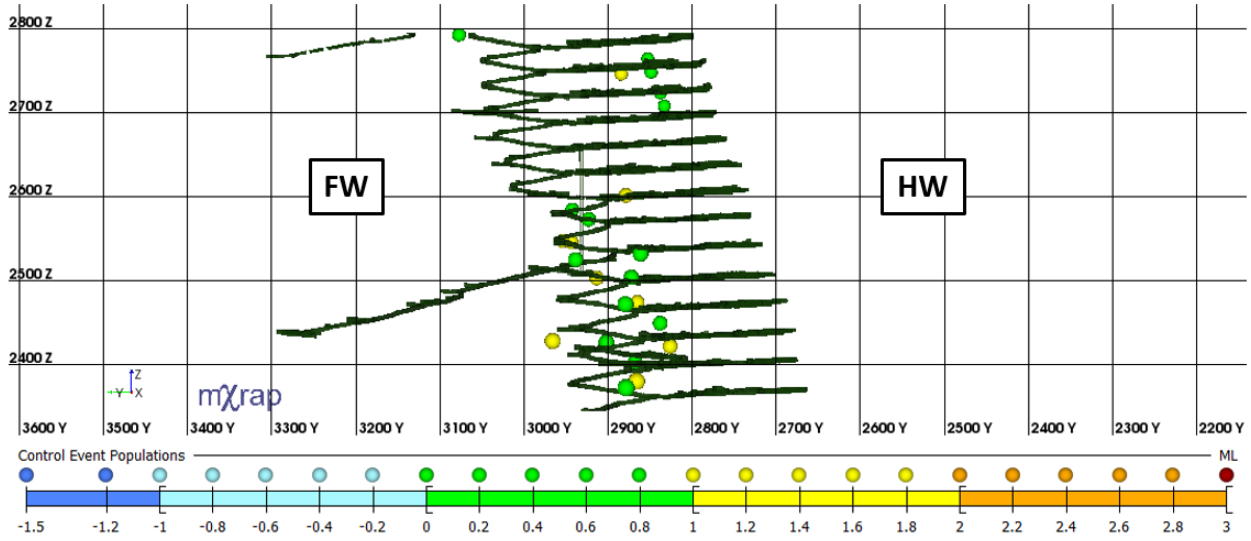

Figure 44: Cross-sectional projection looking east of LaRonde showing events selected for test populations - coloured by Local magnitude.

Test populations are predominately concentrated in the FW. With 93% of the largest events included in populations generated from these central points, the test populations represent virtually all of the large events near excavations, in this section of the mine.

4.1.2 « Control Populations »

Control populations are representative of areas of moderate or low seismic hazard. Similar to the test populations, they were generated using a central point and a 30 m search radius. In order to ensure there was no bias in the selection of central points, a grid was placed over the entire area of interest. An equally spaced grid of 50 m minimizes the overlap of seismicity in populations generated from adjacent grid points. Each grid point was used as a central point to generate a seismic population using the 30 m search radius. Any populations containing events $M_L \geq 0$ or located farther than 50 m from excavations were eliminated. The 25 grid points with the largest number of seismic events within the search radius were selected as central points to generate control populations. In cases where adjacent grid points were both selected as control populations, the one with the lower number of events was eliminated. This process endeavours to identify control populations that are representative of the entire area of interest.

While all control populations contain only seismic events less than $M_L = 0$, this on its own is not indicative of low seismic hazard. Forecasting seismic hazard requires the ability to identify populations with elevated hazard prior to the occurrence of a large seismic event. In such cases, where the large event has not yet occurred but there is an abnormal seismic response to mining, the hazard level is referred to as moderate.

In order to quantify what constitutes an abnormal seismic response to mining in the absence of a large event, a cumulative distribution of Local magnitude for all 2093 of the macroseismic events contained within the 50 sample populations (test and control populations) was used. In order to minimize the influence of mining processes events, only macroseismic events ($M_L \geq -1$ or $M_R \geq 0$) are considered.

In Figure 45, the 90th percentile corresponds to Local magnitude 0.0. Populations containing events of this size or greater will be considered representative of high hazard (the test populations). The 70th percentile corresponds to a Local magnitude larger than -0.5. Populations containing events greater than or equal to this size but less than magnitude zero will be considered representative of moderate hazard. Any populations that contain only events $M_L < -0.5$ will be considered representative of low hazard.

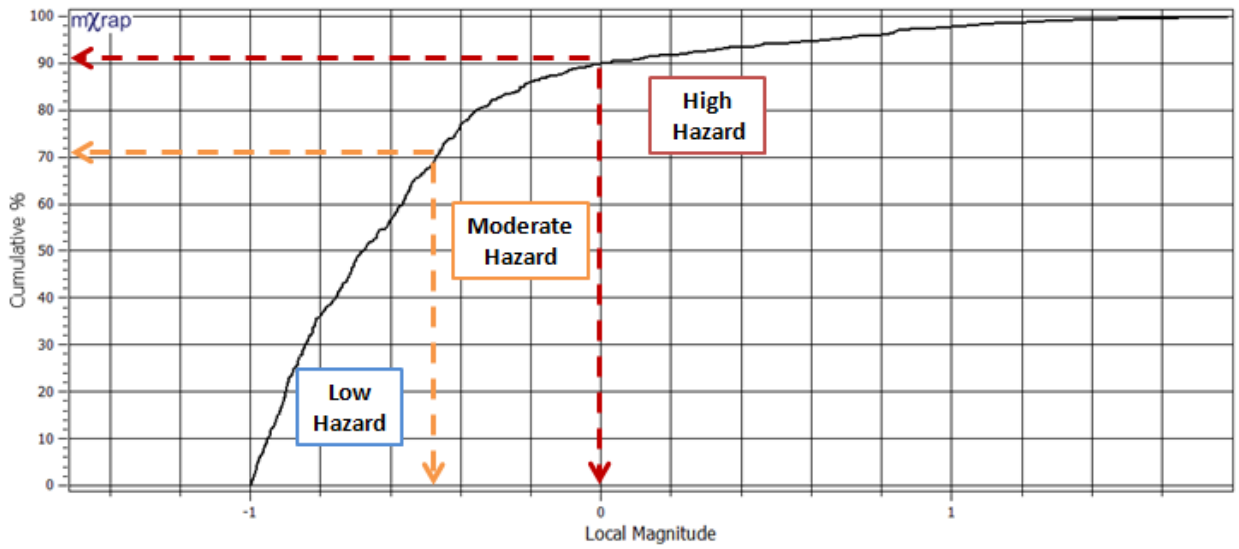

Figure 45: Cumulative distribution of Local magnitude for all events $M_L \geq -1$ contained within the 50 sample populations of the area of interest at LaRonde. Magnitude regions corresponding to low, moderate, and high hazard are labeled.

Each of the control populations is designated as moderate or low seismic hazard based on the largest event contained within the population. Table 6 summarizes the 25 grid point locations selected as central points for the generation of control populations.

Table 6: Summary of events selected as central points for control populations.

ID	Location X	Location Y	Location Z	Number of Events	Largest Event (M_L)	Seismic Hazard
26	6950	3000	2522	100	-0.38	Moderate
27	6700	2850	2422	98	-0.11	Moderate
28	6950	3100	2722	68	-0.53	Low
29	7100	2950	2722	61	-0.42	Moderate
30	7050	2900	2622	41	-0.03	Moderate
31	7050	3050	2672	35	-0.25	Moderate
32	6950	2900	2622	34	-0.40	Moderate
33	7200	2850	2722	34	-0.19	Moderate
34	6950	2900	2522	29	-0.37	Moderate
35	6850	2900	2522	27	-0.36	Moderate
36	6800	2700	2372	26	-0.16	Moderate
37	6950	3000	2622	23	-0.50	Moderate
38	6800	2850	2372	21	-0.07	Moderate
39	6950	2800	2472	18	-0.93	Low
40	6950	2900	2422	17	-0.09	Moderate
41	6850	2900	2622	15	-0.29	Moderate
42	7100	2850	2672	15	-0.31	Moderate
43	6850	2950	2372	14	-0.42	Moderate
44	6700	2700	2372	13	-0.60	Low
45	6950	3050	2722	13	-1.10	Low
46	7100	3050	2722	13	-0.55	Low
47	6950	2800	2722	12	-0.32	Moderate
48	7050	3000	2522	12	-0.02	Moderate
49	6950	2900	2722	11	-0.68	Low
50	6850	3000	2472	10	-0.20	Moderate

Six populations contain only events less than Local magnitude -0.5 and are representative of low seismic hazard. All other control populations contain events with Local magnitudes between the 70^{th} and 90^{th} percentile values and are therefore representative of moderate seismic hazard. A larger number of moderate hazard populations is expected as the majority of low hazard seismic regions within the area of interest at LaRonde do not contain sufficient quantities of seismic events $M_L \geq -1.5$. Seismic activity in these areas would be composed nearly entirely of mining processes events and are therefore underrepresented in this analysis.

Figure 46 and Figure 47 provide a visual representation of the central locations for the control populations. Populations of moderate and low seismic hazard are represented by orange and blue spheres respectively.

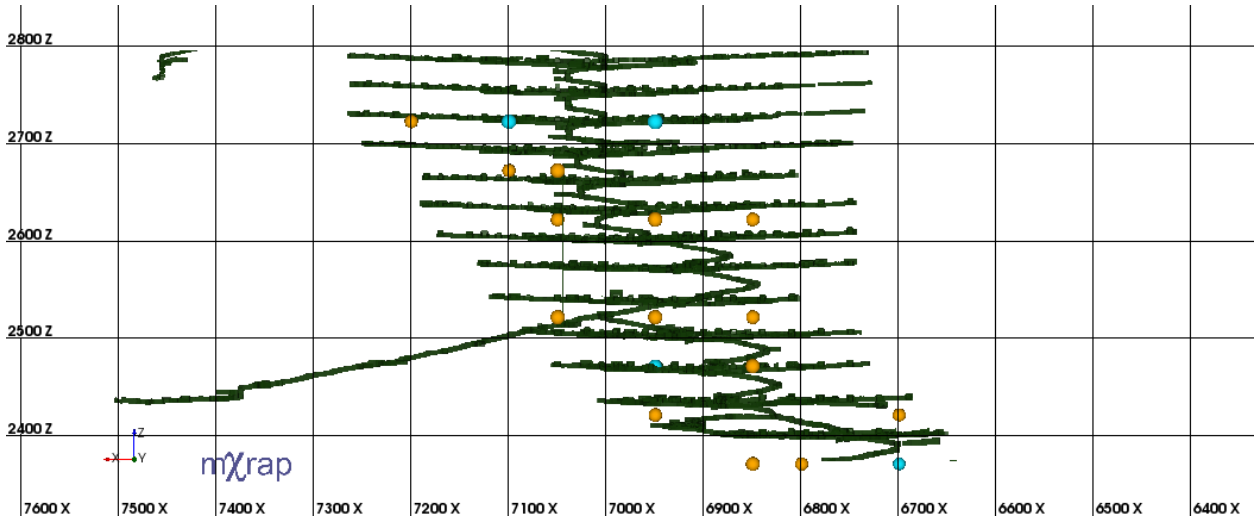

Figure 46: Longitudinal projection looking south of LaRonde showing central locations selected for control populations. Low and moderate seismic hazard points are shown in blue and orange respectively.

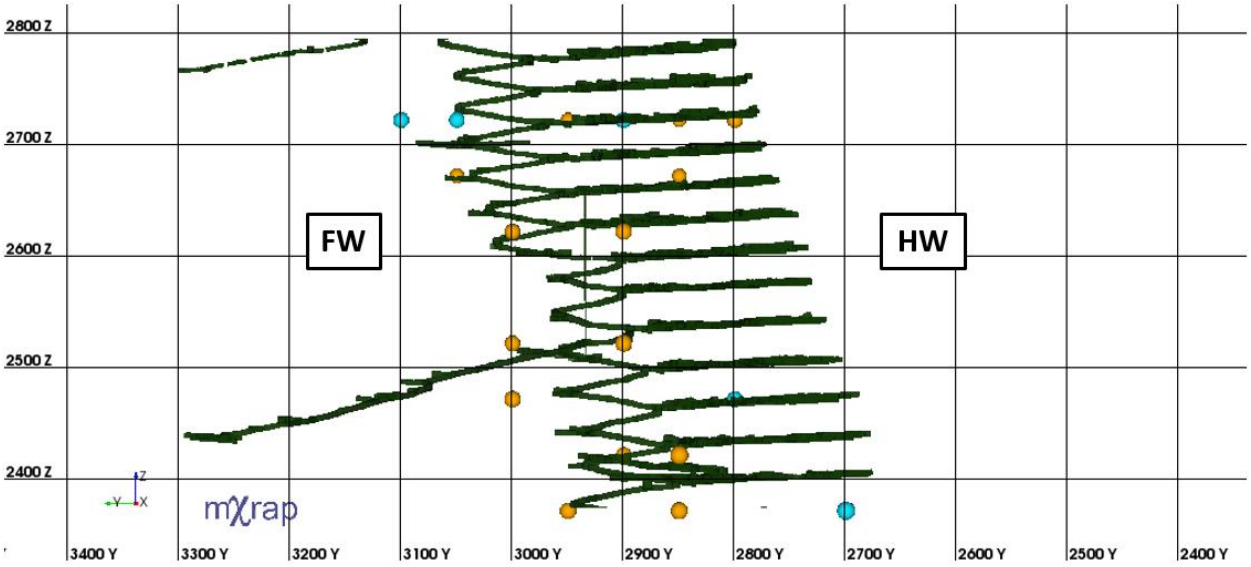

Figure 47: Cross-sectional projection looking east of LaRonde showing central locations selected for control populations. Low and moderate seismic hazard points are shown in blue and orange respectively.

Control populations are dispersed representatively throughout the area of interest without bias, for regions of both low and moderate seismic hazard. The populations generated from these

locations are used to demonstrate that seismic hazard forecasted using apparent stress can be applied to various hazard levels and is not solely successful for identifying high hazard populations.

4.2 « Hazard Assessment »

The primary factor for hazard assessment in this methodology is the seismic source parameter apparent stress. High apparent stress values are indicative of increasing stress conditions within the rock mass (Mendecki, 1993). For different mines, determining what constitutes high apparent stress can vary greatly with changes in geological and stress conditions. Current methods that utilize apparent stress for hazard assessment, such as ASTH, select an arbitrary single threshold value to represent high apparent stress. There are disadvantages in using this approach, as it needs to be customized to represent changes in local rock mass conditions. What may be high apparent stress for one mine, or a region within a mine, may be moderate or even relatively low apparent stress for another mine or region.

Figure 48 is a cumulative distribution of apparent stress for two different mines. One mine is representative of rock with a high uniaxial compressive strength (UCS) and is being mined at depths greater than 1500 m. The second mine is representative of rock with a low UCS and is being mined at depths less than 800 m.

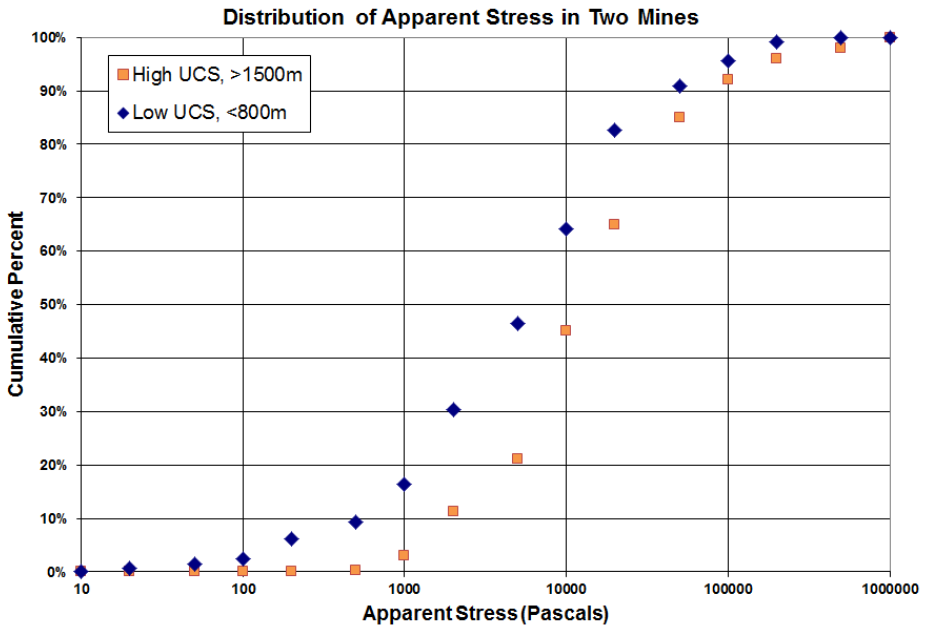

Figure 48: Apparent stress distributions for a mine representative of high UCS and mining at depths greater than 1500 m and a mine representative of low UCS and mining at depths less than 800 m (Hudyma 2014).

A significant difference is evident in the apparent stress distributions of the two mines. The mine with a higher UCS and mining depth (high stress), has larger apparent stress values relative to the mine with a lower UCS and mining depth (low stress). To apply a singular threshold value to both mining environments, meant to be indicative of high apparent stress, would not be meaningful.

Stress conditions increase with depth and can result in large variations in what is considered high apparent stress within a single mine. Figure 49 depicts apparent stress distributions for events from varying levels at LaRonde mine.

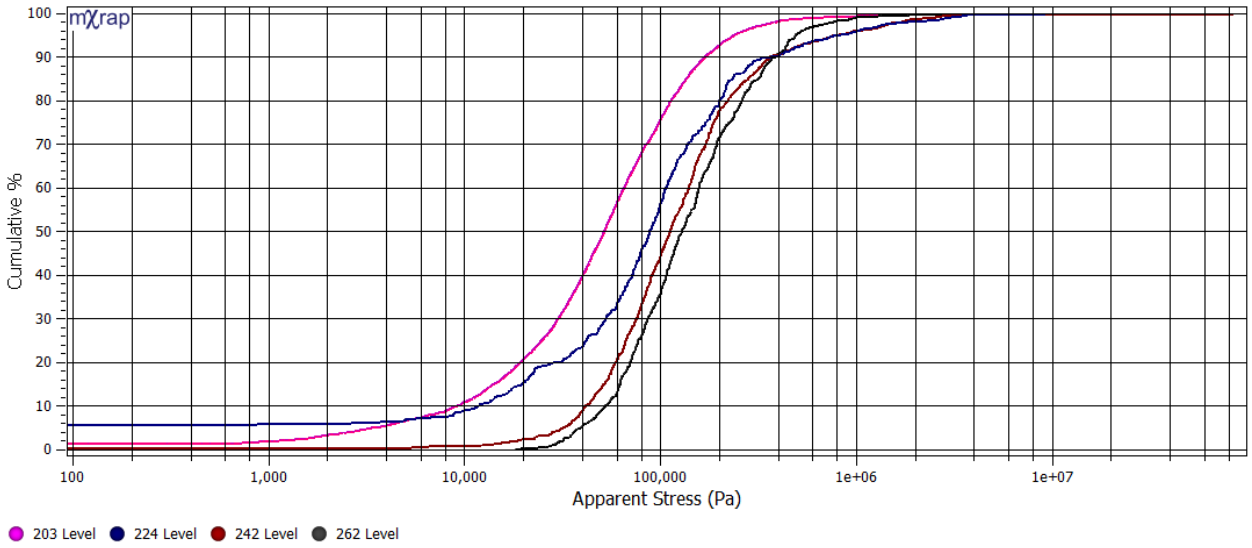

Figure 49: Apparent stress cumulative distributions for 203, 224, 242, and 262 Level at LaRonde.

Figure 49 demonstrates the variations in apparent stress between different levels at LaRonde - 203 Level is approximately 2030 metres below surface and 262 Level is approximately 2620 metres below surface. As the depth of mining increases, the AS distribution shifts to the right. The 50th percentiles for the 203, 224, 242 and 262 Levels are 55 kPa, 87.7 kPa, 111.8 kPa, and 127.8 kPa respectively. With such large variation contained within a single mining sector, it is clear single value thresholds cannot be reliably applied across large regions - even within a single mine. In order to overcome this limitation, apparent stress will be analyzed using a relative ratio. This will allow the seismic response to local stress and geological conditions to be compared relative to itself.

4.2.1 « Apparent Stress Ratio (ASR) »

The intent of apparent stress ratio (ASR) is to identify increasing apparent stress within a seismic population as a proxy for increasing stress conditions within a rock mass. For any given population the ASR value is calculated as the ratio of the apparent stress 80th percentile to the 20th percentile for a cumulative distribution.

$$\text{ASR} = \frac{\text{AS}_{80}}{\text{AS}_{20}}$$

where,

AS_{80} = Apparent Stress 80th Percentile

AS_{20} = Apparent Stress 20th Percentile

Example Calculation:

Using the AS distribution shown in Figure 49 for the 224 Level, the 20th and 80th percentiles are approximately 30 kPa and 199 kPa respectively.

$$\text{ASR} = \frac{199\ \text{kPa}}{30\ \text{kPa}}$$

$$\text{ASR} = 6.6$$

Considering all seismic events located near 224 Level, the ASR value for the population is 6.6.

A high ASR suggests that the apparent stress is relatively high within the population and that local stress conditions are high and increasing within the rock mass. A low ASR suggests that the apparent stress is relatively constant or decreasing within the population and that local stress conditions are constant. By using the 20th and 80th percentile values, the majority of the distribution can be considered while minimizing the impact of a few anomalously high or low apparent stress events. The concept of apparent stress ratio is similar to the uniformity co-efficient in soil mechanics, which is used to quantify variations in a particle size distribution.

Using the test populations, ASR values prior to the occurrence of large events will be analyzed to identify trends and compared against ASR values of the control populations. The ASR value

associated with each event is calculated by including itself in the computation. For forecasting purposes, the ASR values preceding a large event will be analyzed.

The apparent stress distribution for all events $M_L \geq -1.5$ in the area of interest is shown in Figure 50.

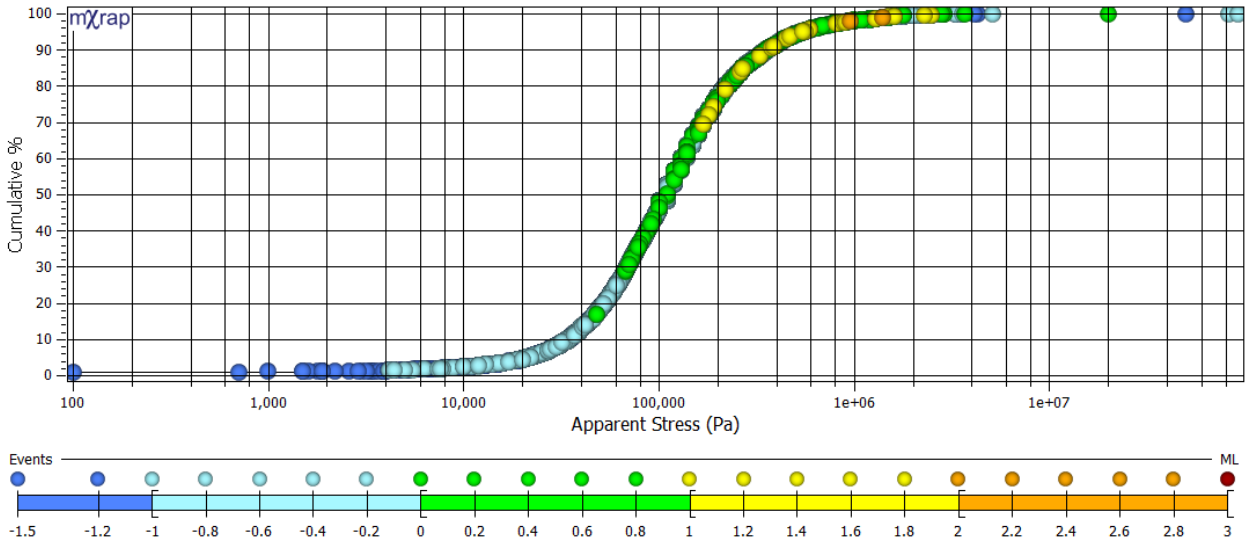

Figure 50: Apparent stress distribution for all events occurring at LaRonde within the area of interest $M_L \geq -1.5$.

Figure 50 depicts the scale dependence of apparent stress. Smaller magnitude events are concentrated at lower AS values, with magnitude increasing as AS values increase. Very few outliers are contained within the data, reasserting the quality of the dataset used in this analysis.

An implicit assumption is that increasing stress conditions within a rock mass lead to rock mass instability and the occurrence of large seismic events. For seismic source mechanisms not related to increasing stress, apparent stress may be unrelated to the occurrence of large seismic events. Determining an uncharacteristically high ASR value to associate with elevated seismic hazard may depend on a number of factors. Potentially one of the most influential factors is the preceding time period over which the ASR value is calculated. Variations in the time periods

considered for calculation could provide insight into long, medium, and short term seismic hazard.

4.2.2 « Time Periods for Hazard Assessment »

Trends in seismic data can be analyzed over varying time periods. This methodology uses ASR to make an assessment of long, medium and short term seismic hazard. When a time period is selected, the ASR value for each event is calculated from only the preceding events contained within the specified time window. For example, assessing hazard using a window of 1 year would result in an ASR that only considers seismicity occurring within the preceding 365 days.

van Aswegen (2005) suggested varying time periods for seismic hazard assessment. Short term seismic hazard refers to hours and days, medium term refers to a monthly planning cycle, and long term refers to a time span that allows for changes in mine design in the order of a year (van Aswegan, 2005). For application of this methodology to LaRonde, short term will be defined as a week, intermediate term will be defined as a typical planning period of 3 months and long term as 1 year.

4.2.2.1 « Long Term Seismic Hazard Assessment using ASR »

Only considering events $M_L \geq -1.5$ in the calculation of ASR greatly reduces the impact from mining process events. Each time a mine blast is taken, many small events occur due to the stress change caused by the new excavation. These small events make up the majority of recorded seismic events and in this thesis are referred to as mining process events. While these events are indicative of where mining activities are taking place, they are often not related to hazardous seismic activity. When large quantities of these smaller magnitude events are included in ASR calculation, the 20^{th} percentile value of a population is lowered (as a result of large quantities of

small events with small AS values), which in turn generates high ASR values. Without including these events however, the total number of events contained within a population is greatly reduced, the time period between individual events increases and the ASR value of a population potentially decreases.

When ASR is calculated for long term seismic hazard, it includes a substantial number of events enabling longer term trends in the local rock mass stress conditions to be identified. For long term seismic hazard assessment, ASR values are calculated using a time window of the preceding year. The 20th and 80th percentile values used for the calculation of ASR are taken from an apparent stress distribution that only considers the seismic events occurring within the preceding 365 days. Figure 51 is an example Magnitude-Time History chart for a high hazard seismic population. The red box is used to highlight the previous year of seismic activity in reference to a large magnitude seismic event occurring in the beginning of Jan 2014.

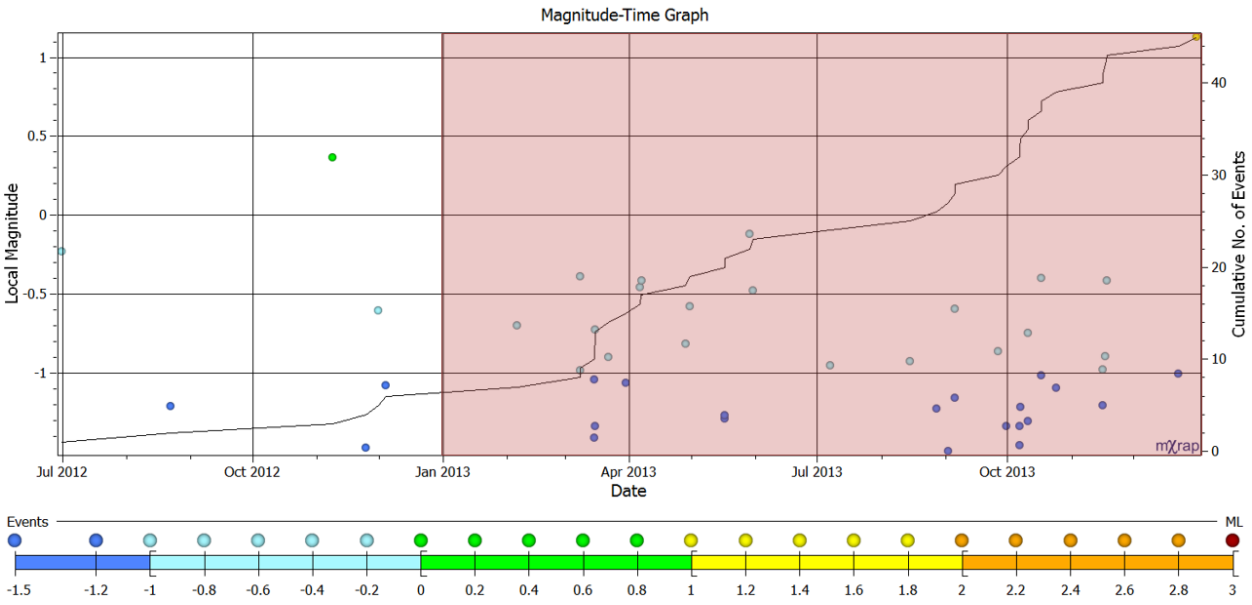

Figure 51: Magnitude-Time History chart for a high hazard seismic population (ID: 7). The red box highlights the ASR calculation time period of 1 year for long term seismic hazard assessment for a large magnitude seismic event.

Long term seismic hazard assessment includes a substantial quantity of seismic events. As a result the addition of each new event has less of an impact on the apparent stress cumulative distribution used for obtaining 20th and 80th percentile values. This generates less variation in ASR values over time compared to other seismic hazard assessment periods. Figure 52 shows a cumulative distribution of the preceding ASR values for large events contained within the test populations - coloured by Local magnitude.

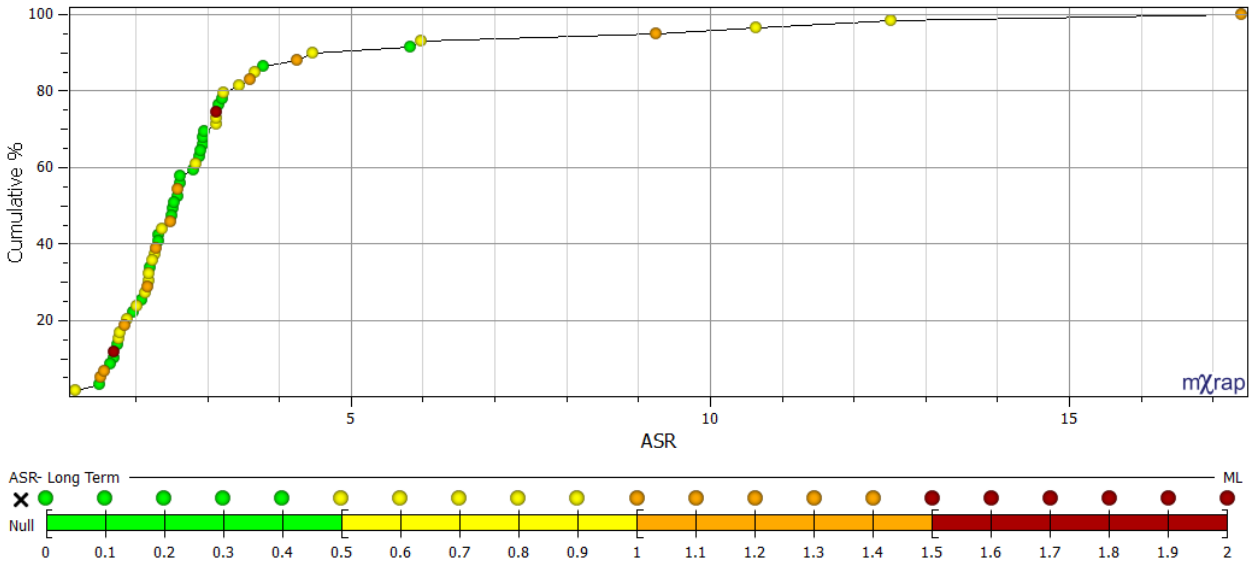

Figure 52: Cumulative distribution of proceeding ASR value calculated based on the previous year for all large events contained within the test populations.

Long term ASR calculations allow for investigation of stress conditions in areas of the rock mass where the stress increase is quite gradual. The 20th percentile for the cumulative distribution in Figure 52 corresponds to an ASR value of approximately 2. This indicates that the vast majority of large seismic events contained within the area of interest have a preceding ASR value greater than or equal to 2. Figure 53 shows a cumulative distribution of the median ASR values calculated for long term seismic hazard for the 25 control populations. The use of median ASR

as a representative value for an entire population will be discussed in 4.2.4 « ASR as an Alarm Tool ».

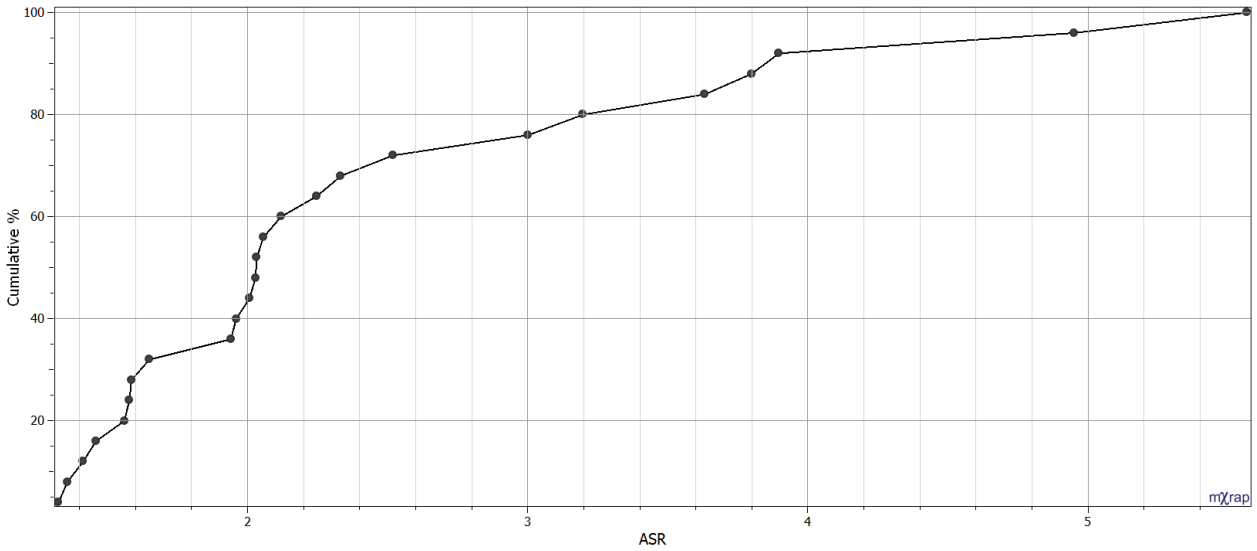

Figure 53: Cumulative distribution of median ASR values calculated based on long term seismic hazard assessment for all control populations.

Median ASR values for control populations are significantly smaller than ASR values preceding large events in test populations. A value of 2 corresponds to nearly the 50th percentile for the cumulative distribution in Figure 53, compared to the 20th percentile for large events. This indicates that larger ASR values may be associated with elevated seismic hazard.

A disadvantage to using a long assessment time period is the extended influence from previous seismic activity that may no longer be relevant to the current stress state in the rock mass. Large quantities of smaller events from nearby development mining can potentially decrease the 20th percentile value of an apparent stress distribution, as previously discussed. Large magnitude events, with large apparent stress values, that may have occurred up to a year earlier will increase the 80th percentile. Both of these factors negatively impact the ability of ASR to reflect changes

in the rock mass conditions subsequent to these small and large events, particularly when extended time windows of seismicity are used in the calculation of ASR.

4.2.2.2 « Medium Term Seismic Hazard Assessment using ASR »

By reducing the time window for ASR calculation from 1 year to 3 months, a significant number of events are no longer included in the apparent stress distribution used for determining the 20^{th} and 80^{th} percentiles. The shortened time period reduces the impact from older events that may no longer be relevant to the current stress state in the local rock mass, while ensuring a sufficient number of events are still included in the calculation.

For medium term seismic hazard assessment, ASR values are calculated using a time window of the previous 3 months. The 20^{th} and 80^{th} percentile values used for the calculation of ASR are taken from an apparent stress distribution that only considers the seismic events occurring within the preceding 91.31 days. Figure 54 is an example Magnitude-Time History chart for a high hazard seismic population. The red box is used to highlight the previous 3 months of seismic activity in reference to a large magnitude seismic event occurring in the beginning of Jan 2014.

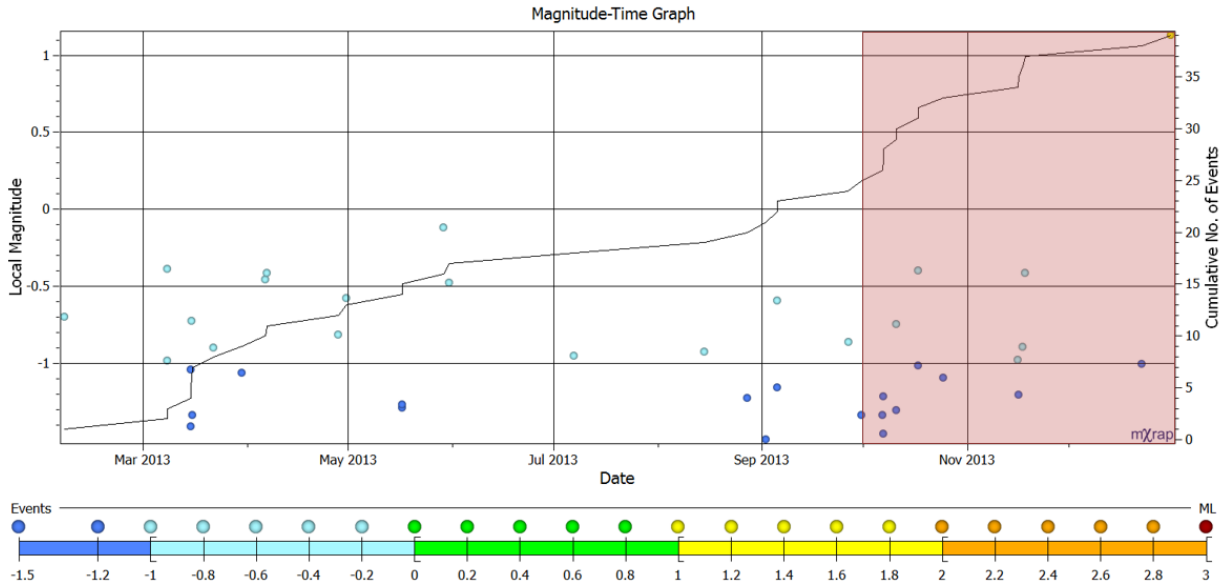

Figure 54: Magnitude-Time History chart for a high hazard seismic population (ID: 7). The red box highlights the ASR calculation time period of 3 months for medium term seismic hazard assessment for a large magnitude seismic event.

By reducing the time period from one year, shown in long term seismic hazard assessment (Figure 51), to 3 months for medium term seismic hazard assessment, less data is considered. As a result, only changes occurring within a 3 month period can be reflected and more gradual changes are underrepresented. Figure 55 shows a cumulative distribution of the preceding ASR values for the large events contained within the test populations - coloured by Local magnitude.

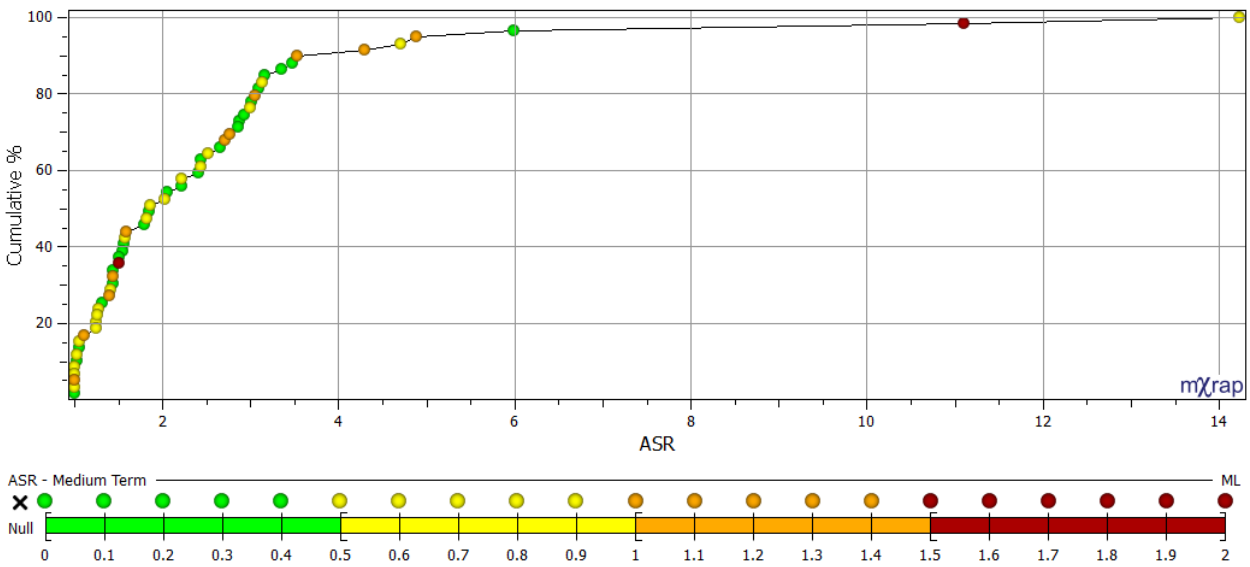

Figure 55: Cumulative distribution of proceeding ASR value calculated based on the previous 3 months for all large events contained within the test populations.

A clear difference can be seen in the scale of ASR values when compared to those calculated using a longer time period (Figure 52). The 20th percentile has been reduced to approximately 1.3 from 2 (using long term seismic hazard assessment). This is a direct reflection of the reduced time period. Longer time periods allow for a much more gradual change in local stress conditions to be observed, and as a result the 20th and 80th apparent stress percentile values typically have a larger degree of separation. Approximately 10% of events in Figure 55 have a preceding ASR value of 1, indicating there were no seismic events in the preceding 3 months. Figure 56 shows a cumulative distribution of the median ASR values calculated for medium term seismic hazard for all control populations.

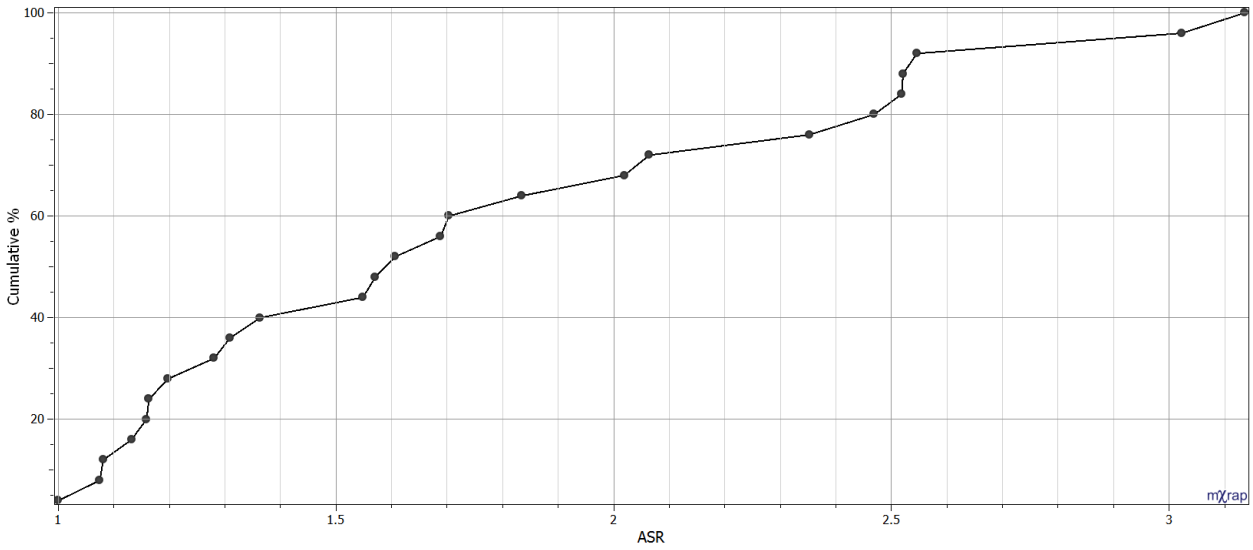

Figure 56: Cumulative distribution of median ASR values calculated based on medium term seismic hazard assessment for all control populations.

Similar trends to those seen in the ASR values preceding large events for the test populations is reflected in the median ASR values for the 25 control populations. Values are smaller than those calculated using long term seismic hazard assessment, but ASR values preceding large events are typically higher than median values for control populations. Only a single control population has a median value of 1. Using a longer calculation time period, such as the preceding year, increases both the value of ASR and the degree of separation between lower values for moderate/low hazard populations and larger values for high hazard populations.

With a medium term time period such as 3 months, the 20th percentile can, in the best case, only reflect apparent stress values from the 3 preceding months. If local stress conditions have been consistently increasing over a longer time period, this will not be reflected in ASR. For this purpose long term seismic hazard assessment may provide the best means of reflecting local stress conditions.

4.2.2.3 « Short Term Seismic Hazard Assessment using ASR »

For short term seismic hazard assessment, ASR values are calculated using a time window of the previous week. In other words, the 20th and 80th percentile values used for the calculation of ASR are taken from an apparent stress distribution that only considers seismic events occurring within the preceding 7 days. Figure 57 is an example Magnitude-Time History chart for a high hazard seismic population. The red box is used to highlight the previous week of seismic activity in reference to a large magnitude seismic event occurring in the beginning of Jan 2014.

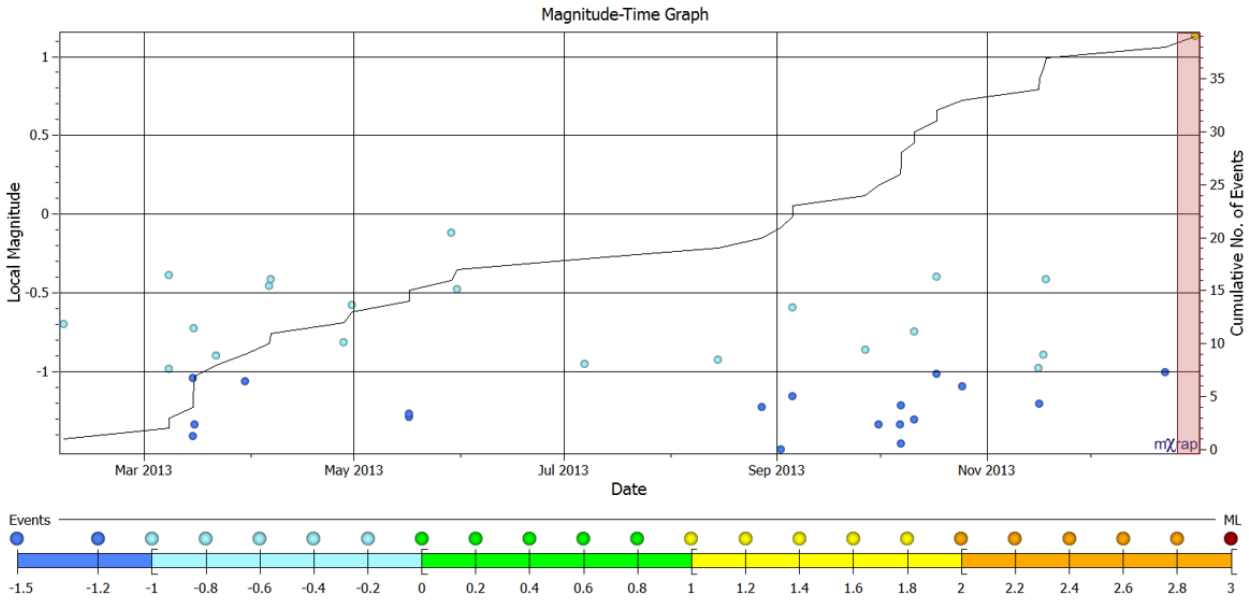

Figure 57: Magnitude-Time History chart for a high hazard seismic population (ID: 7). The red box highlights the ASR calculation time period of 1 week for short term seismic hazard assessment for a large magnitude seismic event.

Because there are no other seismic events occurring within the preceding week, the ASR value preceding the large magnitude event highlighted in Figure 57 is 1. Figure 58 shows a cumulative distribution of the preceding ASR values for all of the large events contained within the test populations - coloured by Local magnitude.

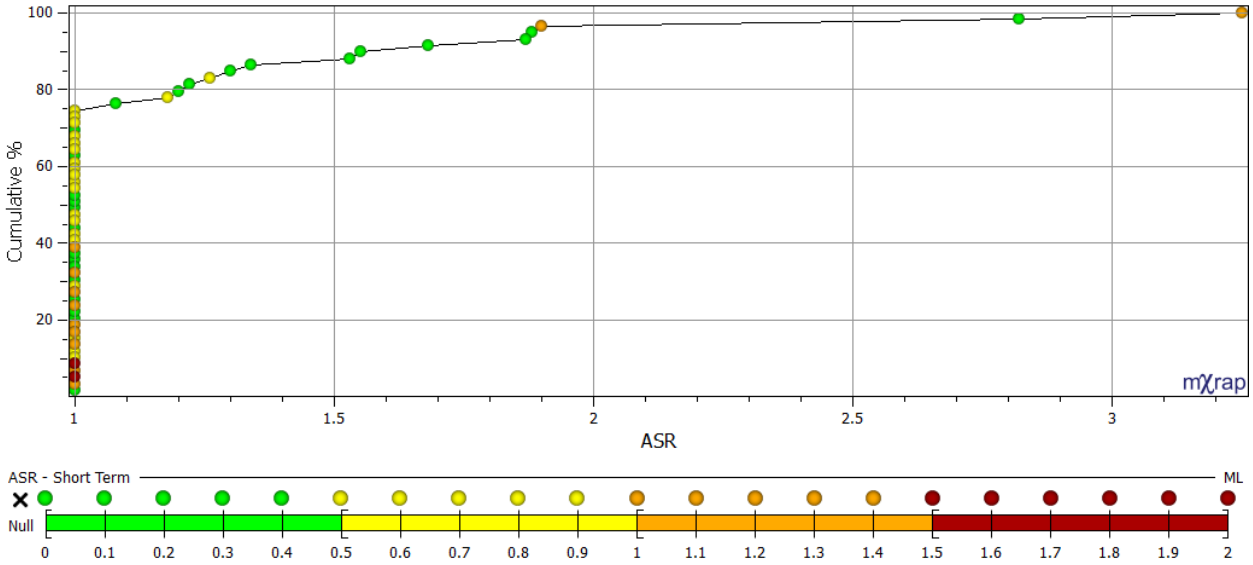

Figure 58: Cumulative distribution of proceeding ASR value calculated based on the previous week for all large events contained within the test populations.

In the vast majority of populations, there are extended periods of time in which event frequency is equal to or less than one event per week - generating ASR values of 1. The majority of large events, approximately 75%, have a preceding ASR value of 1. This indicates that in most cases a time period exceeding one week is required to incorporate an appropriate number of events to quantify an increasing stress state. Cases in which the ASR value was greater than 1, at the time of a large event, indicate an increase in the local stress conditions occurred rapidly. This does not appear to be related to increasing event magnitude, as events of varying size have both one and non-one values. Figure 59 shows a cumulative distribution of the median ASR values calculated for short term seismic hazard for all control populations.

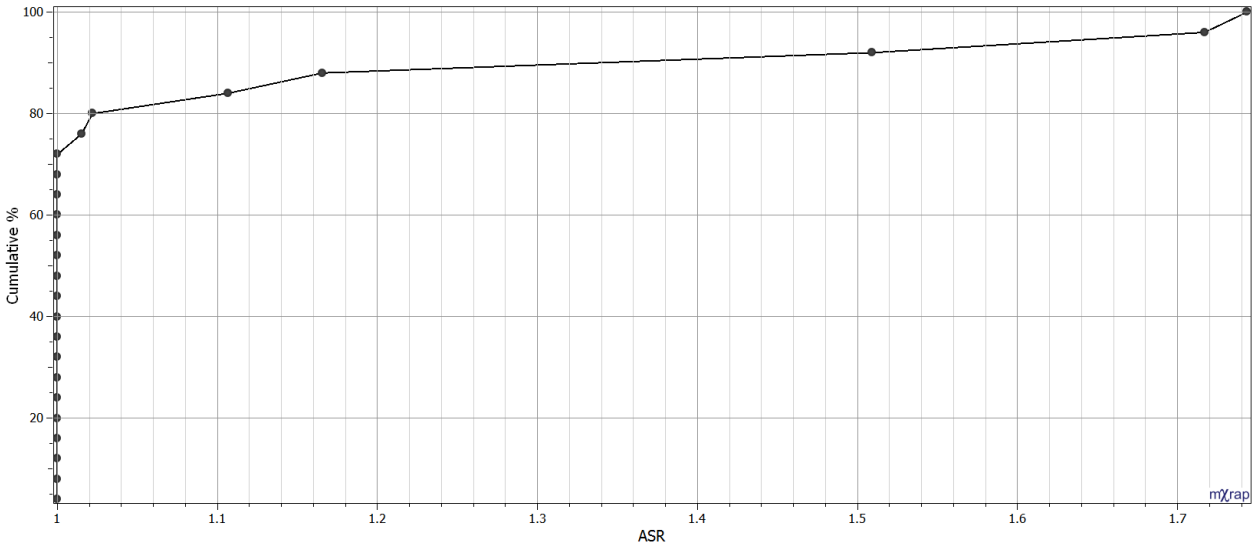

Figure 59: Cumulative distribution of median ASR values calculated based on short term seismic hazard assessment for all control populations.

Just as was seen for the ASR values preceding large events, the majority of control populations have a median ASR value of 1. This is due to event frequency rates less than the short term assessment period of 1 week. As a result, the use of ASR for short term hazard assessment at LaRonde provides little useful information about elevated short term seismic hazard.

ASR values can vary substantially based on the selected time period. Short time periods, in the order of days to weeks, are very limited in their application as populations with relatively low event rates over extended periods of time do not allow for substantial stress change to be observed. Longer time periods result in larger ASR values, as a more gradual change in stress conditions is included in the preceding events used for ASR calculation.

4.2.3 « ASR as an Analysis Tool »

Seismic analysis tools are used to gain insight into the local seismic response to mining. Selecting an appropriate preceding time period is a crucial component to effectively using ASR as an analysis tool. As stress increases within a rock mass, the individual apparent stress

measurements of seismic events increases. If stress builds quickly within the rock mass, generating substantial seismicity within short time periods, short term (1 week) ASR calculations may be meaningful. In most cases, a medium term time period (3 months), appears to provide insight into changing stress conditions in the rock mass while minimizing the impact from previous seismicity that may no longer be relevant to the current stress conditions. Long term (1 year) ASR values may be the best indicator of long term trends in seismic hazard as they are less susceptible to small quantities of anomalous seismic activity and allow for trends in the long term gradual buildup of stress within a rock mass to be identified.

An effective way of presenting ASR values is on an Apparent Stress Ratio Time History chart (ASRTH). Figure 60 is an example of an ASRTH chart for a high hazard seismic population using a calculation time window of the preceding year for ASR values (displayed on the secondary y-axis). Events are coloured according to apparent stress.

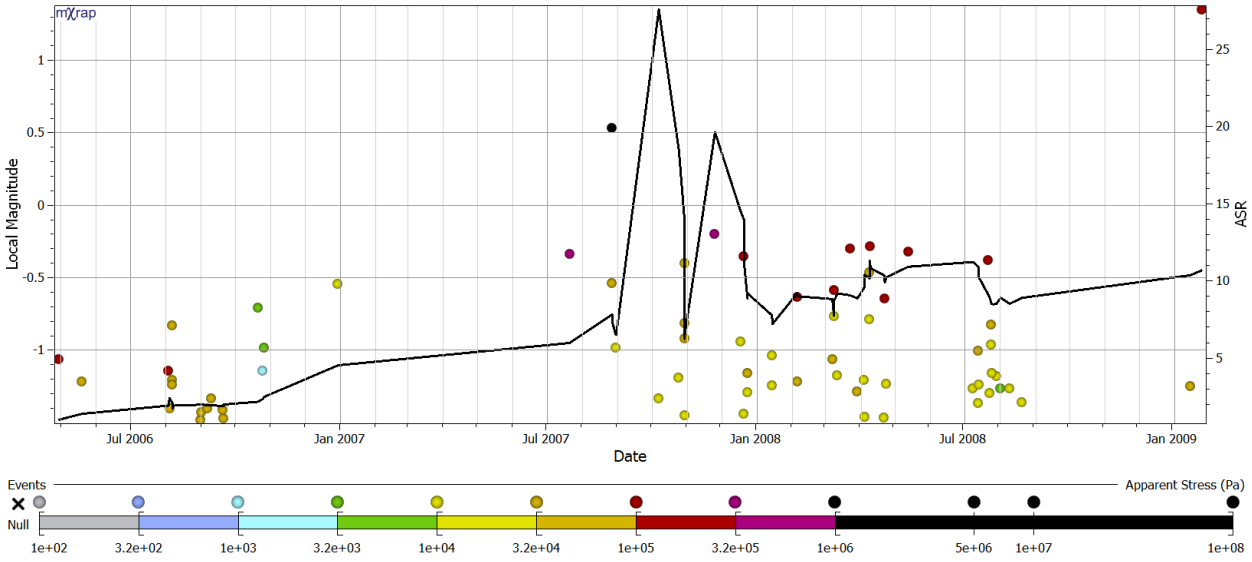

Figure 60: ASRTH chart of a high hazard population (ID: 3). ASR values are calculated based on long term seismic hazard (preceding year).

The seismic population shown in Figure 60 possesses extended time periods of high apparent stress, during which two large seismic events occur. In the beginning of the population life, ASR

values are relatively low, but begin to increase in Nov 2006. After this date the population contains a mix of high and low apparent stress events, generating large ASR values. Displaying ASR on an ASRTH chart allows the user to gain insight into the historic seismic response of the population and how it relates to event frequency, magnitude, and apparent stress.

When ASR values increase, it may be a result of an increasing 80^{th} percentile value or a decreasing 20^{th} percentile value. By colouring the events according to apparent stress, it allows the user to identify which of these two possibilities is occurring. This is an important component of assessing stress increase, as an increasing 80^{th} percentile value is indicative of increasing stress conditions, while a decreasing 20^{th} percentile value may be a result of various factors such as the quantity of small events considered in the ASR calculation. To better understand the factors driving trends in ASR, an Apparent Stress Percentile chart (ASP) can be used for secondary analysis. Figure 61 is an example of an ASP chart for the high hazard seismic population shown in Figure 60. The primary y-axis represents apparent stress and is used to display the 20^{th} and 80^{th} apparent stress percentile values. The secondary y-axis show the cumulative number of events but can alternatively be used to display ASR. Events are plotted according to apparent stress and coloured by Local magnitude.

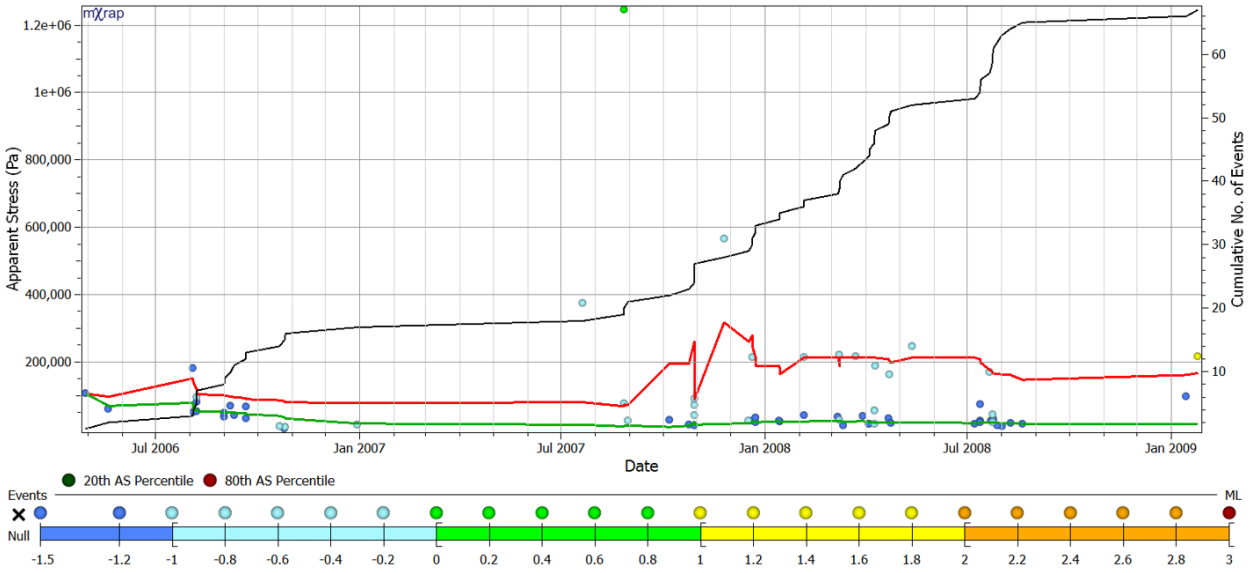

Figure 61: ASP chart of a high hazard population (ID: 3). ASR values are calculated based on long term seismic hazard (preceding year).

It is clear the increase in ASR for the population shown in Figure 61 is a direct result of an increase in the apparent stress 80th percentile value. This increase is driven by larger apparent stress events contained within the population or a reduction in the number of small apparent stress events considered as time, and consequently the calculation time window, progresses. In this example, the apparent stress 20th percentile values remain relatively constant throughout the population life. In order to use ASR effectively as an analysis tool, the factors influencing increases and decreases in ASR for a population need to be considered.

4.2.3.1 « Peak Apparent Stress Ratio »

The peak apparent stress ratio is an important value in defining the level of seismic hazard associated with a population. It is defined as the largest ASR value reached by a seismic population and serves as an indicator of the maximum stress change possible within the preceding time period in use. The population presented in Figure 60 has a peak ASR of approximately 27. This indicates that over the course of a single year (365 days), the apparent

stress of events within the population were such that the 80th percentile reached a high of 27 times larger than the 20th percentile.

As apparent stress is scale dependent, large ASR values are frequently indicative of the occurrence of large magnitude events. Representing populations by peak ASR values can therefore provide insight into past seismic response. Areas of a mine that have comparatively higher peak ASR values may be associated with elevated seismic hazard. Elevated values indicate that over a constant calculation time period, stress was able to increase substantially more in these areas.

When ASR calculation time periods are varied (long, medium and short), peak ASR values remain meaningful. Figure 62 is the ASRTH chart for the same seismic population shown in Figure 60. ASR values shown below are calculated using a time window of the preceding week (7 days).

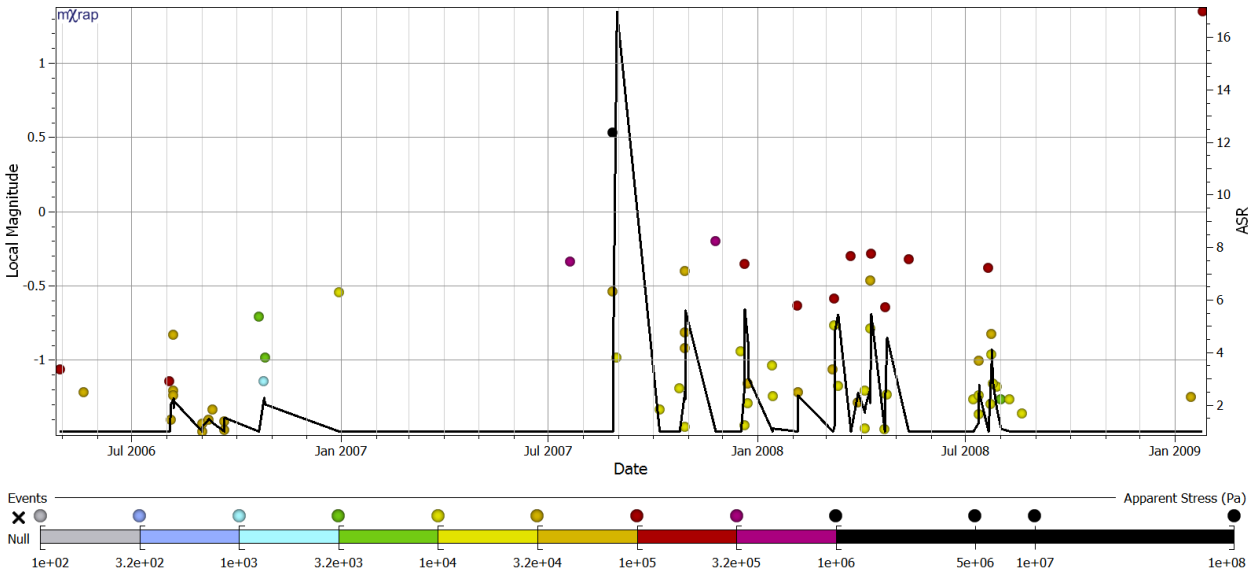

Figure 62: ASRTH Chart of a high hazard seismic population (ID: 3). ASR values are calculated based on short term seismic hazard (preceding week).

By shortening the calculation time window, the peak ASR value for this population is reduced from 27 to approximately 17. This value is still significant as it implies that over the course of a single week (7 days), the apparent stress of events within the population was such that the 80th percentile reached a high of 17 times larger than the 20th percentile.

Peak ASR values are significantly smaller for low seismic hazard populations. Low seismic hazard is a reflection of stability in the rock mass and should be associated with relatively small apparent stress values. Figure 63 is an ASRTH chart for a low hazard seismic population using long term (1 year) hazard assessment.

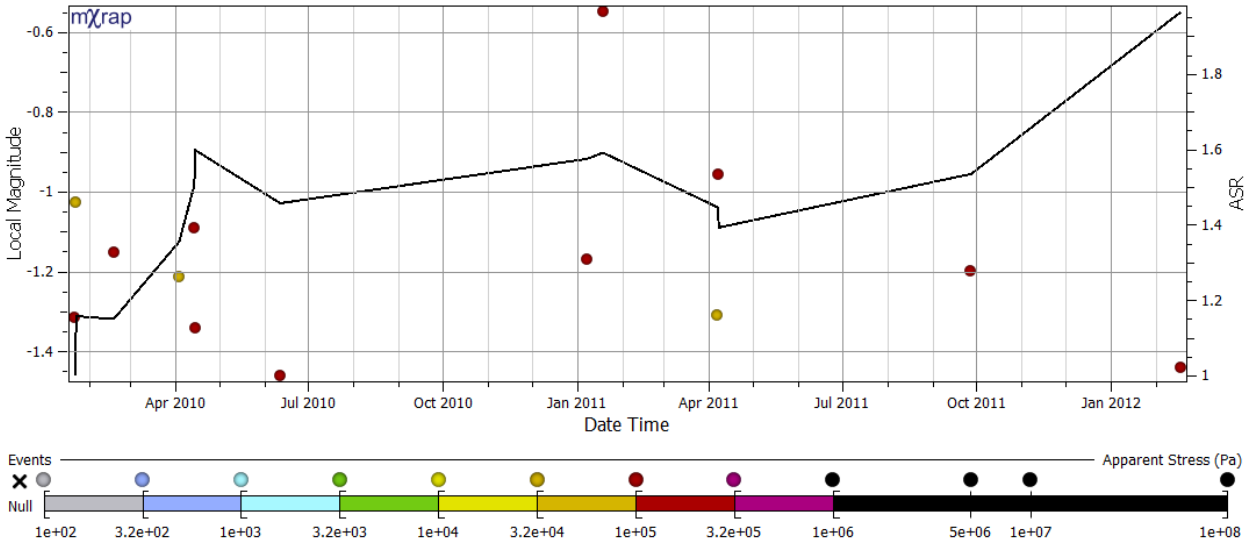

Figure 63: ASRTH Chart of a low hazard seismic population (ID: 46). ASR values are calculated based on long term seismic hazard (preceding year).

With a peak ASR value less than 2, it is clear this population is representative of low apparent stress. No large variations in apparent stress are present throughout the population and as a result, ASR values remain relatively low throughout the duration of the population life. Just as trends of high peak values can be seen over varying time periods for high hazard populations, the

same is true for low hazard populations. Figure 64 is an ASRTH chart using short term hazard assessment for the same low hazard seismic population shown in Figure 63.

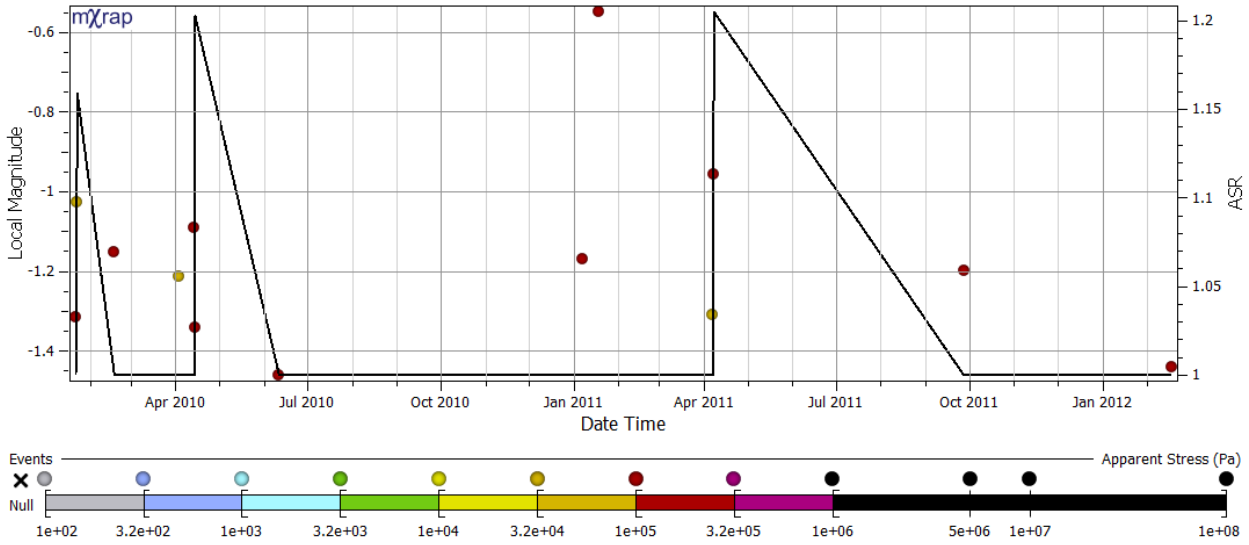

Figure 64: ASRTH Chart of a low hazard seismic population (ID: 46). ASR values are calculated based on short term seismic hazard (preceding week).

With the use of a shorter preceding time period for ASR calculation, the peak ASR value is reduced to approximately 1.2. This is highly indicative of stable stress conditions as the apparent stress values of events occurring within 7 days of one another are nearly identical. Large peak ASR values indicate a significant differences between the apparent stress 80th and 20th percentile values for the calculation time period. Extremely high values, over a shorted time period, indicate changes in local stress conditions are capable of occurring rapidly.

From these examples it is evident that peak ASR can be used as an indicator of seismic hazard for varying degrees of hazard over varying time periods. These trends are seen throughout the entire area of interest at LaRonde and further examples will be provided in 5.1 « Peak ASR: Analysis and Examples ». Peak ASR values are highly indicative of seismic hazard and can be used over varying time frames to provide insight into the local rock mass conditions.

4.2.3.2 « Confidence in ASR »

The number of events considered in the calculation of ASR has a large impact on the confidence of using ASR as an analysis tool. As with most seismic analysis techniques, the more data that is considered, the more confident the user can be in the trends observed. Because ASR is calculated over varying time periods, the number of events included in the apparent stress distribution is continuously changing. When utilizing tools such ASRTH charts, it is important to understand what impact this may have on trends in ASR. When smaller quantities of data are used, anomalous seismic activity is capable of having a much larger influence on ASR values. This is a main reason results from ASR calculated using shorter time periods may produce less meaningful results. Figure 65 is an example of a low hazard seismic population with a very large peak ASR value.

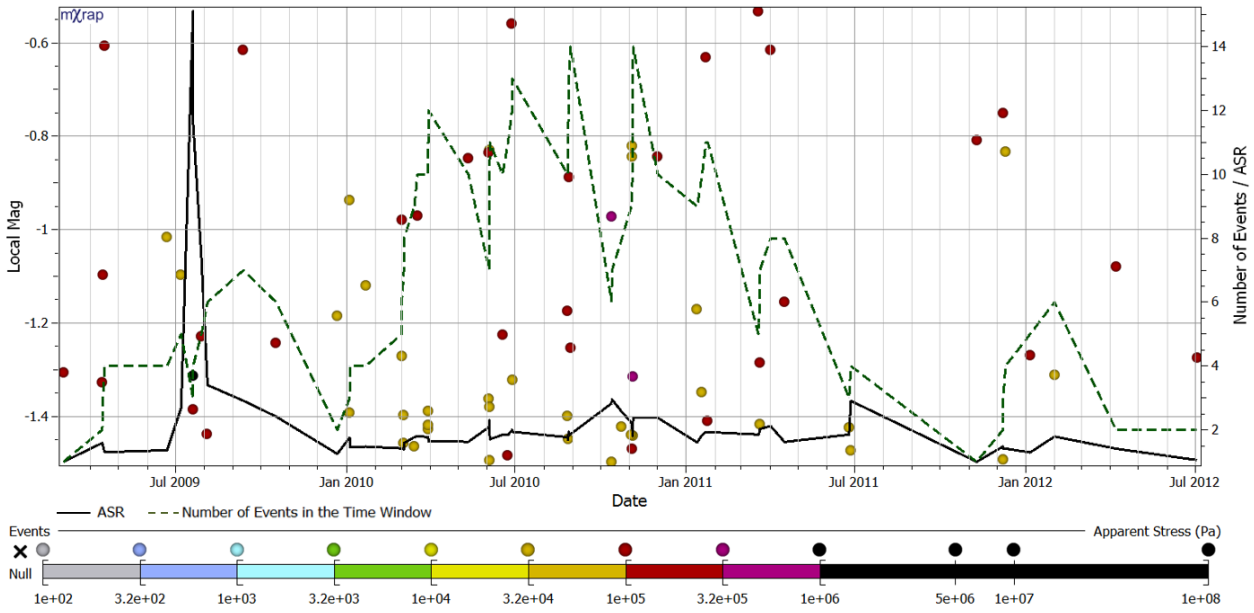

Figure 65: ASRTH Chart of a low hazard seismic population (ID: 28). ASR values calculated for medium term seismic hazard and the number of events contained within the calculation time window are displayed on the secondary y-axis.

The low hazard population shown in Figure 65 has an uncharacteristically high peak ASR of approximately 15, occurring in July 2009. This spike in ASR is the product of a single

anomalously high apparent stress seismic event. As previously discussed, apparent stress is scale dependent and it is uncharacteristic for such a small magnitude event to have such a large apparent stress value. Because of the small quantity of seismic events contained within the three months surrounding this event, it has a large impact on the apparent stress distribution from which the local ASR values are calculated. Due to the minimal number of events considered in ASR calculation for this time period, the confidence in this ASR value is reduced. As the population continues and the seismic event rate increases, ASR values are reduced to levels expected for a low hazard seismic population.

Figure 66 is a Magnitude-Time History chart for the same low hazard seismic population shown in Figure 65.

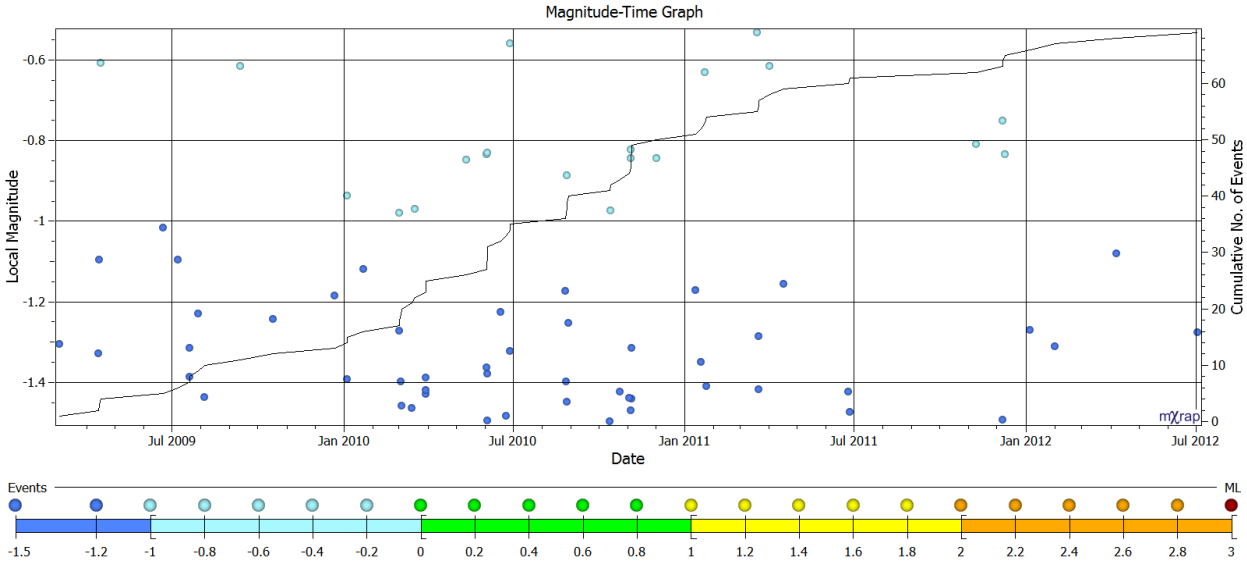

Figure 66: Magnitude-Time History Chart of a low hazard seismic population (ID: 28).

The seismic event rate surrounding July 2009, which corresponds to the large peak ASR value for the population, is significantly less than that for the rest of the population. On either side the slope of the cumulative number of events line is nearly zero for several months. It is due to this low event rate, paired with the three month calculation time period, which enables a single

seismic event to have such a large impact on ASR. For the remainder of the population, ASR values are more characteristic of a low hazard population and confidence levels are increased as a result of the elevated seismic event rate.

When analyzing trends in ASR, it is important to understand the relation between the seismic hazard assessment period being used and the event rate of the population. Uncharacteristically low and high peaks in ASR should be further analyzed, as this is the key to inferring seismic hazard. A high level of confidence cannot be obtained when relatively small quantities of seismic events form the apparent stress distribution, enabling anomalous seismic activity to have a large influence on ASR.

4.2.4 « ASR as an Alarm Tool »

As previous examples have shown, large ASR values are indicative of elevated seismic hazard. The value of peak ASR as an analysis tool has been demonstrated, but ASR in itself is of considerable importance. By pairing trends in the previous occurrence of large events with an alarm tool, a threshold ASR value for potentially forecasting the occurrence of large seismic events may be determined. When the ASR of a population exceeds this threshold, it initiates an alarm indicating that large scale stress changes may be occurring - suggesting elevated seismic hazard.

The selection of a reasonable threshold value for ASR depends on many factors. While a low threshold value will ensure a high rate of success (the number of large events occurring during alarm periods), there may also be a substantial number of false alarms associated with it. False alarm refers to an instance in which an ASR value exceeds the set ASR threshold, but no large event occurs prior to the ASR value returning below the threshold. Instances in which the ASR

value remains high, up to and including the final event in a population, are also considered false alarms for the purposes of this thesis. Using an arbitrary ASR threshold value of 2.5, the ASRTH chart in Figure 67 depicts a low hazard seismic population containing two false alarms, or two time periods in which ASR exceeds the threshold but no large seismic event occurs.

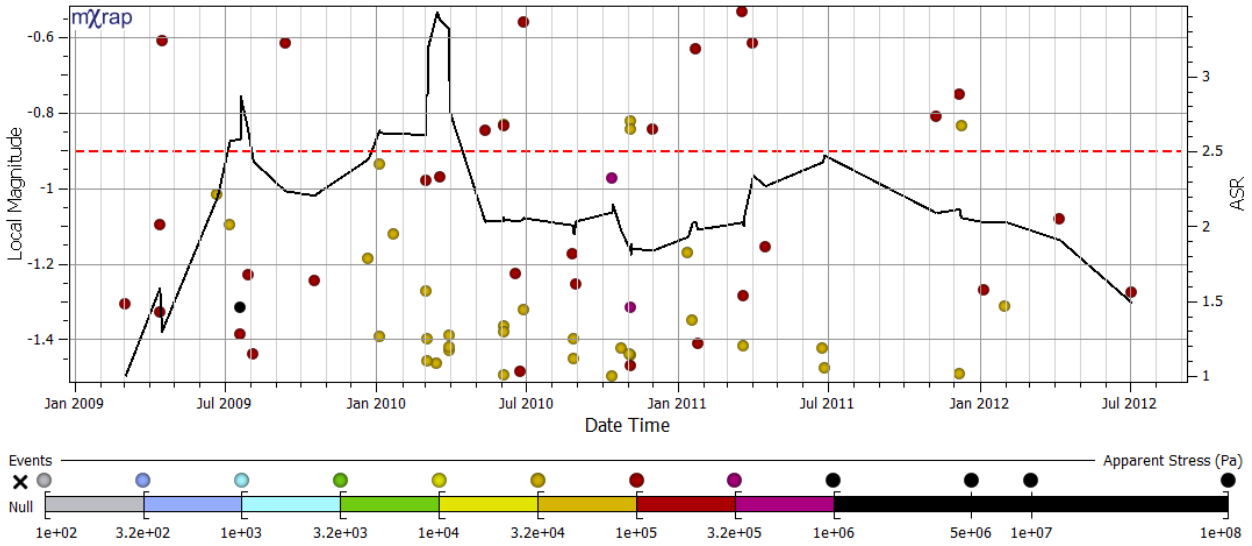

Figure 67: ASRTH chart for a low hazard seismic population (Id: 28) with an ASR alarm threshold of 2.5. ASR values are calculated based on long term seismic hazard (preceding year).

The first alarm begins in Jul 2009, when the threshold of ASR = 2.5 is exceeded due to the occurrence of a high apparent stress event. It lasts approximately a month and then the ASR value falls below the threshold. Because no large events occurred during this time period, this is classified as a false alarm. The second alarm occurs in Jan 2010 when the threshold is again exceeded, and lasts until mid-April 2010. Again no large events occur during this time period and it is classified as a false alarm.

It is clear from Figure 67 that a decrease in the ASR alarm threshold value would increase both the frequency and duration of false alarms for the population. Determining an acceptable threshold value depends on the level of tolerable risk for the area in question. An area with a low tolerance for risk, such as a refuge station or garage, may require a lower threshold value for

example. Although the number of false alarms will increase, the likelihood of a large event occurring during a time of alarm (elevated hazard awareness) also increases. For an area with a high tolerance for risk, such as an active heading with remote and enclosed equipment, a suitable threshold value may be considerably higher. The number of false alarms would decrease, while still being able to provide an indication of when large changes in local stress conditions may be occurring.

The following sections discuss the process of selecting a threshold value for the various time periods of hazard assessment using ASR (long, medium, short). For simplification, a general threshold ASR value is selected to apply to all sample populations, regardless of variations in risk tolerance. These values are determined by comparing the ASR values preceding large events in test populations to median ASR values for control populations.

Representing populations by median ASR values minimizes the impact of anomalous seismic activity that may lead to large ASR values. Short periods of large ASR, that are not necessarily representative of the entire seismic population, can be generated due to a variety of factors. Such factors include the influence of nearby mining activities (such as development or production blasting), and anomalously high or low apparent stress events occurring in times of reduced seismic activity. As was discussed in 4.2.3.2 « Confidence in ASR », relatively large or small apparent stress events can have a large impact on ASR when few events are included in the calculation time period, leading to uncharacteristically high peak ASR values. These values are short lived and not representative of the entire population. Figure 68 is an example of a low hazard seismic population with a peak ASR of 13.

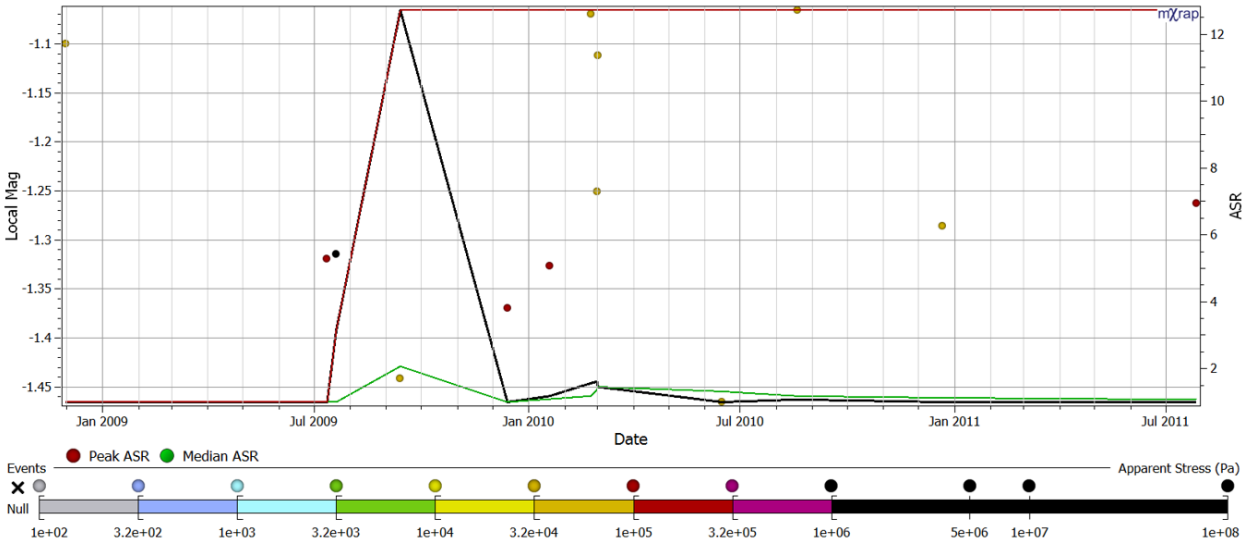

Figure 68: ASRTH Chart of a low hazard seismic population (ID: 45). ASR values calculated for medium term seismic hazard are displayed on the secondary y-axis.

The low hazard population shown in Figure 68 has an uncharacteristically high peak ASR of approximately 13 occurring in September 2009. This is due to a single seismic event that has uncharacteristically low apparent stress compared to the other events contained within the same 3 month period. The other two events have relatively high apparent stress values, and with only 3 events comprising the entire apparent stress distribution for the ASR calculation time frame, the resultant ASR value is very large. For the other events contained within the population, ASR values are low and within expected ranges for a low hazard population. The median ASR for the entire population is approximately 1.1. Using a value of 1.1 versus 13 allows for a much lower and more representative threshold value to be selected.

Figure 69 shows cumulative distributions for ASR values preceding large seismic events in test populations, as well as median and peak ASR values for control populations.

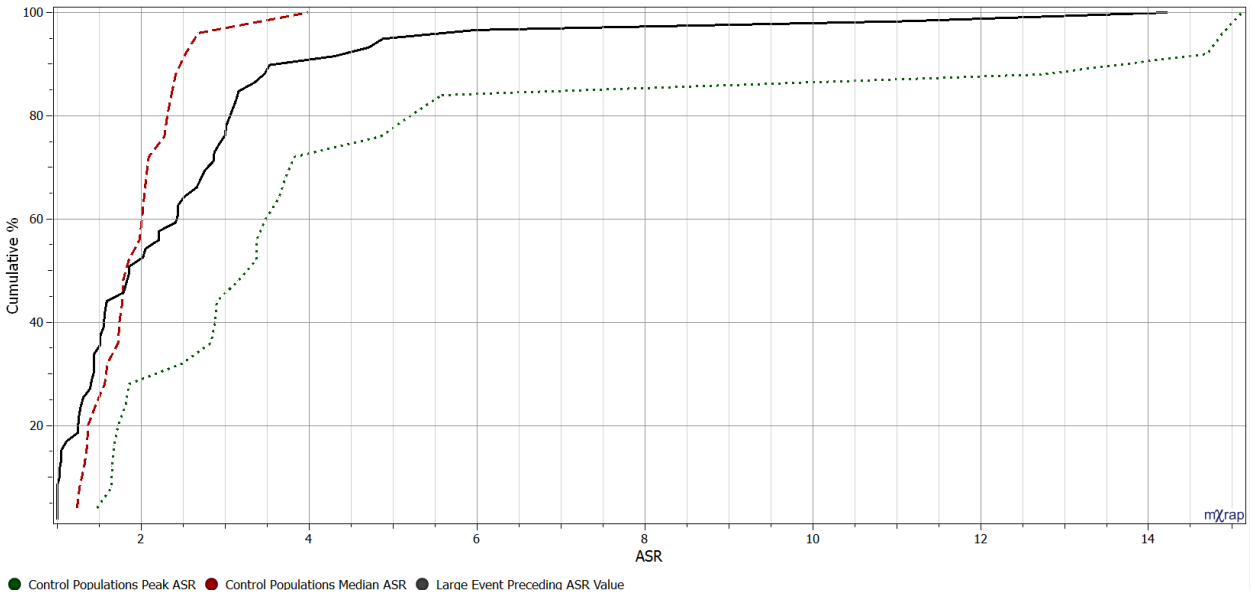

Figure 69: Cumulative distribution of ASR values preceding large events, median ASR values and peak ASR values for all control populations. All ASR values are calculated based on medium term seismic hazard assessment.

Median ASR values for control populations are better suited for comparison against ASR values preceding large events. The significant difference between peak ASR values for control populations and ASR values preceding large events prevents the selection of a reasonable threshold value. As previously discussed, the purpose of a threshold value is to maximize the level of success while minimizing the number of false alarms. This cannot be completed using peak ASR values, as they are not necessarily representative of the typical response of a seismic population to mining.

4.2.4.1 « ASR as an Alarm Tool for Long Term Hazard »

Long term hazard assessment is based on the seismic activity occurring over the preceding year (365 days). It allows for a very gradual stress change in the rock mass to be observed, but may incorporate the influence of any anomalous seismic activity for an extended period of time. Figure 70 shows a cumulative distribution for the ASR values preceding large events located

within the test populations, as well as the median ASR values for test and control populations - all calculated use one year as the preceding time window.

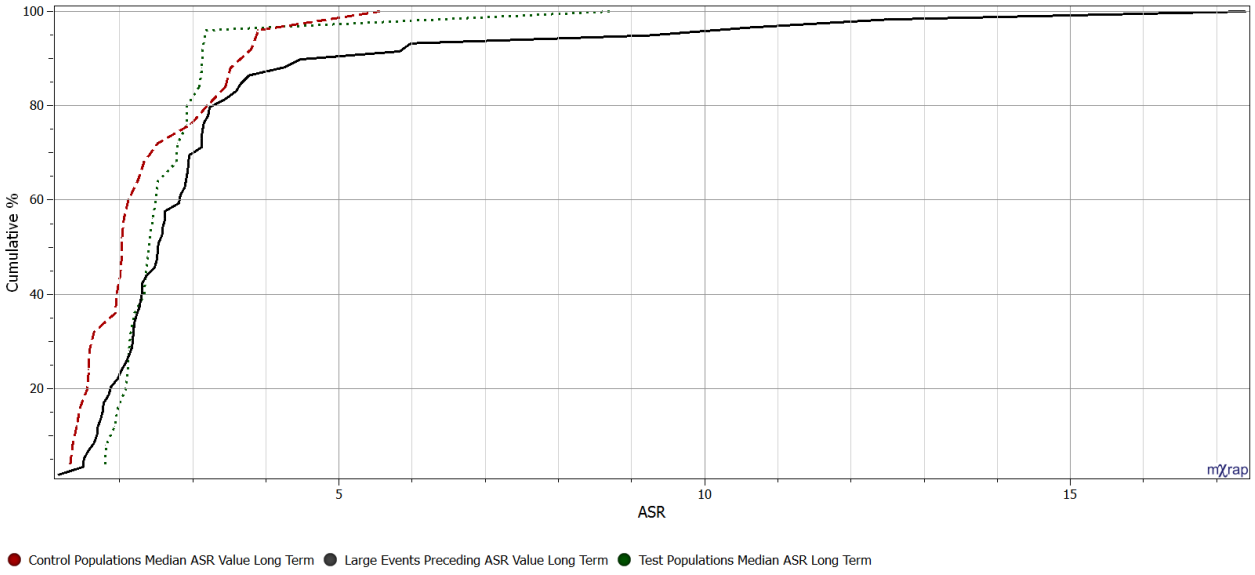

Figure 70: Cumulative distribution of ASR values preceding large events, and median ASR values for all test and control populations. All ASR values are calculated based on long term seismic hazard assessment.

Using long term seismic hazard assessment virtually all ASR values are greater than 1, with the distribution for ASR values preceding large events approximating the distribution for median ASR values of test populations. This is indicative of the smoothing of trends in seismic parameters that occurs when larger quantities of seismic events are included in analysis (over extended time periods). Single events have less of an impact on the 20th and 80th apparent stress percentile values and therefore fluctuations in ASR are minimized.

The process of selecting an alarm tool threshold requires a trade-off of expected false alarms to successful forecasts. For the purposes of this thesis, an ASR value of 2.2 will be used to distinguish long term seismic hazard. Approximately 66% of large events occur at a preceding ASR of 2.2 and while only 40% of control populations have a median ASR value of 2.2 or greater. This appears to be a reasonable trade between successful forecasts and the number of

potential false alarms. This topic of a reasonable threshold ASR value will be discussed further in 5.6.3 « Discussion of Parameter Value Selection ».

4.2.4.2 « ASR as an Alarm Tool for Medium Term Hazard »

Medium term hazard assessment is based on the seismic activity occurring over the preceding planning period (3 months). It allows for a gradual stress change to be observed while minimizing the long term impact of abnormal seismic activity. Figure 71 shows a cumulative distribution for the ASR values preceding large events within the test populations, and median ASR values for test and control populations - all calculated using 3 months as the preceding time window.

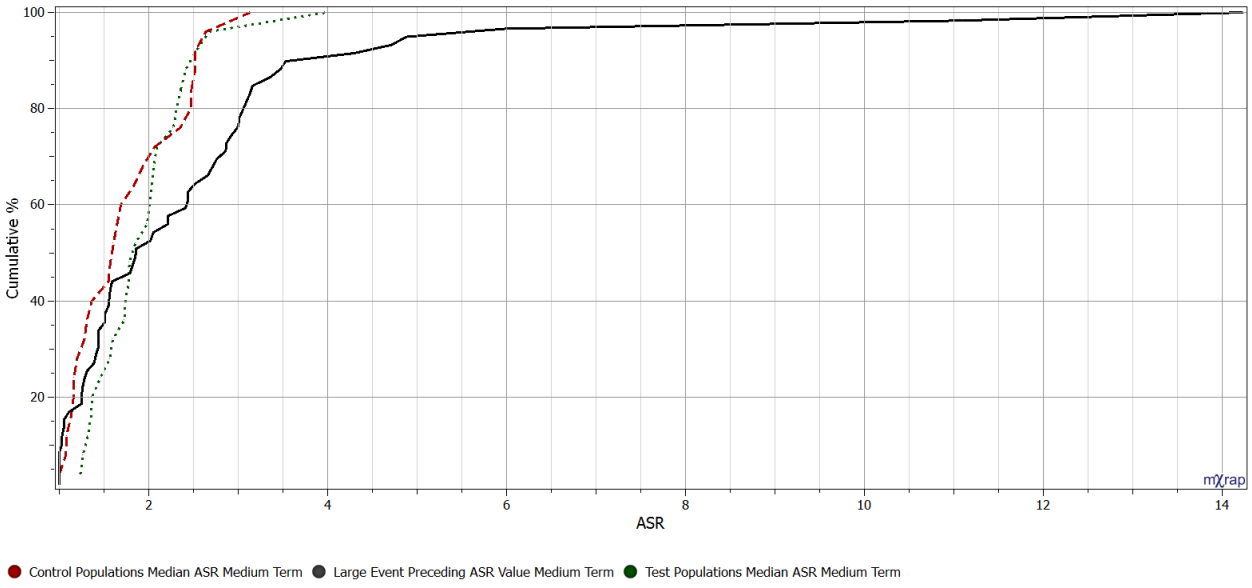

Figure 71: Cumulative distribution of ASR values proceeding large events, and median ASR values for all test and control populations. All ASR values are calculated based on medium term seismic hazard assessment.

Compared to Figure 70, which shows the cumulative distributions for long term seismic hazard, the distributions have shifted to the left. The shortened time frame allows ASR to represent stress change only occurring over a 3 month period and as a result ASR values are typically smaller.

For the purposes of this thesis, an ASR threshold value of 1.8 will be used to distinguish medium term seismic hazard in conjunction with an alarm tool. This value has been selected as approximately 54% of large events occur at a preceding ASR of 1.8, while only 40% of control populations have a median ASR value of 1.8 or greater. This appears to be a reasonable trade between successful forecasts and the number of potential false alarms.

4.2.4.3 « ASR as an Alarm Tool for Short Term Hazard »

Short term hazard assessment is based exclusively on the seismic activity occurring over the preceding week (7 days). It ensures that only the most recent events and changes in stress conditions are considered. As previously discussed however, it is not effective for forecasting large events in most seismic populations at LaRonde. The frequency of occurrence for events in the sample populations is commonly less than 1 event per week, generating ASR values of 1. Figure 72 shows a cumulative distribution for the ASR values preceding large events within the test populations, and median ASR values for test and control populations - all calculated using 1 week as the preceding time window.

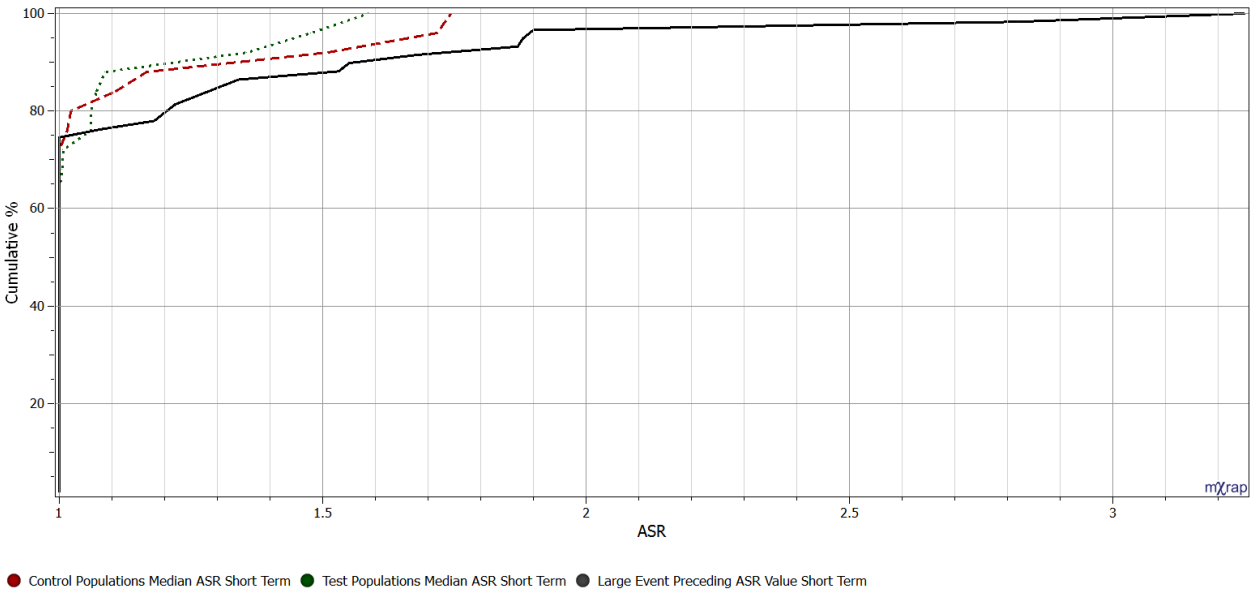

Figure 72: Cumulative distribution of ASR values preceding large events, and median ASR values for all test and control populations. All ASR values are calculated based on short term seismic hazard assessment.

All of the distributions shown in Figure 72 are dominated by ASR values of 1. The 75th percentile for ASR values preceding large events is 1, indicating there was only a single event in the preceding time period of 1 week. For this reason, the application of ASR as an alarm tool for short term seismic hazard is not recommended and will not be discussed further in this thesis.

4.2.5 « ASR as it Relates to Source Mechanism »

The ratio of energy of the secondary and primary seismic waves, referred to as ES:EP, can be an indicator of seismic source mechanism. For fault-slip events, the secondary wave contains considerably more energy than the primary wave (Boatwright and Fletcher, 1984). Ratios greater than 10 are highly indicative of fault-slip type events. When ratios are considerably lower, typically ranging from 1-3, they are indicative of stress related volumetric fracturing (Urbancic et al., 1992). Figure 73 is a cumulative distribution of the ES:EP values for all large seismic events ($M_L \geq 0$) contained within the sample populations.

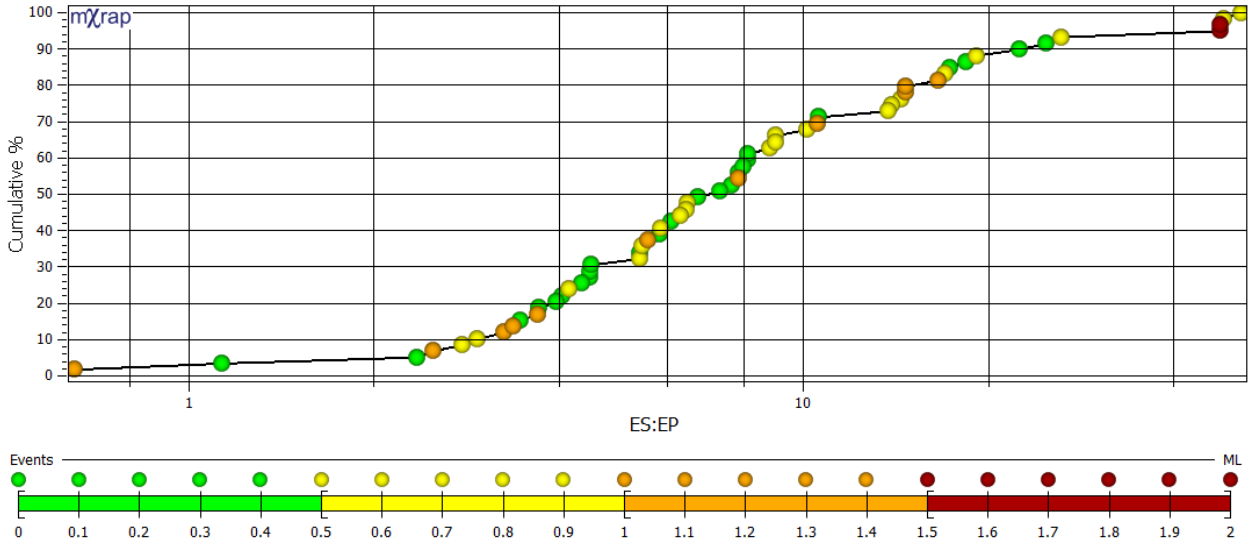

Figure 73: Cumulative distribution of ES:EP for all large events contained with the sample populations. Events are coloured according to Local magnitude.

The majority of large events from the test populations have an ES:EP value ranging from 3 to 10. Approximately 10% of events have an ES:EP value less than 3, indicating a stress related volumetric fracturing source mechanism. Approximately 30% have an ES:EP value greater than 10 (including the two largest magnitude seismic events within the populations), indicating a fault-slip source mechanism. Past studies have shown that apparent stress analysis techniques are typically poorly related to large magnitude events along geological structures - fault-slip events (Young, 2012). Trends in ASR values however appear to be meaningful for seismic hazard evaluation of fault slip type events. Figure 74 is a cumulative distributions of ASR values preceding large events ($M_L \geq 0$) calculated for medium term seismic hazard assessment.

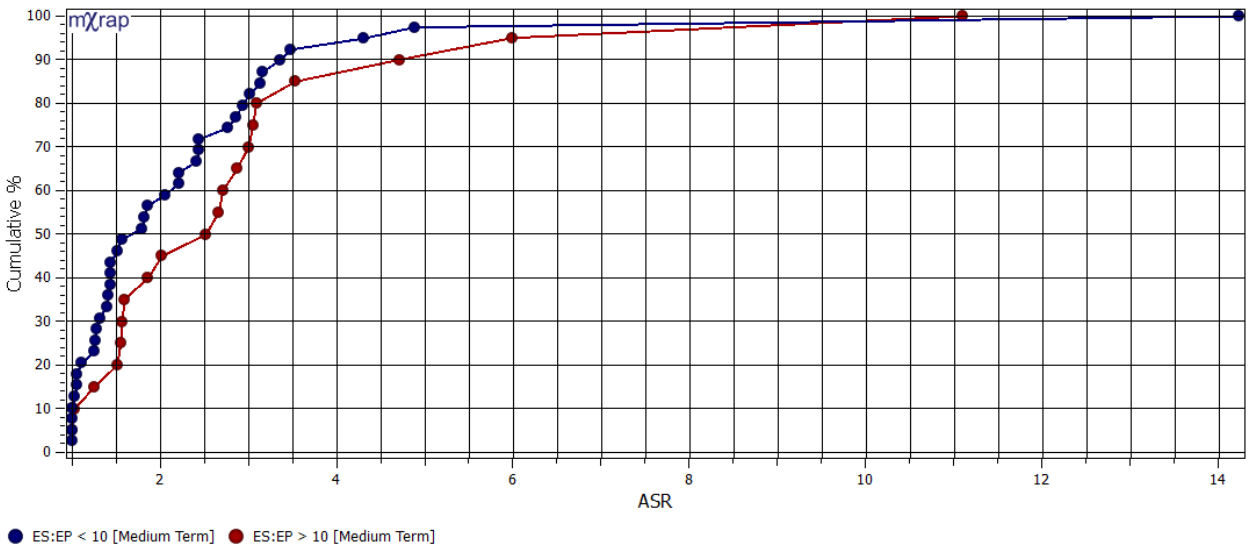

Figure 74: Cumulative distribution of ASR values preceding large events ($M_L \geq 0$) separated by events with ES:EP greater than and less than 10. ASR values are calculated based on medium term seismic hazard (preceding 3 months).

When ASR values are calculated for medium term seismic hazard, there is a significant difference in the values for events with a fault slip source mechanism (inferred from ES:EP). Large ES:EP ratio events typically have larger preceding ASR values. This implies that the use of high ASR values for medium term seismic hazard assessment may be more effective than other apparent stress based analysis techniques, such as ASTH, for fault slip type events. Figure 75 shows the same distribution, but using ASR values calculated for long term seismic hazard.

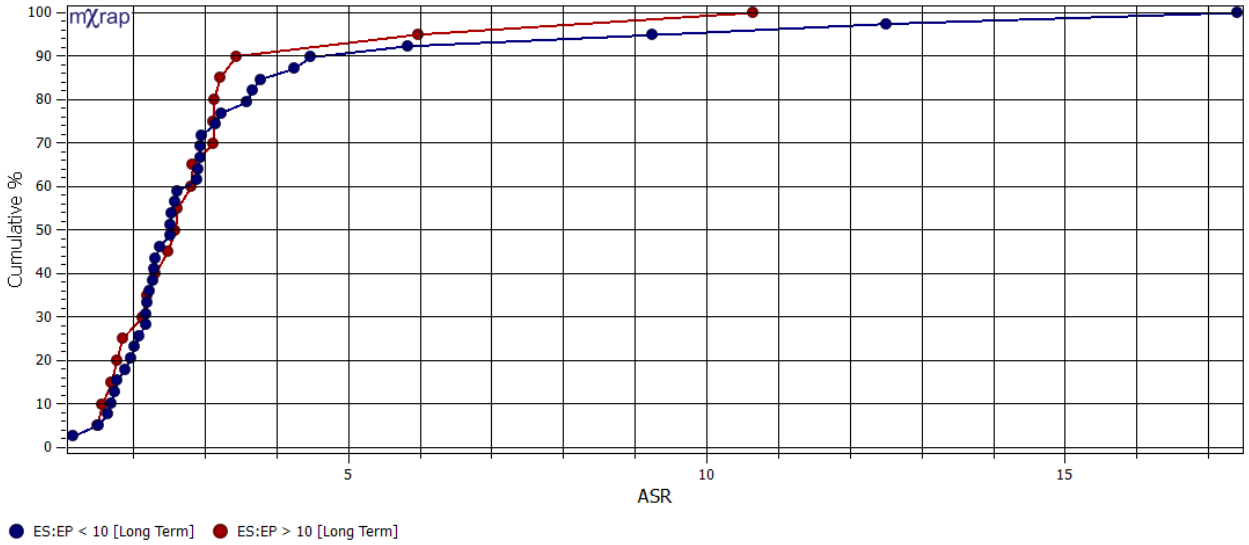

Figure 75: Cumulative distribution of ASR values preceding large events ($M_L \geq 0$) separated by events with ES:EP greater than and less than 10. ASR values are calculated based on long term seismic hazard (preceding year).

In contrast to the difference seen for medium term ASR values, long term values are relatively independent of ES:EP. The two distributions shown in Figure 75 are nearly identical, indicating that use of high ASR values for long term seismic hazard assessment is equally sensitive regardless of source mechanism of large events.

Where other methods of hazard assessment using apparent stress fall short, ASR may be effective. By using a relative ratio as opposed to a singular threshold value, changes in the local rock mass conditions may be identified whether a predominately volumetric fracturing or fault slip source mechanism is generating large and potentially damaging seismic events.

4.3 « Chapter Summary »

The 224 Level to 262 Level of LaRonde mine has been well covered by the microseismic monitoring system through development and production mining. A high quality database of seismic events, $M_L \geq -1.5$, exists for this area. Fifty sample populations have been selected as representative of this area with varying degrees of seismic hazard (25 high hazard populations, 19 moderate hazard populations, and 6 low hazard populations).

Previous attempts to analyze seismic hazard in relation to apparent stress have employed the use of thresholds. Events with AS values exceeding these thresholds were considered high apparent stress events and indicative of elevated seismic hazard. This methodology introduces a new and alternative way of quantifying AS - the apparent stress ratio (ASR). This value is a relative ratio of the 80^{th} to 20^{th} percentile for a cumulative apparent stress distribution of the population. This distribution can be fixed to long, medium, or short term hazard assessment by increasing and decreasing the time window of preceding events to be considered.

An Apparent Stress Ratio Time History (ASRTH) chart can provide insight into a seismic population and the local rock mass conditions. The ASR and peak ASR values for a seismic population provide information relevant to seismic hazard. There is also a potential application for the use of ASR in conjunction with an alarm tool to generate awareness of areas within a mine that are experiencing large changes in local stress conditions.

Chapter 5

5 « Analysis of Results »

The application of peak ASR and ASR for use as an alarm tool has been analyzed in reference to a large area of interest at LaRonde. Examples of the methodology presented in Chapter 4 and results as they pertain to low, moderate, and high hazard populations for long, medium and short term hazard assessment are presented. The objective of this chapter is to demonstrate how ASR can be used in a variety of ways to provide insight into local rock mass conditions and how those conditions translate to seismic hazard.

This analysis chapter:

- Provides examples of peak ASR for long, medium and short term seismic hazard assessment periods.
- Introduces ASR and peak ASR hazard mapping along with examples and analysis.
- Discusses the selection of the percentile values used in the calculation of ASR and an appropriate search radius for generating seismic populations.
- Quantifies the success of ASR as an alarm tool as it applies to an area of interest at LaRonde mine.
- Discusses the selection of appropriate parameter values for use in conjunction with an alarm tool.

5.1 « Peak ASR: Analysis and Examples »

As previously discussed, peak ASR refers to the largest ASR value in a seismic population. It serves as an indicator of the maximum stress change possible within the time period used for calculation of ASR values (long, medium or short). Populations with higher peak ASR values should be considered more hazardous, as the stress conditions within the local rock mass are capable of changing significantly more within the same time period.

Peak ASR values typically surround large magnitude (high apparent stress) events. Prior to the occurrence of a large magnitude event, apparent stress values are often high. Following the large event, local stress conditions are typically reduced and subsequent events have much lower AS values. This results in a large degree of separation between the AS of events prior to and following large events. Large peak ASR values are therefore commonly representative of areas that have experienced large seismic events.

For each time period of seismic hazard assessment, a cumulative distribution of peak ASR values of test and control populations is presented. Test populations contain large events ($M_L \geq 0$) and represent high hazard conditions. Control populations do not contain large events and represent moderate and low hazard conditions. Examples are provided of both expected and unexpected results.

5.1.1 « Long Term Seismic Hazard »

Calculating ASR values for long term seismic hazard (1 year) allows for larger quantities of data to be included, relative to medium and short term seismic hazard, and is therefore capable of representing more gradual changes in stress conditions. Figure 76 is the cumulative distribution of peak ASR values for all test and control populations calculated for long term seismic hazard.

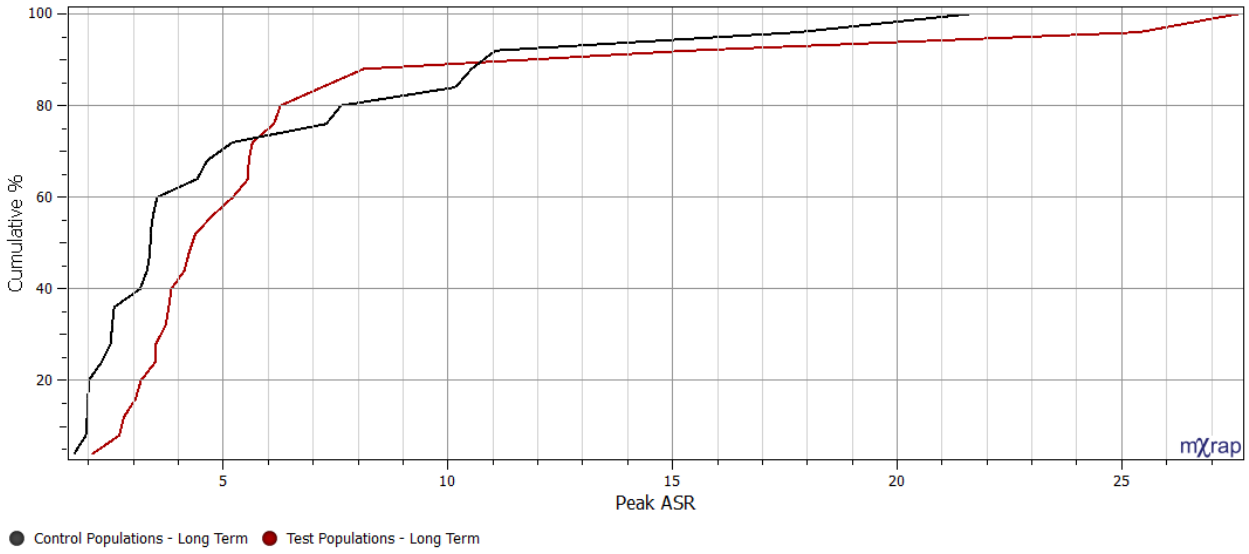

Figure 76: Cumulative distribution for control and test population peak ASR values calculated using long term seismic hazard.

There is a significant separation between the peak ASR values for test and control populations. Unique to long term assessment, the distributions come together and cross at a peak ASR value of approximately 5.7, just above the 70th percentile. This cross over is driven largely by the moderate hazard populations that also generate high peak ASR values when longer time periods are considered.

5.1.1.1 « Long Term Seismic Hazard: Examples »

It is expected that high hazard seismic populations have larger peak ASR values compared to moderated and low hazard populations calculated over the same time period. Figure 77 is a high hazard population with a peak ASR of approximately 12.

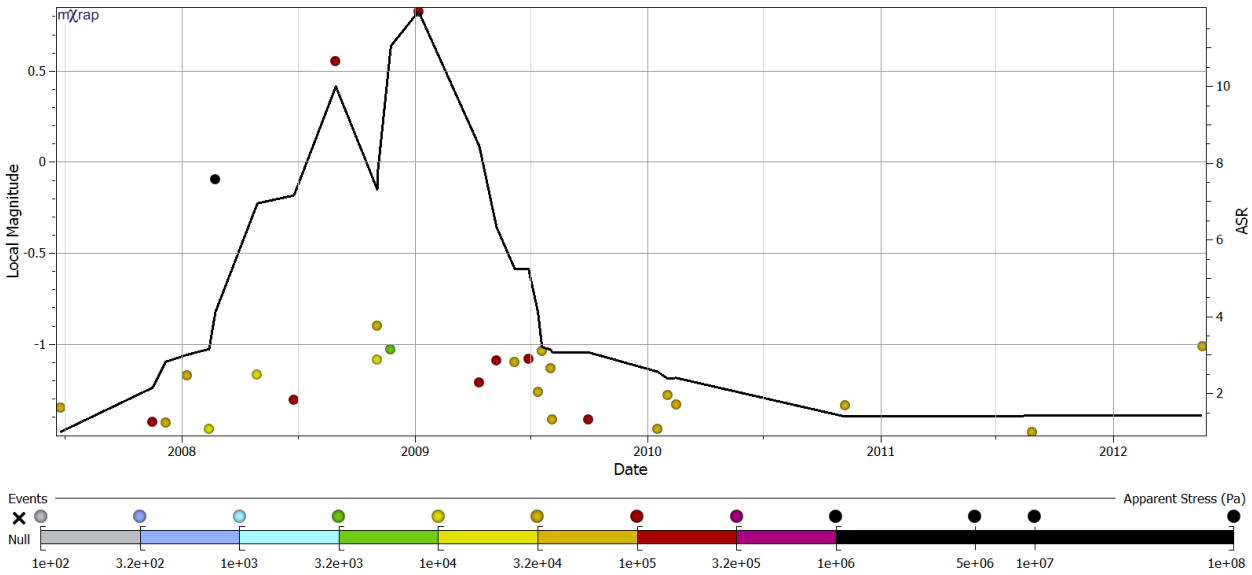

Figure 77: ASRTH Chart of a high hazard seismic population (ID: 18). ASR values calculated for long term seismic hazard are displayed on the secondary y-axis.

ASR values are high throughout the life of this population. ASR reaches a high of approximately 7 prior to the occurrence of the first large event (Aug 2008). The addition of this event to the apparent stress distribution for the population generates a large ASR value of approximately 10. ASR values subsequently drop, but reach a new peak of approximately 11 preceding the largest event contained within this population. This event (Jan 2009), generates the peak of 12, and subsequent ASR values drop as the time window progresses forward and large magnitude and apparent stress events are no longer included. In this population, peak ASR is an excellent indicator of seismic hazard and serves as a successful forecast to the occurrence of large and potentially damaging events.

Moderate hazard populations should have lower peak ASR values than high hazard populations. As discussed in the previous chapter, the classification of seismic populations as moderate hazard indicates the presence of an abnormal response to mining. This is reflected in the peak

ASR values which typically fall between low and high seismic hazard populations. Figure 78 is an example of a moderate seismic hazard population with a peak ASR of approximately 3.5.

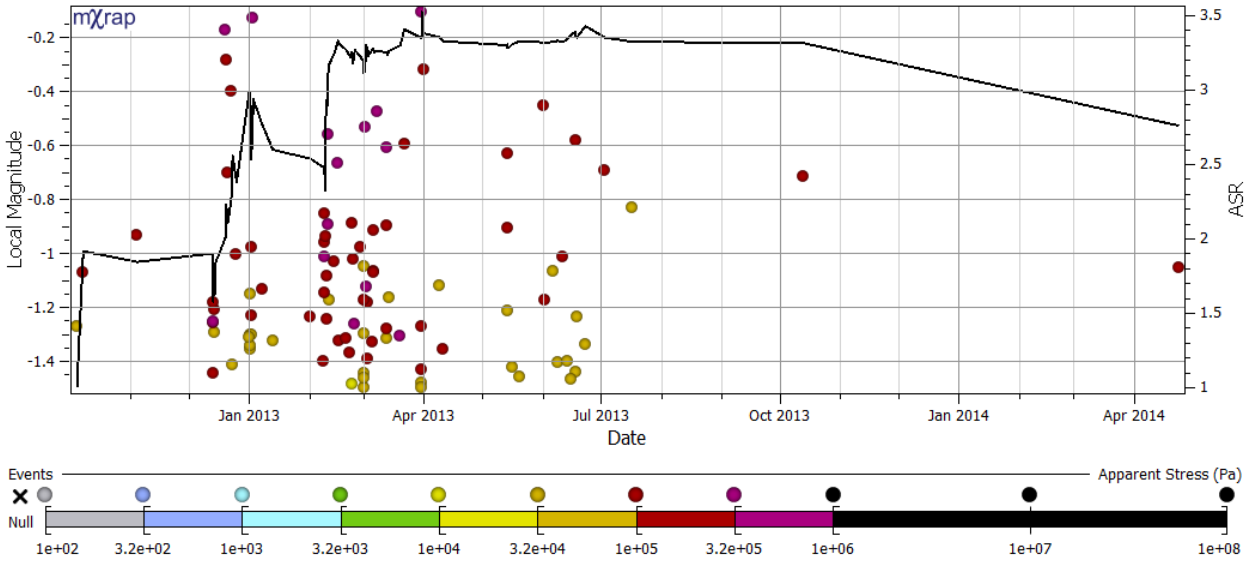

Figure 78: ASRTH Chart of a moderate hazard seismic population (ID: 27). ASR values calculated for long term seismic hazard are displayed on the secondary y-axis.

A peak ASR value of 3.5 indicates there is a reasonable amount of stress increase occurring in the local rock mass. Long time periods allow for events to be included in the apparent stress distribution for an extended period of time and as a result the ASR remains relatively high (compared to low hazard), even after the event rate drops drastically in July 2013.

Low hazard seismic populations should have considerably lower peak ASR values compared to high and moderate hazard populations. Figure 79 is a low hazard population with a peak ASR of approximately 1.7.

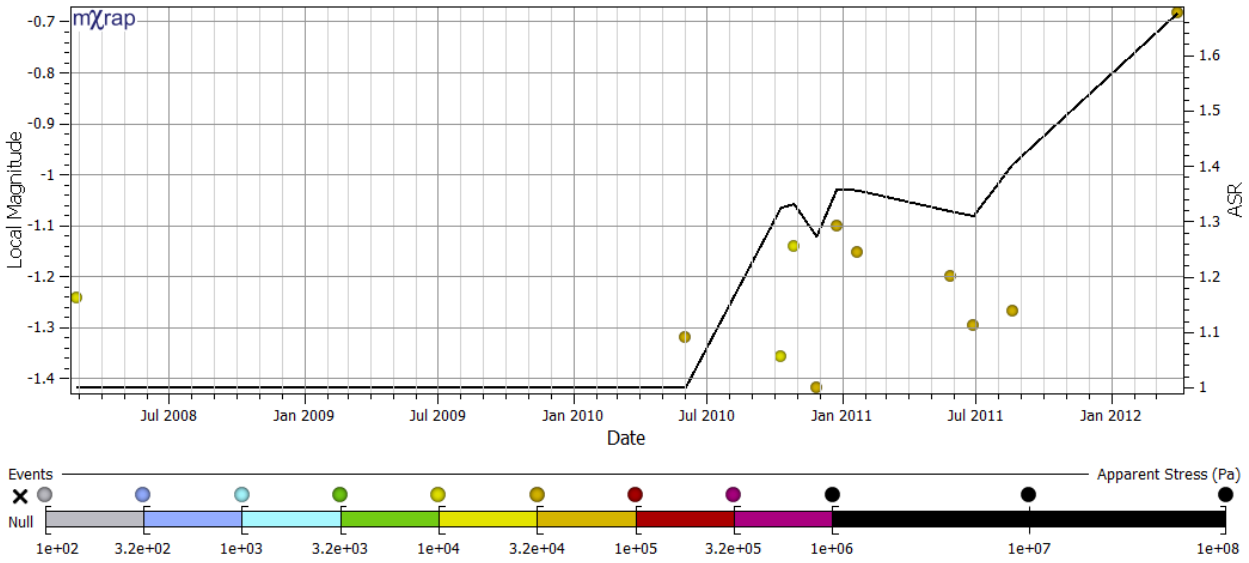

Figure 79: ASRTH Chart of a low hazard seismic population (ID: 49). ASR values calculated for long term seismic hazard are displayed on the secondary y-axis.

There is not much variation in apparent stress values for the events contained within this population. A peak ASR of 1.7 is indicative of low stress increase and low hazard which is clearly representative of this population. There are very few events and all have relatively small magnitudes.

A variety of factors can influence trends in ASR and generate unexpected results. Figure 80 is a high hazard population with a peak ASR of approximately 2.1.

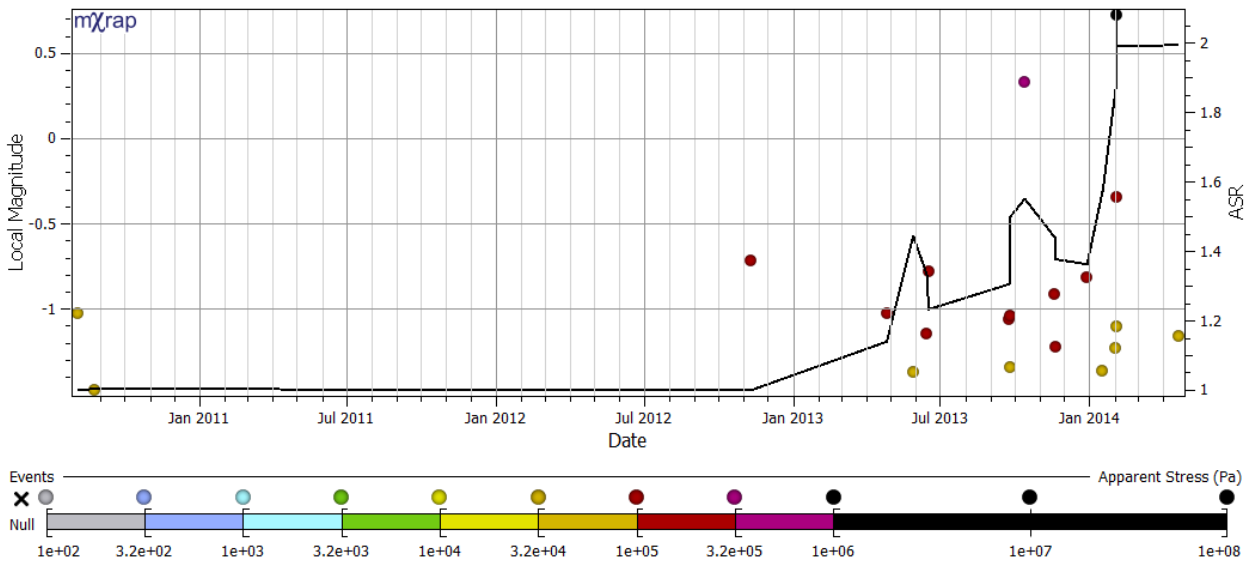

Figure 80: ASRTH Chart of a high hazard seismic population (ID: 22). ASR values calculated for long term seismic hazard are displayed on the secondary y-axis.

This high hazard population has a low event frequency relative to the other populations with a similar hazard classification. As was discussed in 4.2.3.2 « Confidence in ASR », when the event frequency is low, confidence in conclusions drawn from ASR is reduced. The variation of apparent stress values contained within a single calculation time period for this population is not substantial enough to generate the high peak ASR values typical of high hazard populations. Even the occurrence of a very high apparent stress event in January 2014 only generates an ASR value of approximately 2.1. Values of this scale are typically associated with low hazard populations.

In an opposite effect, the low hazard population show in Figure 81 has uncharacteristically high ASR values, including a peak ASR of 11.

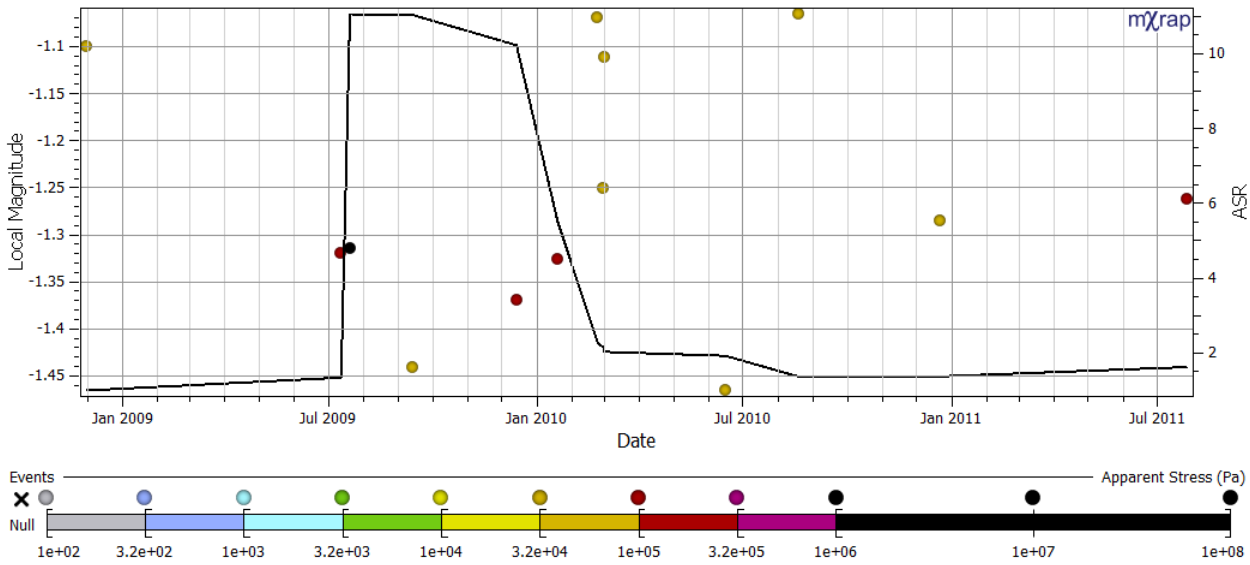

Figure 81: ASRTH Chart of a low hazard seismic population (ID: 45). ASR values calculated for long term seismic hazard are displayed on the secondary y-axis.

Due to the 1 year hazard assessment time frame, a small apparent stress event occurring in December 2008 is included in the calculation for the events in July 2009 and generates the large peak ASR value of 11. If this small event were not included, the ASR value would not be as large. This ASR value is calculated using only 3 seismic events, including an anomalously high AS event, suggesting low confidence in the produced results. When ASR values are calculated using larger quantities of events, they begin to drop to expected values for low hazard populations of less than 2.

Long term ASR values include a longer period of time and are therefore more representative for areas of the rock mass experiencing gradual changes in stress conditions. Even with the extended time period however, the effect of anomalous and small quantities of events on ASR need to be considered. Because the time period is extended, seismic activity that is anomalous or no longer representative of the current stress state affects the ASR values longer.

5.1.2 « Medium Term Seismic Hazard »

Just as with long term peak ASR values, medium term peaks typically surround the occurrence of large magnitude events. Figure 82 is the cumulative distribution of peak ASR values for all test and control populations calculated for medium term seismic hazard.

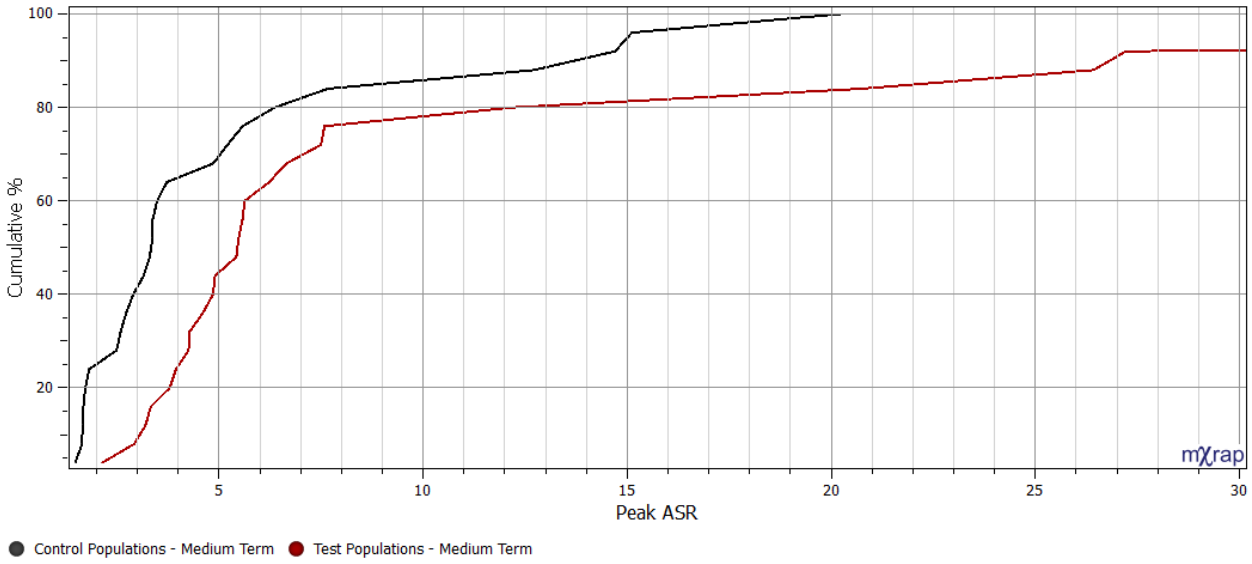

Figure 82: Cumulative distribution for control and test population peak ASR values calculated using medium term seismic hazard.

Medium term peak ASR values for control and test populations possess a large degree of separation. For the distribution shown in Figure 82, a peak ASR value of 5 is equivalent to the 70th percentile for control populations. A peak ASR value of 2 is equivalent to less than the 5th percentile for the test populations. Values less than 2 will therefore be considered indicative of low seismic hazard.

5.1.2.1 « Medium Term Seismic Hazard: Examples »

Just as was demonstrated for long term hazard assessment, high hazard seismic populations should have high peak ASR values when compared to those of moderated and low hazard

populations calculated over the same time period. Figure 89 is a high hazard population with a peak ASR of approximately 27.

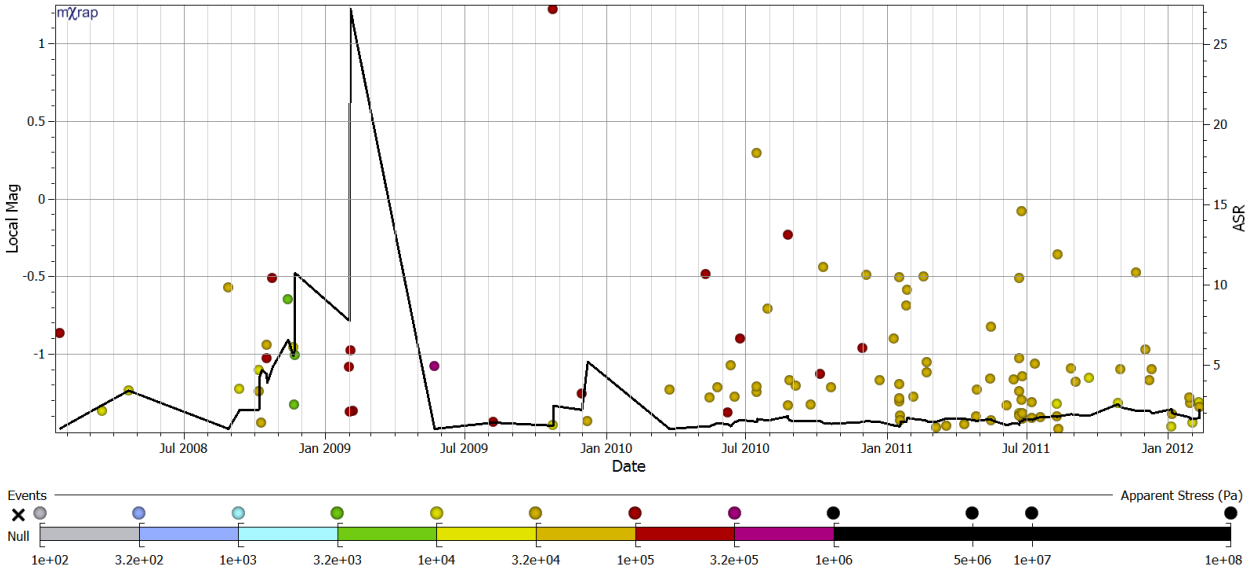

Figure 83: ASRTH Chart of a high hazard seismic population (ID: 6). ASR values calculated for medium term seismic hazard are displayed on the secondary y-axis.

A peak ASR value of 27 is indicative of very high seismic hazard. This indicates the 80th percentile value reached a peak of 27 times larger than the 20th percentile over only a 3 month period. For the population shown in Figure 83, a large degree of variation in the AS values for the events preceding the peak ASR value (August 2008 to March 2009) can be seen. Even in the absence of large events, the ASR values are indicative of high seismic hazard. This indication of high hazard is supported by the large event that occurs just less than a year following the peak ASR.

In terms of moderate hazard seismic populations, peak ASR values should be high but lower than those of high hazard populations. Figure 84 is an example of a moderate seismic hazard population with a peak ASR of approximately 4.8.

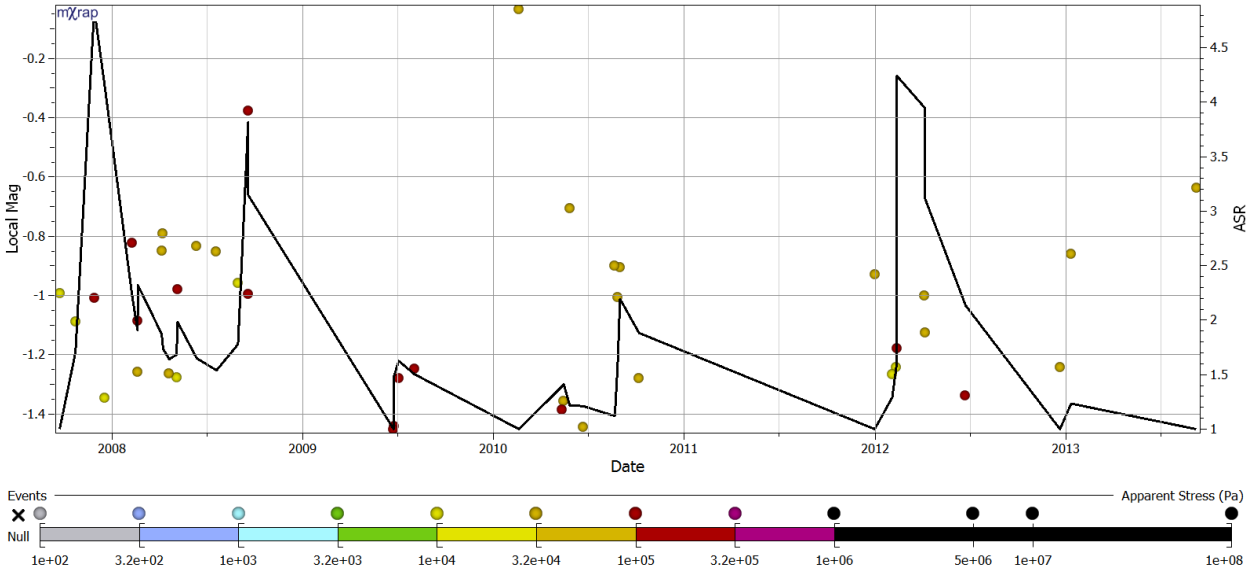

Figure 84: ASRTH Chart of a moderate hazard seismic population (ID: 30). ASR values calculated for medium term seismic hazard are displayed on the secondary y-axis.

It is clear this population represents moderate hazard as it contains a substantial number of seismic events, including one that is nearly $M_L = 0$. Although it has not crossed into the high seismic hazard classification, with a peak ASR of approximately 4.8, it should be considered a moderate seismic risk with future potential to produce large and damaging seismic events.

Low hazard seismic populations should have considerably lower peak ASR values. Figure 85 is a low hazard population with a peak ASR of approximately 1.6.

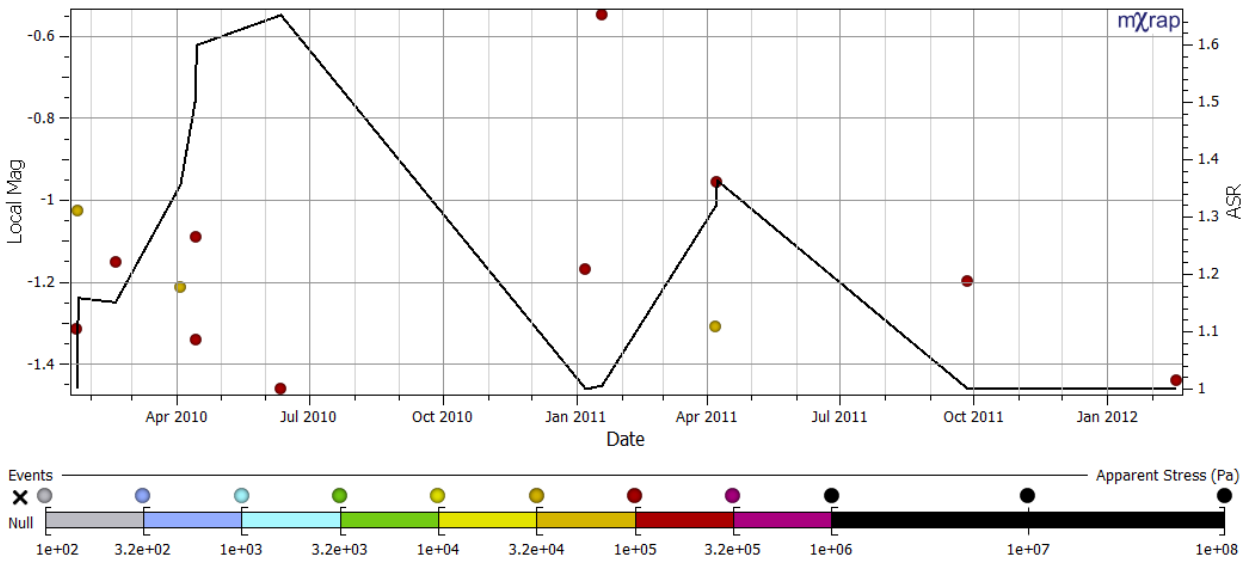

Figure 85: ASRTH Chart of a low hazard seismic population (ID: 46). ASR values calculated for medium term seismic hazard are displayed on the secondary y-axis.

A peak ASR value of 1.6 falls below the set threshold of 2 and is therefore indicative of low seismic hazard. There is very little variation in the apparent stress values of events throughout the entire life of the population and this is reflected in the low ASR values.

Just as before, anomalous seismic activity generates unexpected results for some populations. Figure 86 is a high hazard population with a peak ASR of approximately 2.9.

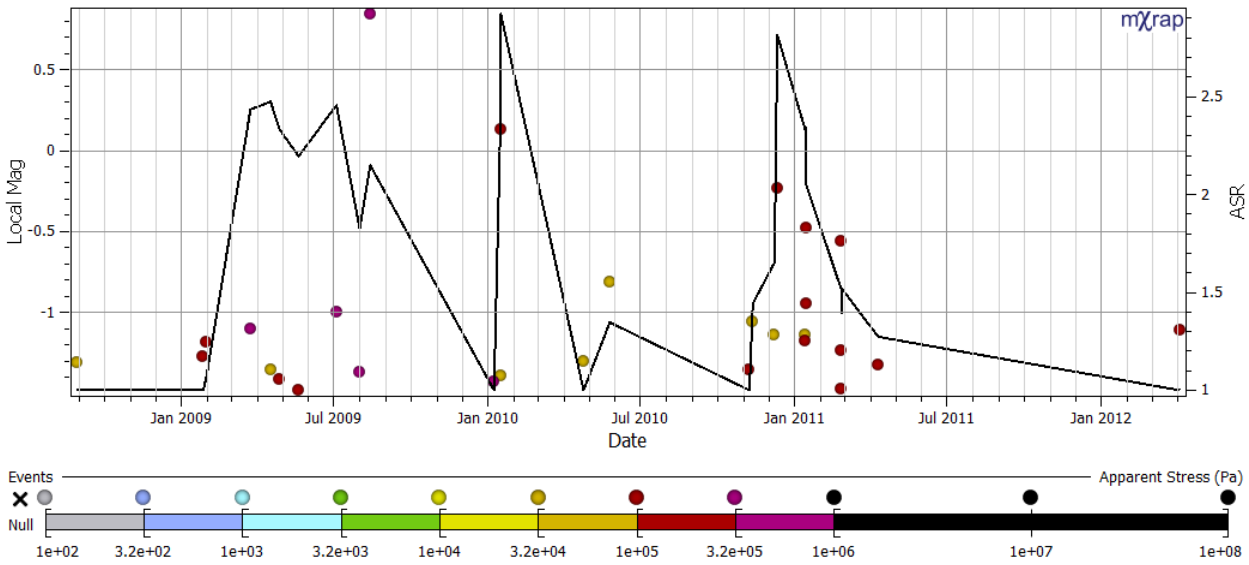

Figure 86: ASRTH Chart of a high hazard seismic population (ID: 15). ASR values calculated for medium term seismic hazard are displayed on the secondary y-axis.

Even with the presence of two large magnitude events, the variation of apparent stress values is not substantial enough for this population to exceed on ASR of 3. Unlike most high hazard npopulations, the first large event in September 2009 does not generate a significant change to local stress conditions. As a result there is no large peak in ASR.

Figure 87 is a low hazard population with a peak ASR of approximately 15. This is substantially higher than expected and would be considered high and hazardous for any population.

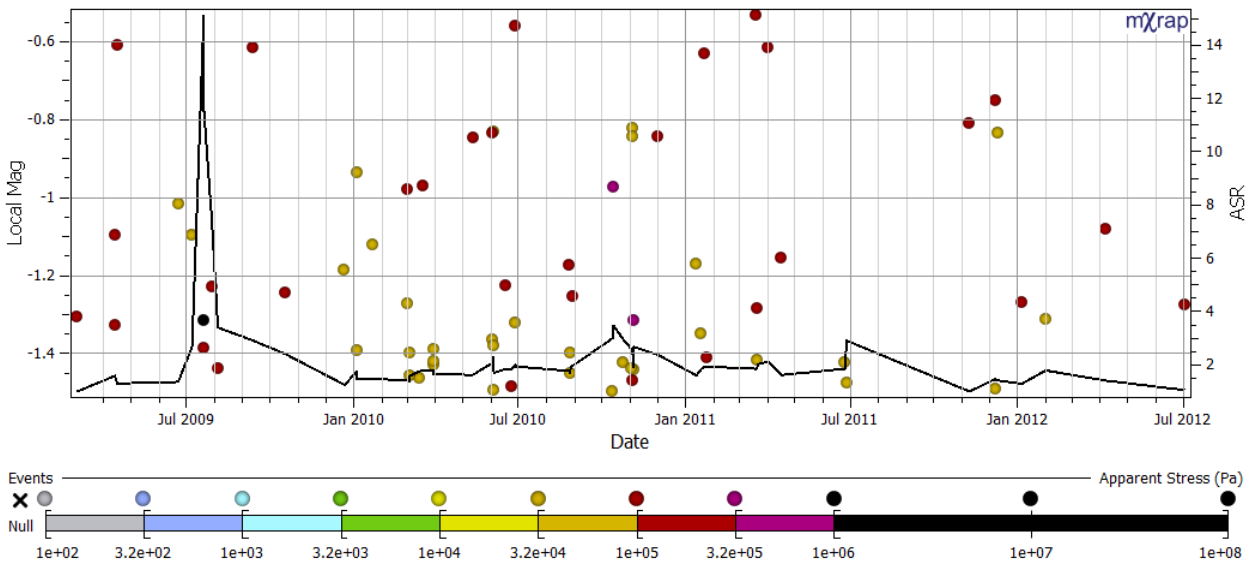

Figure 87: ASRTH Chart of a low hazard seismic population (ID: 28). ASR values calculated for medium term seismic hazard are displayed on the secondary y-axis.

As populations are classified for seismic hazard based on the largest magnitude event they contain, this population is low hazard. Compared to most low hazard populations however it has an abnormally high quantity of seismic events. This population has previously been analyzed in 4.2.3.2 « Confidence in ASR ». The large peak ASR value is a result of an anomalously high AS event contained within a small sub population used for medium term seismic hazard assessment.

Peak ASR values calculated based on medium term hazard assessment are capable of being an indicator of seismic hazard. Like long term seismic hazard assessment they are capable of representing a gradual change in local stress conditions. Because the time period is reduced, anomalous seismic activity influence ASR values for smaller periods of time, but shorter time periods reduce the total quantity of events taken into consideration for ASR value calculations.

5.1.3 « Short Term Seismic Hazard »

Large peak ASR values for short term seismic hazard indicate large increases in stress conditions over very short periods of time (1 week). Figure 88 is the cumulative distribution of peak ASR values for all test and control populations calculated for short term seismic hazard.

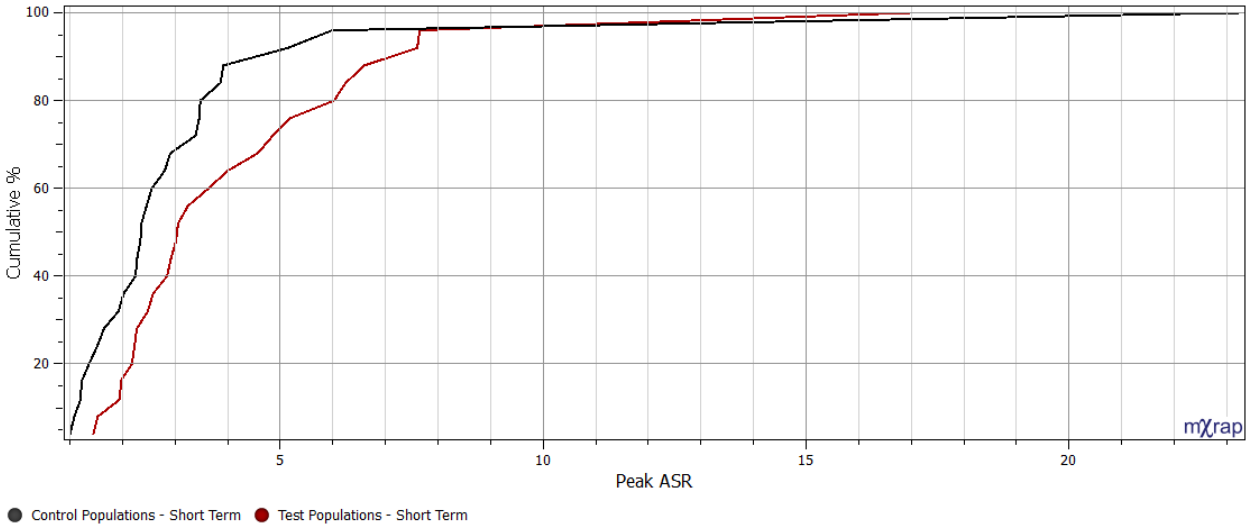

Figure 88: Cumulative distribution for control and test population peak ASR values calculated using short term seismic hazard.

There is a significant difference between the test and control population distributions in Figure 88. Unlike ASR values, peak ASR values are capable of providing meaningful information about seismic hazard over short time periods. Populations that contain large events (test populations) have larger peak ASR values. A peak ASR value of 3 corresponds to approximately the 50^{th} percentile for test populations and the 70^{th} percentile for control populations. The large separation between the test and control populations can be largely attributed to the influence of increased stress conditions and the occurrence of large events.

5.1.3.1 « Short Term Seismic Hazard: Examples »

For high hazard seismic populations, peak ASR values should be high when compared to those of moderate and low hazard populations calculated over the same time period. Figure 89 is a high hazard population with a peak ASR of approximately 6.

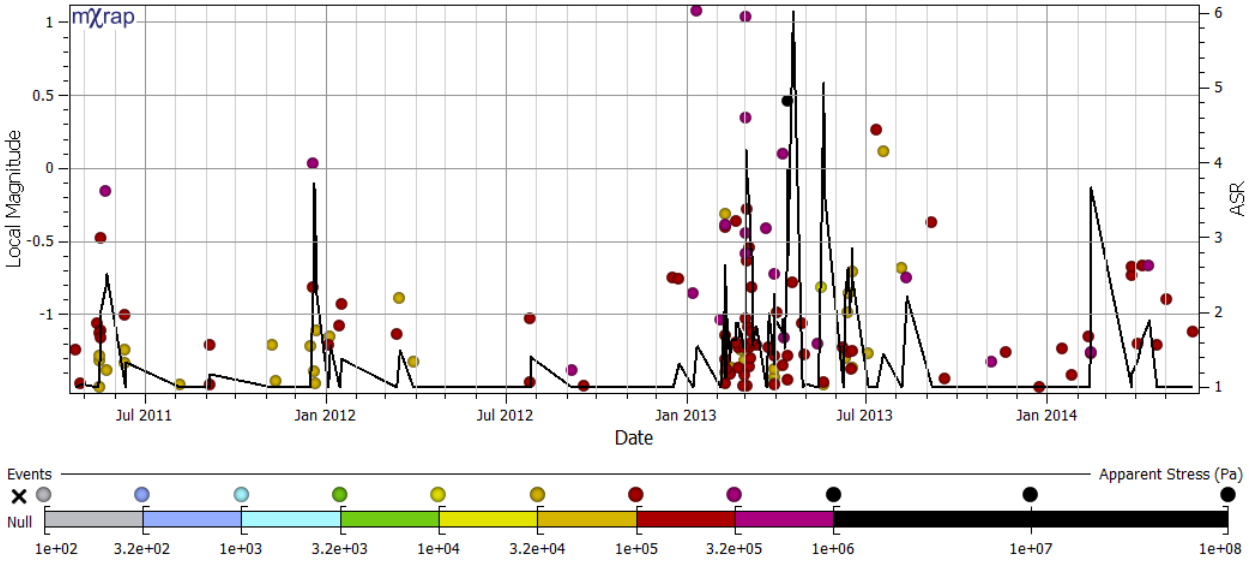

Figure 89: ASRTH Chart of a high hazard seismic population (ID: 9). ASR values calculated for short term seismic hazard are displayed on the secondary y-axis.

A peak ASR value of 6 is indicative of high seismic hazard. It indicates the 80th percentile for the population reached a high of 6 times the 20th percentile over the course of a single week. For the population shown in Figure 89, there are many peaks in ASR that exceed 3. A value of 3 is equivalent to the 70th percentile for control populations and could be considered indicative of moderate to high apparent stress. The first and smallest of the large events within the population generates a peak ASR of approximately 3.8, indicating a high hazard population (Dec 2011). As time progresses and more large events occur within the population, the peak ASR value continues to increase. It reaches an overall peak of 6 in April 2013.

Moderate hazard seismic populations may also contain large peak ASR values, although because they have not had a large event, ASR values may not have reached the same extremes as those of high hazard populations. Figure 90 is an example of a moderate seismic hazard population with a peak ASR of approximately 2.6.

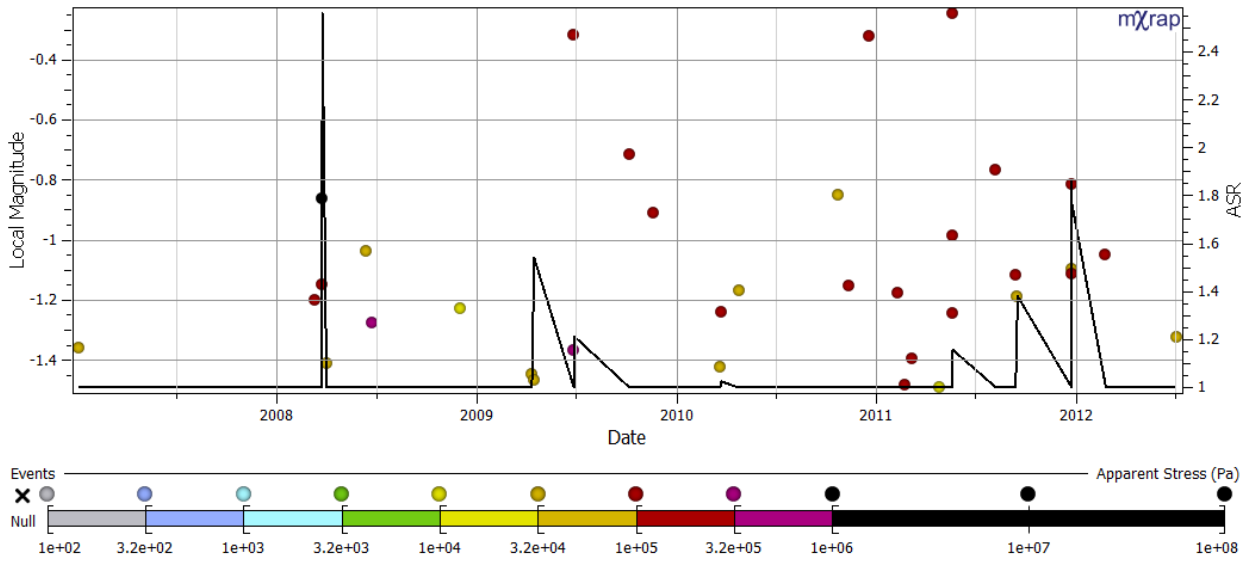

Figure 90: ASRTH Chart of a moderate hazard seismic population (ID: 31). ASR values calculated for short term seismic hazard are displayed on the secondary y-axis.

A peak ASR value of 2.6 is indicative of an elevated but not significantly high stress condition within the rock mass. Low hazard populations are expected to have a peak less than 2, approximately the 10th percentile for test populations. The peak ASR for this population exceeds 2, indicating the 80th percentile more than doubled the 20th percentile over the course of one week.

For low hazard seismic populations, peak ASR values should be much smaller relative to those of high and moderate hazard populations calculated over the same time period. Figure 91 is a low hazard population with a peak ASR of approximately 1.9.

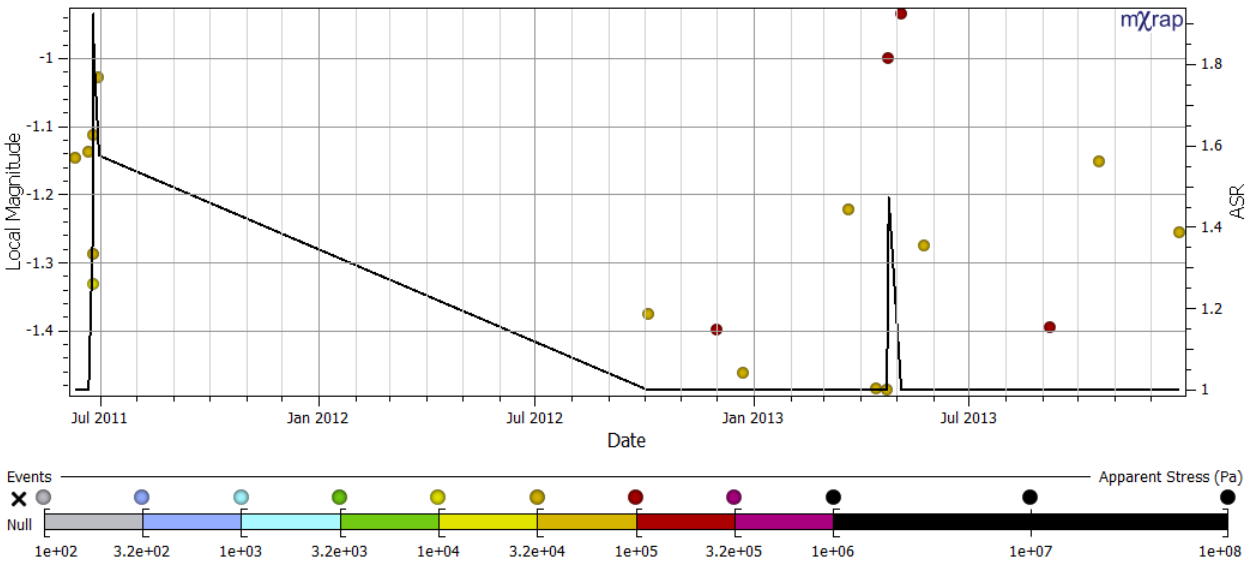

Figure 91: ASRTH Chart of a low hazard seismic population (ID: 39). ASR values calculated for short term seismic hazard are displayed on the secondary y-axis.

A peak ASR value of 1.9 is indicative of low seismic hazard. Even with the increased event frequency generating the peak value at the beginning of the population (July 2011), all events possess very similar apparent stress values and therefore the peak ASR is low.

Similar to the other time periods used for seismic hazard assessment, anomalous seismic activity is capable of generating unexpected results within a population. Using a short time period for ASR value calculations means each individual event that occurs within a population has a substantial impact on the overall AS distribution for the time period. Figure 92 is a high hazard population with a peak ASR of approximately 1.5.

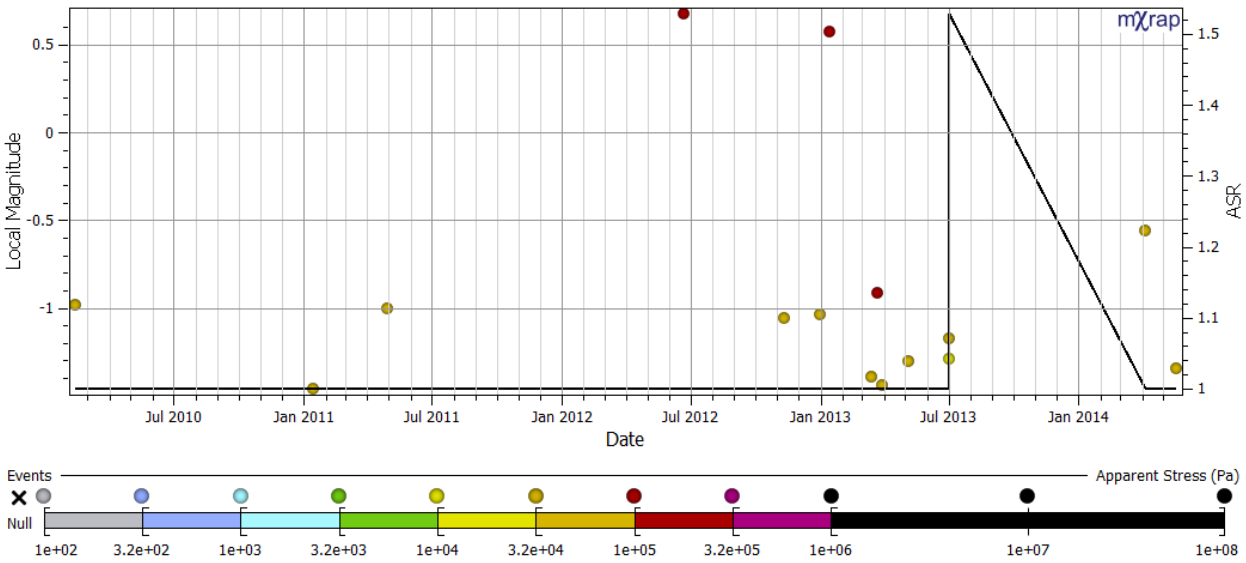

Figure 92: ASRTH Chart of a high hazard seismic population (ID: 25). ASR values calculated for short term seismic hazard are displayed on the secondary y-axis.

Although this population contains events with large magnitudes and varying apparent stress values, the ASR value for nearly the entire life of the population is 1. This is due to the low event rate. There is only a single instance of more than one event occurring over the course of a week. This corresponds to the peak value, but as the two events have nearly the same apparent stress values, the peak ASR is only 1.5. This is the largest drawback to using shortened time periods for seismic hazard assessment. When event frequency is less than the selected time period, ASR values are not meaningful and rarely provide insight into seismic hazard.

As previously discussed, low hazard seismic populations are expected to have a peak ASR value less than 2 when calculated for short time periods. Figure 93 is a low hazard population with a peak ASR of approximately 5.

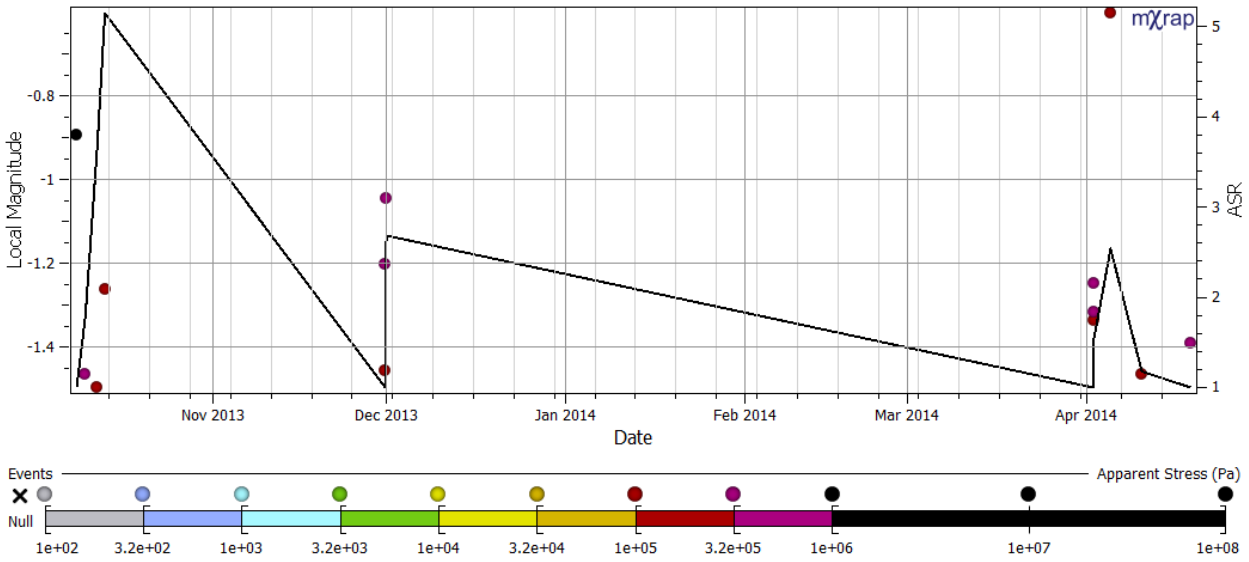

Figure 93: ASRTH Chart of a low hazard seismic population (ID: 44). ASR values calculated for short term seismic hazard are displayed on the secondary y-axis.

The abnormally high peak ASR for this population, occurring in the beginning of October 2013, is a result of a single seismic event with a very high AS value. All events contained within this population have apparent stress values higher than would be expected for such low event magnitudes and frequency. This is an anomalous population that does not conform to typical results and has unexpectedly high ASR values for a population classified as low hazard.

Overall peak ASR values are reasonable indicators of seismic hazard when used for short term assessment. They provide an indication of what areas in a rock mass are capable of increasing/decreasing stress conditions over very short periods of time. When populations contain smaller quantities of seismic events however, short term assessment can produce ASR values that are unrepresentative of the population and consequently the associated hazard.

5.1.4 « Summary of Peak ASR Results »

All three time periods for hazard assessment (long, medium and short), can be used to generate meaningful results in terms of peak ASR values. Short term is more effective for identifying areas of high hazard that experience large scale changes in the local stress conditions very quickly, while medium and long term is more effective for representing areas that experience a more gradual stress increase. For peak ASR values that are more representative of high, moderate, and low hazard areas a medium or long term hazard assessment should be used. Long term calculations are able to accurately represent areas of very gradual stress increase, but any anomalous seismic activity within the population may skew the apparent stress distribution for an extended period of time.

5.2 « Hazard Mapping: ASR »

Hazard maps allow for the spatial variation of seismic parameters, such as ASR, to be easily visualized. In order to generate hazard maps for the area of interest at LaRonde, an approach similar to grid-based hazard mapping is used. Consecutive points, referred to as minodes, along mine excavations are used to generate independent seismic populations as shown in Figure 94.

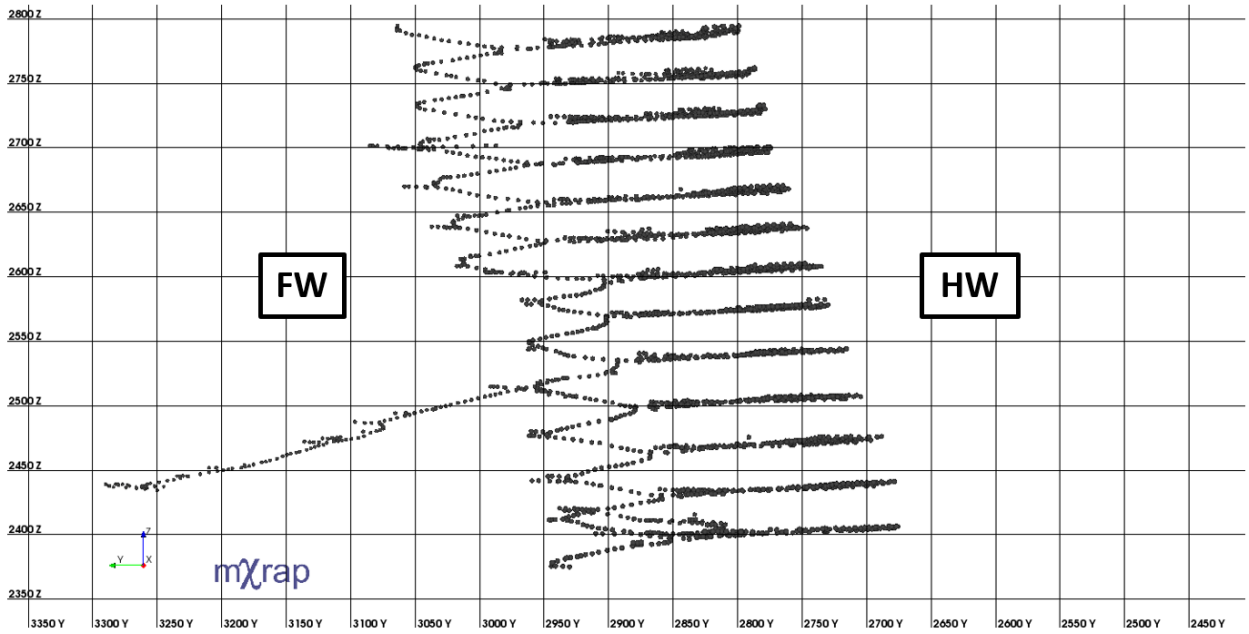

Figure 94: Cross-sectional projection looking East of LaRonde showing minodes used for creating hazard maps.

The minodes shown in Figure 94 are typically less than 5 m apart. Each point is used as a central location for the generation of a seismic population. Each population consists of all seismic events contained within a 30 m search radius, similar to the methodology used to generate sample populations. The ASR value for each population is assigned to the respective minode. Because only the events within the preceding time period of the hazard map creation date are considered, hazard is capable of decreasing over time. This enables ASR to reflect areas that may have yielded and are no longer prone to increasing stress conditions.

Long term ASR seismic hazard assessment appears to generate more stable and meaningful results, relative to medium and short term ASR hazard assessment. For this reason, it is the time period used to analyze the results of ASR hazard mapping. Medium term hazard maps appear to also produce meaningful results and allow for the identification of areas with increasing stress

conditions. Short term ASR hazard maps are dominated by ASR values of 1 and are not recommended to infer seismic hazard.

5.2.1 « Long Term ASR Hazard Mapping Example »

The 255 Level at LaRonde contains large seismic events ($M_L \geq 0$) and consequently areas of elevated seismic hazard. Figure 95 depicts the location of minodes used to generate a long term ASR hazard map for the level.

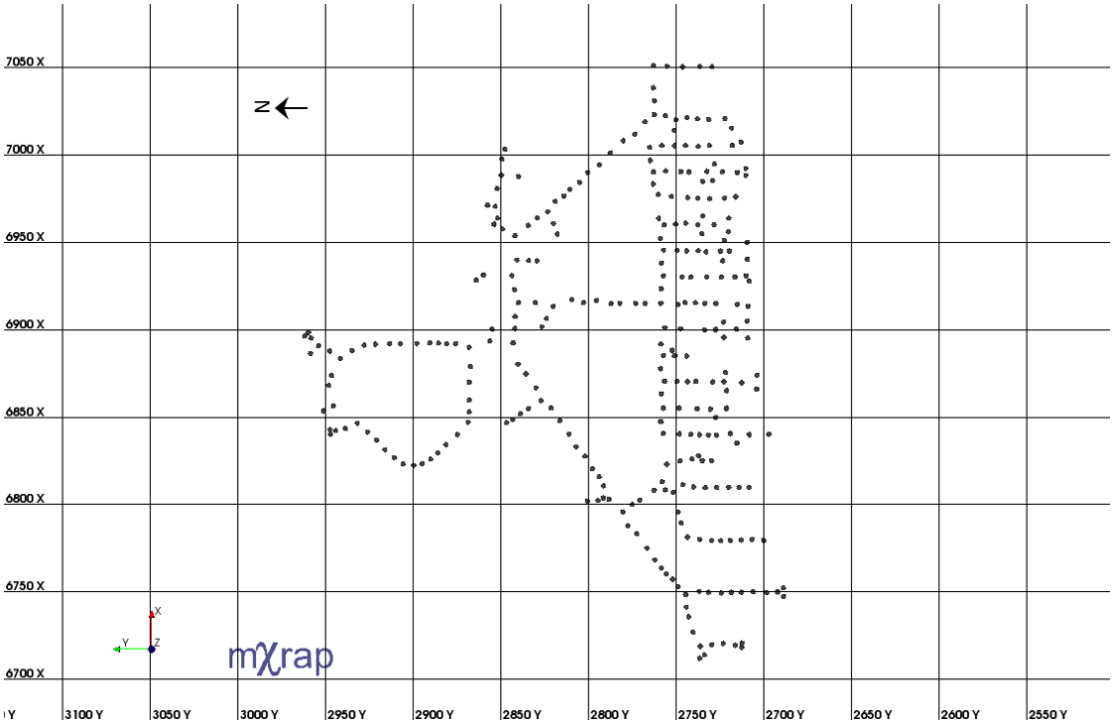

Figure 95: Minodes used for the creation of a hazard map for the 255 Level at LaRonde.

As previously mentioned, only the seismic activity contained within the preceding time period is taken into consideration in an ASR hazard map. Figure 96 is an ASR hazard map using long term seismic hazard assessment as of June 2012 for the 255 Level at LaRonde.

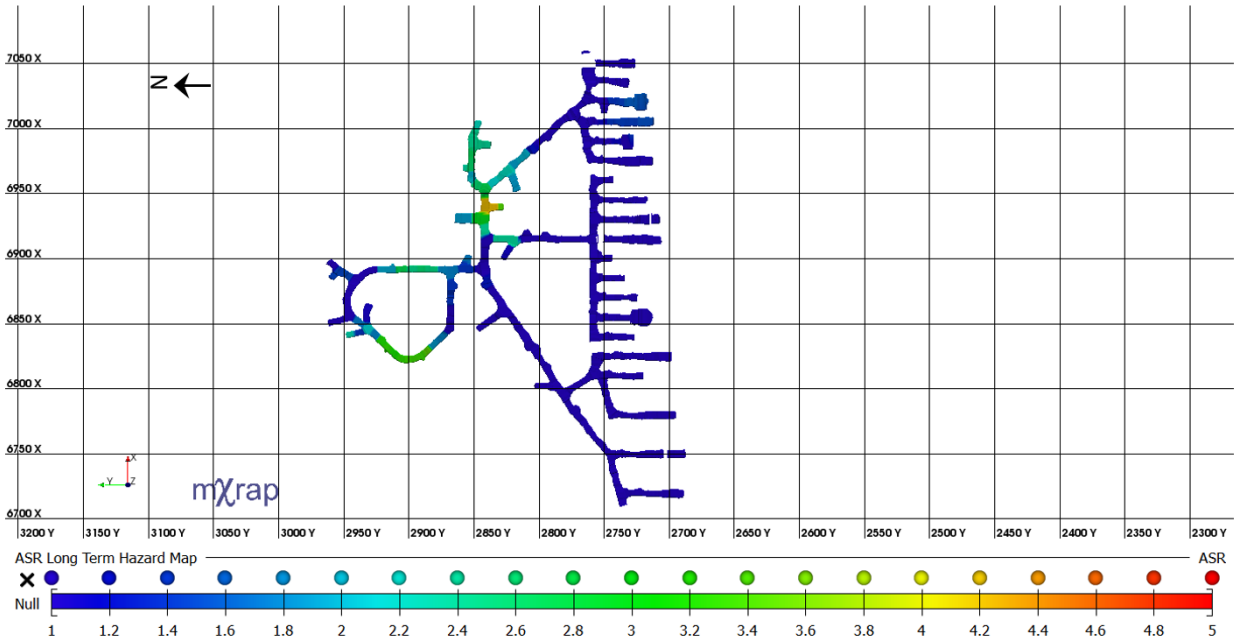

Figure 96: Long term ASR seismic hazard map for the 255 Level at LaRonde generated based on data prior to 06/2012.

This hazard map is based primarily on seismic activity related to development mining as production blasting for this level does not begin until Jan 2013. Areas of elevated hazard appear to be isolated to the FW of the level and ramp area. Figure 97 is an ASR hazard map using long term seismic hazard assessment as of Oct 2013 for the 255 Level at LaRonde.

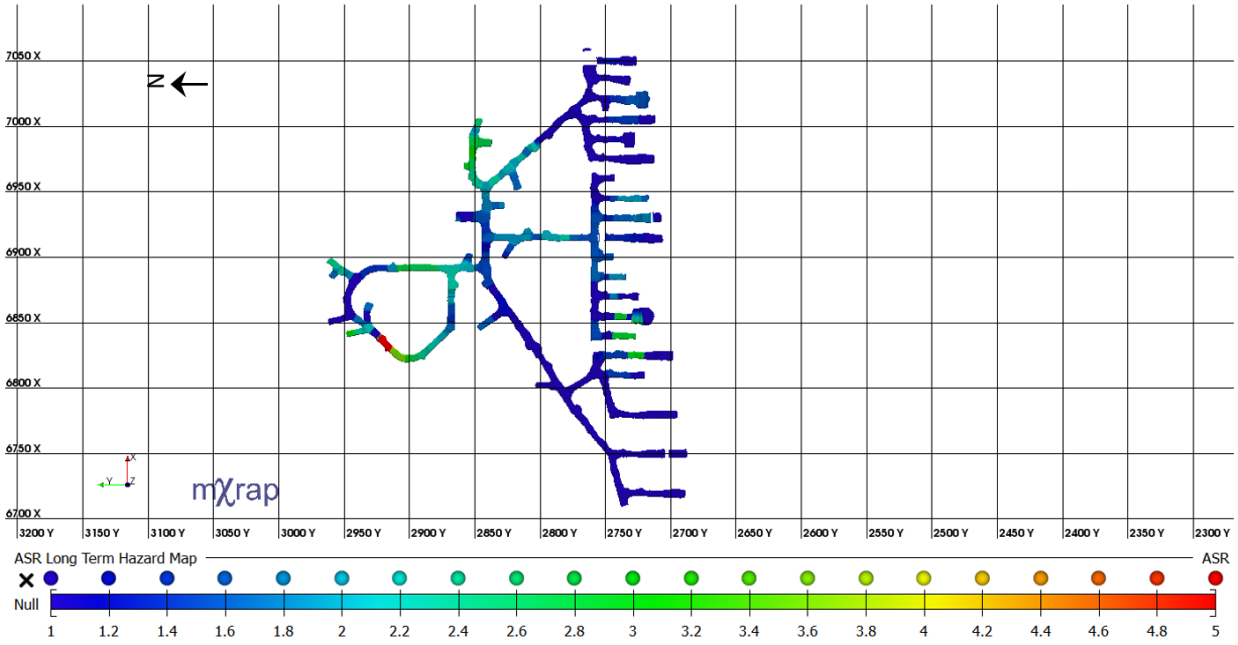

Figure 97: Long term ASR seismic hazard map for the 255 Level at LaRonde generated based on data prior to Oct 2013.

Slight variations in ASR are evident between Figure 97 and Figure 96. The influence from production blasting produces slightly increased ASR values throughout the stoping area. The same areas contained within the FW and ramp area continue to be representative of elevated hazard (Figure 96 and Figure 97). This is significant as more than 1 year separates the date of the two maps and therefore they are based on completely different seismic events. Figure 98 is the same seismic hazard map shown in Figure 97, but with the location of large event (M_L = 0.33) occurring mid-October 2013.

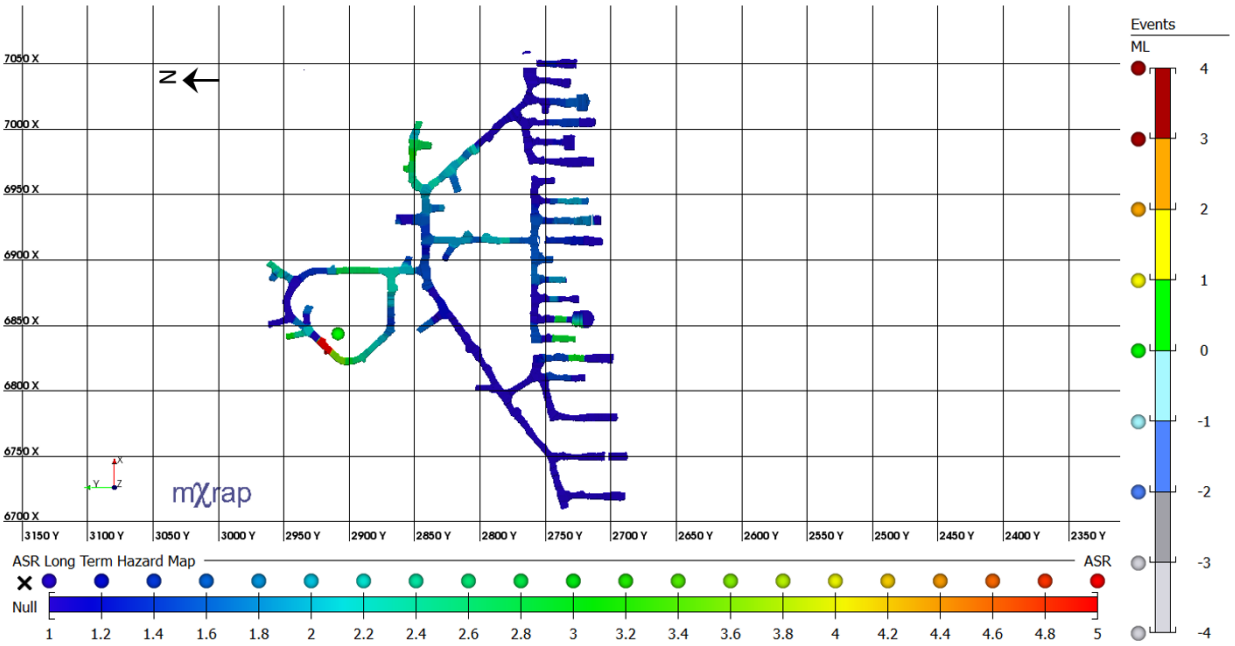

Figure 98: Long term ASR seismic hazard map for the 255 Level at LaRonde generated based on data prior to Oct 2013. A large event (M_L = 0.33) occurring in mid-October 2013 is shown.

Areas identified as having increased stress conditions, high ASR, should be considered more likely to generate large seismic events. The large event occurring in mid-October 2013 (Figure 98), is located in close proximity to areas previously identified as being representative of elevated seismic hazard.

Figure 99 is an ASR hazard map using long term seismic hazard assessment as of Nov 2013 for the 255 Level at LaRonde. The location of two large seismic events (M_L = 0.11 and M_L = 0.5) occurring in mid-November are shown.

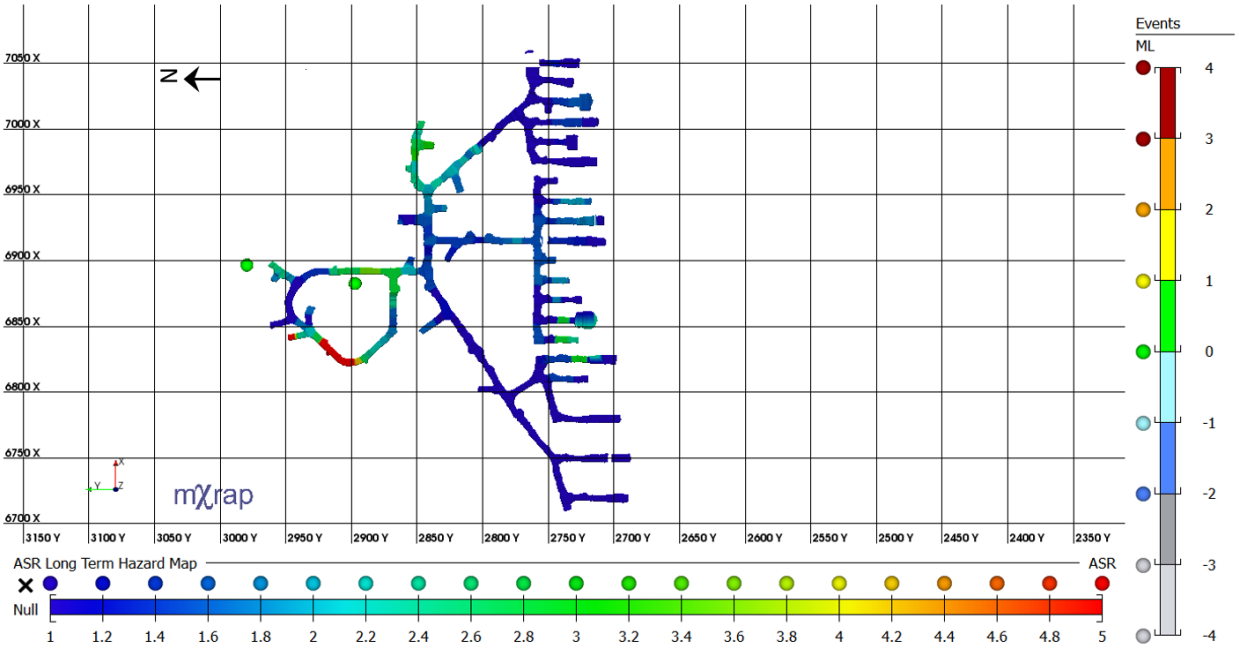

Figure 99: Long term ASR seismic hazard map for the 255 Level at LaRonde generated based on data prior to Nov 2013. Two large events (M_L = 0.11 and M_L = 0.5) occurring on in mid-November are shown.

The hazard map shown in Figure 99 is based solely on data prior to the occurrence of the two events. Similar to the previous example, the location of the two events correspond to areas of increased stress and ASR.

Figure 100 is an ASR hazard map using long term seismic hazard assessment as of Dec 2013 for the 255 Level at LaRonde. The location of a large seismic event (M_L = 1.13) occurring at the end of December is shown.

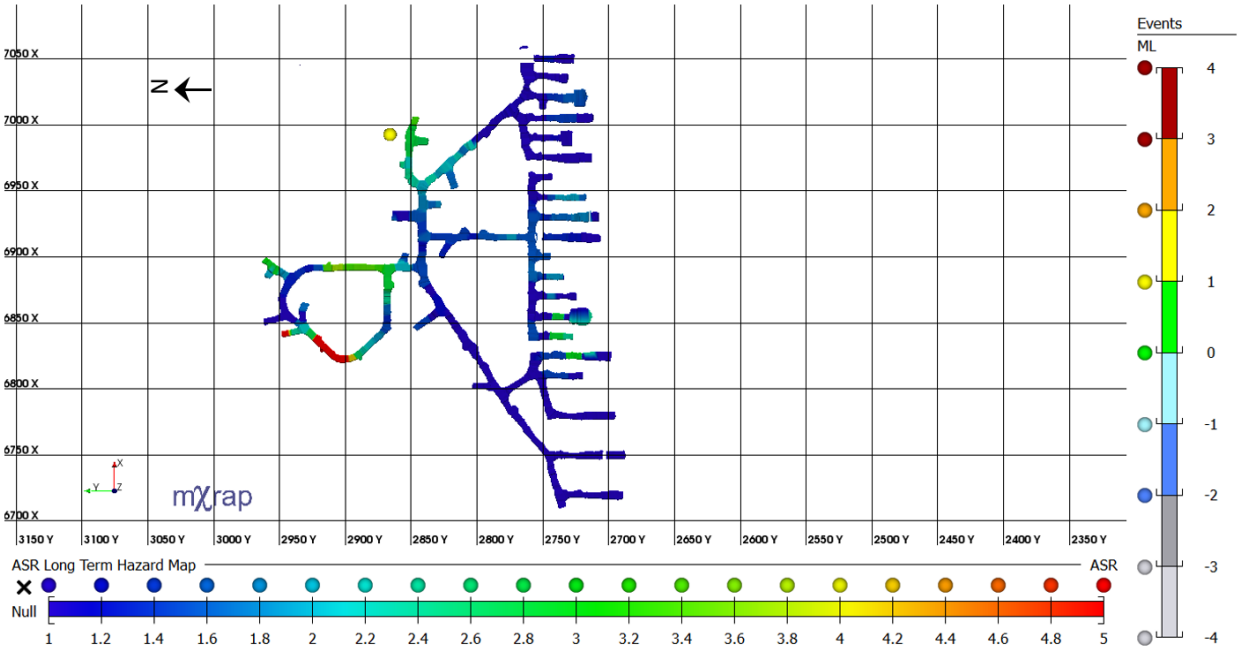

Figure 100: Long term ASR seismic hazard map for the 255 Level at LaRonde generated based on data prior to 12/2013. A large event (M_L = 1.13) occurring on 31/12/2013 is shown.

The location of this event, the largest to occur on the level, corresponds to an area that was originally identified (Figure 96) as possessing elevated ASR values and seismic hazard. Areas where large events have previously occurred, such as the ramp area, continue to show increasing stress conditions.

Figure 101 is an ASR hazard map using long term seismic hazard assessment as of Feb 2015 for the 255 Level at LaRonde.

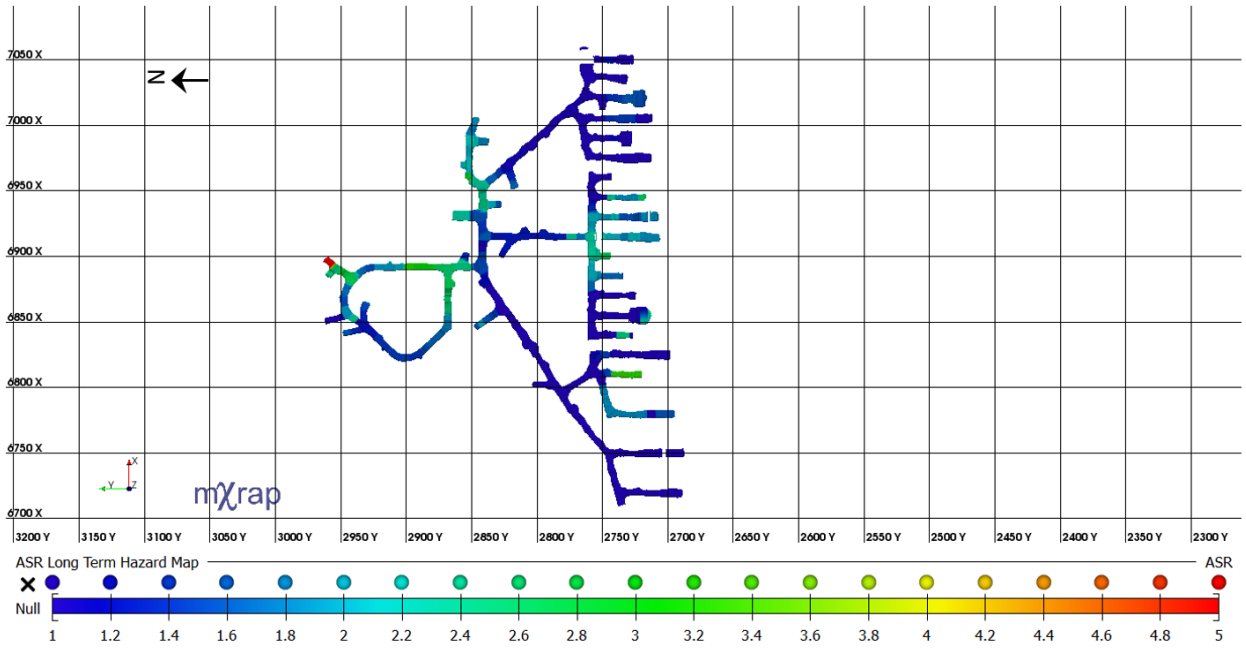

Figure 101: Long term ASR seismic hazard map for the 255 Level at LaRonde generated based on data prior to 02/2015.

With over one year separating the hazard maps shown in Figure 100 and Figure 101, they are generated based on entirely different seismic events. Areas that have been previously identified as possessing increasing stress conditions and elevated seismic hazard, now have reduced ASR values. Drifts within the orebody have larger ASR values then seen in previous hazard maps, which may be attributed to the continued influence of stope blasting.

5.2.2 « Summary of ASR Hazard Mapping Results »

Hazard maps generated using ASR values are capable of providing a visual representation of areas within a mine that may be experiencing increased stress. These areas change over time in correlation to recent seismic activity. This allows for long and short term trends to be identified within the rock mass. Areas that maintain ASR values indicative of moderate to high seismic hazard over extended periods of time should be considered of particular concern. When the historic and present seismic response is similar, it may indicate the presence of factors such as

unfavourable geological conditions or areas of stress concentration. Areas that have large ASR values for shorter periods of time may be of less concern as they could represent local stress redistribution that will shift and diminish over time.

5.3 « Hazard Mapping: Peak ASR »

Peak ASR appears to be an effective indicator of increasing stress conditions and elevated seismic hazard. High hazard populations are characterized by large peak ASR values and low hazard populations are characterized by smaller peak ASR values. Unlike ASR, peak ASR serves as an indicator of seismic hazard across all time assessment periods (long, medium and short).

Peak ASR hazard maps employ the same methodology used to generate ASR hazard maps. Different from ASR based maps however, peak ASR maps incorporate and represent the entire historic seismic response to mining in the area. Assessment time periods are only considered in the calculation of individual ASR values, and the peak ASR value is taken from all previously calculated ASR values. As a result, peak ASR values cannot decrease over time.

5.3.1 « Long Term Peak ASR Hazard Map »

Large peak ASR values calculated based on long term hazard assessment have been shown to correspond well to areas of increasing stress conditions and elevated seismic hazard. Figure 102 and Figure 103 are longitudinal and cross-sectional projections of a peak ASR hazard maps generated using long term seismic hazard assessment for LaRonde.

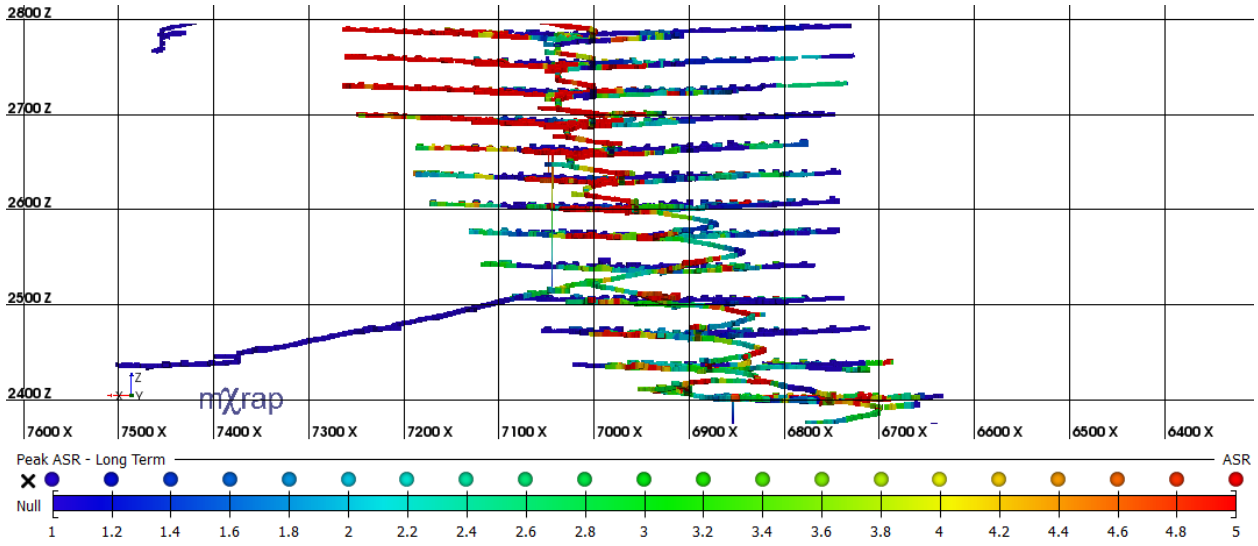

Figure 102: Longitudinal projection looking south of a peak ASR hazard map for LaRonde. Drifts are coloured according to peak ASR values calculated for long term seismic hazard assessment.

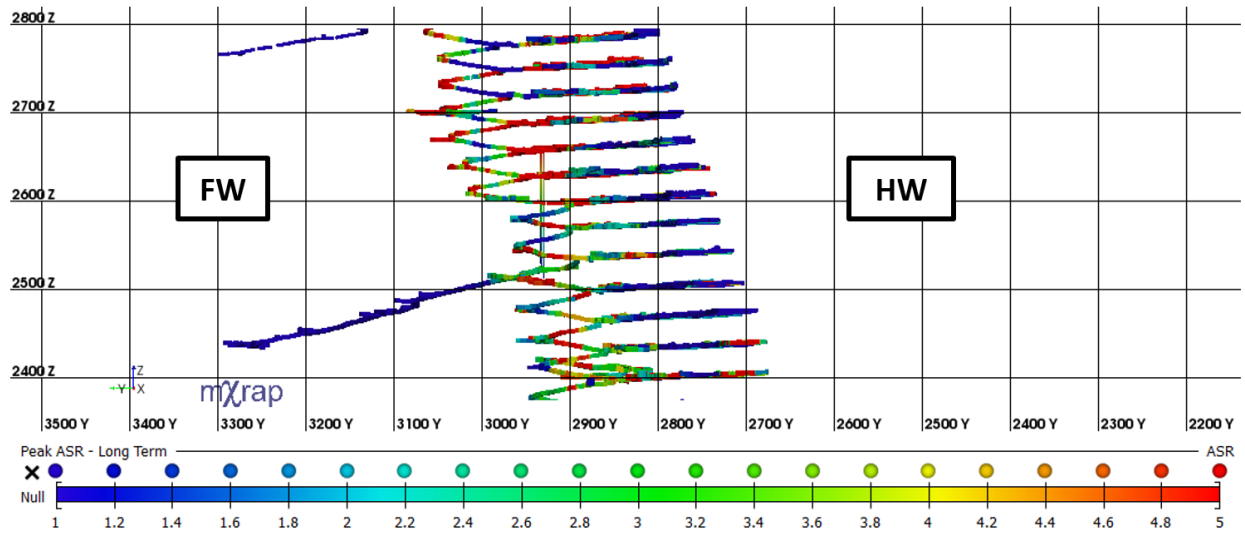

Figure 103: Cross-sectional projection looking east of a peak ASR hazard map for LaRonde. Drifts are coloured according to peak ASR values calculated for long term seismic hazard assessment.

Areas of elevated hazard appear to be concentrated in the FW and Eastern portion of the orebody. These regions correspond to the location of the majority of large events at LaRonde.

Based on the typical seismic response and geological conditions present at LaRonde, elevated hazard areas are expected to be concentrated in the FW and Eastern portion of the orebody. Both of these trends are clearly evident in the hazard map shown in Figure 102 and Figure 103.

5.3.1.1 « Long Term Peak ASR Hazard Map: Examples »

Individual hazard maps of the 224, 242 and 262 Levels are shown in Figure 104, Figure 105, and Figure 106 respectively. These levels were selected as the represent the top, middle and bottom of the area of interest at LaRonde. In each level map, the trends shown previously in the long and cross sections are clearly visible. The location of all large events ($M_L \geq 0$) are shown to provide an indication of where high hazard areas with large peak ASR values should be concentrated.

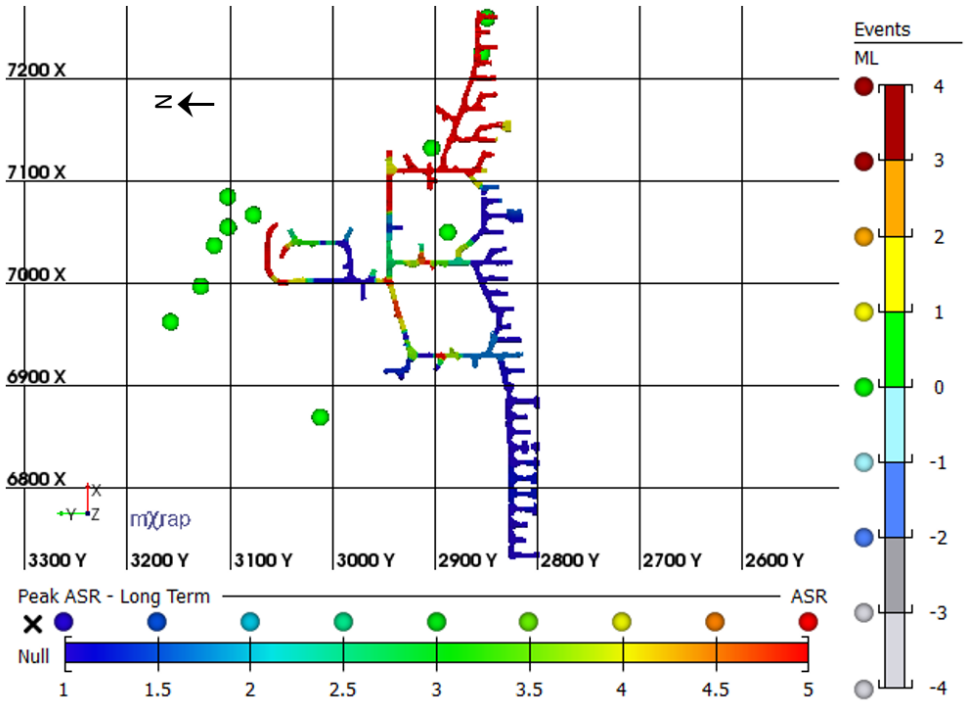

Figure 104: Peak ASR hazard map for 224 Level. Drifts are coloured according to peak ASR values calculated for long term seismic hazard.

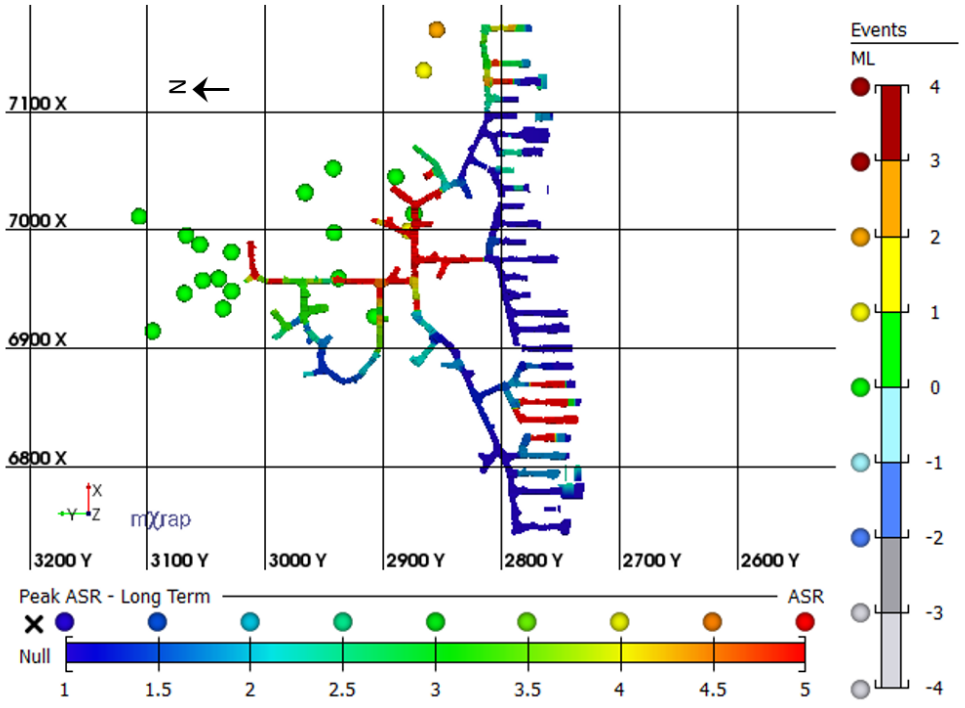

Figure 105: Peak ASR hazard map for 242 Level. Drifts are coloured according to peak ASR values calculated for long term seismic hazard.

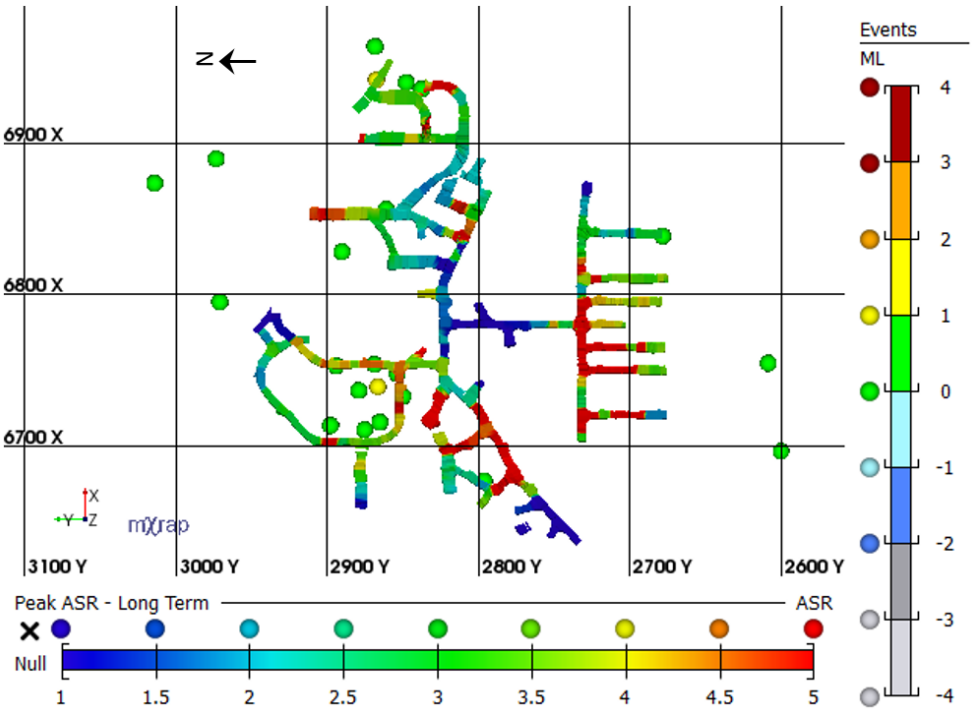

Figure 106: Peak ASR hazard map for 262 Level. Drifts are coloured according to peak ASR values calculated for long term seismic hazard.

The locations of large events clearly correspond to regions of moderate and high seismic hazard based on peak ASR values. The Eastern side of the orebody and drifts located into the FW appear to be primarily representative of moderate and high seismic hazard, while the Western side of the orebody represents low seismic hazard. These trends are expected based on the historical seismic response and known geological conditions at LaRonde.

5.3.2 « Medium Term Peak ASR Hazard Map »

As was previously demonstrated, medium term hazard assessment for peak ASR values is capable of providing meaningful results. Figure 107 and Figure 108 are longitudinal and cross-sectional projections of peak ASR hazard maps generated using medium term seismic hazard assessment for LaRonde.

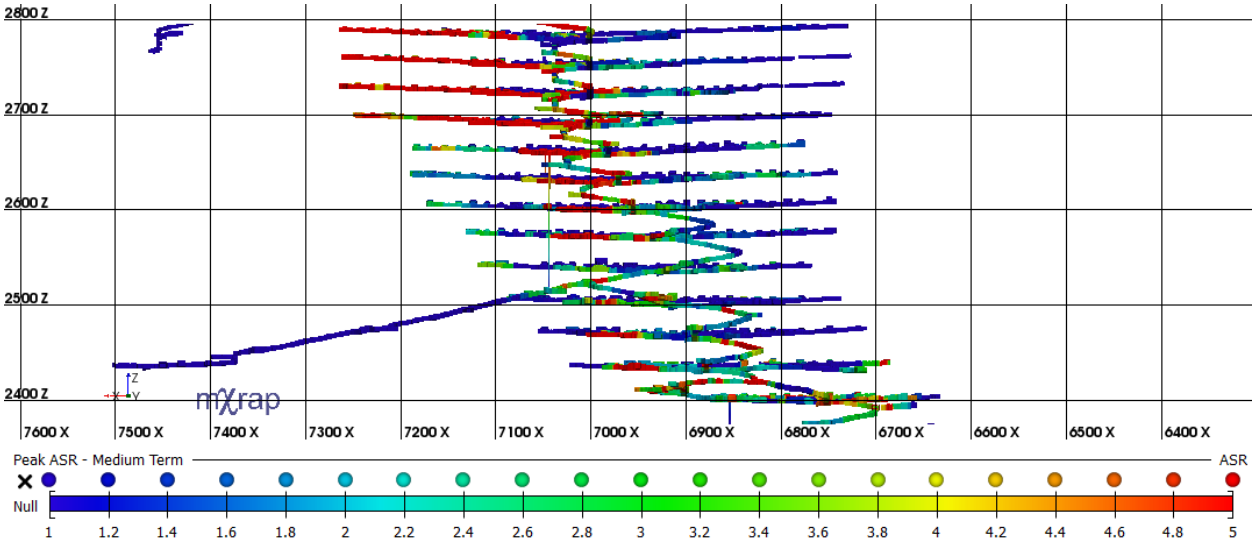

Figure 107: Longitudinal projection looking south of a peak ASR hazard map for LaRonde. Drifts are coloured according to peak ASR values calculated for medium term seismic hazard assessment.

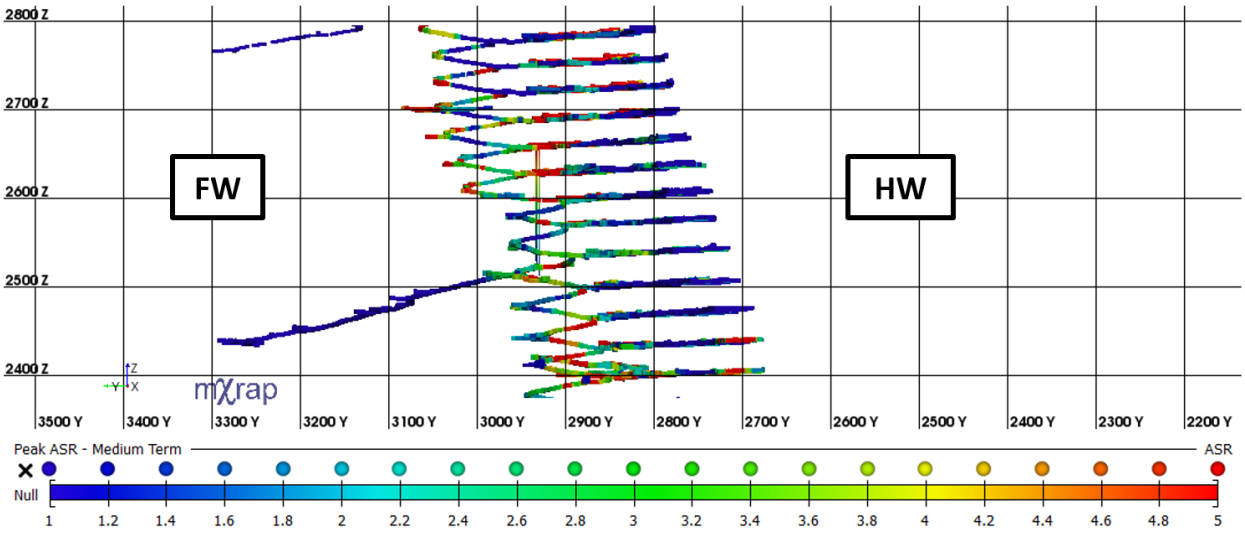

Figure 108: Cross-sectional projection looking east of a peak ASR hazard map for LaRonde. Drifts are coloured according to peak ASR values calculated for medium term seismic hazard assessment.

The same trends evident in hazard map based on long term assessment are present in Figure 107 and Figure 108. Areas with large peak ASR values are concentrated in the FW and Eastern portion of the orebody.

5.3.2.1 « Medium Term Peak ASR Hazard Map: Examples »

Hazard maps of 224 Level, 242 Level and 262 Level are shown in Figure 109, Figure 110, and Figure 111 respectively. All large events ($M_L \geq 0$), are plotted on the levels to indicate areas that should be considered representative of high and moderate seismic hazard.

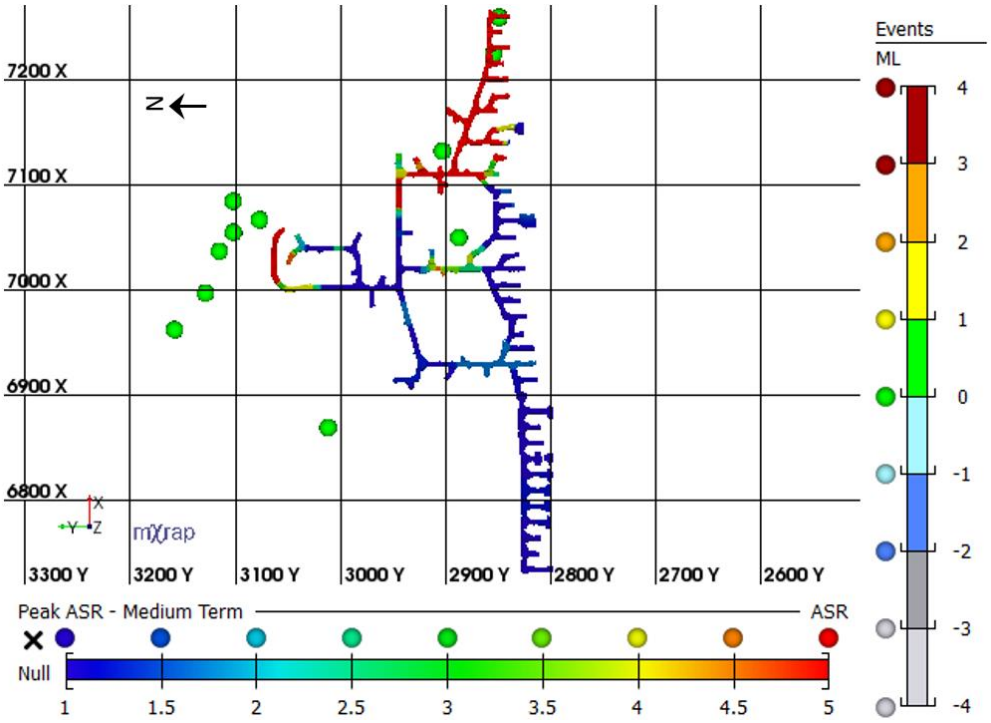

Figure 109: Peak ASR hazard map for 224 Level. Drifts are coloured according to peak ASR values calculated for medium term seismic hazard.

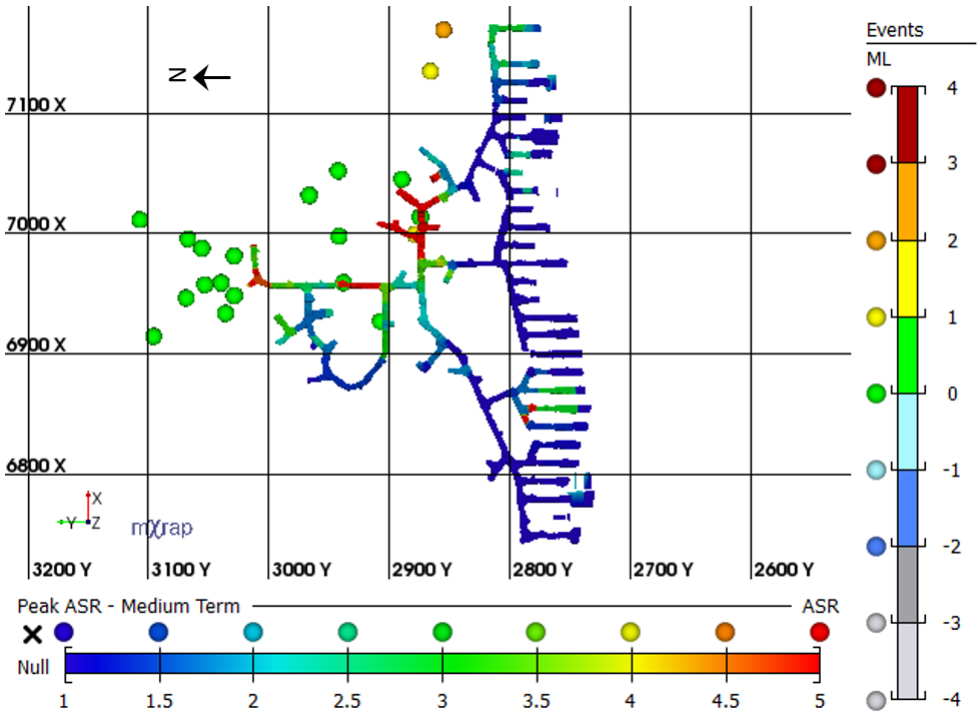

Figure 110: Peak ASR hazard map for 242 Level. Drifts are coloured according to peak ASR values calculated for medium term seismic hazard.

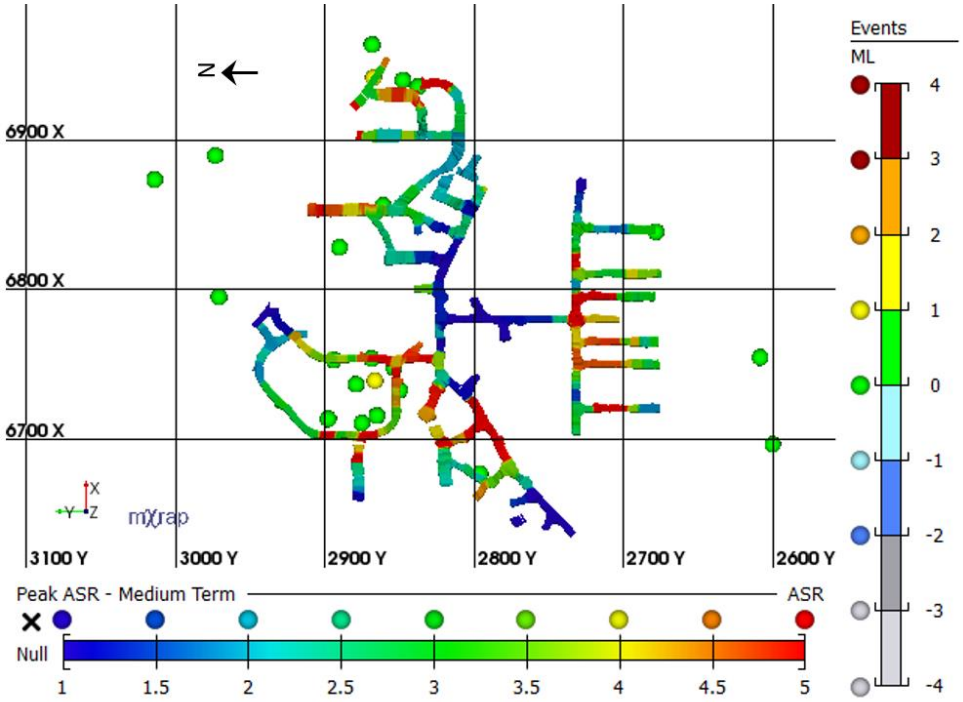

Figure 111: Peak ASR hazard map for 262 Level. Drifts are coloured according to peak ASR values calculated for medium term seismic hazard.

Hazard maps generated using medium term hazard assessment are very similar to those generated using long term hazard assessment. Both maps have concentrated areas of large peak ASR values corresponding to areas previously identified at LaRonde as representing elevated seismic hazard (primarily the FW).

5.3.3 « Short Term Peak ASR Hazard Map »

Peak ASR values calculated using short term hazard assessment are more meaningful than ASR values calculated over the same time period for hazard assessment. Because there are many populations within the area of interest that have an event frequency less than 1 event per week, the majority of ASR values calculated for short term seismic hazard assessment are 1. Peak ASR values however represent areas that experienced large stress increases within the short assessment time period of 1 week. Figure 112 and Figure 113 are longitudinal and cross-

sectional projections of a peak ASR hazard maps generated using short term seismic hazard assessment for LaRonde.

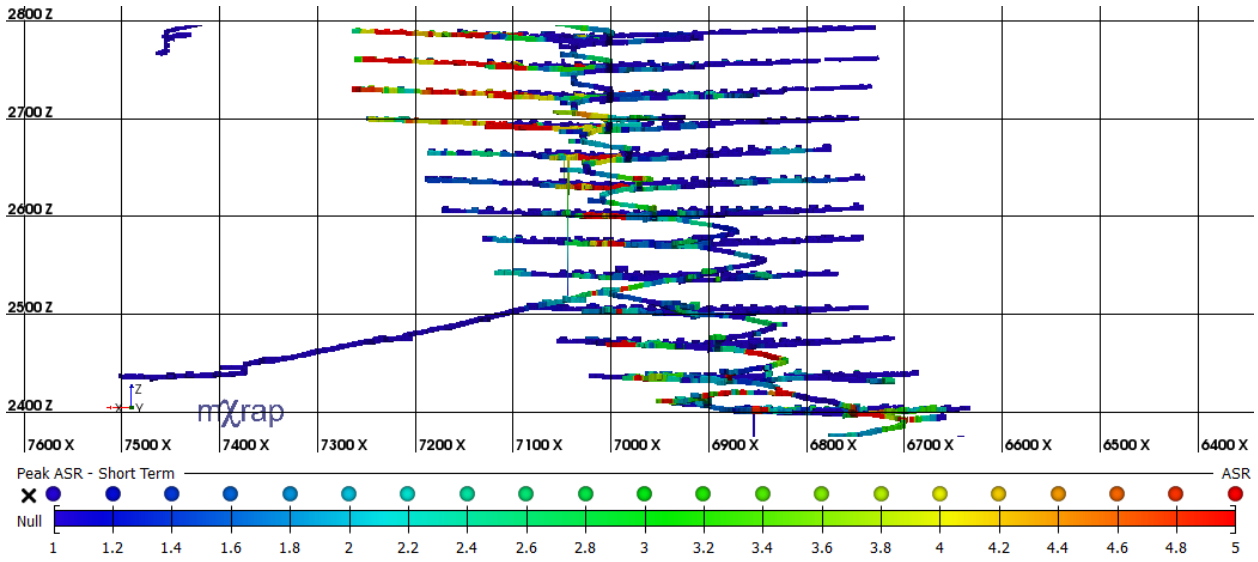

Figure 112: Longitudinal projection looking south of a peak ASR hazard map for LaRonde. Drifts are coloured according to peak ASR values calculated for short term seismic hazard assessment.

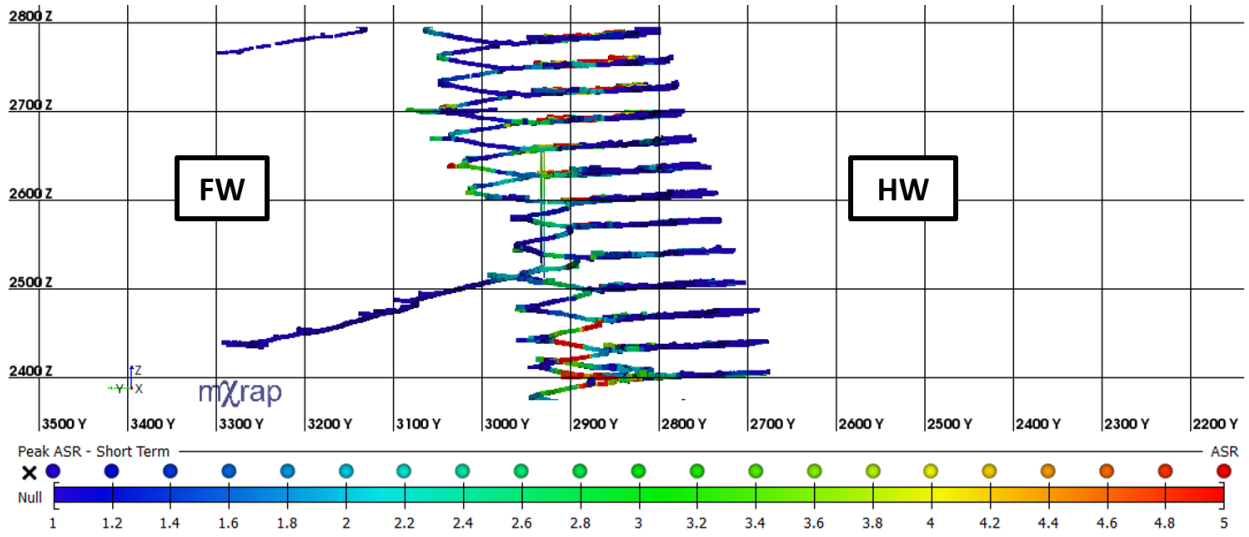

Figure 113: Cross-sectional projection looking east of a peak ASR hazard map for LaRonde. Drifts are coloured according to peak ASR values calculated for short term seismic hazard assessment.

Similar to the hazard maps generated using long and medium term seismic hazard assessment, areas characterized by large peak ASR values are concentrated in the FW and Eastern portion of the orebody.

5.3.3.1 « Short Term Peak ASR Hazard Map: Examples »

Hazard maps of the 224, 242 and 262 Levels are shown in Figure 114, Figure 115, and Figure 116 respectively. All large events ($M_L \geq 0$), are plotted on the levels to represent areas that should be considered representative of high and moderate seismic hazard.

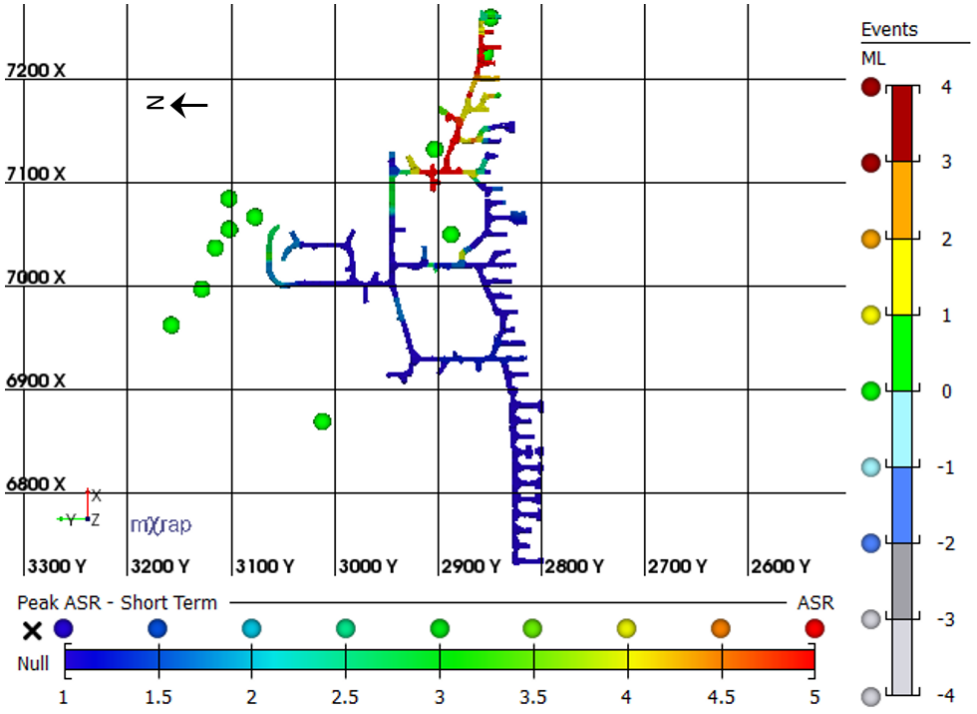

Figure 114: Peak ASR hazard map for 224 Level. Drifts are coloured according to peak ASR values calculated for short term seismic hazard.

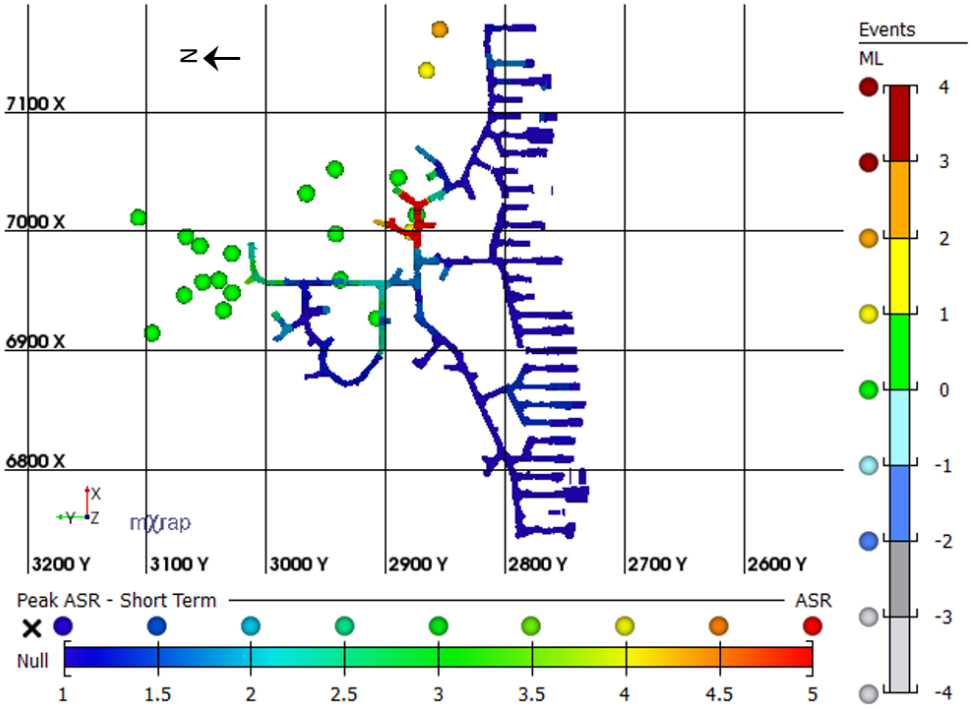

Figure 115: Peak ASR hazard map for 242 Level. Drifts are coloured according to peak ASR values calculated for short term seismic hazard.

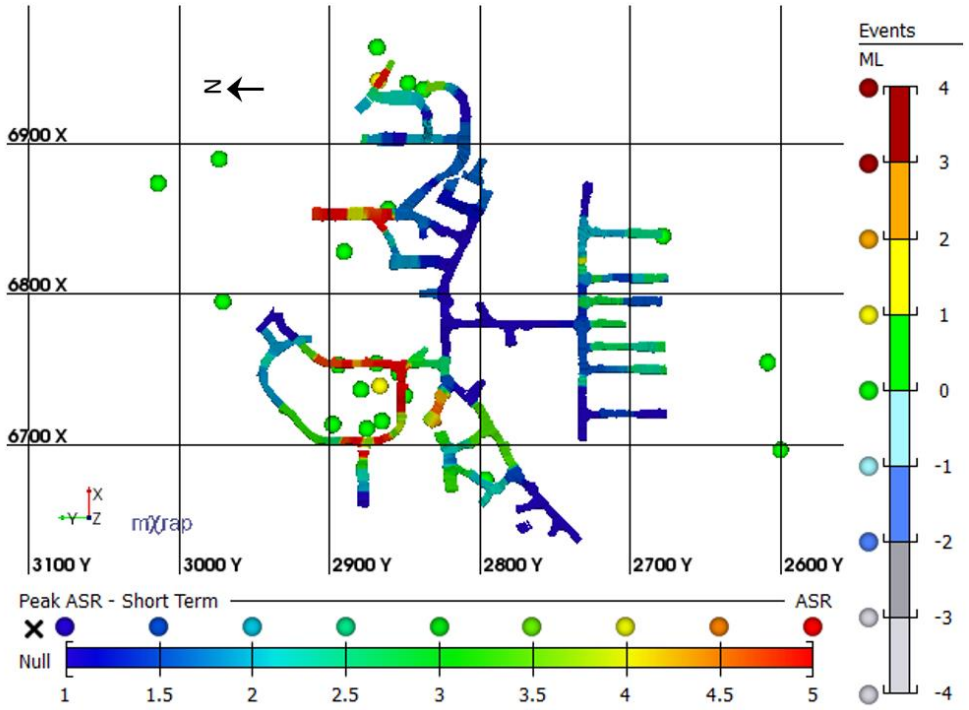

Figure 116: Peak ASR hazard map for 262 Level. Drifts are coloured according to peak ASR values calculated for short term seismic hazard.

Short term seismic hazard assessment identifies areas in the rock mass that are capable of large scale changes in local stress condition over very short periods of time. Areas that require a more gradual buildup of stress or have a very low event frequency may be under estimated by using a short term hazard assessment.

5.3.4 « Summary of Peak ASR Hazard Mapping Results »

Peak ASR values can be effectively translated into hazard maps. These maps show correlations between large peak ASR values and areas where large magnitude events have occurred in the past. Hazard map results for all three time frames are fairly consistent with their ability to identify high hazard areas from peak ASR values. Comparisons between the examples provided for all time frames show similarities for high hazard areas. Unlike short term seismic hazard assessment, medium and long term assessment effectively identify areas of moderate hazard and may be more useful for an overall assessment of elevated hazard within the rock mass.

5.4 « Discussion of Percentiles Used in the Calculation of ASR »

The 80^{th} and 20^{th} percentile values were selected for the calculation of ASR as they allow for the majority of an apparent stress distribution to be sampled while minimizing the impact of a few anomalously high or low apparent stress events. For a typical seismic population, the 80^{th} and 20^{th} percentile values usually approximate the beginning and end of the linear portion of the dataset, as shown in Figure 117.

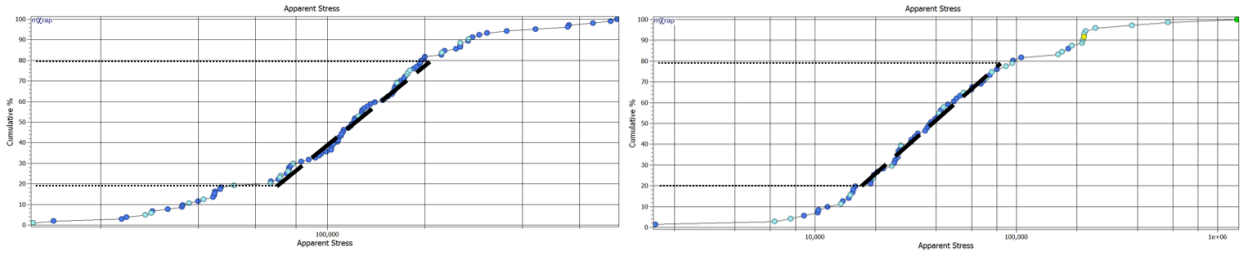

Figure 117: Apparent stress cumulative distributions for a control population (ID: 26) shown on the left and a test population (ID: 3) shown on the right.

As shown in Figure 117, both test and control populations typically possess a linear data relation between the 80th and 20th percentiles for a cumulative apparent stress distribution. As the separation between the percentiles used for ASR calculation is reduced, for example to the 60th and 40th percentiles, ASR values decrease. Due to the small separation between the 60th and 40th percentiles, ASR values calculated using these percentiles are significantly smaller with very little variation. As a result, these values are not well suited for analyzing the distribution of apparent stress for a seismic population. As the separation is increased, for example to the 90th and 10th percentiles, ASR values increase, but include data outside the linear relation. As the separation between the percentiles used increases, the ASR values increase and consequently ASR values calculated using the 90th and 10th percentiles are the largest. Because these percentiles exists outside of the linear limits of a cumulative distribution of apparent stress, as shown in Figure 117, they are however more susceptible to the influence of anomalously high and low apparent stress events. Figure 118 shows the cumulative distributions for ASR values preceding large events using these varying percentiles.

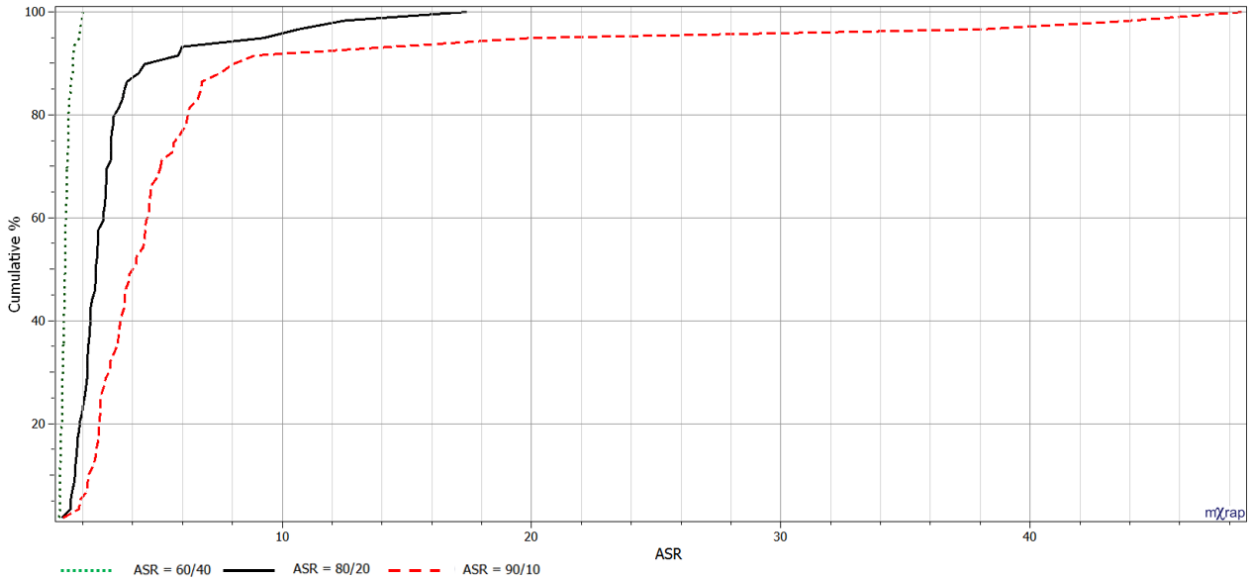

Figure 118: Cumulative distributions of ASR values preceding large events using 60/40, 80/20 and 90/10 percentiles to calculate ASR.

The same overall trends in ASR for seismic populations are observed for values calculated using both 80/20 and 90/10, however the degree of variability in ASR values is significantly larger for those calculated using 90/10. Figure 119 is an ASRTH Chart for a high hazard population showing ASR values using all three percentile ranges (90/10, 80/20 and 60/40). ASR values are calculated using long term seismic hazard assessment.

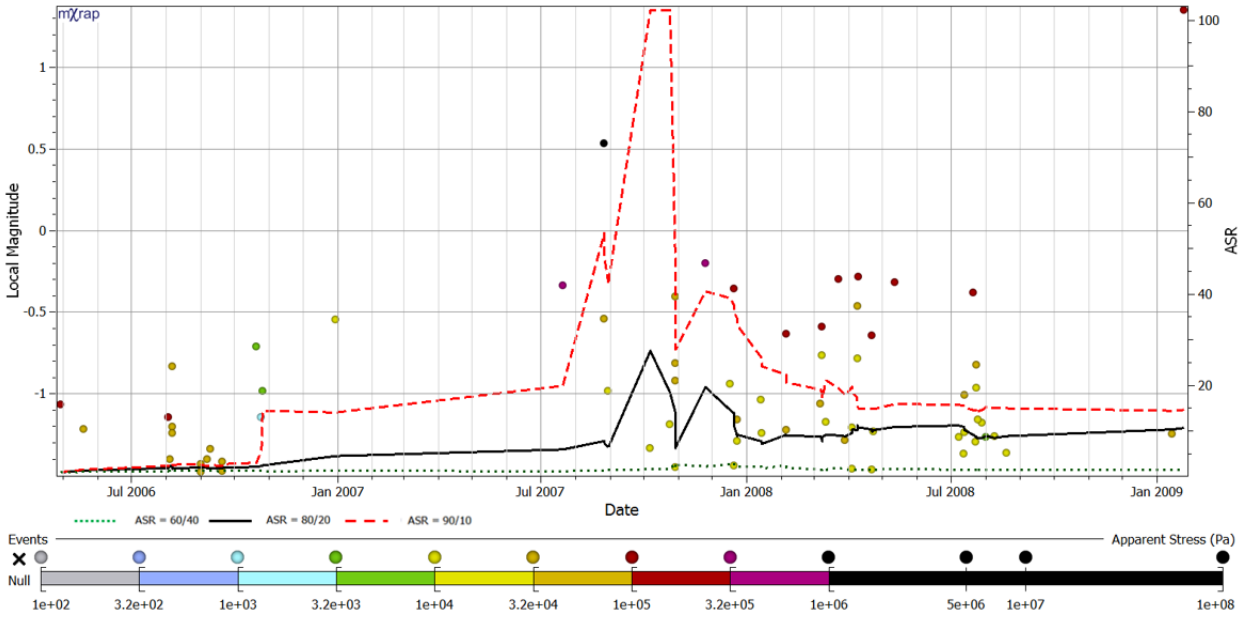

Figure 119: ASRTH Chart for a high hazard population (ID: 3) showing ASR values using all three combinations of percentiles (90/10, 80/20 and 60/40). ASR values calculated for long term seismic hazard are displayed on the secondary y-axis.

The same trends seen in the 80/20 ASR values are seen in the 90/10 ASR values, however the 90/10 values are significantly higher – with a peak exceeding 100 in Figure 119. The 60/40 ASR values are significantly smaller, with very little variation throughout the life of the population.

Figure 120 is an ASRTH Chart for a low hazard population showing ASR values using all three combinations of percentiles (90/10, 80/20 and 60/40). ASR values are calculated using long term seismic hazard assessment.

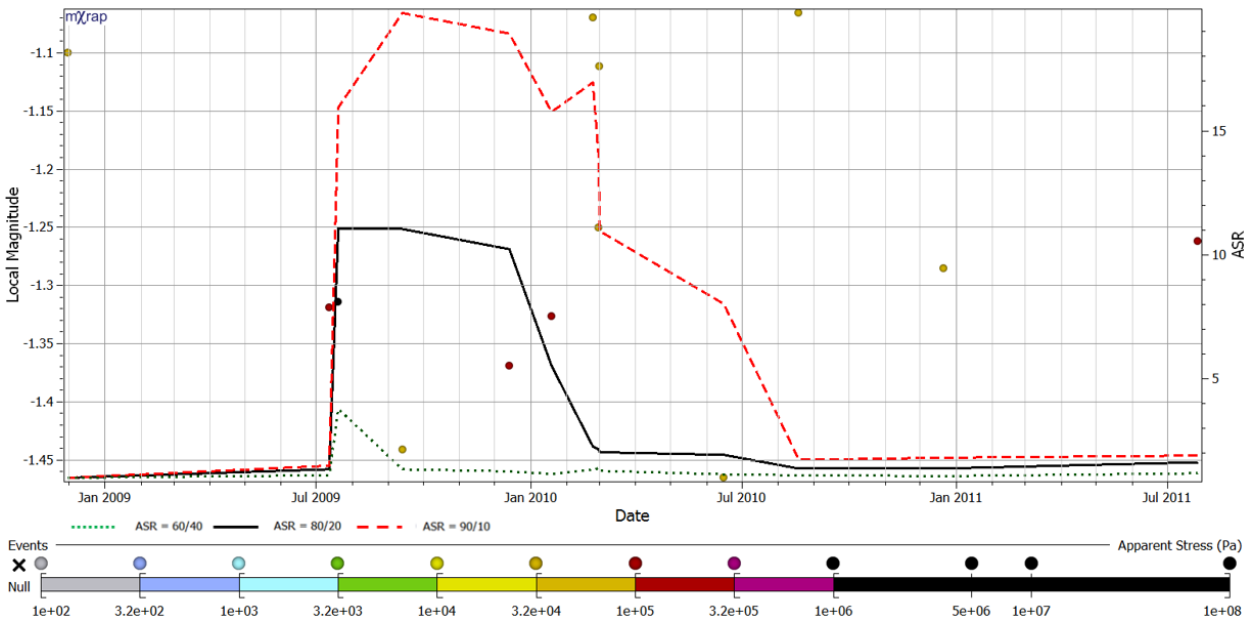

Figure 120: ASRTH Chart for a low hazard population (ID: 45) showing ASR values using all three combinations of percentiles (90/10, 80/20 and 60/40). ASR values calculated for long term seismic hazard are displayed on the secondary y-axis.

In Figure 120 the influence on ASR of the anomalously high apparent stress event, occurring in July 2009, is proportional to the degree of separation in the percentiles used for ASR calculation increases. While the 80/20 ASR decreases to levels more representative of a low hazard population in Feb 2010, the 90/10 ASR remains high until a full year has passed and the event is no longer considered in the ASR calculation.

In summary, the 80th and 20th percentiles have been selected for the calculation of ASR in this thesis due to their ability to sample the majority of a seismic population apparent stress distribution without allowing for an extended influence of anomalously high or low apparent stress events.

5.5 « Discussion of Search Radius »

As previously discussed, a search radius of 30 m was selected for the generation of seismic populations at LaRonde mine. This value is equivalent to the sublevel spacing for the operation and therefore lends itself well to mine wide application. Generating seismic populations from mine excavations includes all seismic activity up to the level above and below. Figure 121 is a standard Apparent Stress Ratio Time History chart for a high hazard seismic population generated using a 30 m search radius from the largest event contained within the population. ASR values shown are calculated using a time window of the preceding year.

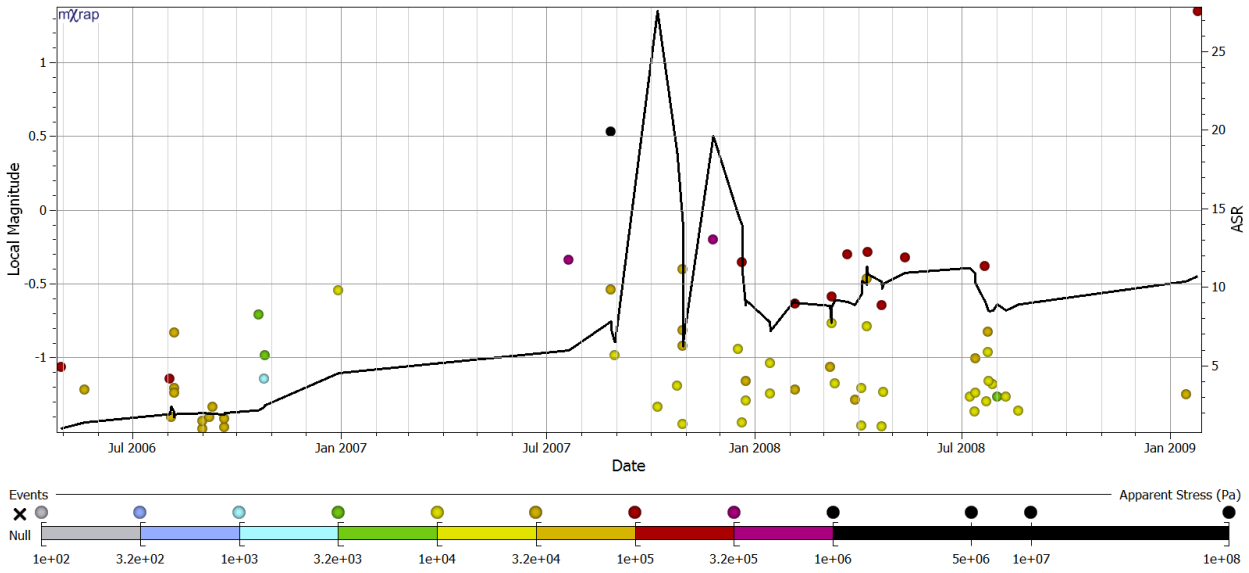

Figure 121: ASRTH chart of a high hazard population (ID: 3) using a 30 m search radius. ASR values are calculated based on long term seismic hazard (preceding year).

Using a 30 m search radius, a sufficient number of events are included in the population to enable ASR to be used as an indicator of seismic hazard for the population. ASR values are indicative of high seismic hazard throughout the entire population, which includes two large seismic events (Aug 2007 and Jan 2009). Figure 122 is an Apparent Stress Ratio Time History chart for the same high hazard seismic population shown in Figure 121, but generated using a 20

m search radius from the largest event contained within the population. ASR values shown are calculated using a time window of the preceding year.

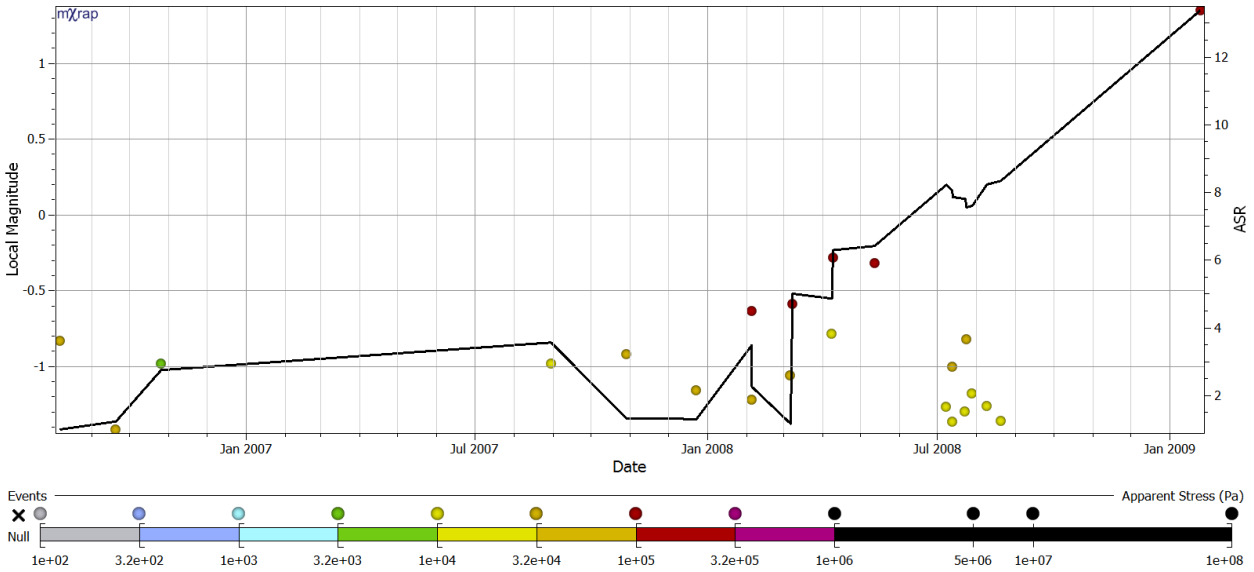

Figure 122: ASRTH chart of a high hazard population (ID: 3) using a 20 m search radius. ASR values are calculated based on long term seismic hazard (preceding year).

Similar trends in ASR can be identified in seismic populations using smaller search radius values. By reducing the search radius to 20 m, a significant number of seismic events are eliminated from the population in Figure 122 – including a large seismic event (Aug 2007). Even with this reduction however, similar trends in ASR are evident throughout the population. Larger magnitude events, with larger apparent stress values, are introduced in Feb 2008. These events generate large ASR values indicative of increasing stress, which continue to rise until a large event occurs in Jan 2009. Reducing search radius values below 20 m is not recommended as seismic populations become very small. Sufficient data is required to reliably apply seismic analysis techniques that utilize precursory trends, such as ASR.

Increasing the search radius increases the risk of including large quantities of unrelated seismic events. Events resulting from varying source mechanisms correspond to different levels of

seismic hazard. Populations from a large volume of ground may contain seismicity as a result of multiple failure mechanisms. This has a negative impact on methodologies that attempt to use precursory trends in data to determine seismic hazard. Because this methodology reduces the impact from mining process events by employing a lower bound of M_L = -1.5, a large quantity of mining process events are not introduced to a population by increasing the search radius. Figure 123 is an Apparent Stress Ratio Time History chart of the same seismic population shown in Figure 121 and Figure 122, but generated using a 100 m search radius from the largest event contained within the population. ASR values shown are calculated using a time window of the preceding year.

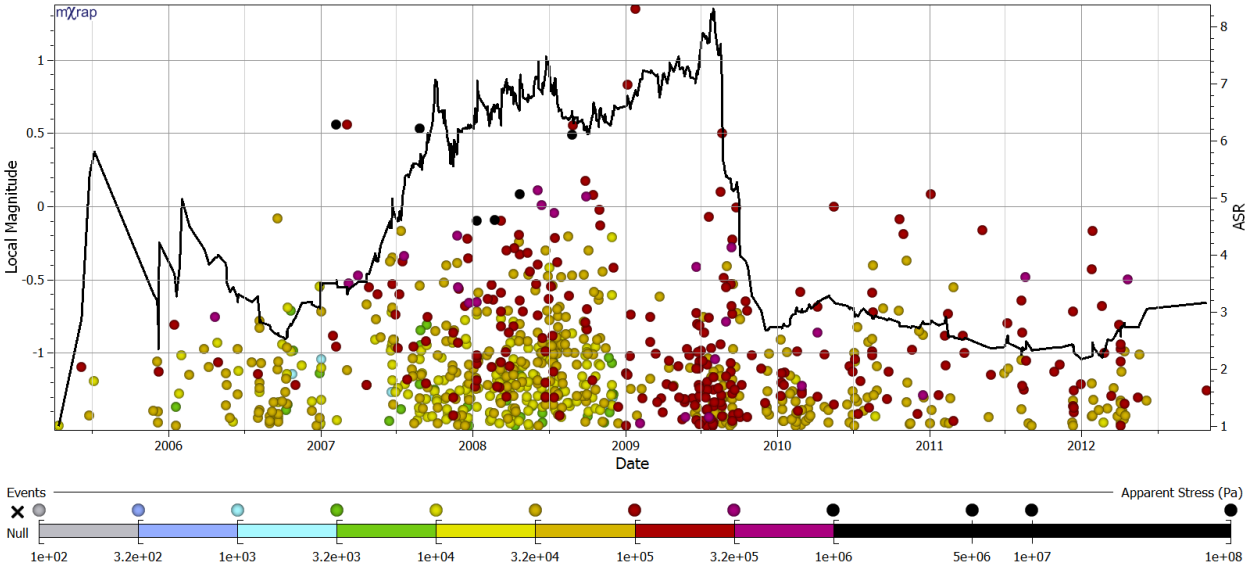

Figure 123: ASRTH chart of a high hazard population (ID: 3) using a 100 m search radius. ASR values are calculated based on long term seismic hazard (preceding year).

Trends in ASR relating to seismic hazard are still evident when the search radius is increased to 100 m. Large ASR values precede nearly all large seismic events, and a clear decrease in ASR is evident around Jan 2010, mirroring a decrease in seismic hazard that is also reflected in the frequency and size of events within the population.

The same trends that are evident using a 30 m search radius for short, medium and long term seismic hazard assessment can be observed in high and moderate hazard populations when the search radius is increased and decreased. Low hazard populations however are more susceptible to changes in search radius values. Because the number of events is initially small, decreasing the search radius reduces many low hazard populations to quantities unfeasible for precursory trend analysis techniques. Figure 124 is a standard Apparent Stress Ratio Time History chart for a low hazard seismic population generated using a 30 m search radius from the largest event contained within the population. ASR values shown are calculated using a time window of the preceding year.

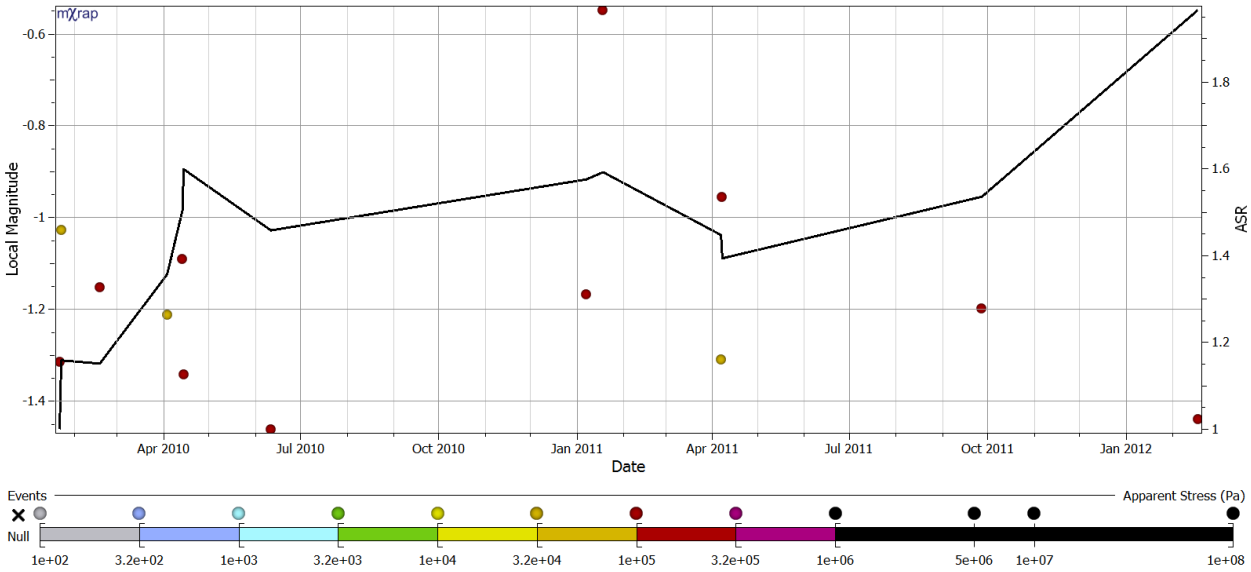

Figure 124: ASRTH Chart of a low hazard seismic population (ID: 46) using a 30 m search radius. ASR values are calculated based on long term seismic hazard (preceding year).

Using a 30 m search radius, a sufficient number of events are included in the population to enable ASR to be used as an indicator of seismic hazard for the population. The ASR values are low throughout the life of the population, indicating low stress conditions and seismic hazard. The peak ASR is also low at approximately 1.95. Figure 125 is an Apparent Stress Ratio Time History chart for the same low hazard seismic population shown in Figure 124, but generated

using a 20 m search radius. ASR values shown are calculated using a time window of the preceding year.

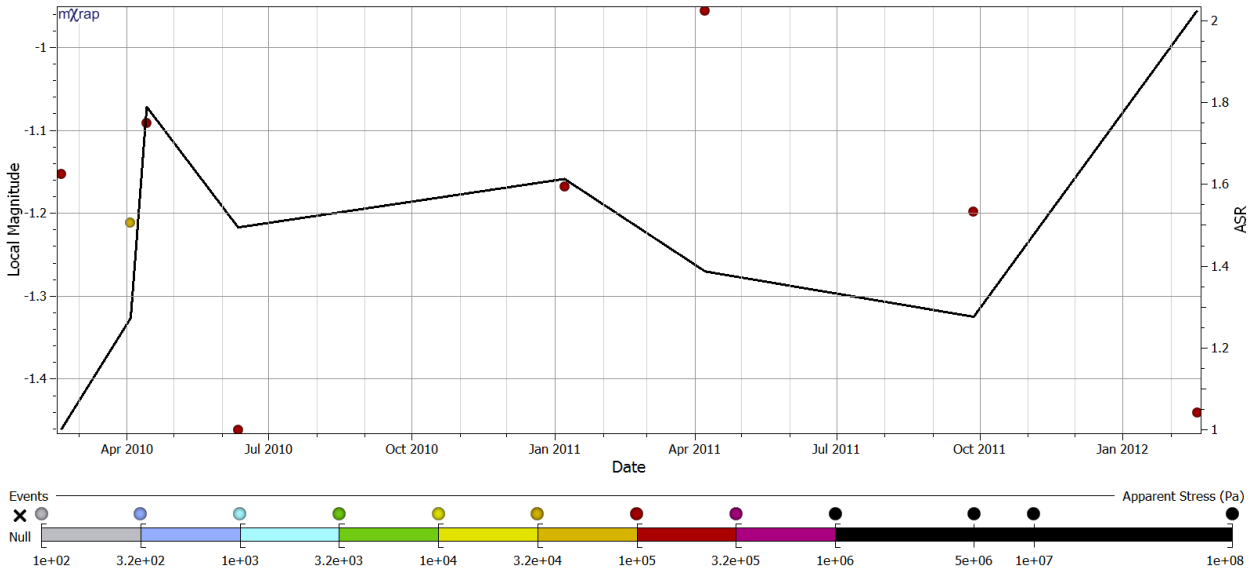

Figure 125: ASRTH Chart of a low hazard seismic population (ID: 46) using a 20 m search radius. ASR values are calculated based on long term seismic hazard (preceding year).

The reduction in search radius does not have a large impact on this population. The same trends are evident in ASR. This is expected as low hazard populations should be representative of areas in the rock mass that have a relatively constant stress state. Reducing the search radius should therefore not impact the trends observed in ASR. Increasing the search radius typically has the opposite result. Figure 126 is an Apparent Stress Ratio Time History chart the same seismic population shown in Figure 124 and Figure 125, but generated using a 50 m search radius. ASR values shown are calculated using a time window of the preceding year.

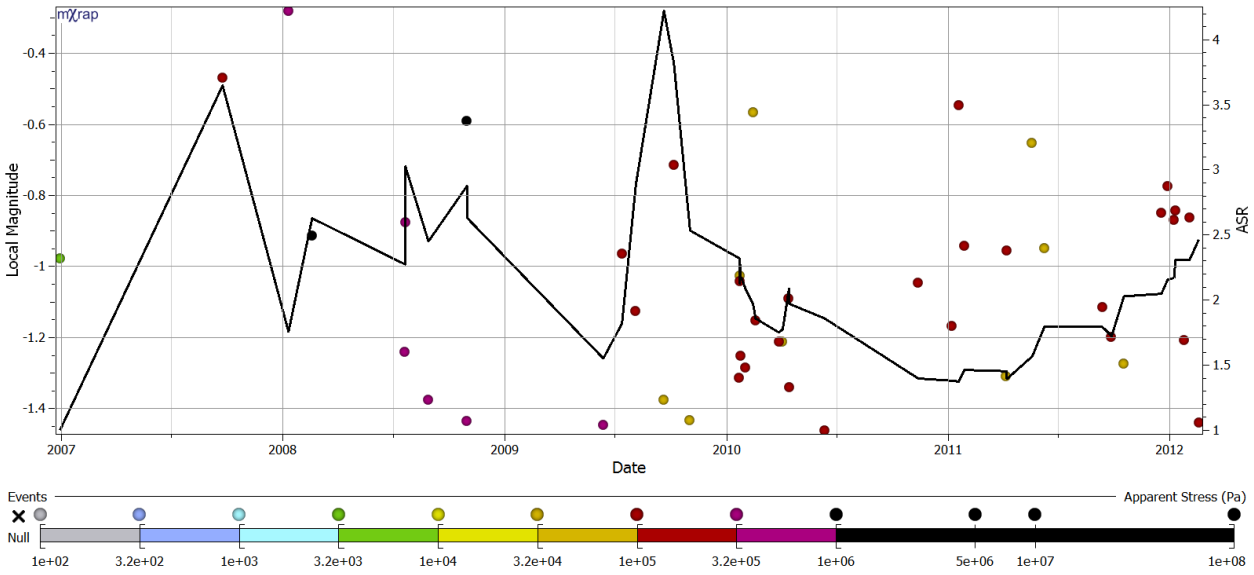

Figure 126: ASRTH Chart of a low hazard seismic population (ID: 46) using a 50 m search radius. ASR values are calculated based on long term seismic hazard (preceding year).

A slight increase in the search radius for the population is significant enough to alter the classification of the population from low to moderate hazard. This change is also reflected in the ASR values, which are calculated using the new seismic events introduced to the population. Incorporating a larger volume of the rock mass includes regions with different and more hazardous failure mechanisms in the population. The peak ASR value for the population is more than double at a value of approximately 4.2.

Reductions in the search radius have a minimal impact on both high and low hazard seismic populations. Care must be taken to not reduce the radius to a point where insufficient quantities of seismic events are present in the populations. High hazard populations are less susceptible to increases in the search radius, as these populations are centered in areas of high hazard. Including surrounding areas of low hazard will not have large impacts on the overall trends in ASR due to the relativity small number of events. Including moderate to high hazard areas within low hazard areas has the opposite effect. Because of the relatively high number of events in

moderate/high hazard areas, they dominate the low hazard area and the population is no longer representative of the local rock mass conditions at the center of the population. Search radius values need to be carefully selected to ensure they are large enough to incorporate a reasonable amount of seismic data for analysis purposes, while attempting to minimize the inclusion of multiple failure modes within the rock mass.

5.6 « ASR as an Alarm Tool »

The objective of using ASR as an alarm tool is to forecast the occurrence of large and potentially damaging seismic events. As previously discussed in the methodology chapter, this requires the selection of a threshold value to indicate increased seismic hazard. These values were selected from cumulative distributions of ASR values preceding large events in test populations and median ASR values for control populations. An optimum threshold value ensures a maximum number of large events occur within alarm periods (when the ASR threshold is exceeded), while minimizing the number of false alarms.

A false alarm denotes when the ASR threshold has been exceeded within a seismic population but no large event occurs by the end of the alarm. An alarm ends when the ASR values fall back below the threshold or there is no further seismic activity in the population. To gain a better understanding of what is occurring during these false alarms, they are subdivided into four categories: standard false alarms, development mining related alarms, end of population alarms, and isolated event alarms.

A standard false alarm indicates that the ASR threshold was exceeded and the ASR for the population eventually declined to values below the threshold without the occurrence of a large

event. This is the most common type of false alarm. Figure 127 is an example of a standard false alarm.

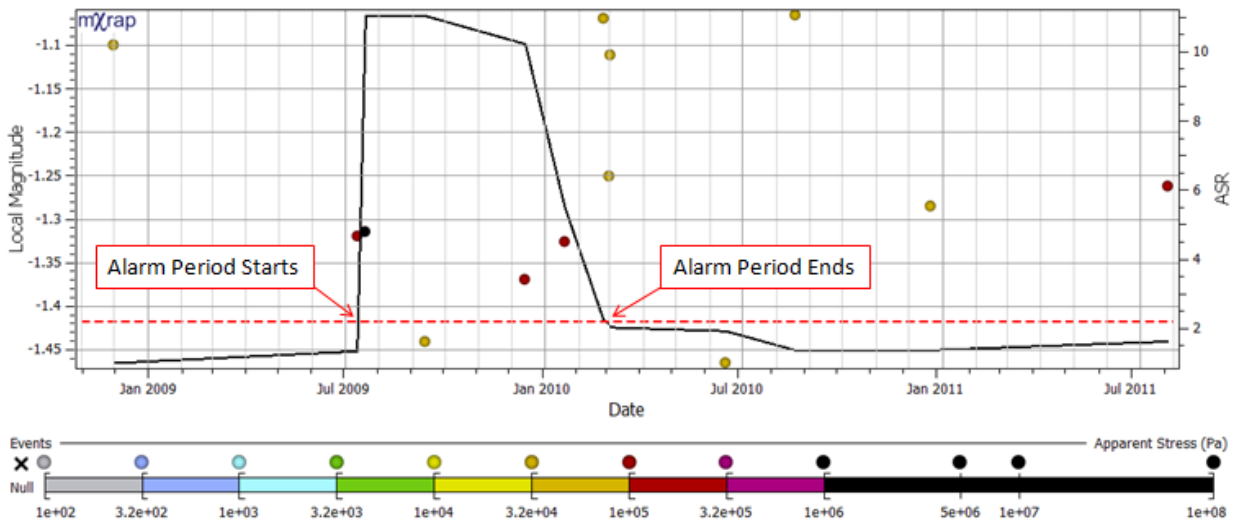

Figure 127: ASRTH chart of a low hazard seismic population (ID: 45). ASR values calculated for long term seismic hazard are displayed on the secondary y-axis. The alarm threshold for long term seismic hazard is represented by a red horizontal line at ASR = 2.2.

At the beginning of the population the ASR is below the ASR alarm threshold of 2.2 (represented by the red dashed line). With the occurrence of high apparent stress events, the ASR value exceeds the threshold in July 2009, beginning an alarm period. ASR value remains high until the end of February 2010, when it falls back below the threshold. As no large magnitude event occurred during the alarm period, this constitutes a standard false alarm.

Development mining related alarms refer to alarm time periods that occur during local development mining. Time periods for which development mining occurred in proximity to sample populations can be found in Appendix V and Appendix W. All seismic events contained within the population shown in Figure 128 occurred during nearby development mining.

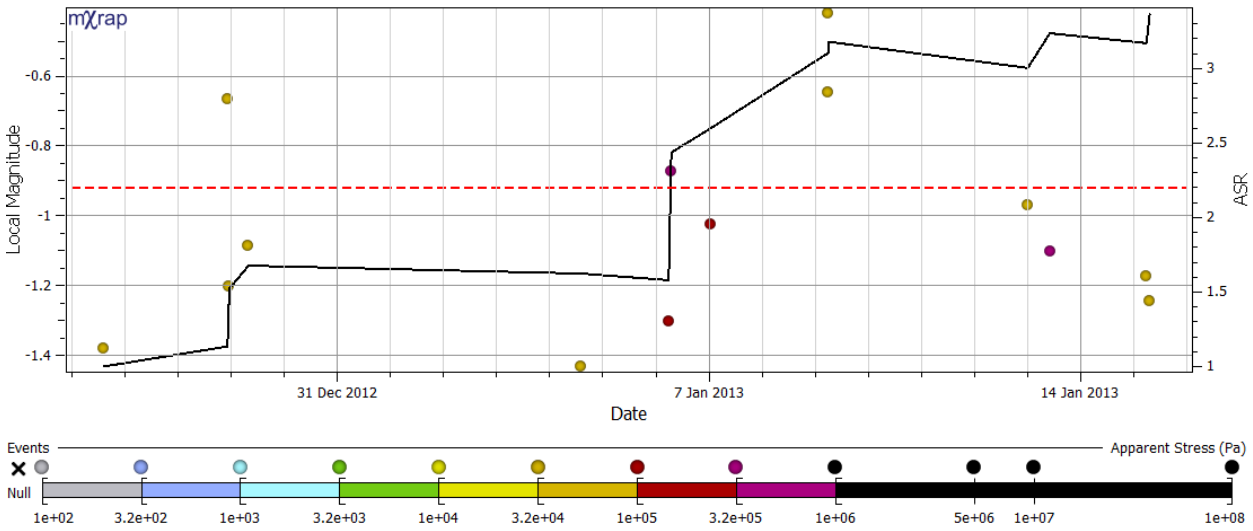

Figure 128: ASRTH Chart of a moderate hazard seismic population (ID: 43). ASR values calculated for long term seismic hazard are displayed on the secondary y-axis. The alarm threshold for long term seismic hazard is represented by a red horizontal line at ASR = 2.2.

For the seismic population in Figure 128, nearby development mining occurs between approximately December 15, 2012 and March 4, 2013. This not only corresponds directly to the time period of the false alarm, but the seismicity for the entire life of the population. High apparent stress values are expected during development mining as new excavations force in-situ stresses to redistribute. False alarms such as this are classified as being related to development mining.

Production blasting is not considered in this analysis. The influence of production blasting cannot be as easily identified and segregated within the sample populations. Figure 129 is a seismic population showing all production blasting on the associated mining level.

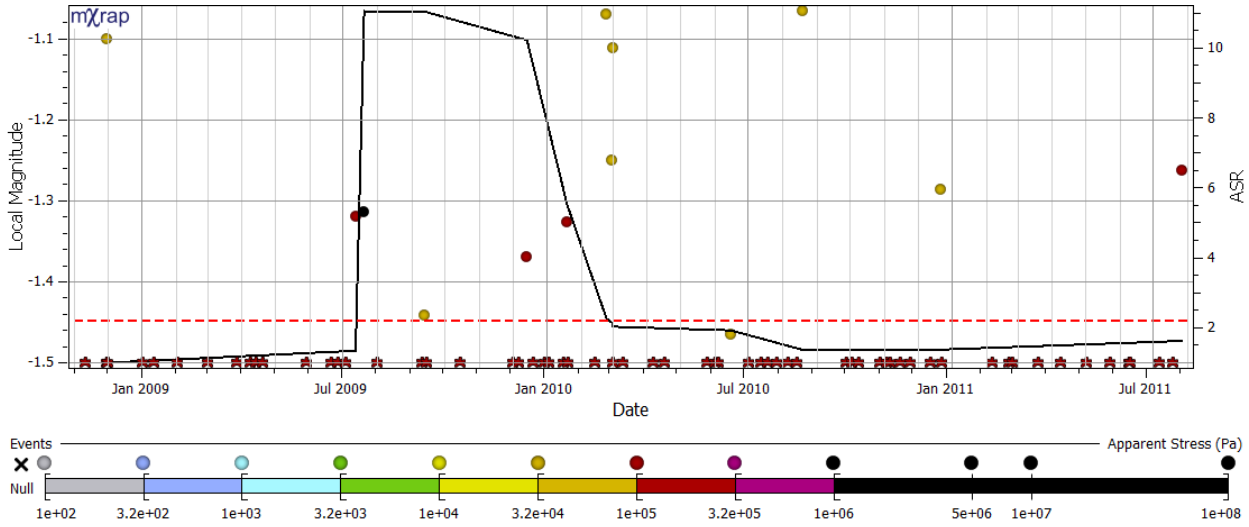

Figure 129: ASRTH Chart of a low hazard seismic population (ID: 45). ASR values calculated for long term seismic hazard are displayed on the secondary y-axis. All red icons presented along the bottom of the chart refer to a single production blast on the 233 Level.

Each of the red icons presented in Figure 129 represents a single production blast for stopes located on the same level as the central point of the sample population. Due to the geometry of the orebody, small sublevel spacing, and predominate location of high hazard populations in the FW, it is difficult to determine the influence of individual production blasts on seismic activity. The high frequency of production blasting, even on a single level, makes it unrealistic to attribute periods of alarm to production blasting.

When ASR values of a population exceed the threshold and continue to remain high until the final event in the population, they are considered end of population alarms. This is a common occurrence and hard to classify. Because the alarm is still active it cannot be stated with certainty that it is a false alarm. In many high and moderate hazard populations, the false alarm extends until the completion of the dataset. For the purposes of this thesis, it is classified as a false alarm but a large event may occur in future during the same period of alarm. Figure 130 is a population including an end of population false alarm.

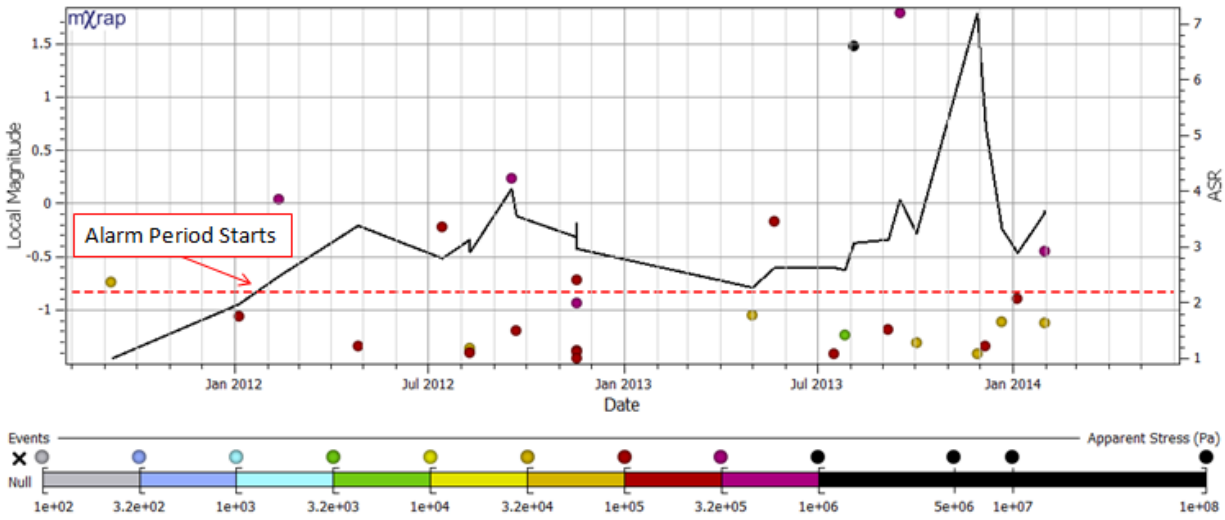

Figure 130: ASRTH Chart of a high hazard seismic population (ID: 1). ASR values calculated for long term seismic hazard are displayed on the secondary y-axis. The alarm threshold for long term seismic hazard is represented by a red horizontal line at ASR = 2.2.

For the high hazard population show in Figure 130, the ASR threshold is exceeded in late January 2012, beginning the alarm period. Large events occur during the alarm period in August and October of 2013. Following the occurrence of a large event, the alarm is classified as a success and the alarm period is reset if ASR values do not return below the threshold value. For this population, following the two successful alarms the ASR values do not decline to levels below the alarm threshold. They continue to remain high until the end of the population life and without the occurrence of another large event. This is classified as an end of population false alarm. Overall the high hazard population shown in Figure 130 has two successful alarms and one false alarm.

Isolated event alarms are rare and typically very short. They occur when the ASR caused by a single event exceeds the threshold value beginning an alarm, but the subsequent event brings the ASR value below the threshold. The entire alarm occurs over the course of a single event and

without the occurrence of a large magnitude event it is classified as a false alarm. Such an alarm is shown in Figure 131.

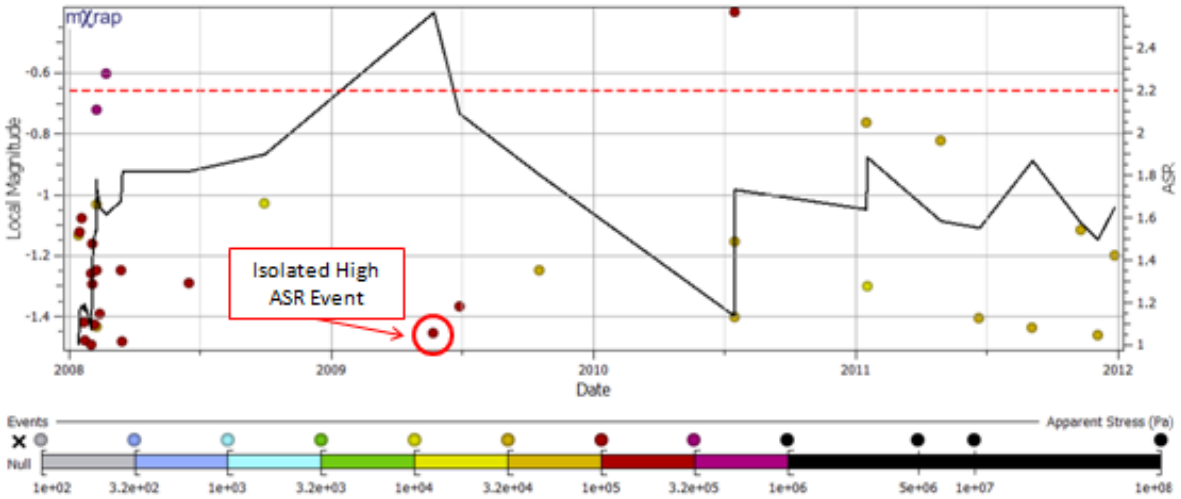

Figure 131: ASRTH Chart of a moderate hazard seismic population (ID: 32). ASR values calculated for long term seismic hazard are displayed on the secondary y-axis. The alarm threshold for long term seismic hazard is represented by a red horizontal line at ASR = 2.2.

The ASR values for the event before and after the isolated high ASR event are both below the threshold value. This is an example of an isolated event false alarm generated by a single seismic event. When this occurs it is not a trend representative of the entire population and is typically an artifact of anomalous seismic activity.

All high, moderate and low hazard sample populations were analyzed for success rates using previously defined threshold values for medium and long term seismic hazard. Short term hazard assessment was not analyzed as the vast majority of ASR values preceding large events was 1. The event rate for these populations using only a preceding week of seismic data potentially allows for meaningful trends to be identified in peak ASR, but it is not applicable for use as an alarm tool.

Simser (2008) found approximately 30% of large seismic events have some precursory microseismic activity that may lend itself to identification with a predictive trend. A further 40% are blast triggered events and the remaining 30% occur with no identifiable precursory seismic activity. The use of ASR does not provide any special consideration for events occurring within blasting time and area restrictions. Success rates in excess of 30% are considered good when based only on precursory microseismic activity. Success rates approaching 70% are ideal as they incorporate both events identified by precursory activity and those triggered by blasting. Success rates on their own however are meaningless without manageable false alarm ratios. Young (2012) concluded that a ratio of false alarms to successful alarms of 2:1 is relatively low.

5.6.1 « Long Term Seismic Hazard »

As previously defined in the methodology chapter, for the purposes of the area of interest at LaRonde mine (224 to 262 Level), an ASR value greater than or equal to 2.2 has been empirically selected as indicative of long term seismic hazard. Long term ASR values are calculated based on the preceding year of seismic activity. The threshold value was determined based on ASR values preceding large events in test populations and median ASR values for control populations. Using this threshold 68% (40 out of 59) of the large events, present in the test populations, occur during a period of elevated seismic hazard. This result is very good as it approaches a success rate of 70%. The following analysis focuses on identifying and classifying false alarms occurring with this threshold.

5.6.1.1 « Test Population Analysis »

The use of 2.2 as an ASR threshold for long term seismic hazard results in a success rate for large events of 68%. A cumulative distribution of the duration of elevated seismic hazard prior to the occurrence of large events is shown in Figure 132.

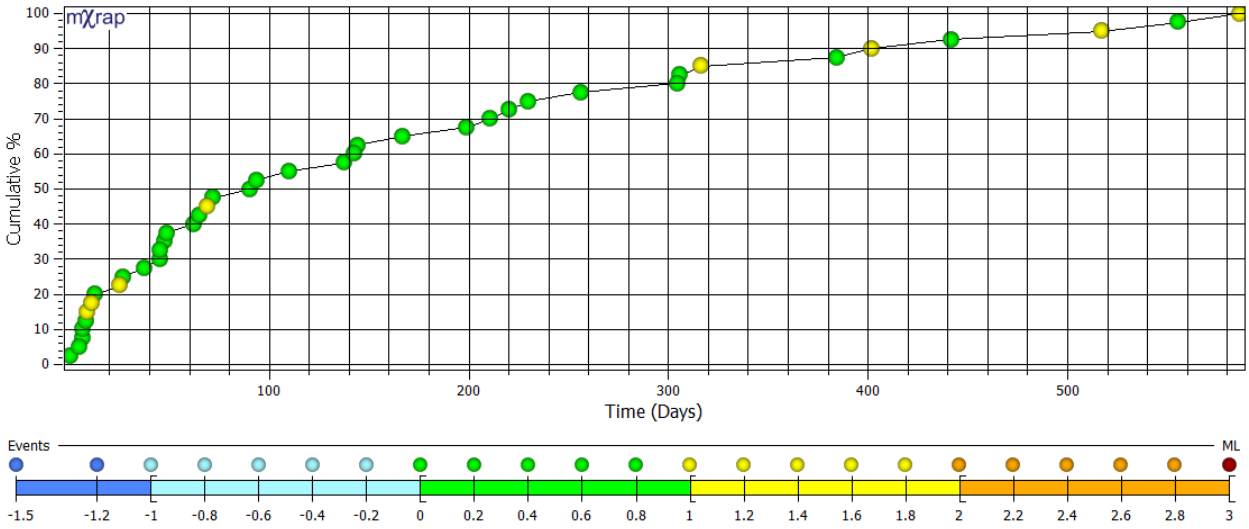

Figure 132: Cumulative distribution for time duration between the beginning of an alarm period and the occurrence of a large event for long term seismic hazard assessment. Events are coloured according to Local magnitude.

The 50th percentile for the cumulative distribution shown in Figure 132 is approximately 90 days. This indicates that half of the large seismic events within the test populations occurred within 3 months of an alarm period. There appears to be no relation between the magnitudes of events and the duration of alarms.

The majority of false alarms that occur with this ASR alarm threshold are generated from high hazard populations. High hazard populations typically experience increases and decreases in ASR values over short periods of time, in which moderate and low hazard populations usually have more stable long term ASR values. Using long term seismic hazard assessment, paired with an alarm threshold value of 2.2 for test populations, generated a total of 54 false alarms.

The percent of false alarms for each category previously discussed is shown in Figure 133.

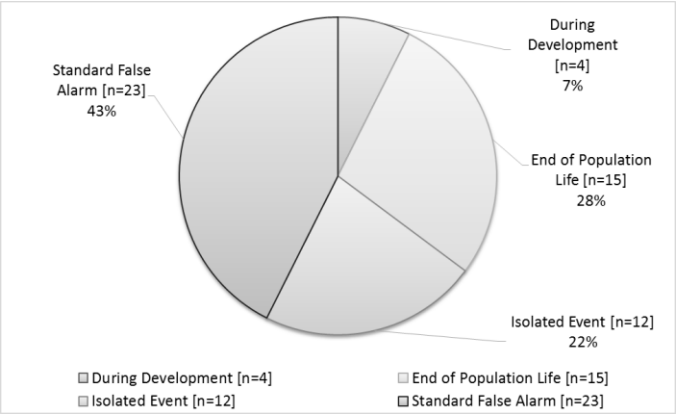

Figure 133: Pie chart showing the percent per category of false alarms related to test populations for long term hazard assessment using an ASR alarm threshold value of 2.2.

The majority of false alarms, 43%, correspond to standard false alarms. This means the alarm threshold was exceeded and after a period of time ASR values returned below the threshold. End of population life alarms represent 28% of the total false alarms. This is expected for high hazard populations. Elevated ASR values up to and including the final event in the population are not necessarily indicative of false alarms, as future large events may occur in the population. Isolated event alarms make up 22% of the total false alarms. They are predominately events with anomalously large or small apparent stress values that have a large influence on the AS distribution due to small quantities of seismic events. Only 7% of the total false alarms occurred during periods associated with develop mining activities. The duration of these false alarms is shown in the cumulative distribution in Figure 134.

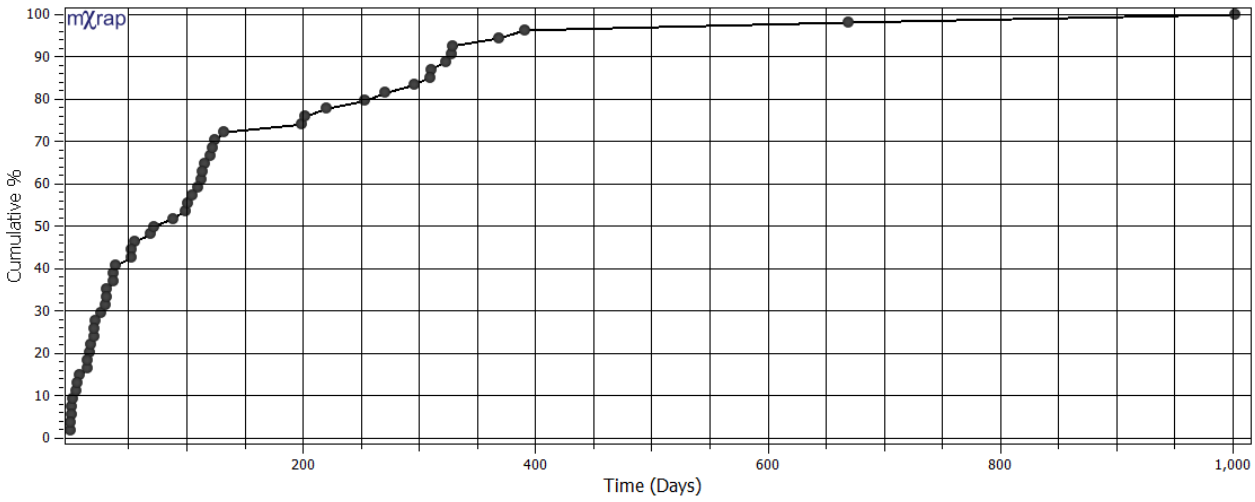

Figure 134: Cumulative distribution for time duration of false alarms in test populations using long term seismic hazard assessment.

The 50th percentile for the cumulative distribution of false alarms shown in Figure 134 is approximately 75 days. This is slightly less than that for successful alarms within the same populations.

5.6.1.2 « Control Populations »

Control populations are representative of a combination of low and moderate hazard seismic populations. The majority of the low hazard populations have very low ASR values throughout the life of the population and false alarms are frequently short. Moderate hazard populations tend to have long duration false alarms and are characterized by more frequent fluctuations in ASR, similar to high hazard populations. Using long term seismic hazard assessment, paired with an alarm threshold value of 2.2 for control populations, generated a total of 30 false alarms. The pie chart in Figure 135 represents the false alarms for control populations using long term seismic hazard assessment.

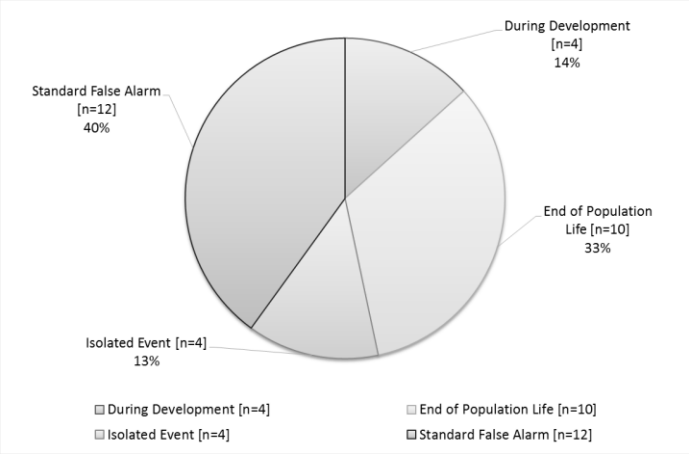

Figure 135: Pie chart showing the percent per category of false alarms related to control populations for long term hazard assessment using an ASR alarm threshold value of 2.2.

The majority of false alarms, 40%, correspond to standard false alarms. This is similar to the trend seen in test populations. The number of end of population life alarms has increased to 33%. This is largely attributed to moderate hazard populations. As previously discussed, it is difficult to determine if these are true false alarms as these populations have the capacity to produce large events moving forward. Isolated event alarms make up 13% of the total number of false alarms. The majority of apparent stress distributions of low and moderate hazard populations contain less variation than high hazard populations. As a result, it is more difficult for a single event to push the ASR value above the threshold without other similar apparent stress events in the population. The percentage of false alarms attributed to local develop mining has doubled to 14% relative to the test populations. This result is expected. For the majority of control populations, the most hazardous time is during development when new excavations are forcing local stresses to redistribute. Because these populations are low to moderate hazard however, these elevated stress and ASR values do not result in large magnitude events. The duration of these false alarms is shown in the cumulative distribution in Figure 136.

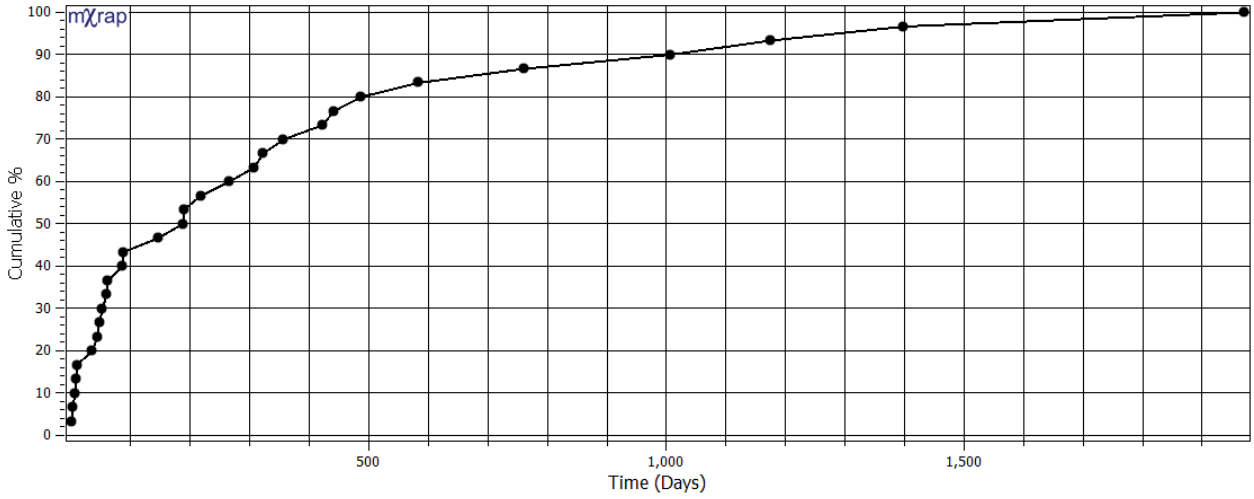

Figure 136: Cumulative distribution for time duration of false alarms in control populations using long term seismic hazard assessment.

The 50th percentile is 190 days, almost twice that of the distributions for false and successful alarms of test populations. It is clear from comparing this distribution to those in Figure 132 and Figure 134, the longer an alarm period is active, the less likely it is to result in a large event.

5.6.1.3 « Summary of Long Term Seismic Hazard »

The success rate for long term hazard assessment of ASR using an alarm threshold of 2.2 is 68%. This is an excellent result that includes the vast majority of events capable of being identified with precursory trends in seismic activity. Using this threshold value, false alarms occur at approximately a 2:1 ratio (84:40). The majority of these false alarms occur in test populations 64.3% (54/84), with just over a third occurring in the control populations 35.7% (30/84). The use of ASR as an alarm tool paired with long term seismic hazard assessment is reasonably accurate and provides insight into areas of the rock mass which should be considered an increased risk over specified time periods.

5.6.2 « Medium Term Seismic Hazard »

As previously defined in the methodology chapter, for the purposes of LaRonde mine in the area of interest (224 to 262 Level), an ASR value greater than or equal to 1.8 has been empirically selected as indicative of medium term seismic hazard. Medium term ASR values are calculated based on the preceding 3 months of seismic activity. The threshold value was determined based on ASR values preceding large events in test populations and median ASR values for control populations. Using this threshold 54% (32 out of 59) of the large events, present in the test populations, occur during a period of elevated seismic hazard. This result is positive and encouraging. The following analysis focuses on identifying and classifying false alarms occurring with the use of this threshold.

5.5.2.1 « Test Population Analysis »

The use of 1.8 as an ASR threshold for medium term seismic hazard results in a relatively good success rate of 54%. The duration of elevated seismic hazard prior to the occurrence of large events is presented in the cumulative distribution shown in Figure 137.

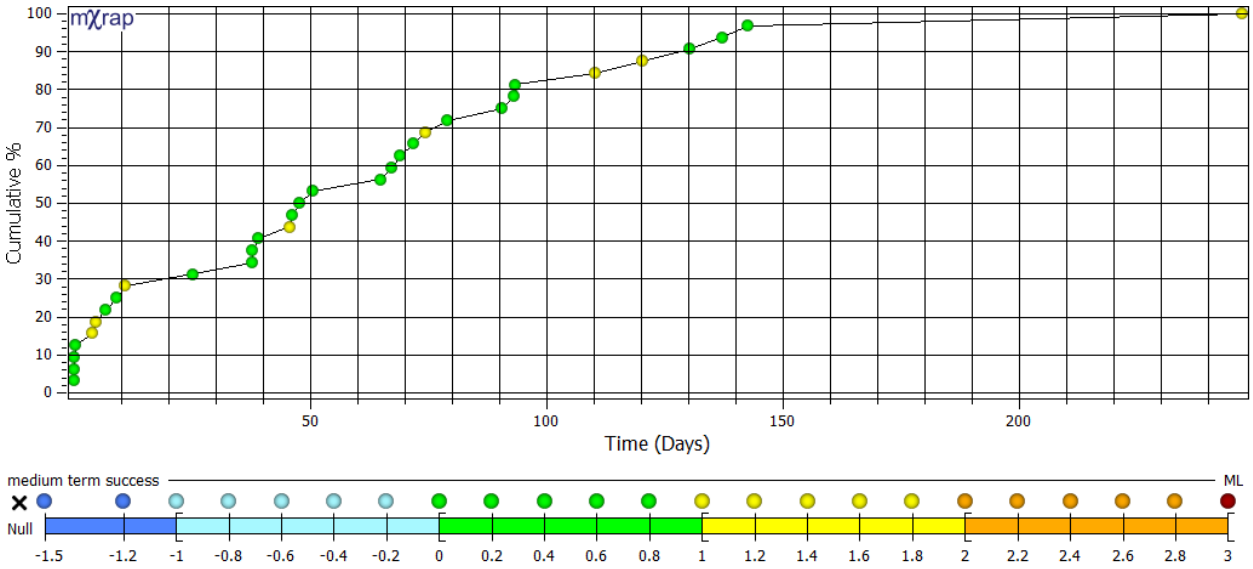

Figure 137: Cumulative distribution for time duration between the beginning of an alarm period and the occurrence of a large event for medium term seismic hazard assessment. Events are coloured according to Local magnitude.

The 50th percentile for the cumulative distribution shown in Figure 137 is approximately 45 days. This means half of the large seismic events within the test populations occurred within 45 days of the start of an alarm period. There appears to be no relation between the magnitudes of events and the duration of alarms.

The majority of false alarms that occur with this ASR alarm threshold are generated from high hazard test populations. High hazard populations typically experience increases and decreases in ASR values over short periods of time, where moderate and low hazard populations usually have more stable long term ASR values. Using medium term seismic hazard assessment paired with an alarm threshold value of 1.8 for test populations generated a total of 85 false alarms. The percent of false alarms for each category previously discussed is shown in Figure 138.

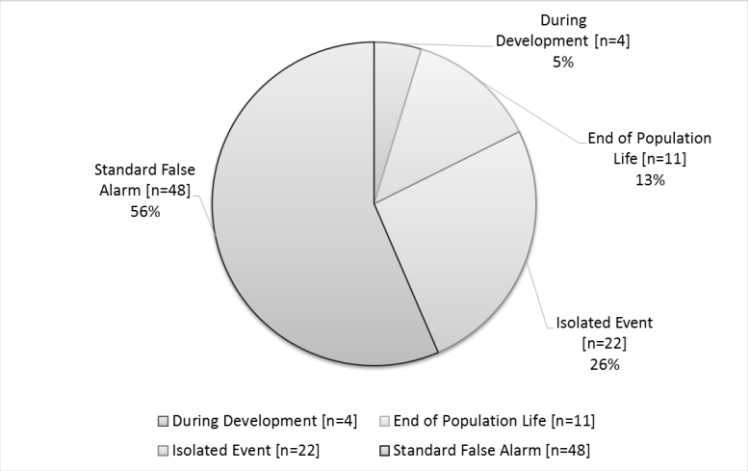

Figure 138: Pie chart showing the percent per category of false alarms related to test populations for medium term hazard assessment using an ASR alarm threshold value of 1.8.

The majority of false alarms, 56%, correspond to standard false alarms. This means the alarm threshold was exceeded and after a period of time, ASR values returned below the threshold. Isolated event alarms make up 26% of the total false alarms. They are predominately events with anomalously large or small apparent stress values and have a large influence on the AS distribution due to small quantities of seismic events. This is particularly common for medium term hazard assessment as the shortened assessment time period allows for each seismic event to have a greater impact on individual apparent stress distributions. End of population life alarms represent 13% of the total false alarms. For high hazard populations this is expected. Elevated ASR values up to and including the final event in the population are not necessarily indicative of false alarms, as large events are potentially still likely to occur in the populations in the future. Only a minimal 5% of the total false alarms occurred during periods associated with develop mining activities.

The duration of all false alarms contained in test populations is shown in the cumulative distribution in Figure 139.

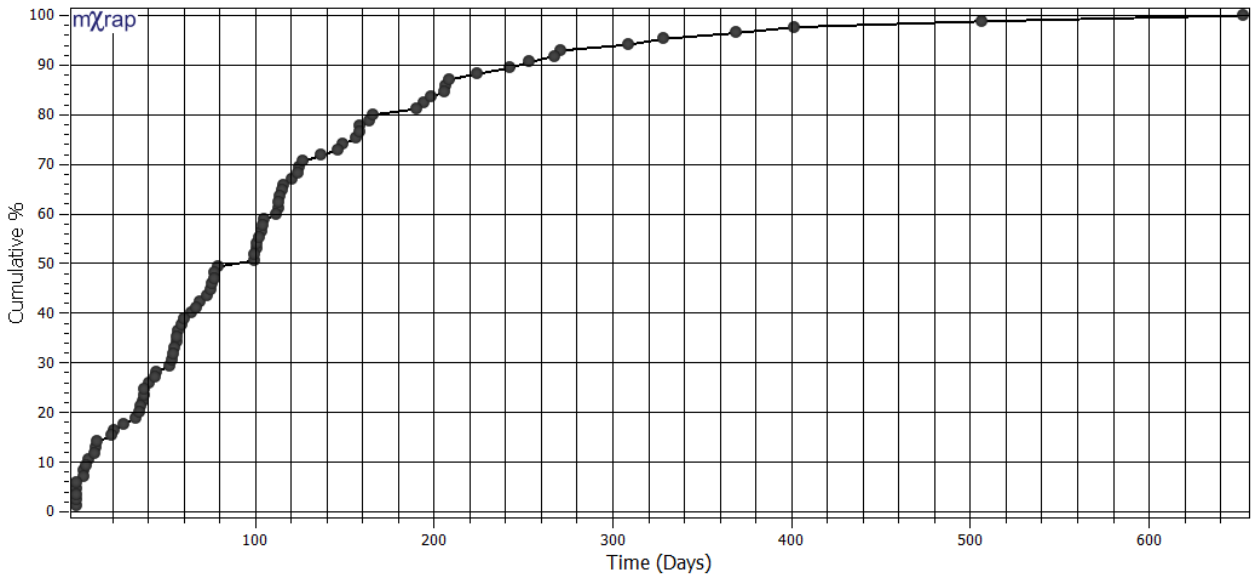

Figure 139: Cumulative distribution for time duration of false alarms in test populations using medium term seismic hazard assessment.

The 50th percentile for the cumulative distribution of false alarms shown in Figure 139 is approximately 90 days. This is twice the number of days for successful alarms contained within the same populations. This indicates that the longer an alarm continues, the more likely it is to be a false alarm. For the distribution of successful alarms shown in Figure 137, the 75th percentile corresponds to approximately 90 days.

5.5.2.2 « Control Population Analysis »

Control populations represent the moderate and low seismic hazard populations and do not contain large seismic events. While low hazard populations typically have very low ASR values throughout the life of the population and consequently short false alarms, moderate hazard populations can produce results similar to those seen in the test populations. Using medium term seismic hazard assessment paired with an alarm threshold value of 1.8, control populations generated a total of 48 false alarms. The pie chart in Figure 140 shows the percent of false alarms classified by category for control populations.

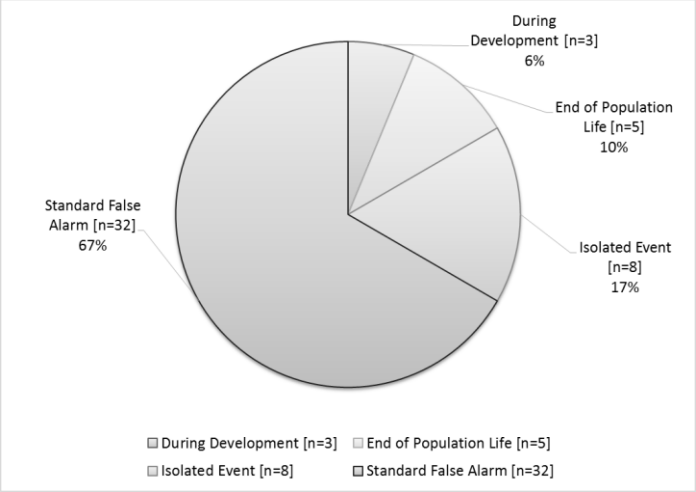

Figure 140: Pie chart showing the breakdown of false alarms related to control populations for medium term hazard assessment using an ASR alarm threshold value of 1.8.

There is a substantial increase in the number of standard false alarms when compared to the test populations shown in Figure 138. This is a result of the moderate hazard populations. ASR values increase and stay high for a time before being reduced to below threshold levels as a result of the shortened assessment period. Other false alarm rates are similar to the test populations. Very similar values for end of population life false alarms (10%) and alarms during development mining (6%) are seen. The increase in standard false alarms appears to have come from a reduction in the number of isolated events (17%). This is expected as low and moderate hazard populations tend to exhibit less fluctuation in ASR values from event to event. As a result, there are less instances in which only a single event exceeds the threshold value. The duration of these false alarms is shown in Figure 141 using a cumulative distribution.

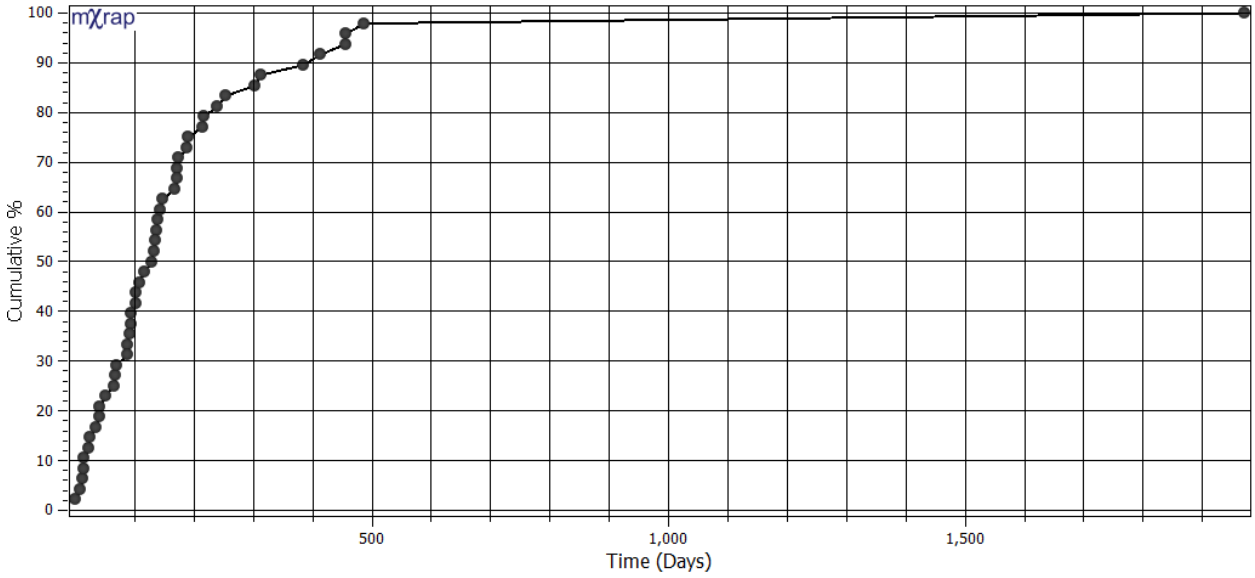

Figure 141: Cumulative distribution for time duration of false alarms in control populations using medium term seismic hazard assessment.

The 50th percentile corresponds to approximately 125 days, while the 50th percentile of 90 days for test populations corresponds to the 40th percentile. This further supports that the longer an alarm periods is active, the less likely it is to result in a large event. This knowledge can be used in conjunction with the alarm tool to assess seismic risk for various areas within the mine.

5.5.2.3 « Summary of Medium Term Seismic Hazard »

The success rate for long term hazard assessment of ASR using an alarm threshold of 1.8 is 54%. This is a relatively good result that begins to approach 70% success. Using this threshold value, false alarms occur at approximately a 4:1 ratio (133:32). The majority of these false alarms occur in test populations 63.9% (85/133), with just over a third occurring in the control populations 36.1% (48/133). These results are encouraging but with a moderate success rate and double the desired ratio of false alarms. By extended the period of assessment from 3 months to 1 year, and using long term seismic hazard assessment, the number of false alarms can be reduced and the success rate increased.

5.6.3 « Discussion of Parameter Value Selection »

A variety of parameters can be altered to effect the success rate and false alarm ratio associated with ASR as an alarm tool. These parameters include the ASR threshold value, the search radius used to generate seismic populations and what magnitude is used to differentiate large events - required to define a successful alarm period. The most prominent of these parameters being the ASR threshold value.

The selection of a singular threshold value to distinguish between acceptable and elevated seismic hazard is challenging. As previously discussed, an increase to the threshold value reduces the number of false alarms but also reduces the success rate. For this reason, it may be more realistic to assign varying threshold values to areas within a mine as opposed to a singular value. Although the analysis applied a single value for simplicity, Table 7 shows the result of increased threshold values for use with long and medium term seismic hazard assessment.

Table 7: Results for various threshold values used for ASR as an alarm tool.

	ASR Threshold Value	Successful Alarms		False Alarms	
		Number	Percent	Number	Ratio
Long Term Seismic Hazard Assessment	2.2	40	68%	84	2:1
	3	14	24%	70	5:1
	4	8	14%	28	4:1
	5	6	10%	27	5:1
Medium Term Seismic Hazard Assessment	1.8	32	54%	133	4:1
	3	11	19%	79	7:1
	4	6	10%	40	10:1
	5	2	3%	30	6:1

The ratio of false to successful alarms increases as the ASR threshold value is increased. The actual number of false alarms and their duration is greatly reduced, but because the number of successful alarms is also reduced, the ratio increases. Ultimately, the selection of the most

appropriate threshold value for mine site application is dependent on the quality of data recorded and objectives of the user.

Selecting an appropriate search radius to generate seismic populations will have a significant effect on the amount of data available for analysis. An ideal search radius includes a sufficient quantity of seismic events in each population to allow for the use of precursory seismic analysis techniques, such as ASR. However, a very large search radius may result in multiple failure mechanisms being included in the same population. It is preferable to have a single mechanism in a population. When multiple populations are present, anomalous trends may be masked or "average out". In 5.5 « Discussion of Search Radius » the effects of increasing and decreasing the search radius of 30 m at LaRonde was investigated. For the application of this methodology to other mining environments, the sublevel spacing for the area of investigation appears to be a good starting point. If no clear distinction between associated hazard levels can be made for the sample populations, the search radius likely needs to be reduced. If the majority of sample populations do not contain a sufficient quantity of seismic activity, the search radius likely needs to be increased.

For the purposes of this thesis a large magnitude event is defined as $M_L \geq 0$. Consequently, only the occurrence of an events of this size constitutes a successful alarm period at LaRonde. By reducing this value, the number of successful alarms is increased and consequently the relative ratio of false alarms is reduced. However, the number of alarms will increase. Based on the frequency-magnitude relation, each decrease of 0.3 in magnitude of interest will result in a 2 fold increase in the number of events of interest. When selecting a magnitude value to associate with a successful alarm period, it is suggested a magnitude threshold that has previously been associated with visible rock mass damage be utilized.

Variation in each of the parameters discussed affects the success and false alarm ratio associated with ASR as an alarm tool. These values should be selected based on the historic seismic response in the area of investigation. Small variations are capable of having a significant influence on this analysis technique, particularly the success rate. An empirical study to determine appropriate values for these parameters should be completed prior to the application of this methodology to other mining environments.

5.7 « Chapter Summary »

ASR has been analyzed for populations of varying hazard over various time periods. Peak ASR, ASR based hazard mapping and ASR as an alarm tool have been presented. Medium and long term assessment periods provide more reliable and representative results for the sample populations selected to represent the area of interest at LaRonde mine. Short term assessment should only be used to identify areas that experience large changes in local stress conditions over very short periods of time. For LaRonde, this is not typical of the larger area and therefore it is a less effective seismic hazard assessment time frame.

Peak ASR provides an indication of the extent to which local rock mass conditions can change in relative periods of time. Short term peak ASR values are most effective in identifying large changes that occur very quickly, typically over the course of less than a week. Medium and long term peak ASR values provide a more representative view of the entire rock mass. They are capable of identifying areas of high, moderate and low seismic hazard.

ASR based hazard mapping allows for spatial visualization of areas within a rock mass that may be experiencing local stress increase. Using points along mine excavations to generate seismic populations reduces bias that may be introduced from user defined groups. Areas within the rock

mass that have experienced large seismic events in the past, correspond well to areas identified as possessing elevated hazard using both ASR and peak ASR hazard maps.

The search radius value used to generate seismic populations for application of ASR analysis needs to be carefully selected. High hazard populations are not exceedingly susceptible to changes in search radius values. Both reductions and increases to the search radius typically generate populations with the same overall trends in ASR. Due to the small quantity of events contained within low hazard populations however, large reductions and increases can have negative impacts on analysis. When the search radius size is reduced the number of events contained within the population can be decreased to insufficient quantities. When the search radius size is increased, it is possible for the local events to be overpowered by large quantities of events located near the outskirts of the population which may be the result of a different failure mechanism.

The use of ASR as an alarm tool is best used with long term seismic hazard. By increasing the preceding time period considered for ASR calculations, individual events have less of an influence on the apparent stress distribution and ASR fluctuation between subsequent events is minimized. By utilizing this more gradual change in ASR values, the number of false alarms associated with ASR for use as an alarm tool are reduced. Furthermore, because longer preceding time periods allow for more gradual changes in local stress conditions to be observed, ASR values are typically higher. This enables the threshold value to be increased when compared to medium term assessment, reducing the number of false alarms while simultaneously increasing the success rate.

Peak ASR, ASR based hazard mapping and ASR as an alarm tool all possess value in terms of seismic hazard assessment. Used in combination they can provide insight into which areas of the rock mass represent elevated seismic hazard and risk. Peak ASR is an analysis technique that can be used to generate hazard maps for large areas. Results from these hazard maps correspond well to the occurrence of large magnitude events and areas that have experienced large stress changes inferred from apparent stress values. ASR for use as an alarm tool with long term seismic hazard assessment produces results of 68% success rate with 2:1 false alarm ratio. The benefits of using ASR as an analysis tool for seismic risk management in mining operations is clear.

Chapter 6

6 « Conclusions »

This thesis investigates precursory trends in apparent stress for forecasting seismic hazard at Agnico Eagle's LaRonde mine. A relative apparent stress ratio concept is presented along with applications for seismic hazard analysis, hazard mapping and use as an alarm tool. Apparent stress ratio (ASR) provides a consistent means of comparing apparent stress measurements in seismic populations across varying stress and geological conditions within a rock mass.

The intent of apparent stress ratio (ASR) is to identify increasing apparent stress within a seismic population as a proxy for increasing stress conditions within a rock mass. Application of ASR to sample seismic populations at Agnico Eagle's LaRonde mine has shown that ASR is a reliable means of analyzing local stress conditions in the rock mass and providing insight into the associated seismic hazard. Unlike previous analysis techniques that primarily consider apparent stress, this methodology incorporates time and does not require the selection of numerous threshold values. By employing a relative ratio, all apparent stress measurements are considered in relation to those contained within the same seismic population. This eliminates the bias introduced to analysis by thresholds values that serve to quantify what is considered high and abnormal apparent stress. The application of ASR to high, moderate, and low hazard seismic populations at Agnico Eagle's LaRonde mine has been investigated over varying time frames and suggests that ASR is strongly correlated with the occurrence of large seismic events - high seismic hazard.

6.1 « Contributions »

The main contribution of this thesis to the field of mining induced seismicity is the use of a relative apparent stress ratio to quantify changes in apparent stress for a given seismic population. The ratio can be used as an analysis tool, to generate hazard maps, or in conjunction with an alarm tool.

6.1.1 « ASR as an Analysis Tool »

Trends in ASR can be effectively analyzed on an Apparent Stress Ratio Time History chart (ASRTH). This chart enables the visualization of trends relating to seismic hazard and the historic rock mass response to mining. A key element that has been identified for hazard assessment of a seismic population is peak ASR.

An excellent measure of seismic hazard in relation to apparent stress is peak ASR. Peak ASR refers to the largest ASR value for a seismic population. This value provides insight into the local rock mass conditions – specifically the ability of the rock mass to buildup and release stress over a specified time window. Areas with relatively high peak ASR values should be considered representative of moderate to high seismic hazard. Low hazard seismic populations typically possess a relatively constant stress state and therefore ASR values tend to be much smaller than those of elevated hazard populations. The identification of areas at LaRonde mine with large peak ASR values correlates very well to high and moderate hazard seismic populations.

Trends in peak ASR over time are relatively consistent over varying calculation time frames. Using long, medium and short term seismic hazard assessment generates similar results in reference to seismic hazard analysis for the sample populations at LaRonde mine. This is an important component of a reliable seismic analysis tool.

6.1.2 « ASR and Peak ASR Hazard Mapping »

Hazard maps are the spatial representation of seismic source parameters and analysis techniques. By subdividing a seismic database into smaller populations and assigning them to local mine excavations, maps of underground workings can be created. ASR hazard maps generated using long term hazard assessment are capable of identifying areas experiencing increased stress conditions within a rock mass. Medium term hazard assessment may also produces meaningful results, but with a shortened time frame, more gradual changes in stress conditions can be underrepresented. It is for this reason that the use of short term seismic hazard assessment, for the generation of hazard maps, is not recommended.

Peak ASR hazard mapping is capable of serving as an indicator of seismic hazard across all three seismic hazard assessment time periods (long, medium, and short). While long and medium term assessment are more consistent, short term enables the user to quickly identify which regions within a rock mass are capable of experiencing large scale stress changes in very short time periods. Peak ASR hazard maps for the area of interest at LaRonde show results consistent with areas in the rock mass that have previously been defined as representative of elevated seismic hazard.

6.1.3 « ASR as an Alarm Tool »

The use of ASR for seismic hazard assessment is not appropriate over any time period when there is no preceding seismic activity. Seismic events that occur "out of the blue" cannot be forecasted based on precursory activity when there is no seismic activity. Long term seismic hazard assessment is the most reliable for use as an alarm tool. As preceding calculation time windows are increased, the apparent stress distribution from which percentile values are obtained

for ASR calculation becomes less susceptible to the influence of individual events. This translates into less volatility in ASR values over time, and therefore is better suited for use as an alarm tool. A success rate of 68% was obtained when using a threshold value of 2.2 for long term seismic hazard at LaRonde mine. Paired with a false alarm ratio of approximately 2:1, most of which occur in high and moderate hazard populations, the results of ASR as an alarm tool are excellent.

6.2 « Recommendations for Further Work »

Apparent stress ratio has been proven effective for application in a large area of interest at Agnico Eagle's LaRonde mine. It is recommended that this methodology be applied to other high stress mining environments. This would allow for the integration of potential improvements, as well as provide reassurance of the ability of this empirical analysis technique for universal application.

Further investigation into trends in ASR of low hazard seismic populations is recommended. Due to the lower bound of M_L = -1.5 applied to this data set, low hazard populations were under represented in analysis. When large quantities of mining process events (M_L < -1.5) are included in ASR analysis, it skews the cumulative apparent stress distribution towards smaller values. By reducing the number of mining process events considered, such as was done in this analysis, this problem is eliminated. Investigation into ASR for large quantities of mining processes events and low hazard populations may provide useful insight into identifying low hazard seismic populations.

While ASR does not appear to be less effective for forecasting hazard associated with large fault-slip source mechanism seismic events, as it relates to LaRonde mine, further investigation using

seismic data from mines with prominent geological structures is recommended. Comparing ASR values for populations associated with shears, faults, dykes and other geological features may provide further insight into potential relations between ASR and fault-slip source mechanism events.

References

Boatwright, J., and J.B. Fletcher. (1984) The partition of radiated energy between P and S waves. *Bulletin of the Seismological Society of America*, Volume 74, pp. 361-376.

Butler, A.G. (1997) Space-time clustering of potentially damaging seismic events and seismic viscosity in Western Deep Levels East and West Mines. *Proceedings of Rockbursts and Seismicity in Mines,* (Editors: S Gibowicz and S Lasocki), Krakow, pp. 89-93.

Collins D.S., Toya, T., Pinnock, I., Shumila, V., and Hosseini, Z. (2014) 3D velocity model with complex geology and voids for microseismic location and mechanism. *Proceedings of the Seventh International Conference on Deep and High Stress Mining*, (Editors: M Hudyma and Y. Potvin), Australian Centre for Geomechanics, Sudbury, pp. 681-688.

Cook, N.G.W. (1976) Seismicity associated with mining. *Engineering Geology,* Volume 10, pp. 99-122.

Dubé, B., Gosselin, P., Mercier-Langevin, P., Hannington, M., and Galley, A. (2007). Gold-rich volcanogenic massive sulphide deposits. *Mineral deposits of Canada: a synthesis of major deposit-types, district metallogeny, the evolution of geological provinces, and exploration methods: Geological Association of Canada, Mineral Deposits Division, Special Publication 5,* pp. 75-94.

Gibowicz, S.J. and Kijko, A. (1994) An introduction to mining seismology. 1st edition. San Diego, Academic Press, 396 p.

Google Maps, May 2015. Pg 37, Fig 18. Pg 48, Fig 26.

Gutenberg, B. and Richter, C.F. (1944) Frequency of earthquakes in California. *Bulletin of the Seismological Society of America,* Volume 34, pp. 185-188.

Hasegawa, H.S., Wetmiller, R.J. and Gendzwill, D.J. (1989) Induced seismicity in mines in Canada - an overview. *Pure and Applied Geophysics,* Volume 129, pp. 432-453.

Heal, D. (2010) Observations and analysis of incidences of rockburst damage in underground mines. PhD Thesis, University of Western Australia, 718 p.

Hedley, D.G.F. (1992) Rockburst handbook for Ontario hardrock mines. CANMET Special Report SP92-1E, 305 p.

Herget, G. (1988) Stresses in rock. A.A Balkema, Rotterdam, Netherlands, 179 p.

Herget, G. (1974) Ground stress determinations in Canada. *Rock Mechanics,* Volume 6, pp. 53-64.

Hoek, E. and Brown, E.T. (1980) Underground excavations in rock. London: The Institution of Mining and Metallurgy, 527 p.

Hudyma, M.R. (2004) Mining-Induced Seismicity in Underground, Mechanised, Hardrock Mines. Australian Centre for Geomechanics, Perth, 138 p.

Hudyma, M.R. (2008) Analysis and interpretation of clusters of seismic events in mines. PhD Thesis, University of Western Australia, 408 p.

Hudyma. (2014) Course notes. ENGR 5356 – Operation and application of seismic monitoring systems in mines. Laurentian University.

Hudyma, M. R., and Brummer, R. K. (2007) Seismic monitoring in mines - Design, operation, tricks and traps. *The 3rd International Seminar on Deep and High Stress Mining*. pp. 1423-1430.

Iamgold. (2012) Cote Gold Project, Ontario. Retrieved May 2015 from http://www.iamgold.com/English/Operations/Development-Projects/Cote-Lake-Ontario/Geology--Mineralization/default.aspx

Kaiser, P.K., McCreath, D.R. and Tannant D.D. (1996) Canadian rockburst support handbook. Geomechanics Research Centre, Laurentian University, Sudbury, 303p.

Mendecki, A.J. (1993) Real time quantitative seismology in mines. *Proceedings of Rockbursts and Seismicity in Mines*, (Editor R.P. Young), Rotterdam. pp. 287-295.

Mendecki, A.J. (1997) Seismic monitoring in mines. London: Chapman and Hall. 262 p.

Mendecki, A.J., van Aswegen, G. and Mountfort, P. (1999) A guide to routine seismic monitoring in mines. A Handbook on Rock Engineering Practices for Tabular Hard Rock Mines. (Editors A.J. Jager and J.A. Ryder), Creda Communications, Cape Town. 371 p.

Mendecki, A.J. and van Aswegen, G. (2001) Seismic monitoring in mines: selected terms and definitions. *In Proceedings of Rockbursts and Seismicity in Mines - RASIM 5, Johannesburg,* (Editors G. van Aswegen, R.J. Durrheim and W.D. Ortlepp), Johannesburg: South African Institute of Mining and Metallurgy, pp. 563-570.

Mercier-Langevin, F. (2010) LaRonde Extension – mine design at three kilometres. *Proceedings of the Fifth International Conference on Deep and High Stress Mining*, (Editors M. Van Sint Jan and Y. Potvin), Australian Centre for Geomechanics, Santiago, pp. 3-15.

Mercier-Langevin, F., Hudyma, M.R. (2007) The development and implementation of a comprehensive seismic risk management plan at Agnico-Eagle's LaRonde mine. *Proceedings of the Fourth International Conference on Deep and High Stress Mining*, (Editor Y. Potvin), Australian Center for Geomechanics, Perth, pp. 221-232.

Nuttli, O.W. (1973) Seismic wave attenuation and magnitude relations for Eastern North America. *Journal of Geophysical Research,* Volume 78, pp. 876-885.

Ortlepp, W.D. (1997) Rock Fracturing and Rockbursts: an illustrated study, *Monograph Series M9,* South African Institute of Mining and Metallurgy, Johannesburg.

Plouffe, M. (1992), Preliminary Local magnitude Scales for Mining-Induced Seismicity at Some Mines in the Sudbury Basin, *Mining Research Laboratories,* Canada.

Richter, C.F. (1935) An instrumental earthquake magnitude scale. *Bulletin of the Seismological Society of America,* Volume 25, pp 1-32.

Simser, B. (2008) Mining in a seismically active fault zone: a case study from Xstrata's Craig mine, Sudbury, Ontario. *Proceedings of the Third International Seminar on Strategic vs Tactical Approaches in Mining,* (Editor J. Hadjgeorgiou), Quebec City, Canada, pp. 272-284.

Simser, B.P., Falmagne, V., Gaudreau, D. and MacDonald, T. (2003) Seismic response to mining at the Brunswick mine. *Canadian Institute of Mining and Metallurgy Annual General Meeting,* Montreal, 12 p.

Turcotte, P. (2014) Practical applications of a rockburst database to ground support design at LaRonde Mine. *Proceedings of the Seventh International Conference on Deep and High Stress Mining,* (Editors: M Hudyma and Y. Potvin), Australian Centre for Geomechanics, Sudbury, pp. 79-92.

Urbancic, T.I., Young, R.P., Bird, S. and Bawden, W. (1992) Microseismic source parameters and their use in characterizing rockmass behaviour: considerations from Strathcona Mine. *In Proceedings of 94th Annual General Meeting of the CIM: Rock Mechanics and Strata Control Sessions,* Montreal, 26-30 April, 1992, pp. 36-47.

van Aswegen, G. (2005) Routine seismic hazard assessment in some South African mines. *In Proceedings of Controlling Seismic Risk - Rockbursts and Seismicity in Mines,* (Editors: Y. Potvin and M.R. Hudyma), Australian Centre of Geomechanics, Perth, pp. 437-444.

Wesseloo, J., Woodward, K. and Pereira, J. (2014) Grid-based analysis of seismic data. *In Proceedings of the 6th South African Rock Engineering Symposium, SARES 2014,* South Africa, 12-14 May, 2014. Southern African Institute of Mining and Metallurgy, Johannesburg.

Wyss, M. and Brune, J.N. (1968) Seismic moment, stress and source dimensions for earthquakes in the California-Nevada region. *Journal of Geophysical Research,* Volume 73, pp. 4681-4694.

Young, D.P. (2012) Energy variations in mining-induced seismic events using apparent stress. MASc Thesis, Laurentian University, 85 p.

Appendices

Appendix A: Magnitude scale relation summary and charts for LaRonde mine.

ACG Richter refers to the magnitude values produced by the local regional macroseismic monitoring network. NRCan Nuttli refers to the magnitude values produced by Natural Resources Canada. ESG Local refers to the magnitude values produced by the ESG microseismic monitoring system. Bounds of ± 0.3 and ± 0.5 are represented on each graph by the solid and dashed lines respectively.

Magnitude Scales	**Relation**	**±0.3**	**±0.5**
ACG Richter & NRCan Nuttli	NRCan Nuttli = ACG Richter + 0.3	85%	94%
ESG Local & NRCan Nuttli	ESG Local = NRCan Nuttli - 1.3	48%	64%
ACG Richter & ESG Local	ACG Richter = ESG Local + 1.0	50%	72%

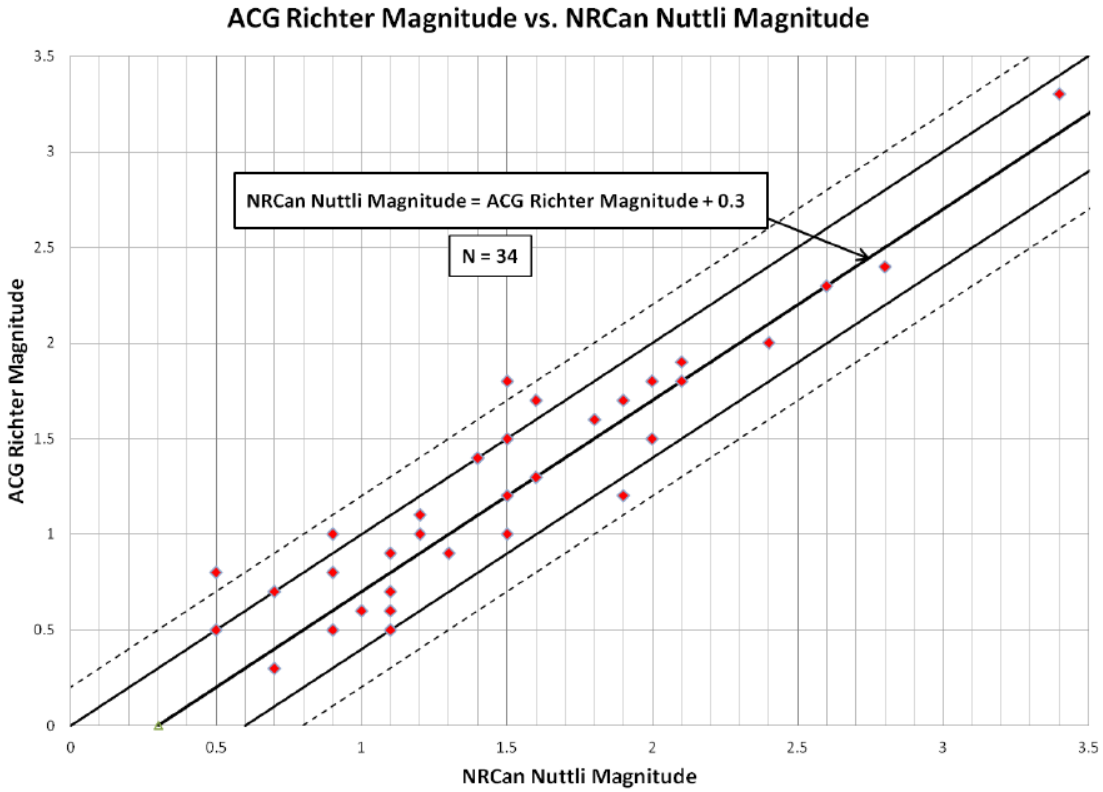

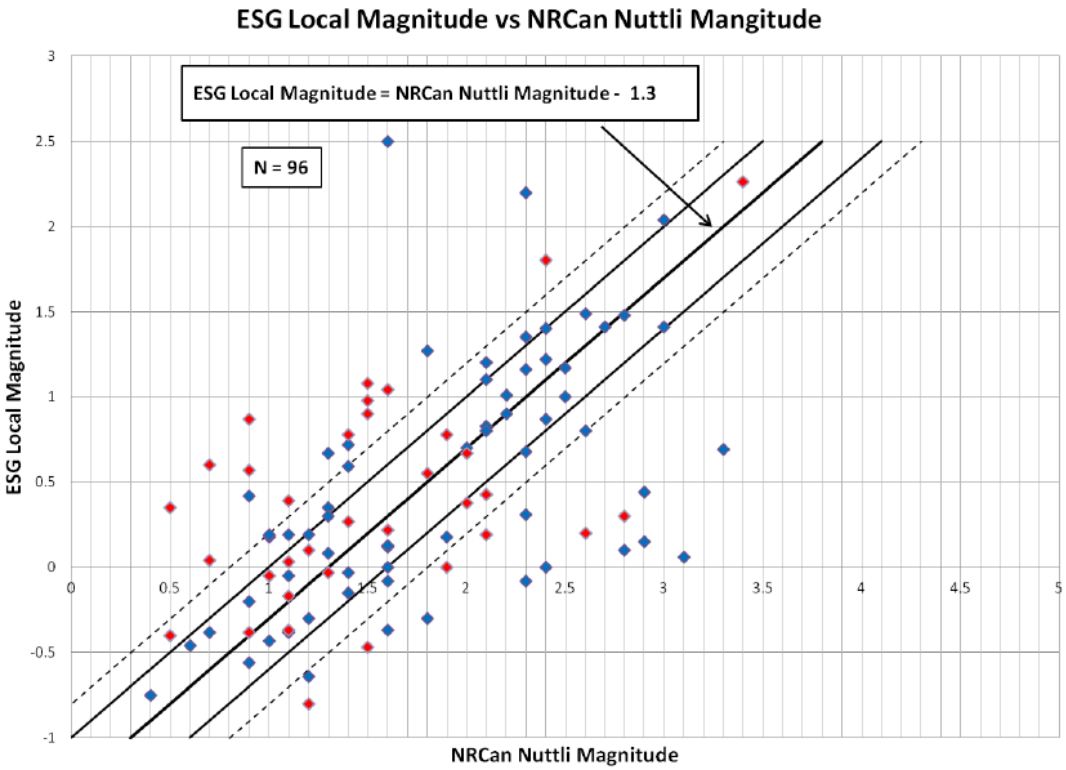
ESG Local Magnitude vs NRCan Nuttli Mangitude
ESG Local Magnitude = NRCan Nuttli Magnitude - 1.3
N = 96
ESG Local Magnitude
NRCan Nuttli Magnitude

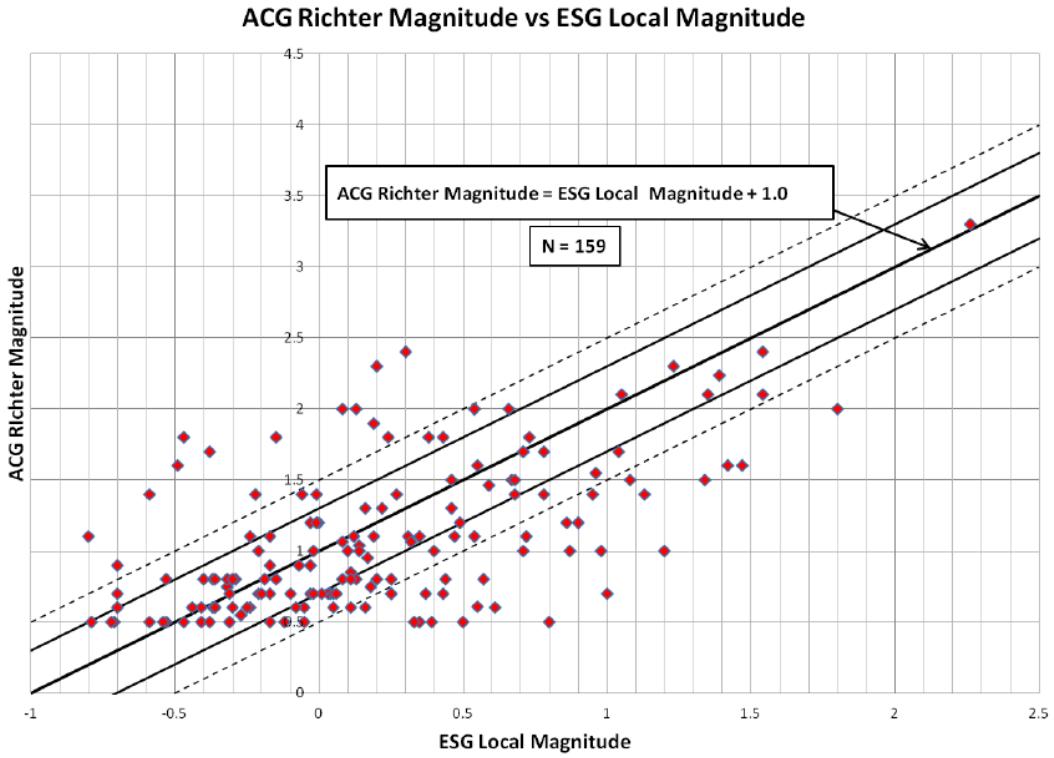
ACG Richter Magnitude vs ESG Local Magnitude
ACG Richter Magnitude = ESG Local Magnitude + 1.0
N = 159
ACG RIchter Magnitude
ESG Local Magnitude

Appendix B: Summary of high hazard sample population ID: 1.

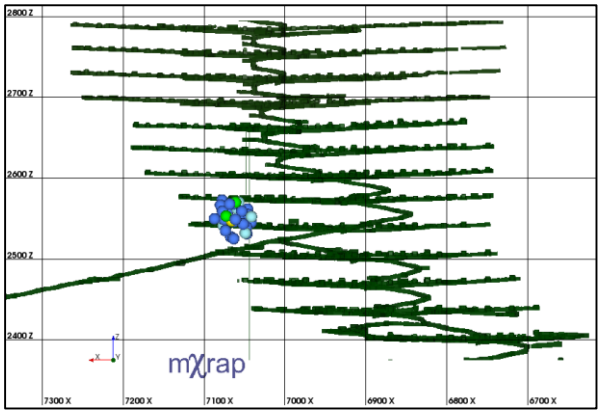

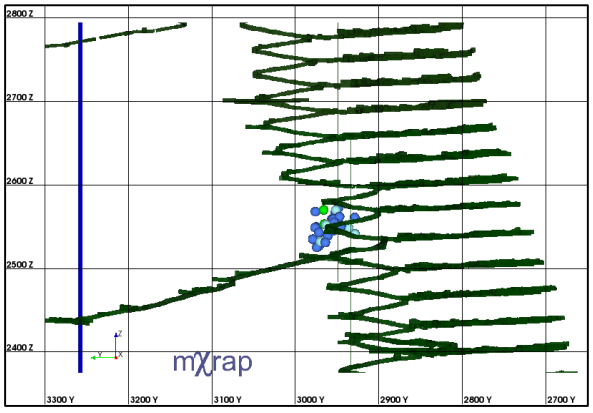

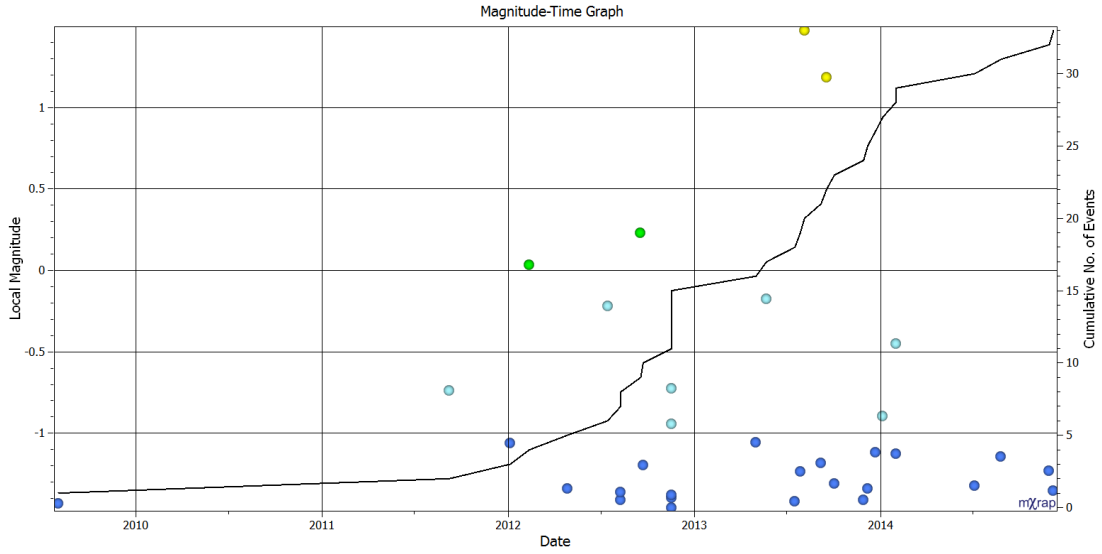

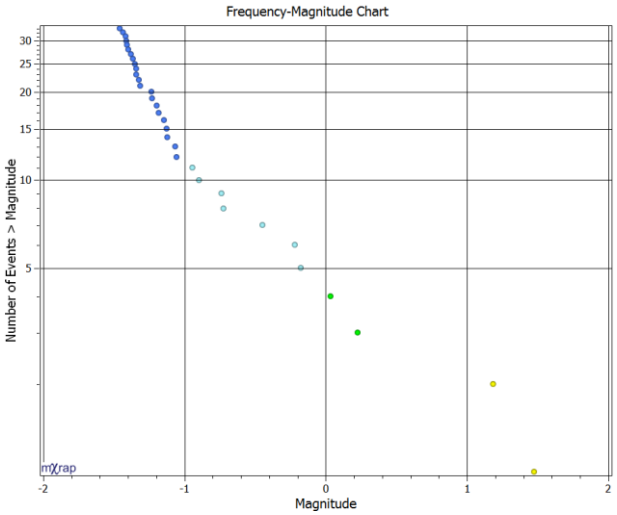

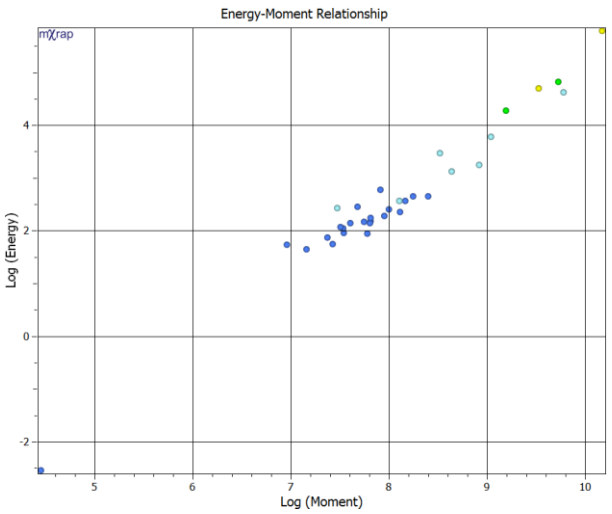

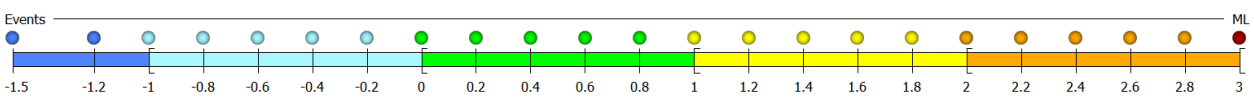

Appendix C: Summary of high hazard sample population ID: 3.

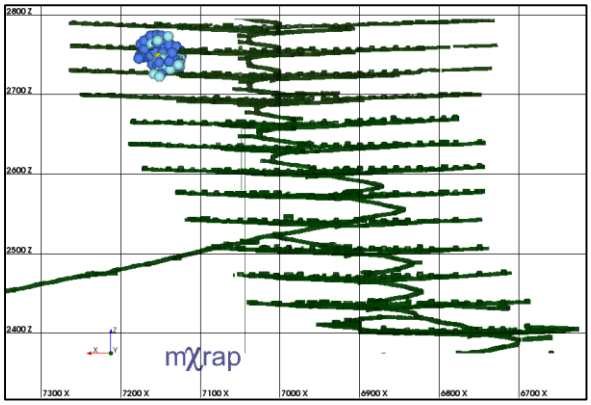

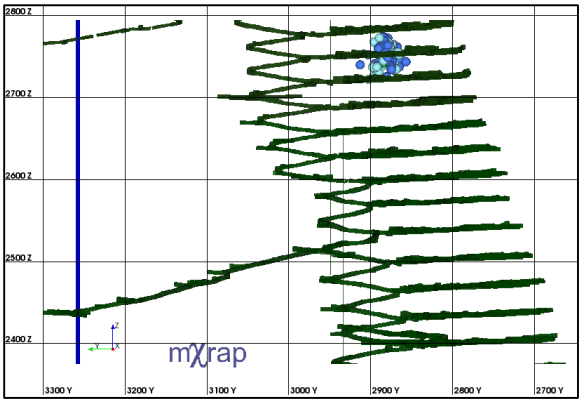

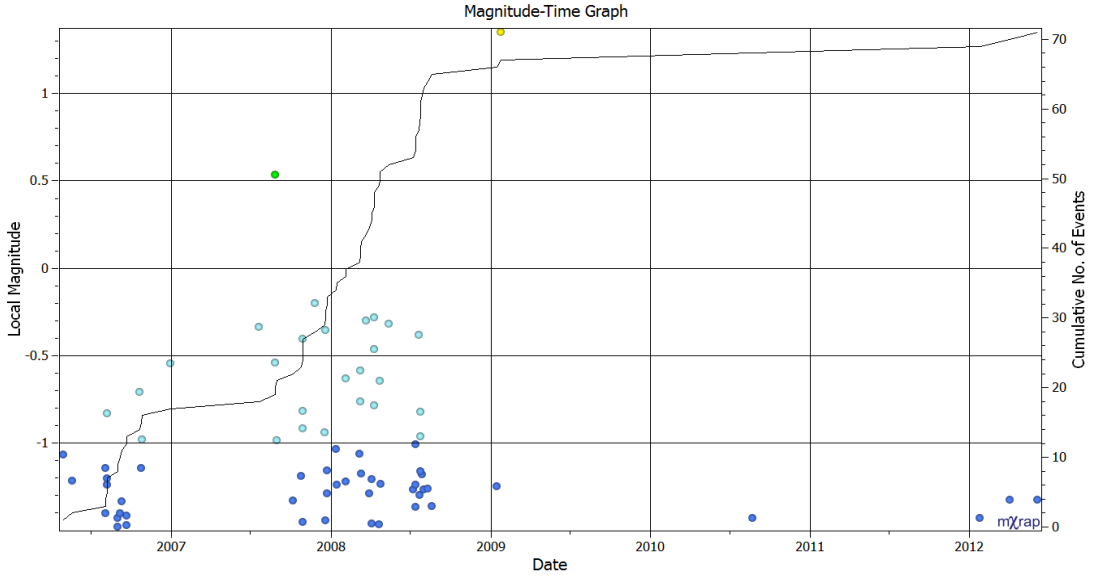

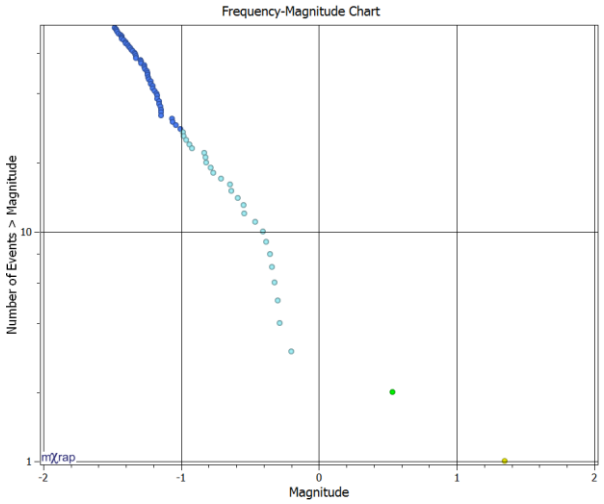

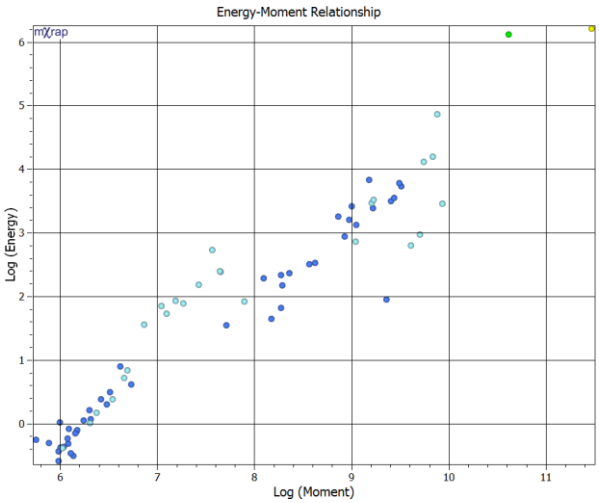

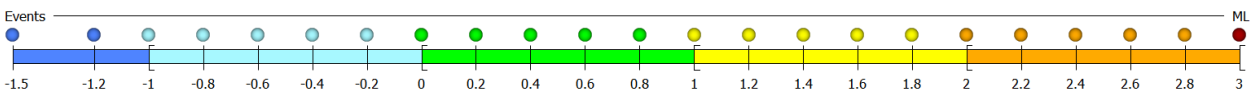

Appendix D: Summary of high hazard sample population ID: 6.

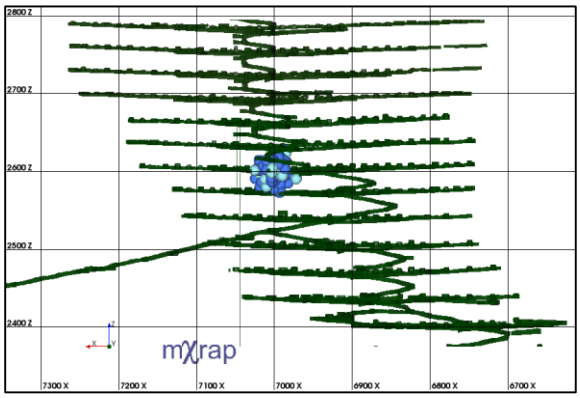

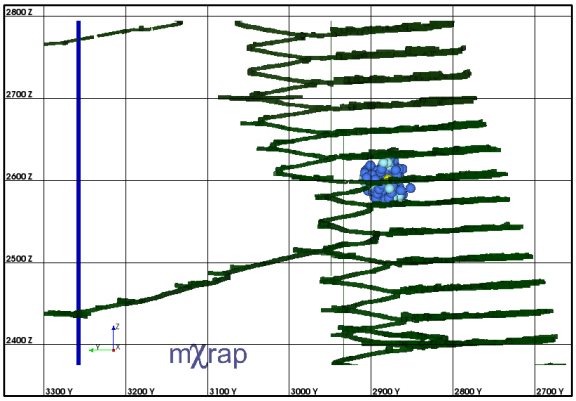

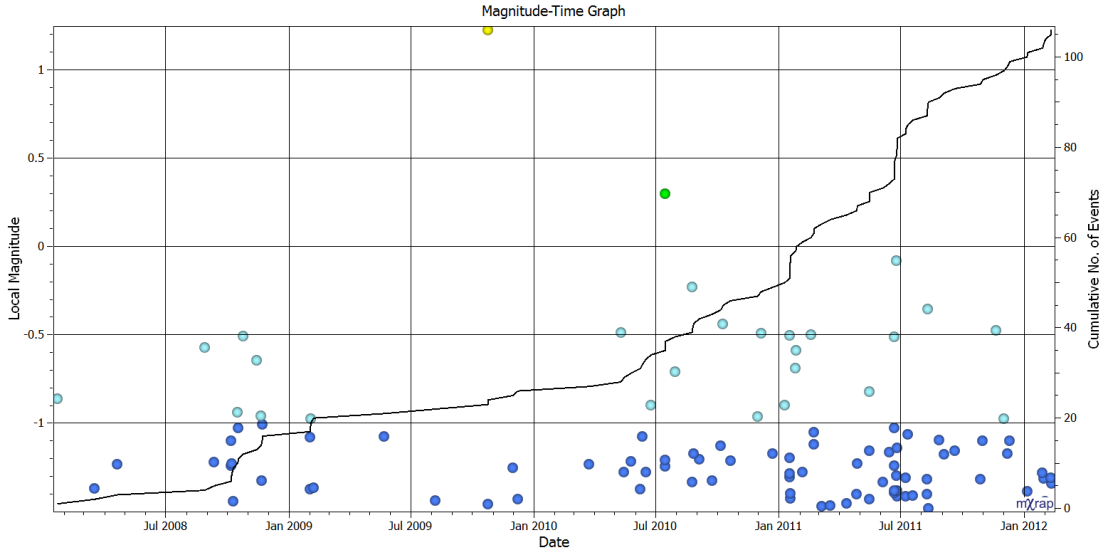

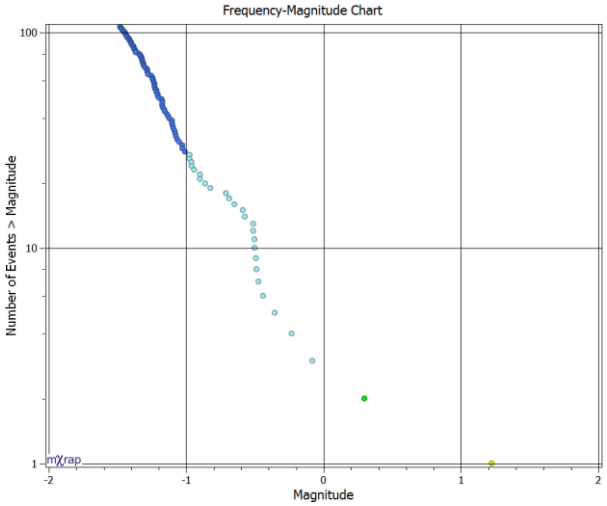

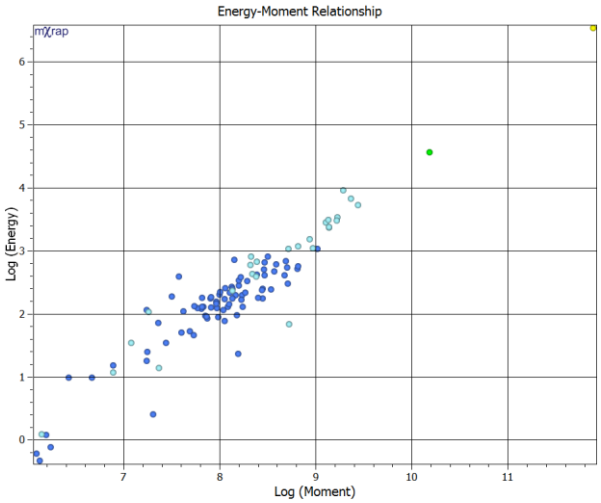

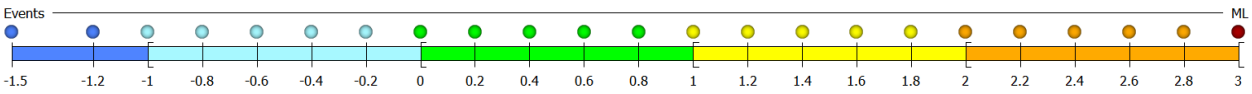

Appendix E: Summary of high hazard sample population ID: 7.

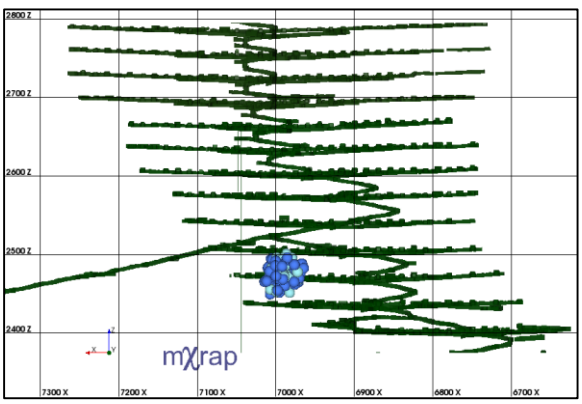

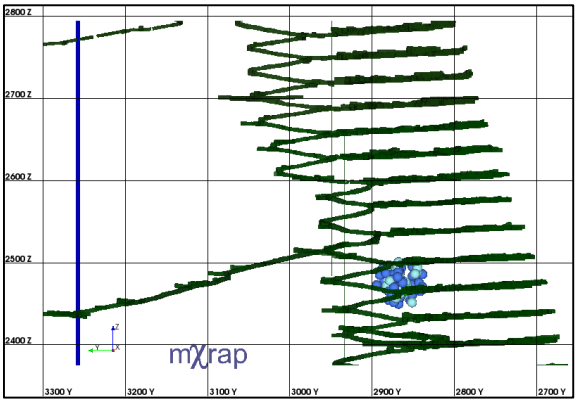

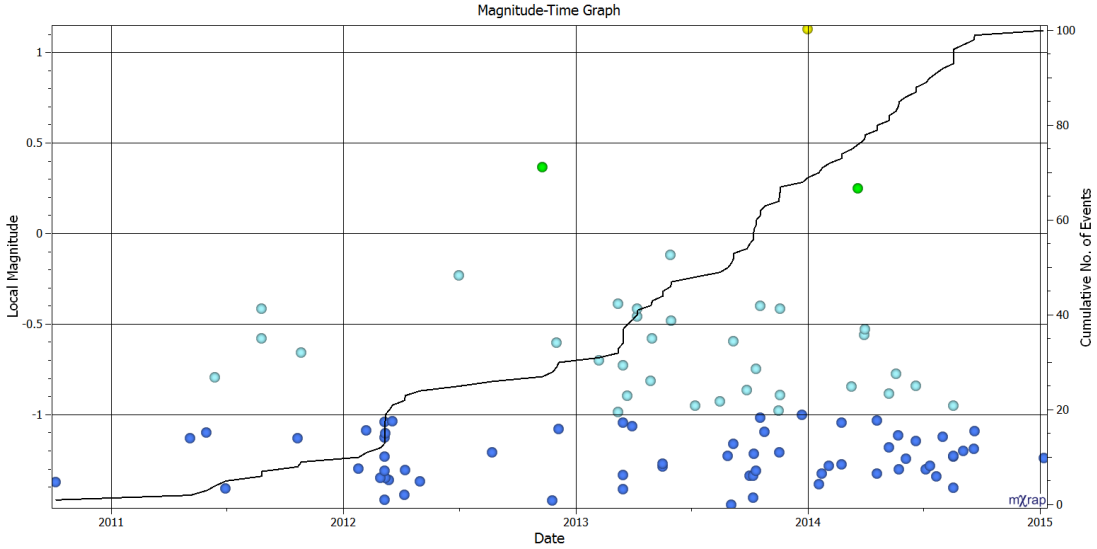

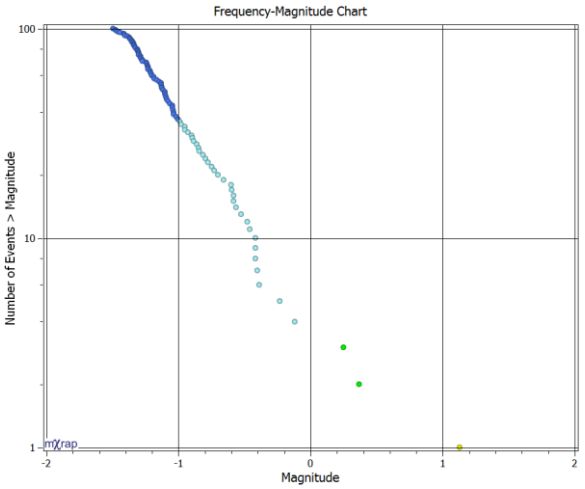

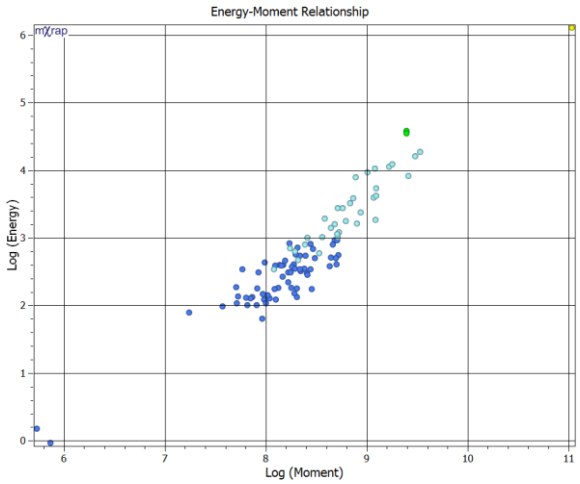

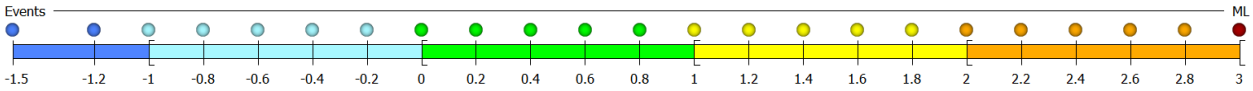

Appendix F: Summary of high hazard sample population ID: 9.

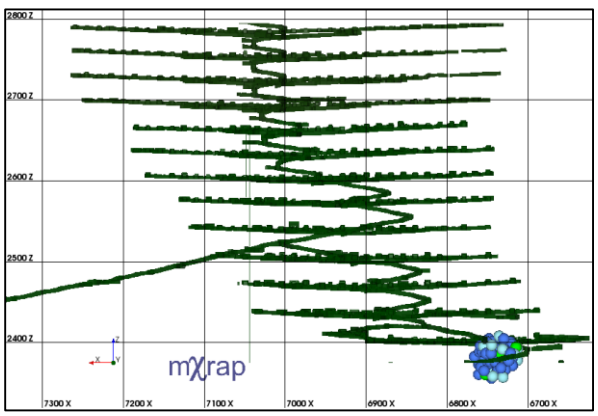

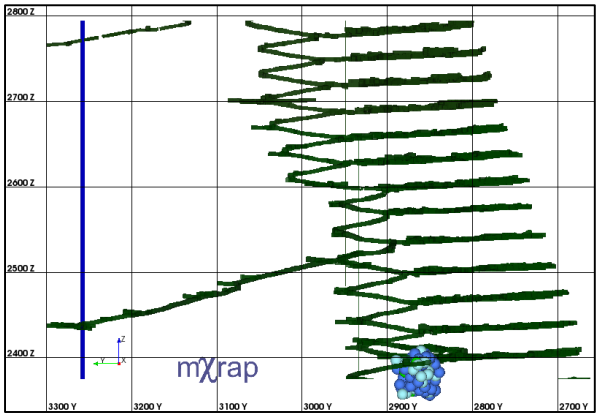

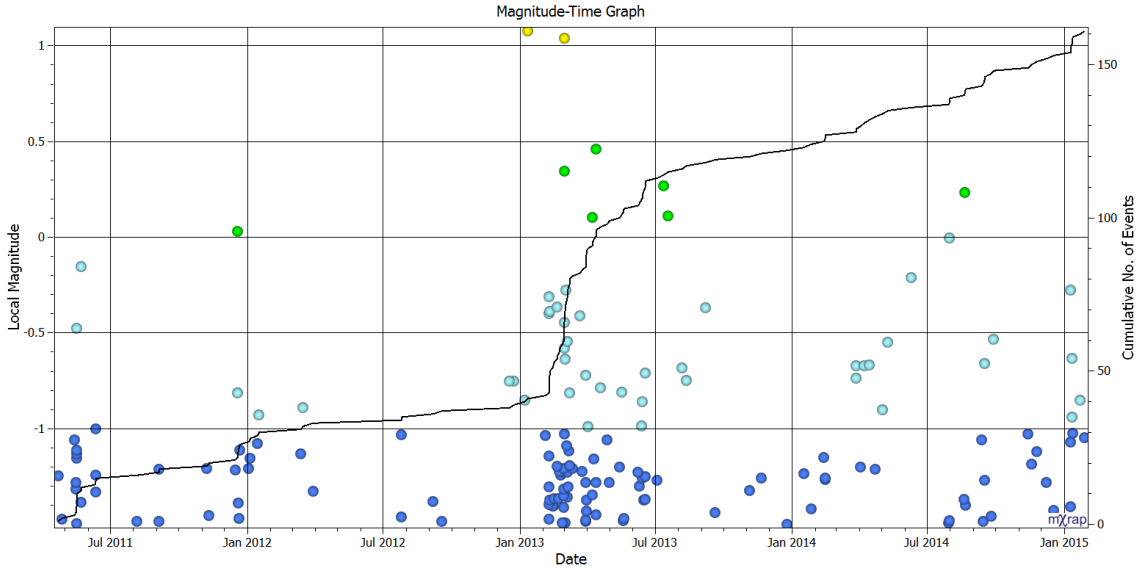

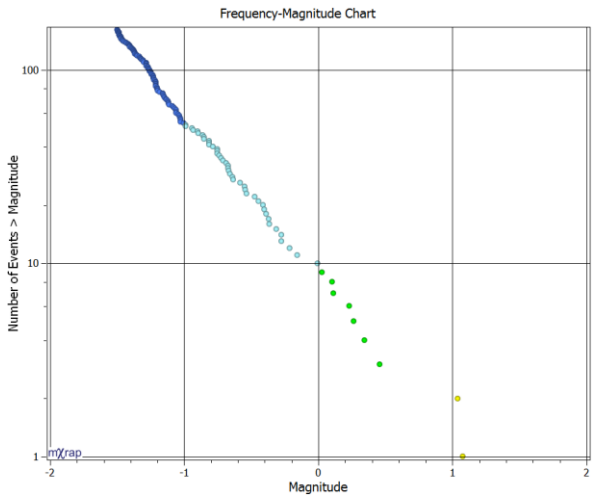

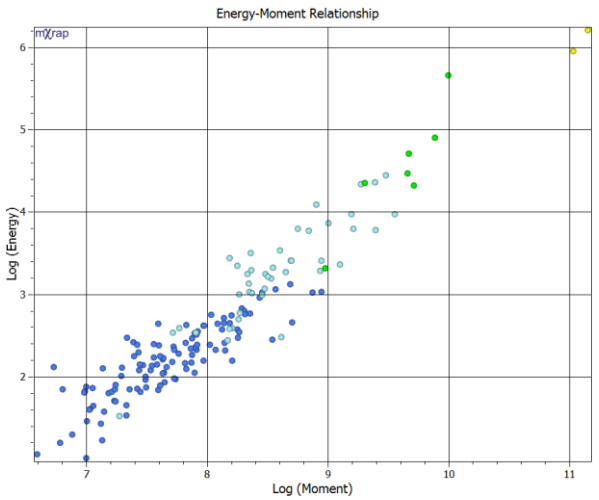

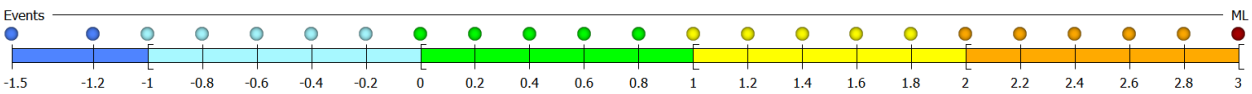

Appendix G: Summary of high hazard sample population ID: 15.

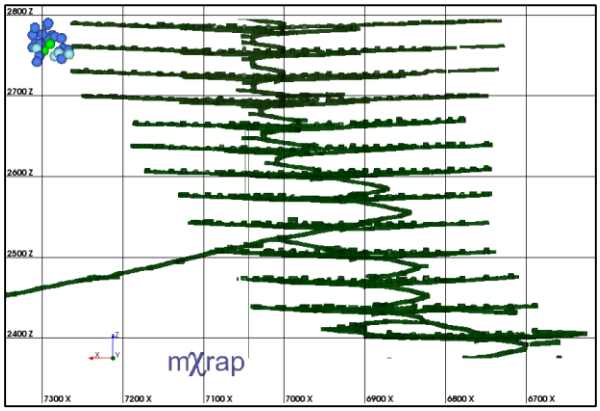

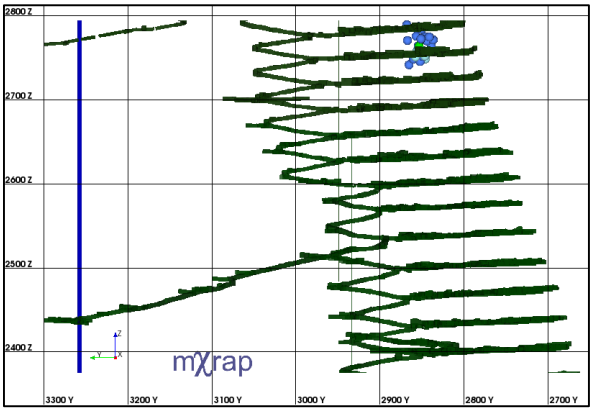

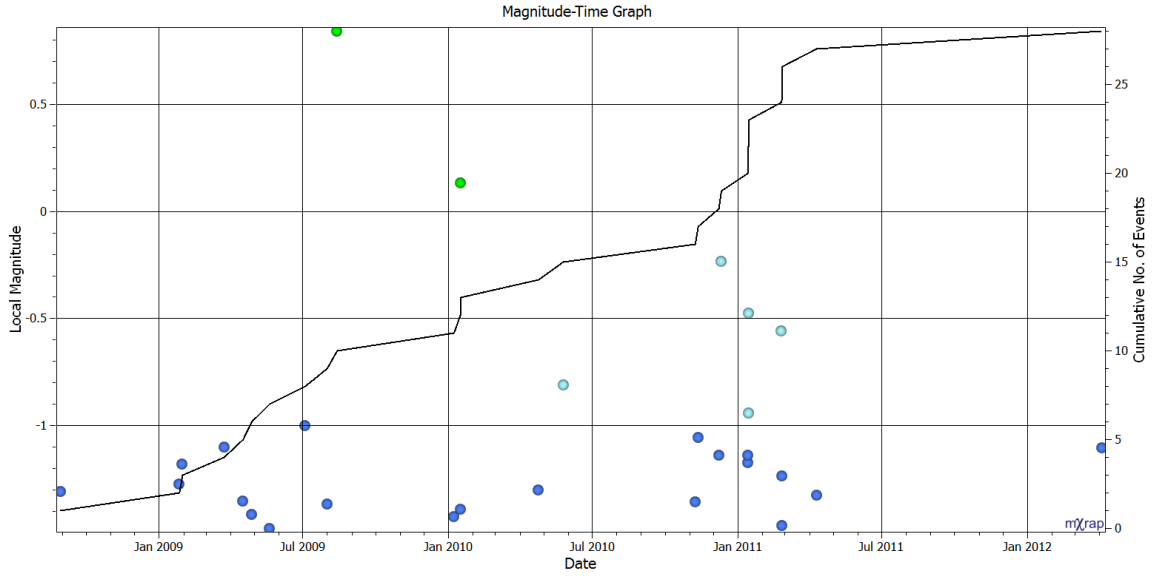

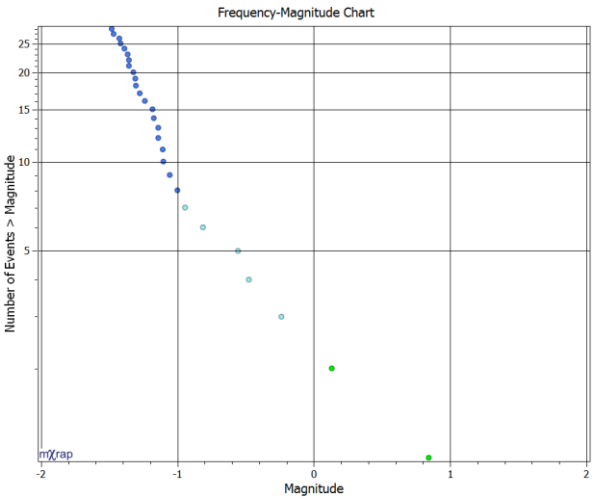

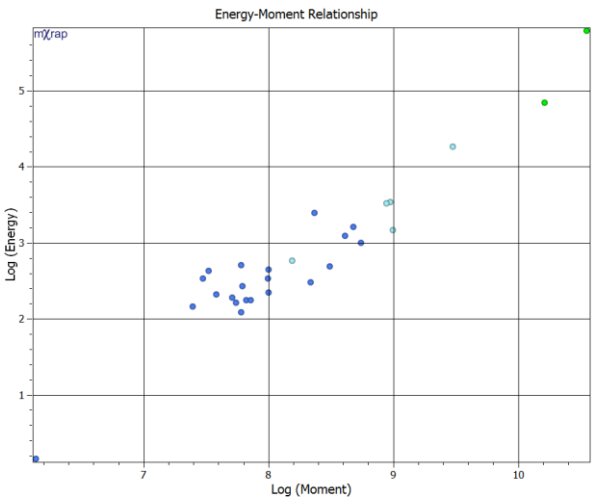

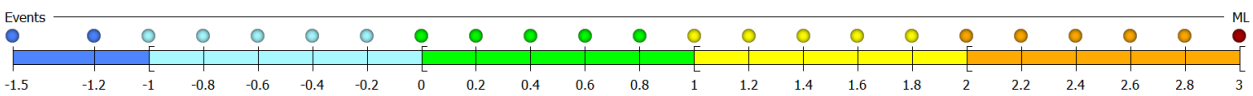

Appendix H: Summary of high hazard sample population ID: 18.

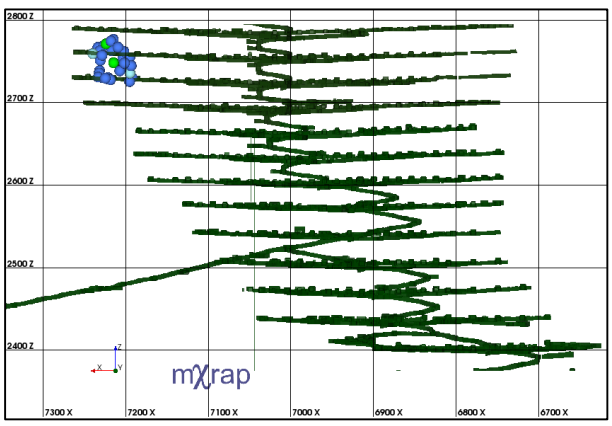

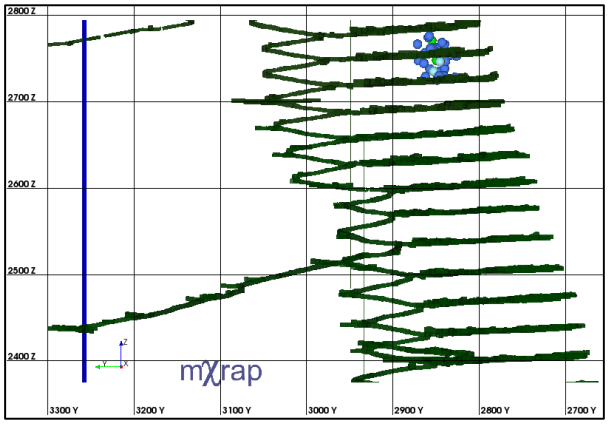

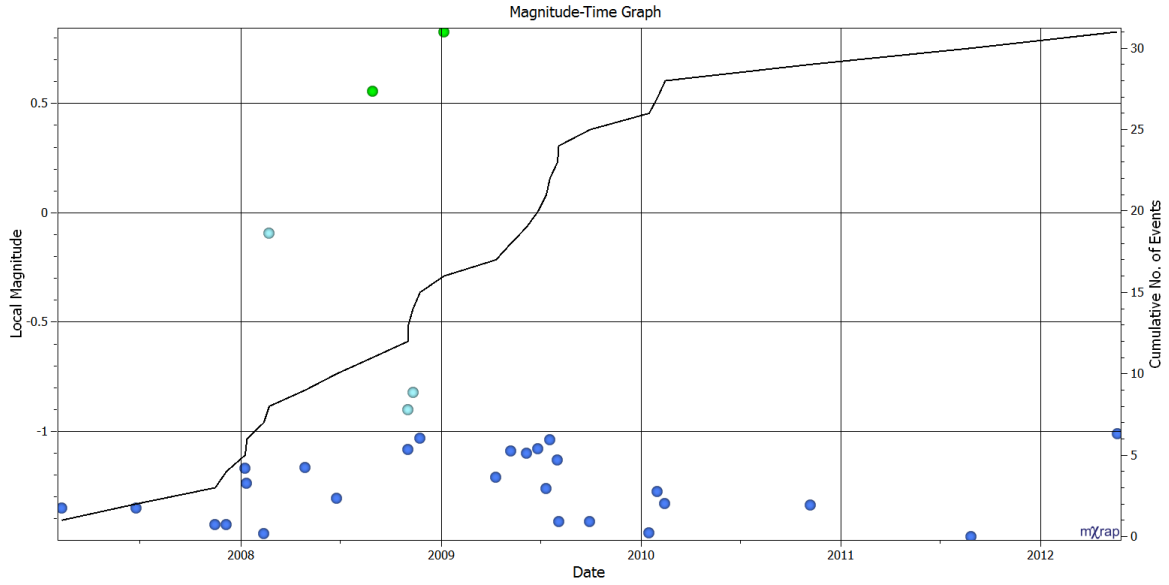

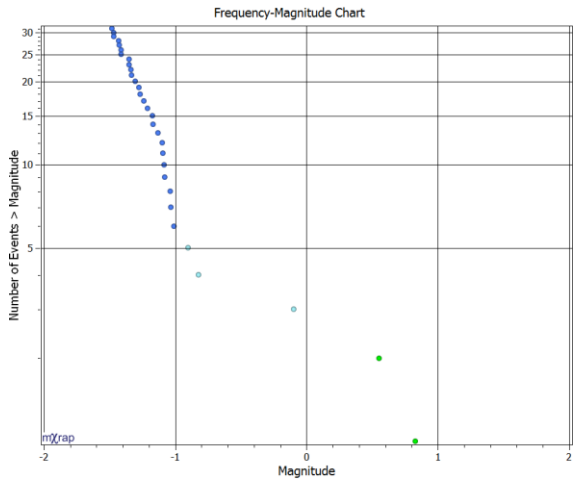

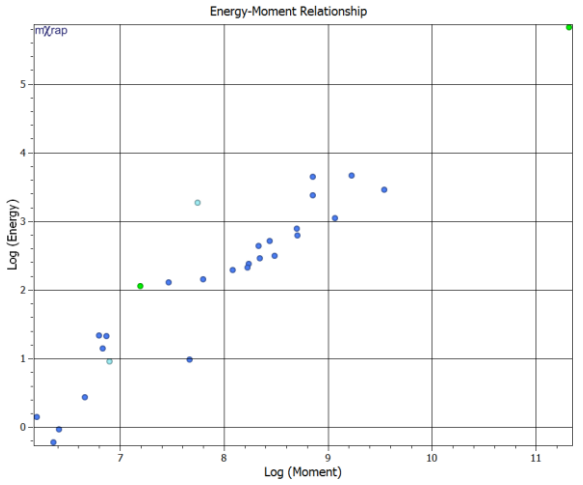

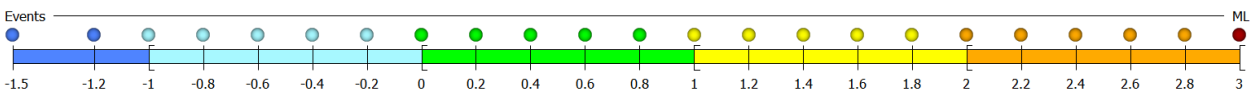

Appendix I: Summary of high hazard sample population ID: 22.

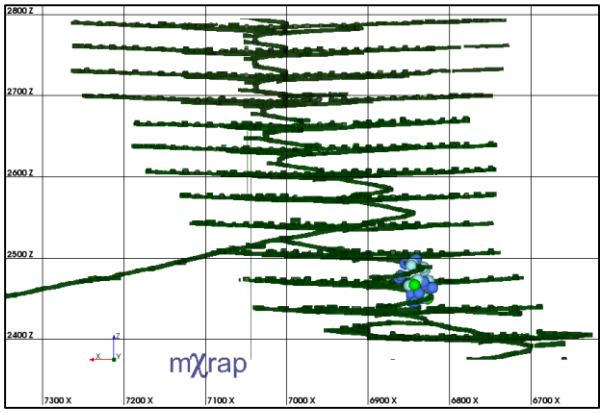

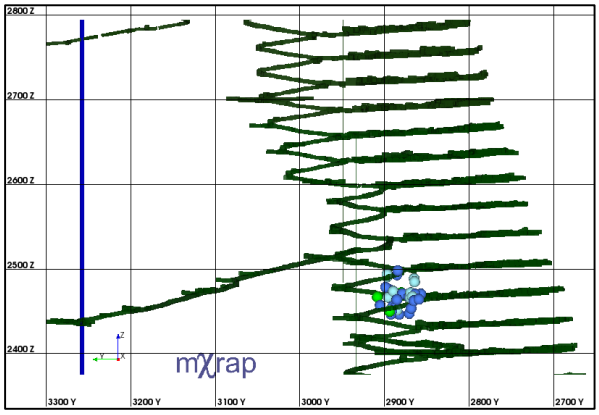

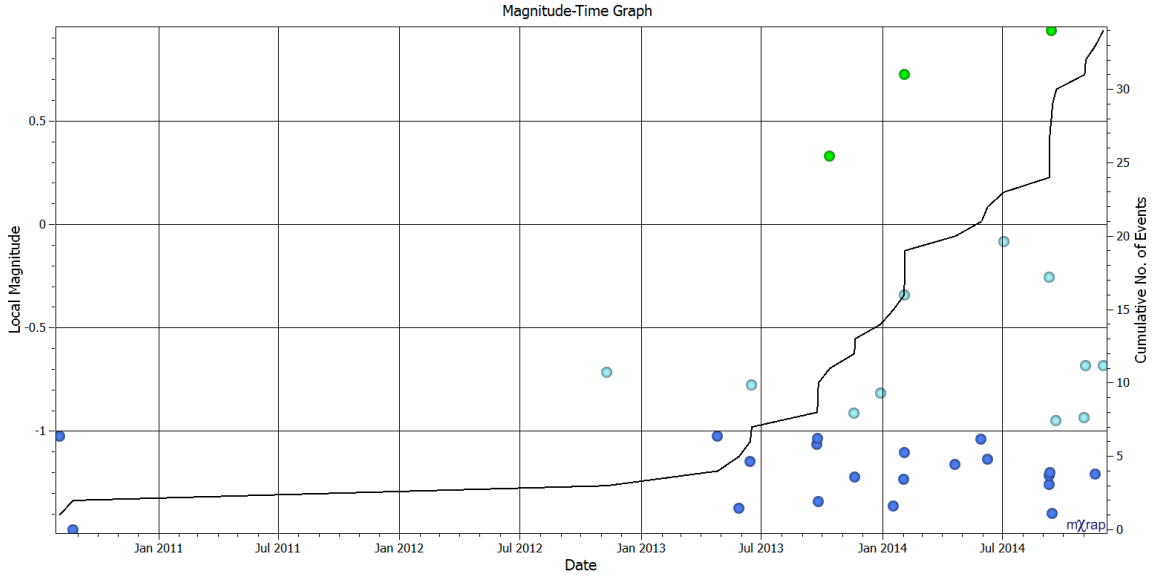

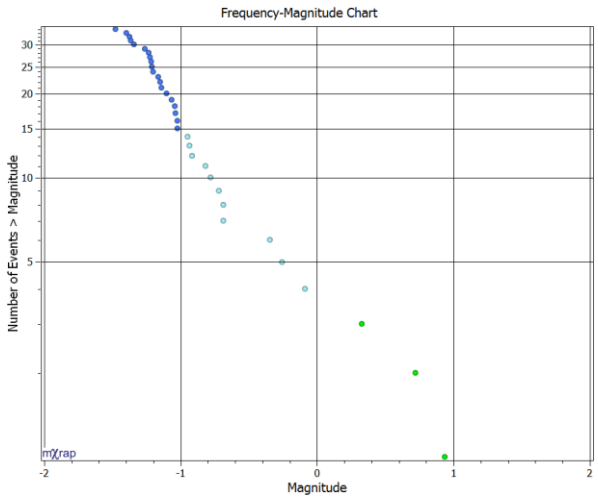

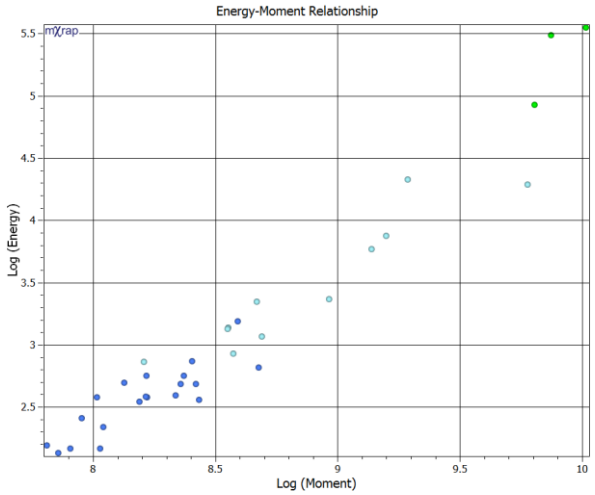

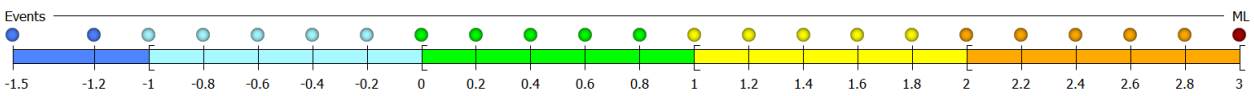

Appendix J: Summary of high hazard sample population ID: 25.

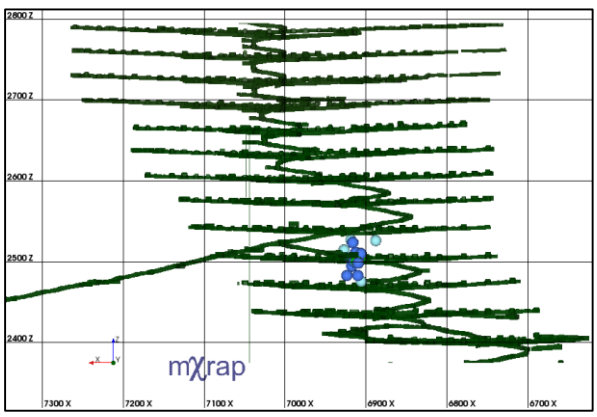

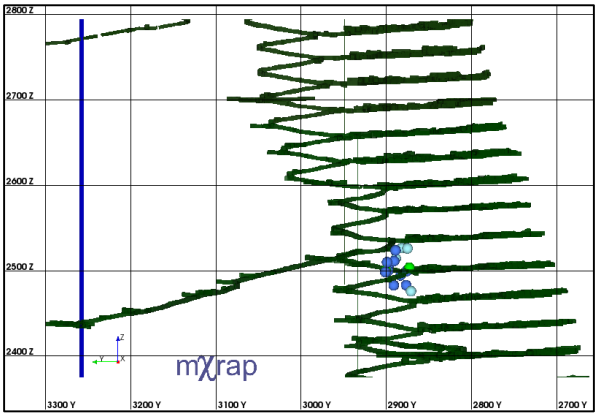

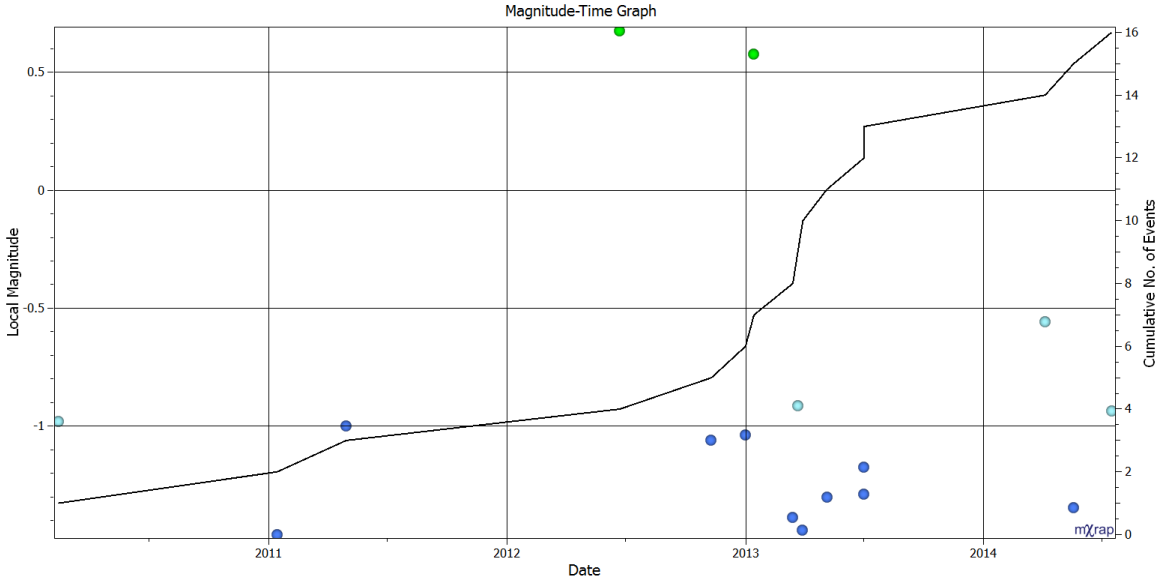

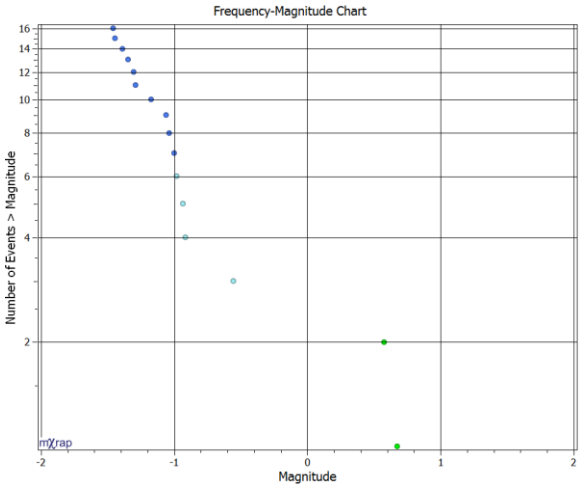

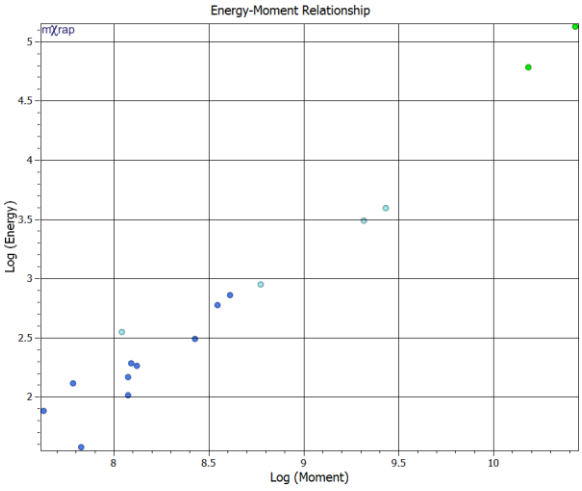

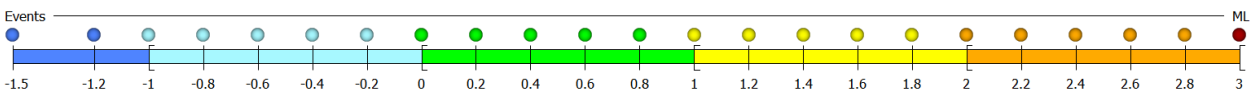

Appendix K: Summary of moderate hazard sample population ID: 27.

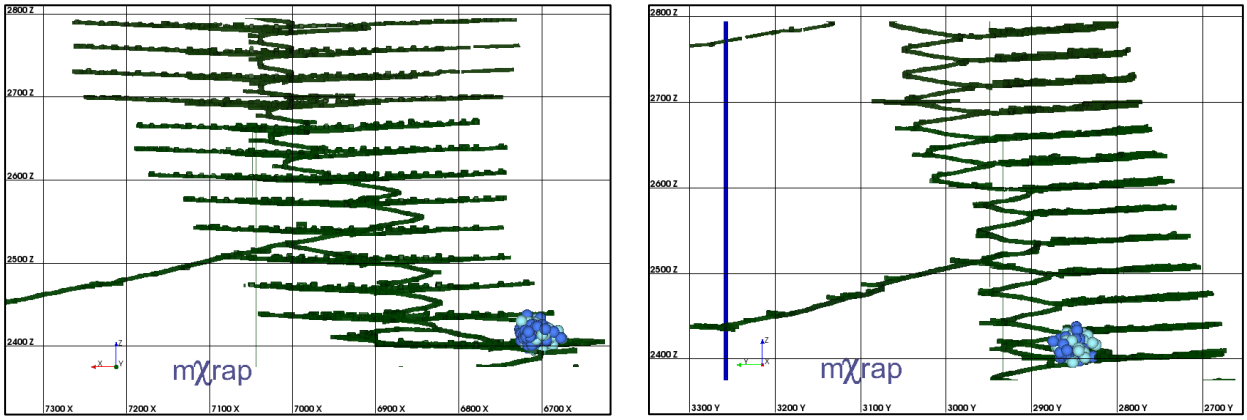

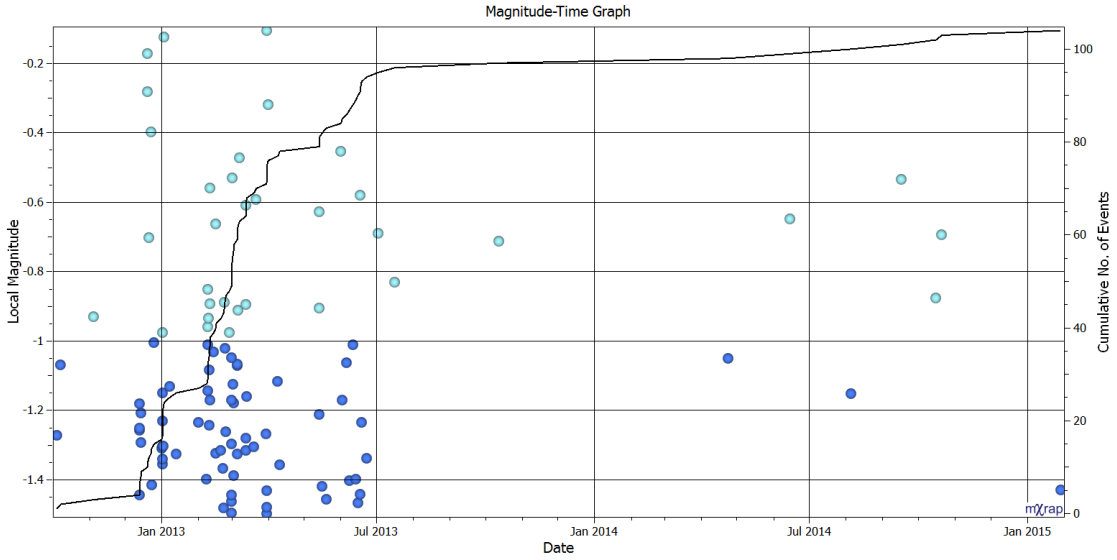

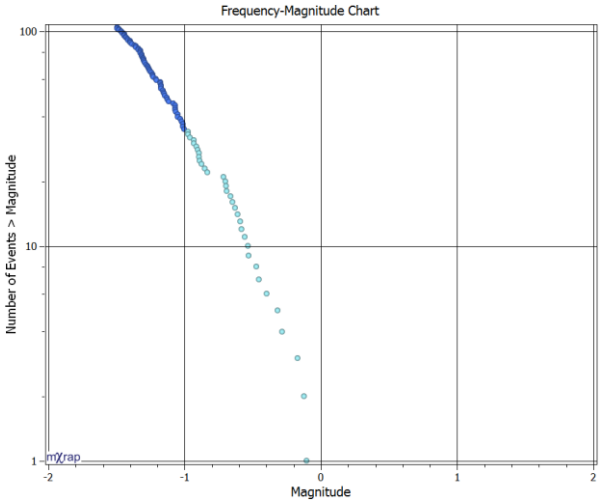

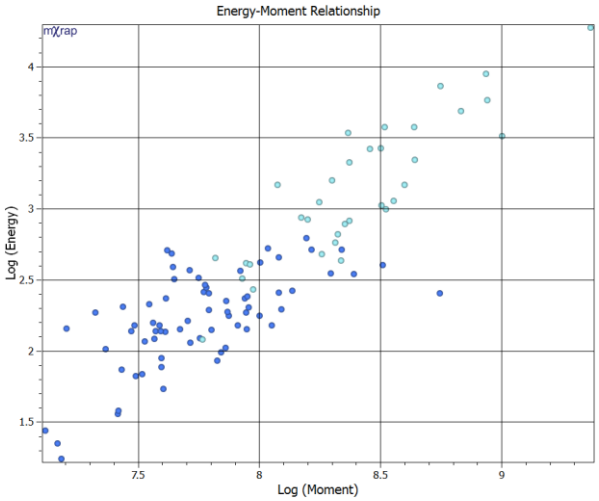

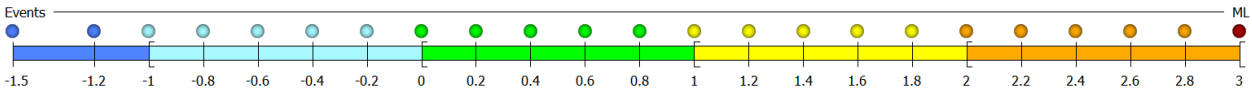

Appendix L: Summary of low hazard sample population ID: 28.

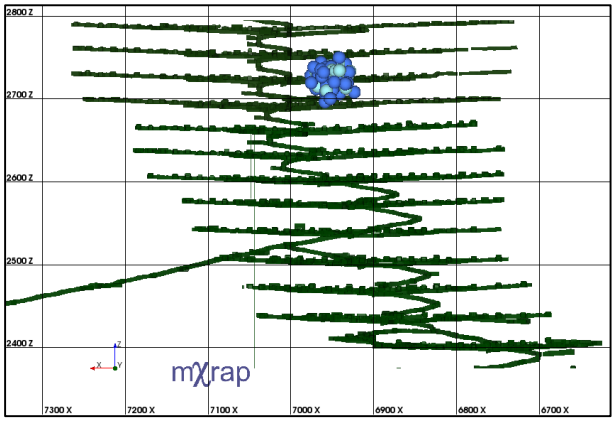

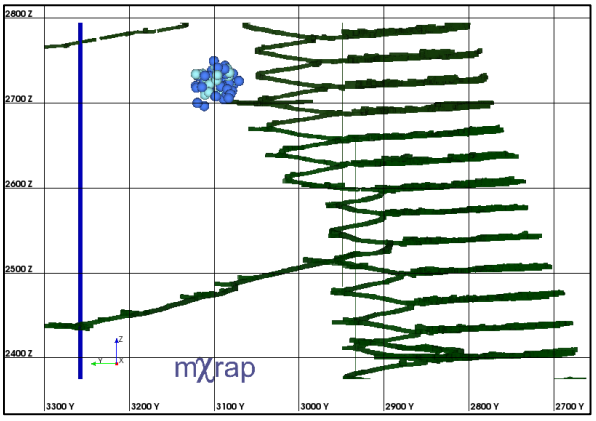

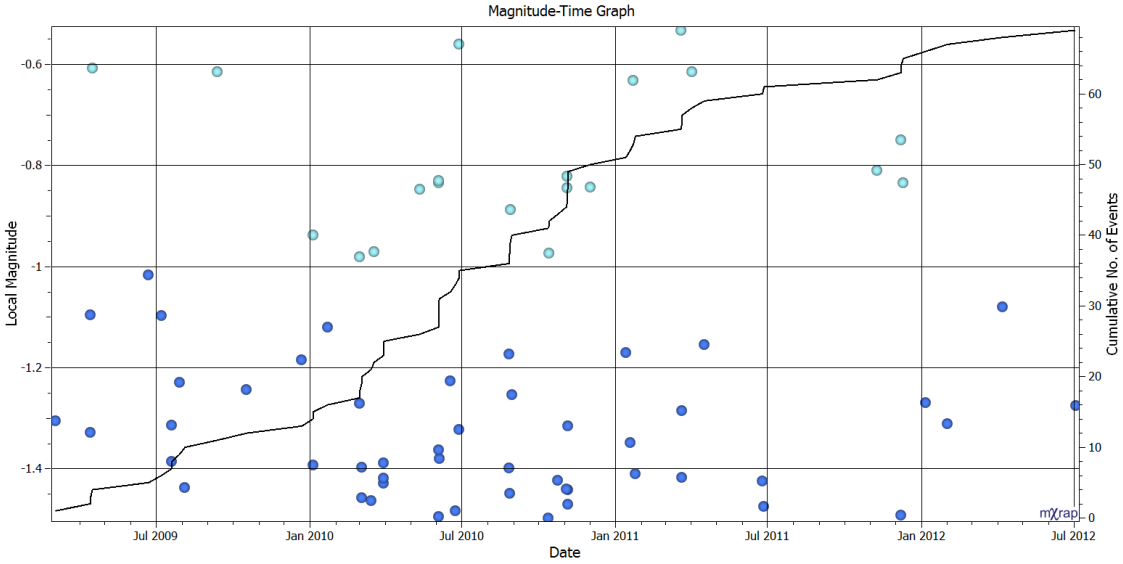

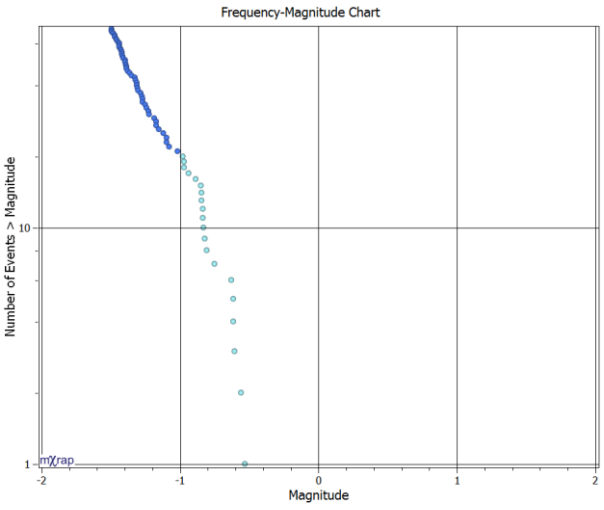

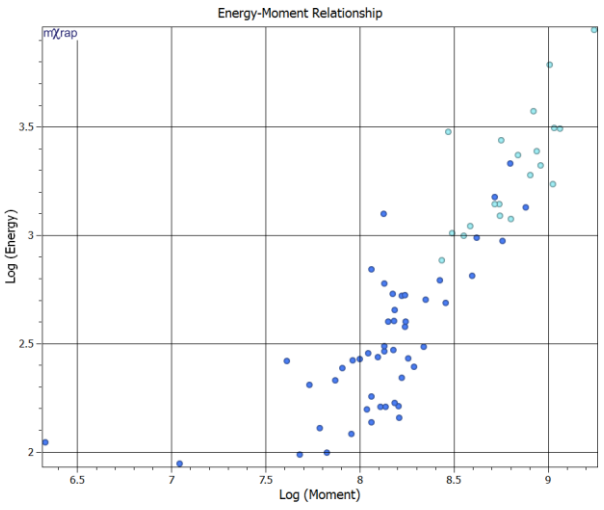

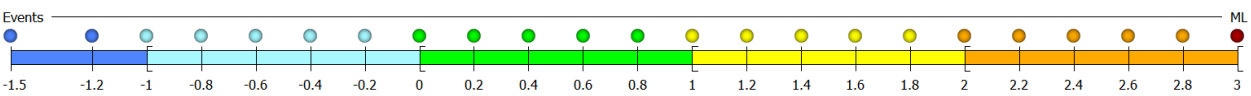

Appendix M: Summary of moderate hazard sample population ID: 30.

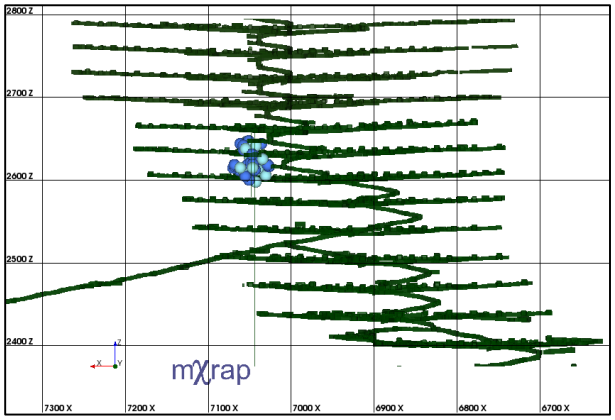

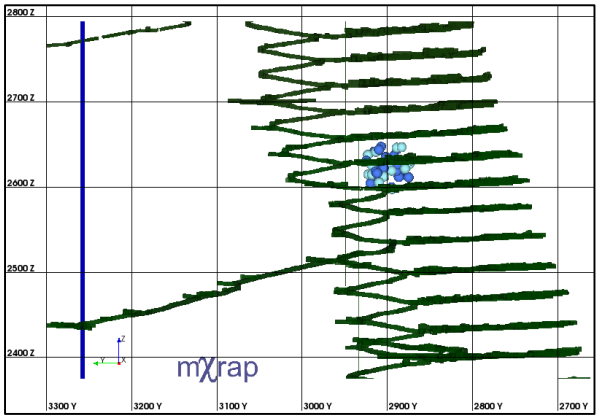

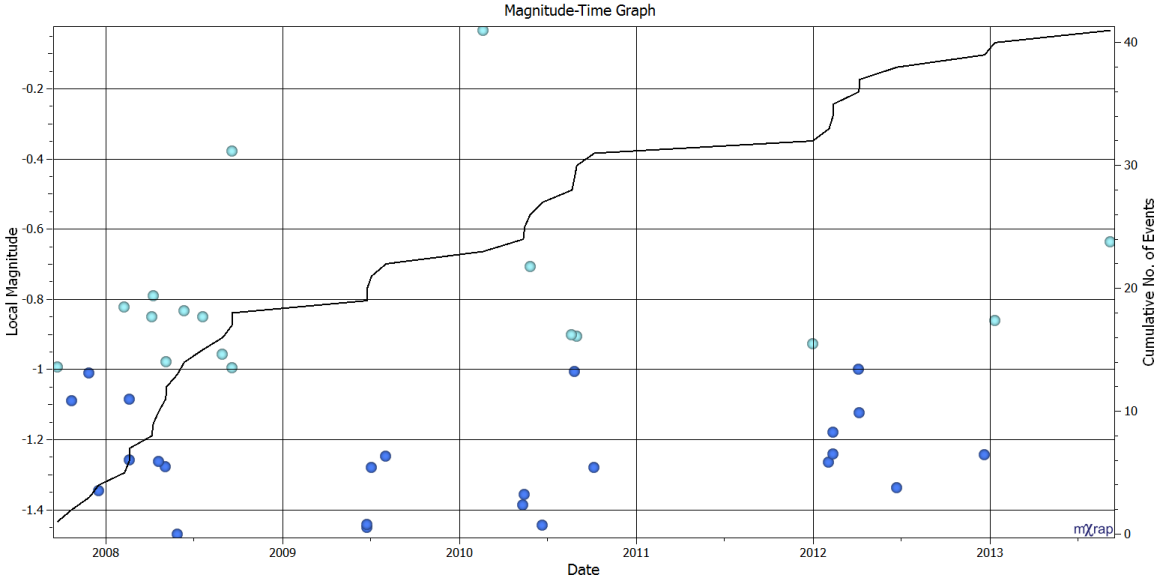

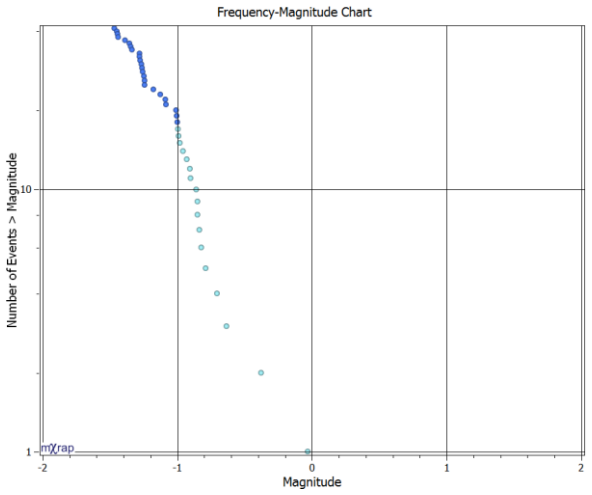

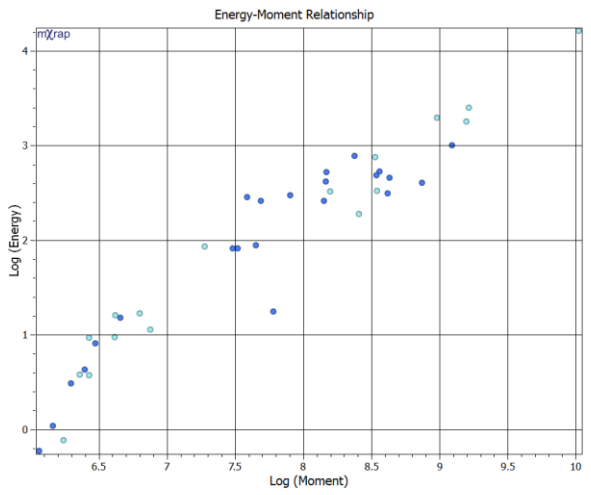

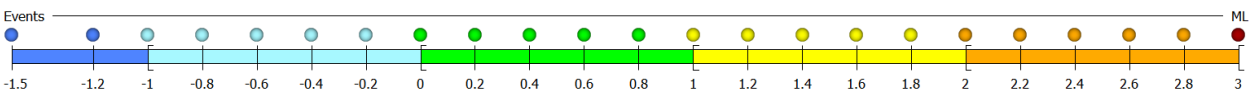

Appendix N: Summary of moderate hazard sample population ID: 31.

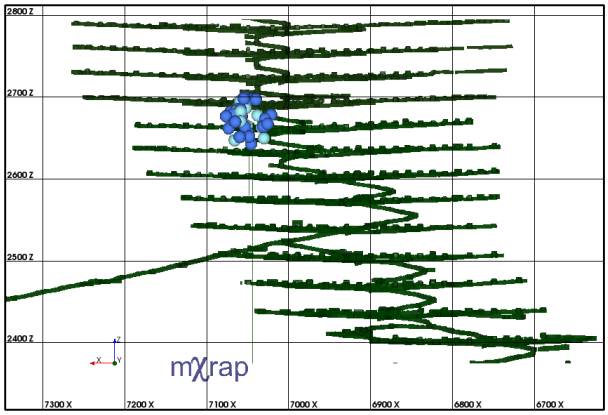

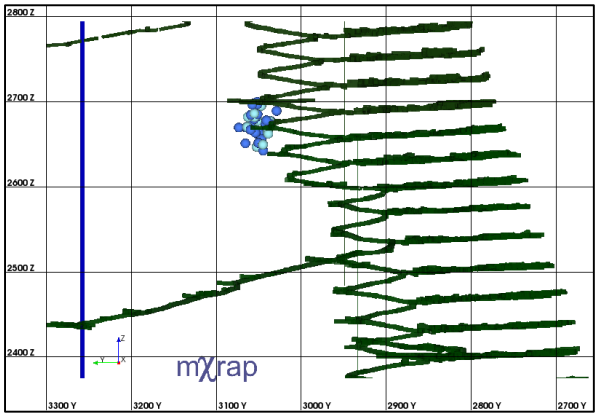

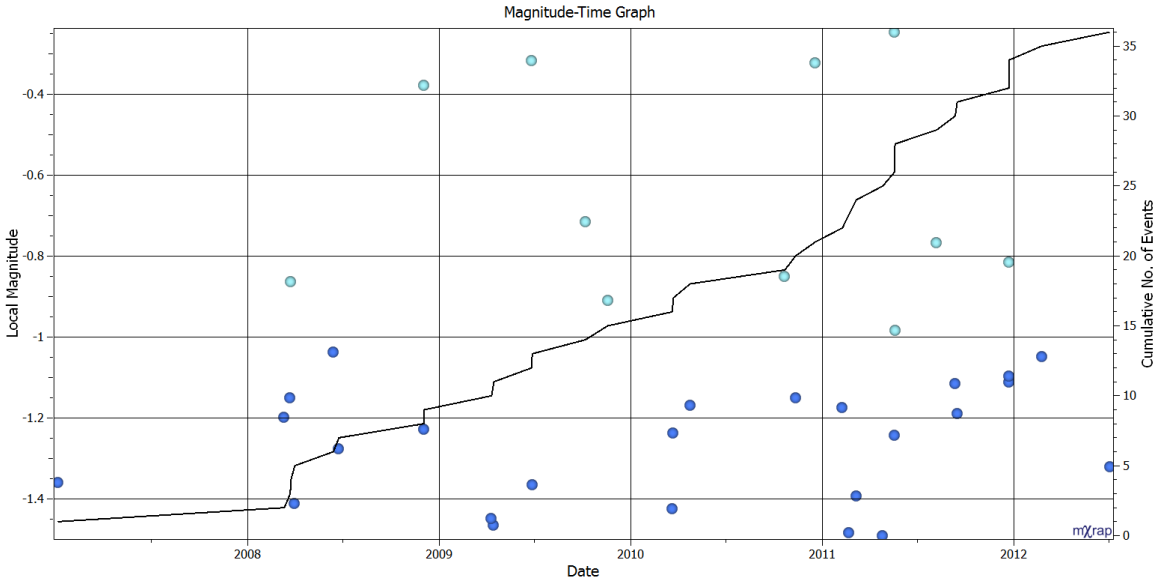

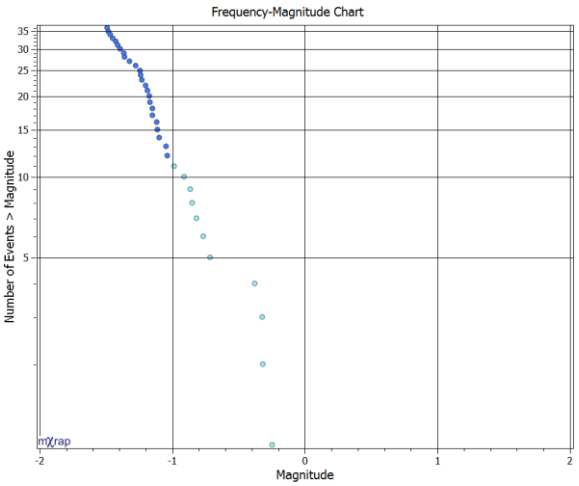

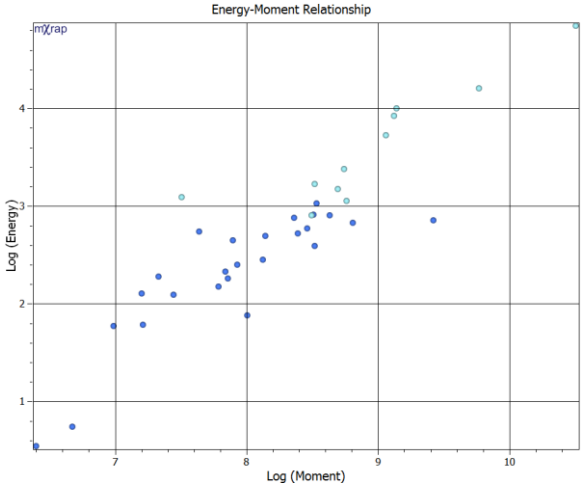

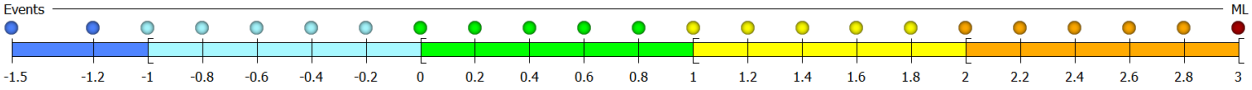

Appendix O: Summary of moderate hazard sample population ID: 32.

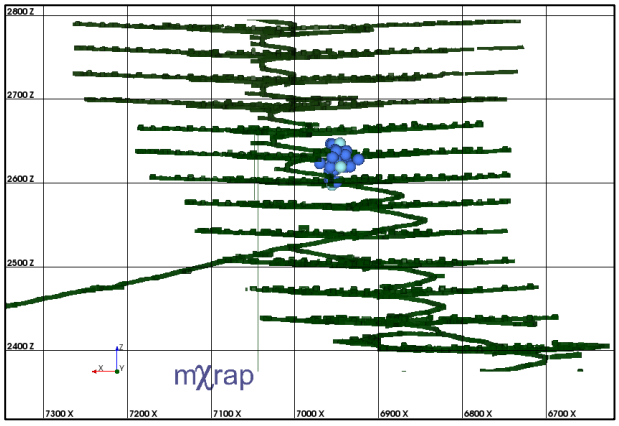

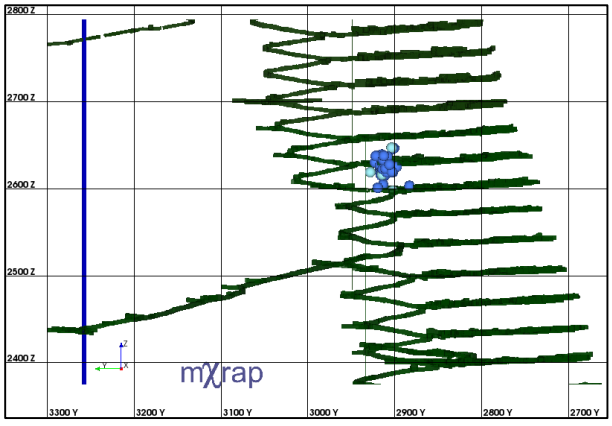

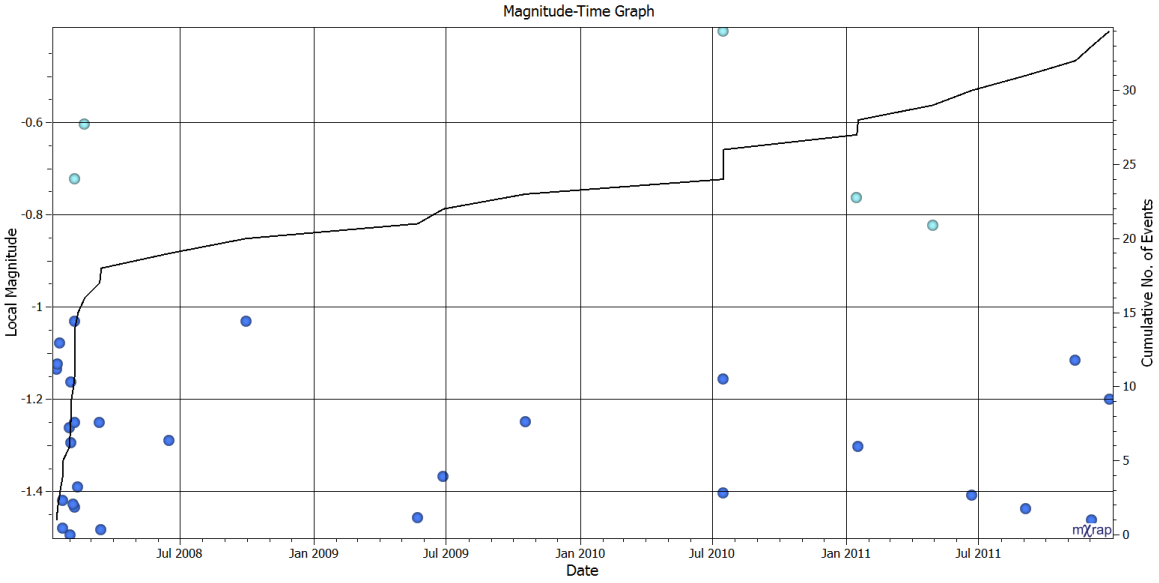

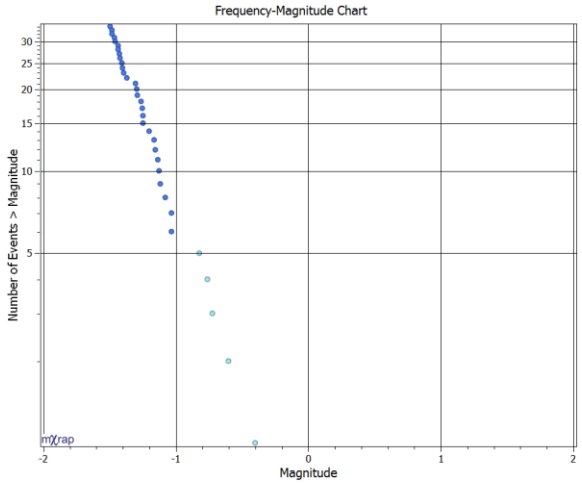

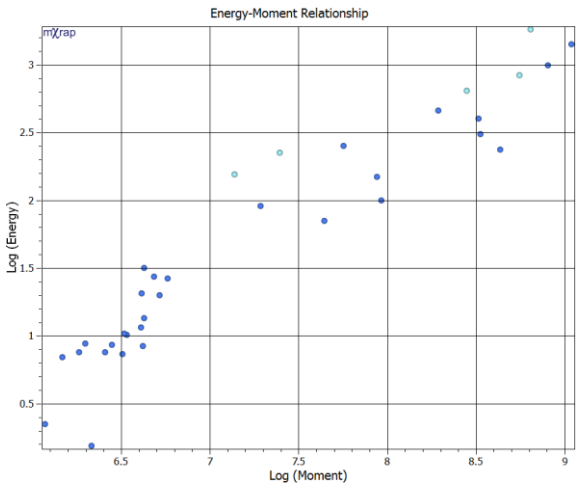

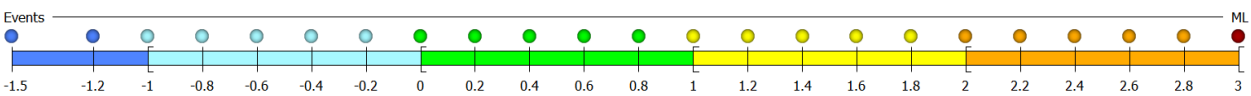

Appendix P: Summary of moderate hazard sample population ID: 39.

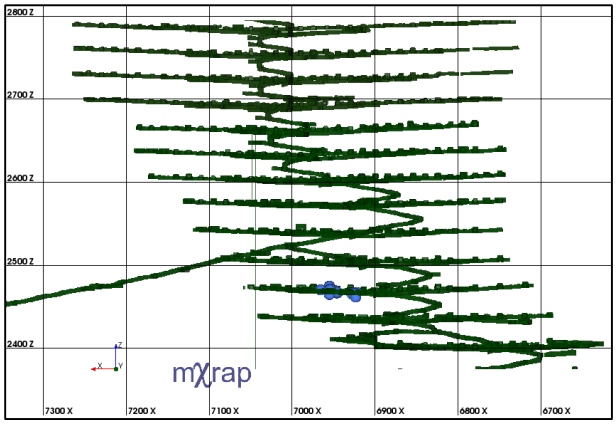

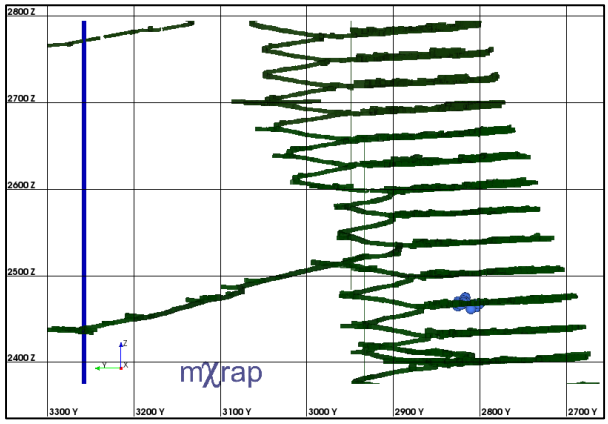

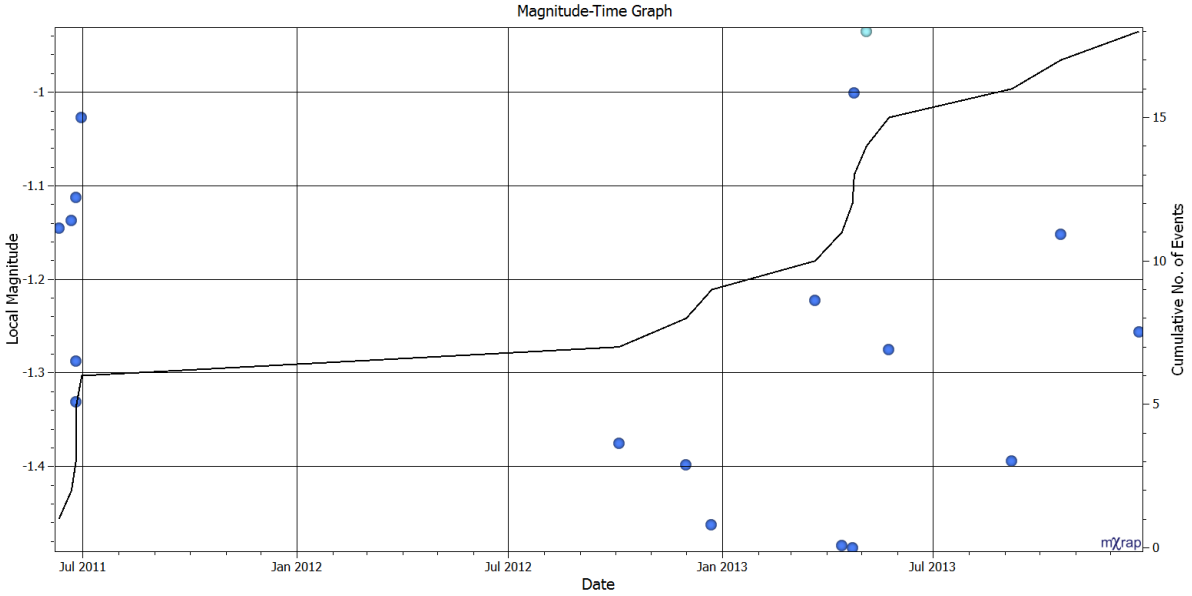

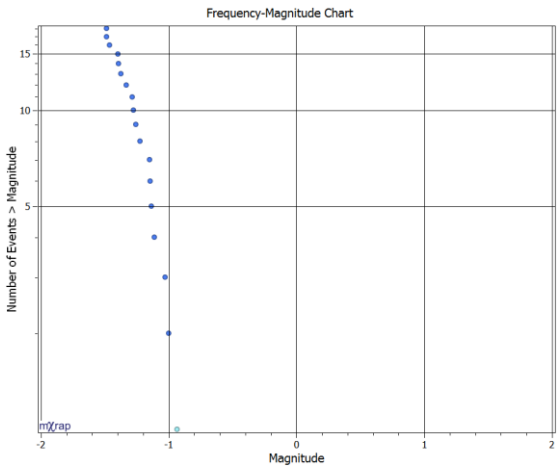

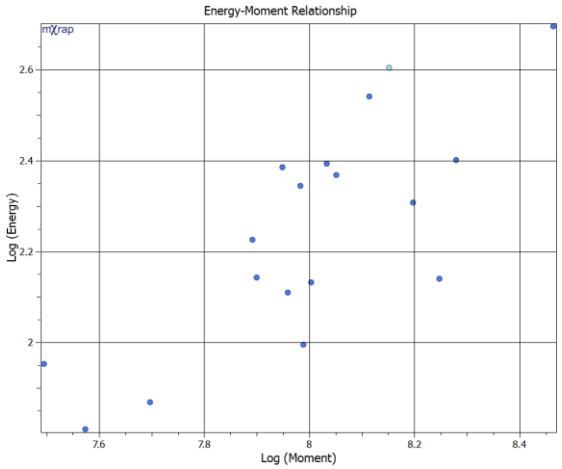

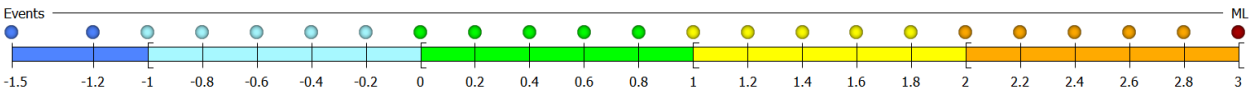

Appendix Q: Summary of moderate hazard sample population ID: 43.

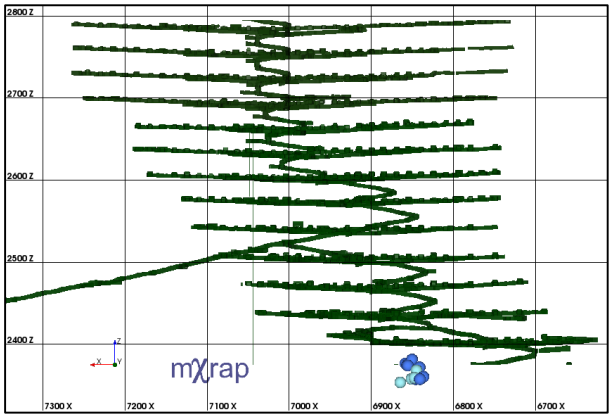

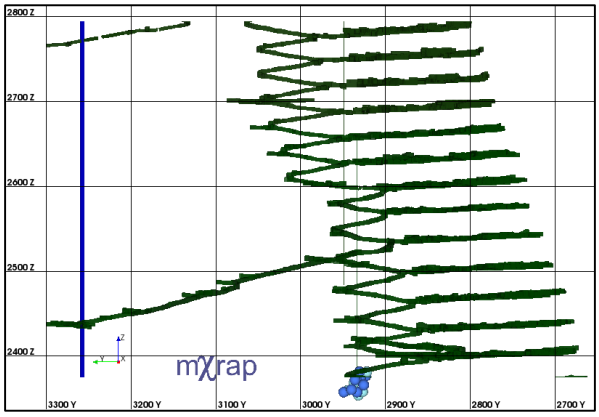

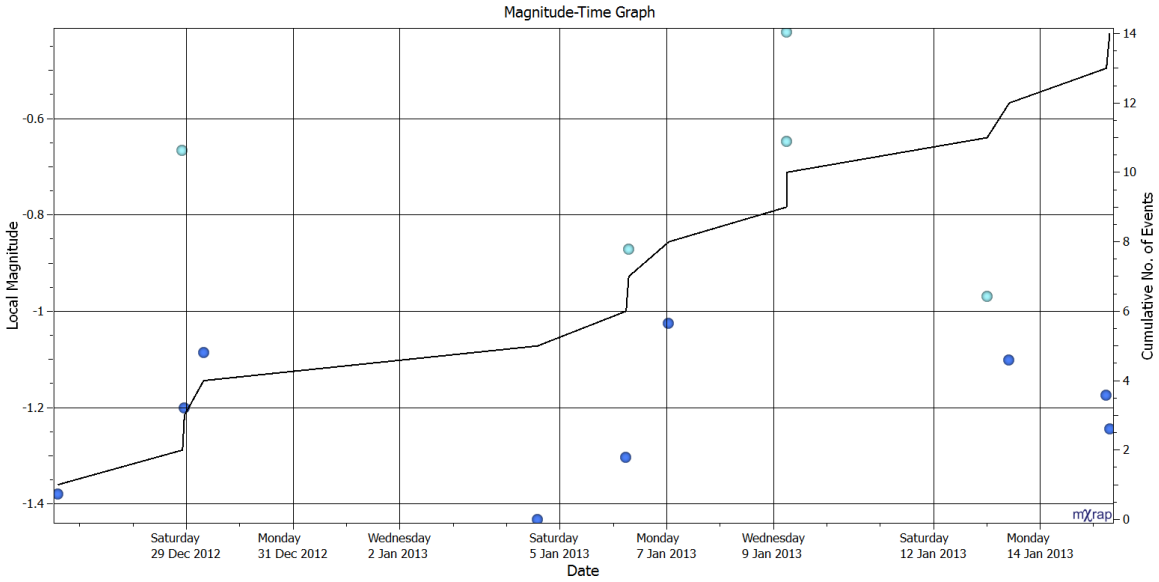

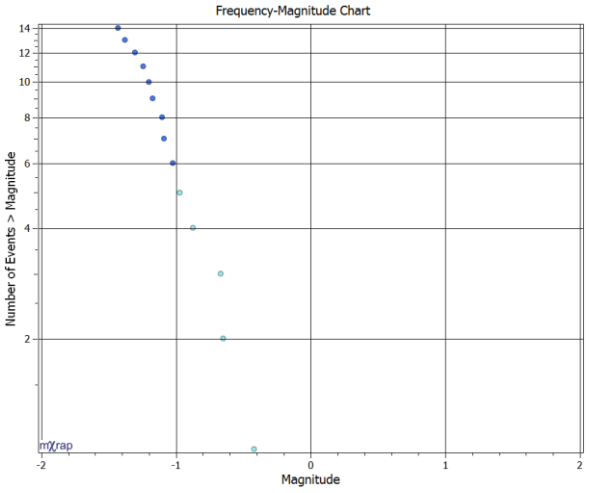

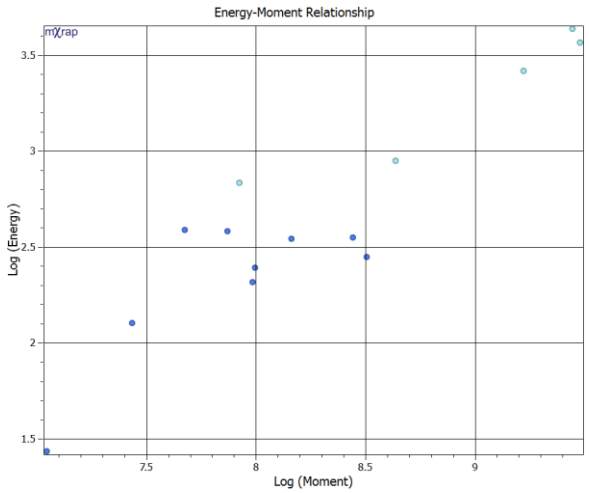

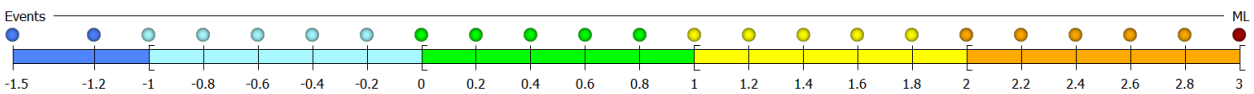

Appendix R: Summary of low hazard sample population ID: 44.

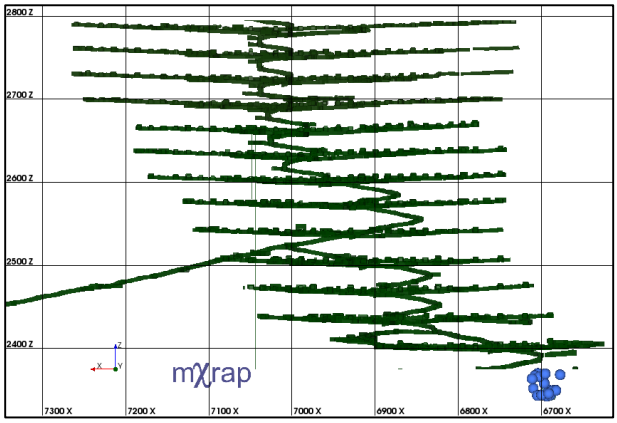

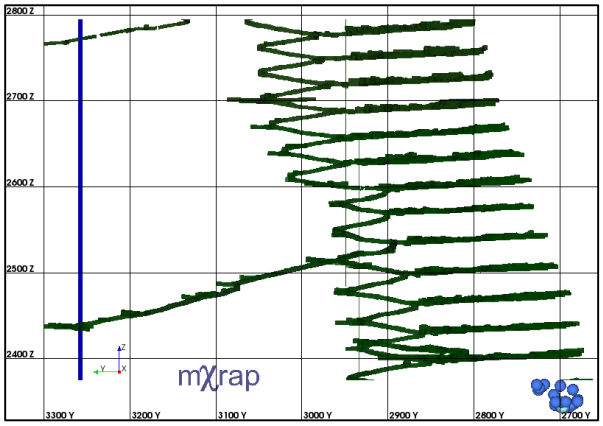

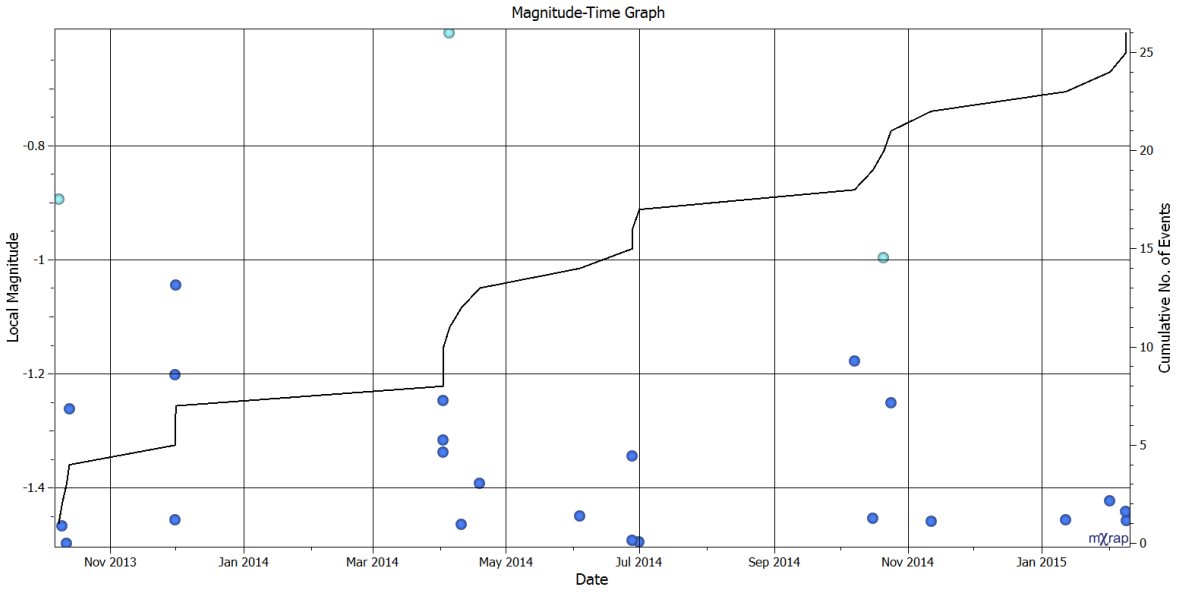

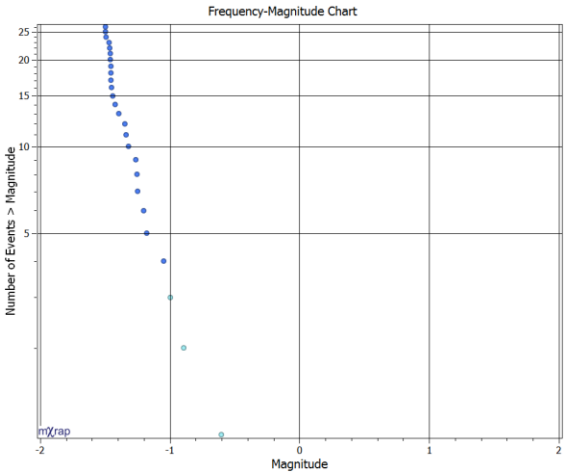

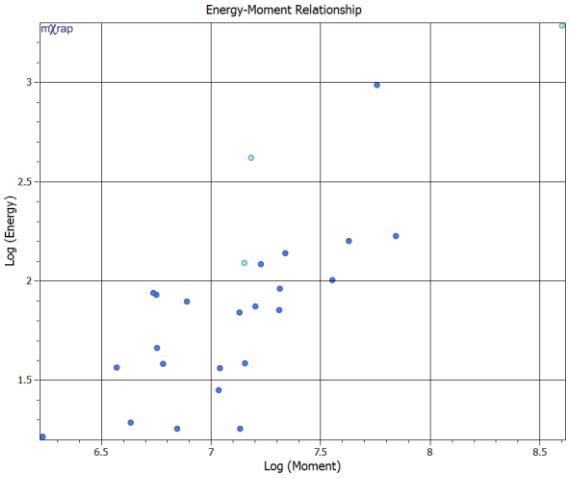

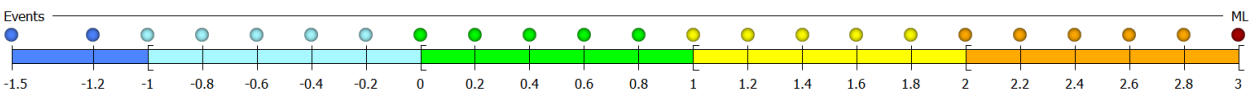

Appendix S: Summary of low hazard sample population ID: 45.

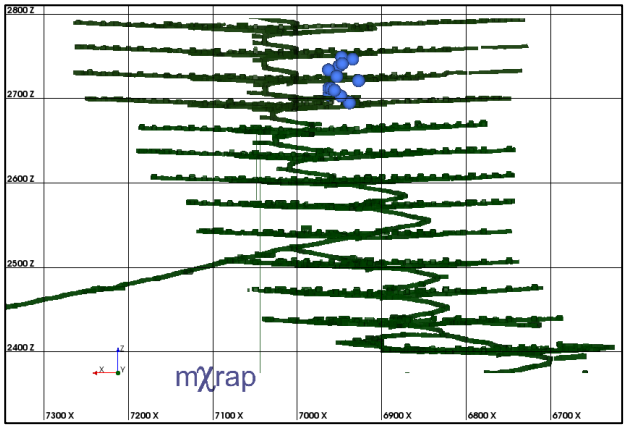

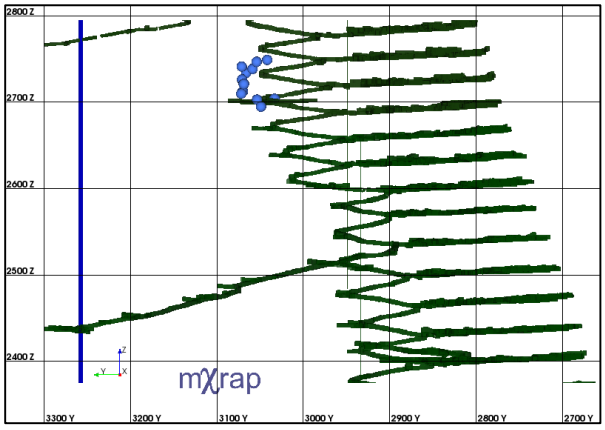

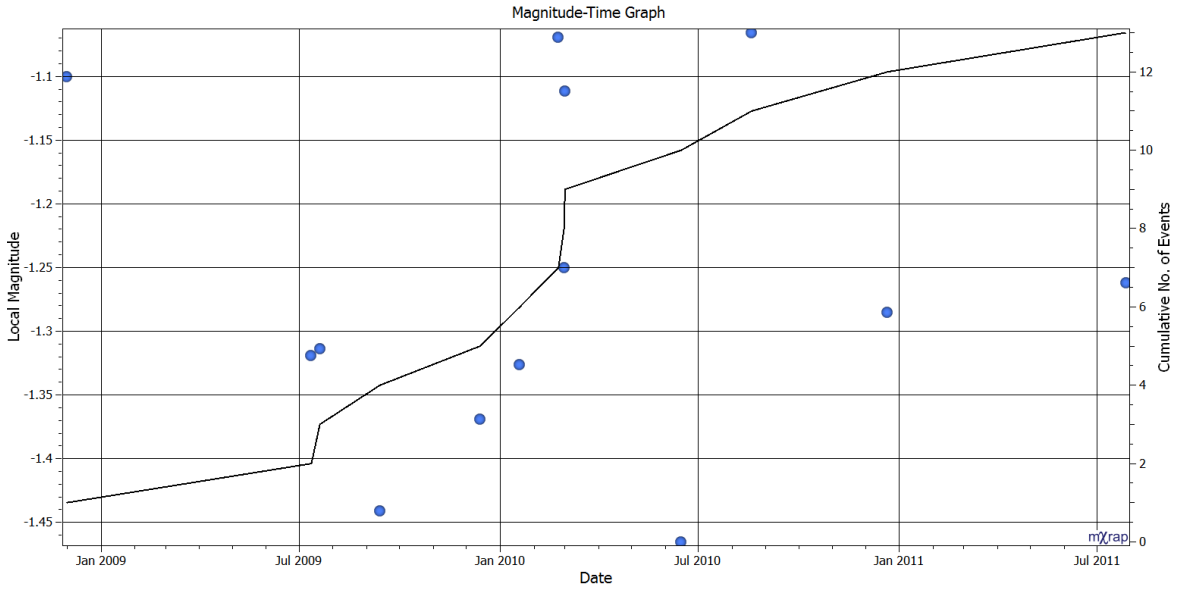

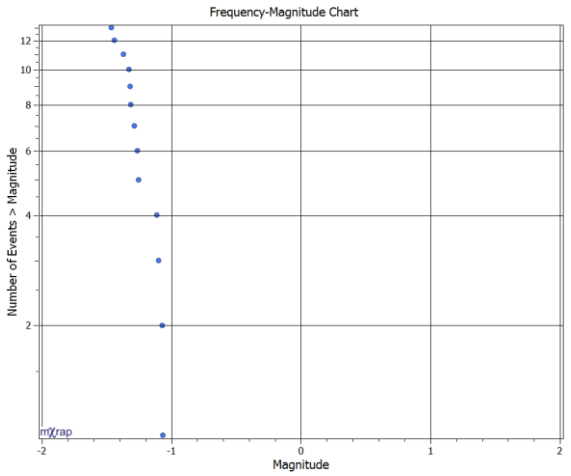

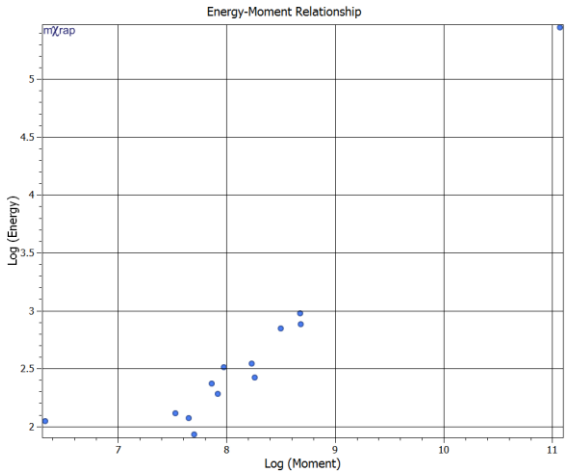

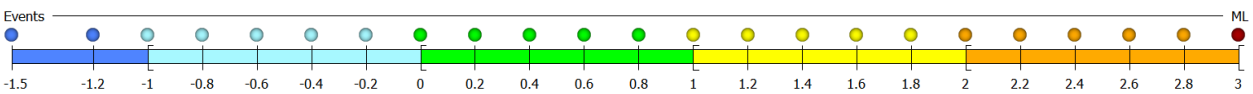

Appendix T: Summary of low hazard sample population ID: 46.

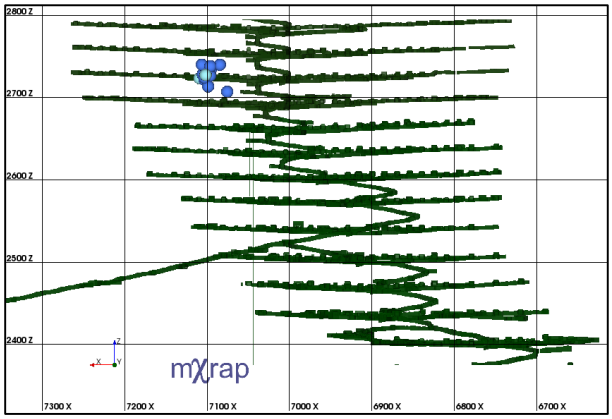

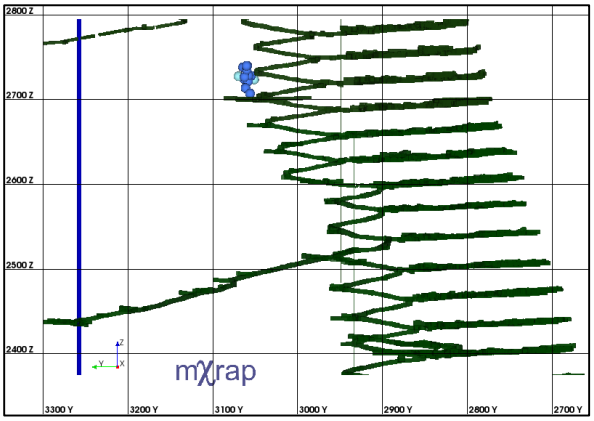

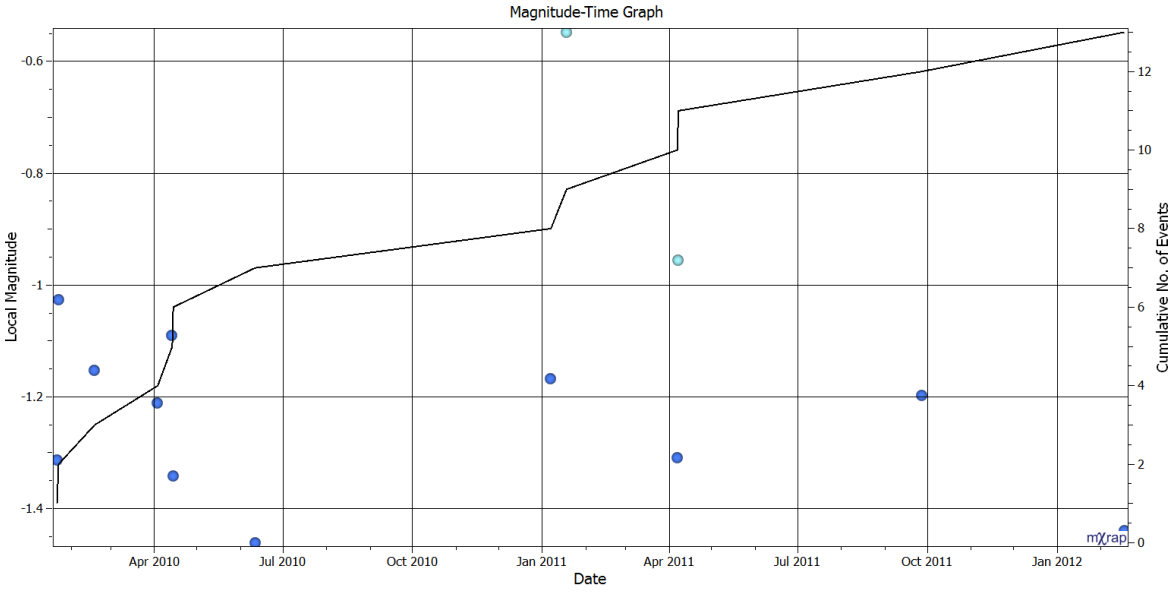

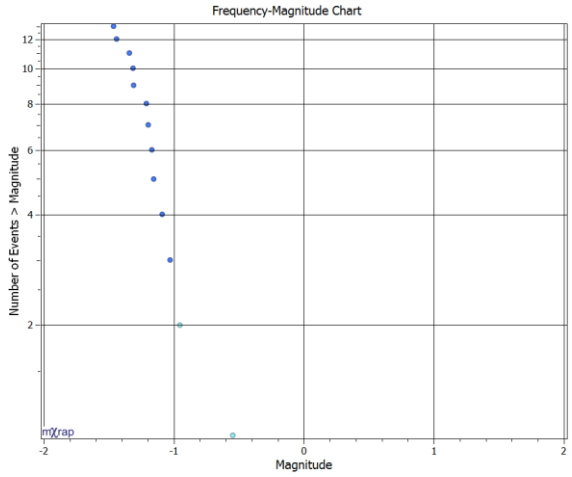

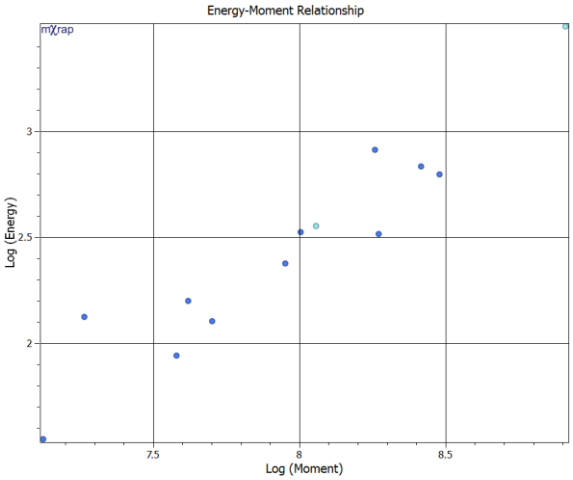

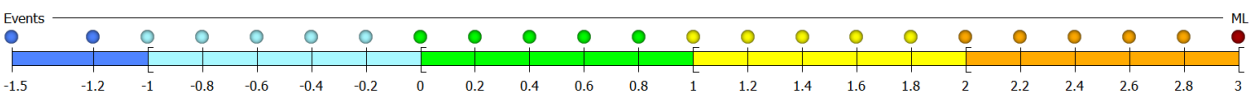

Appendix U: Summary of low hazard sample population ID: 49.

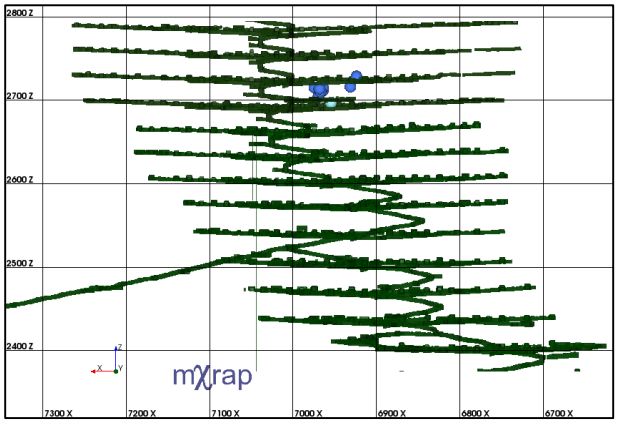

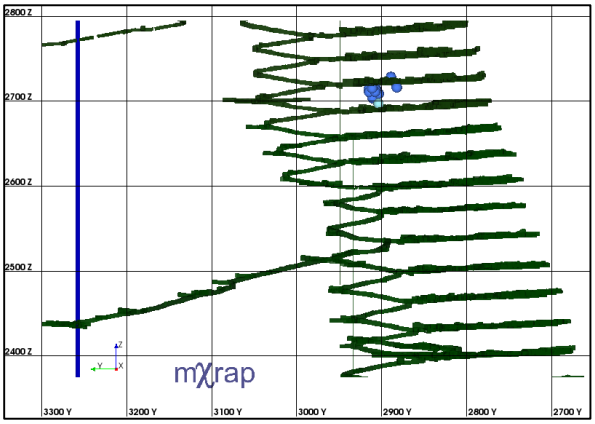

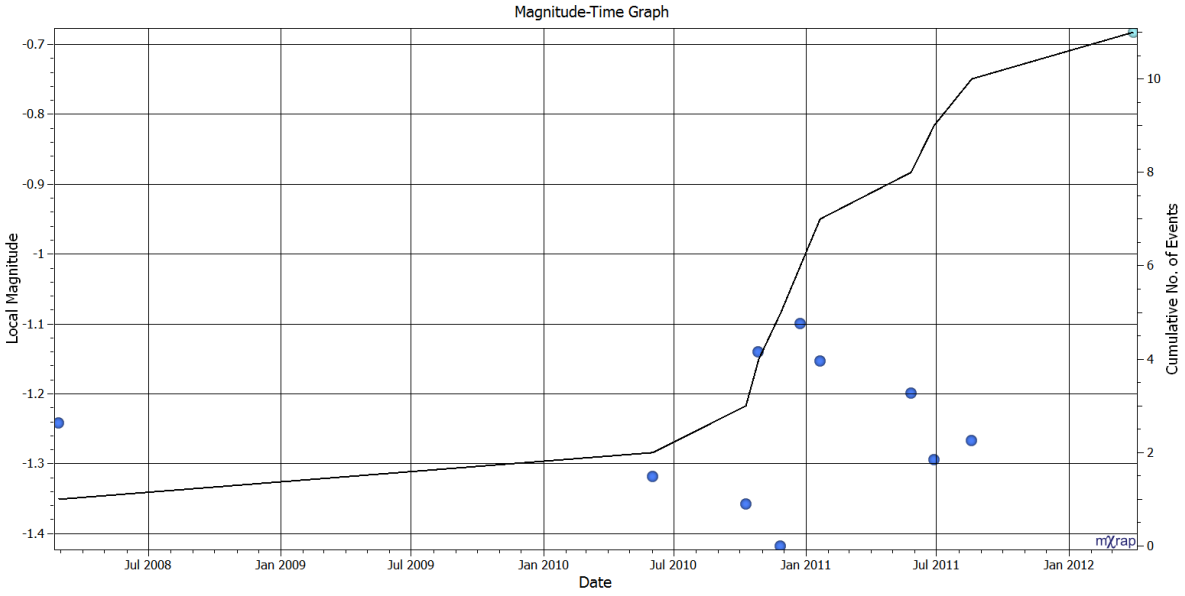

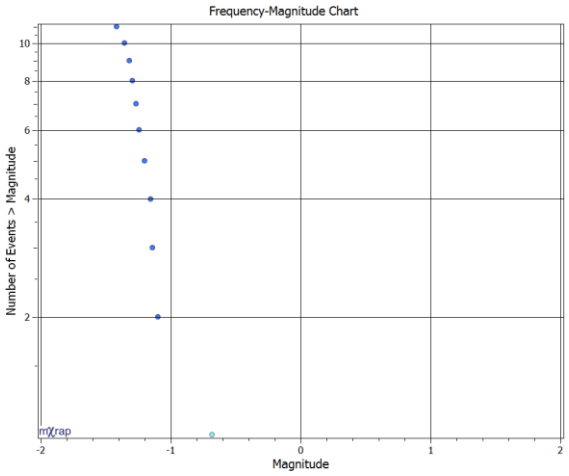

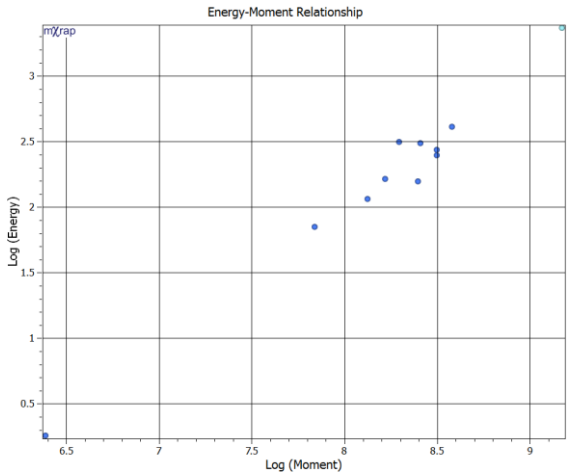

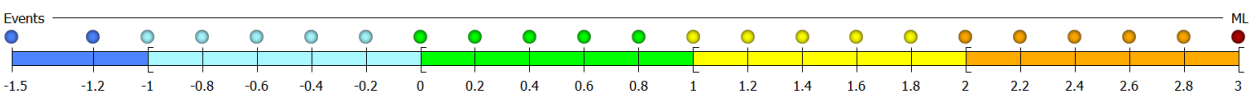

Appendix V: Development mining approximate start and end dates for excavations associated with test populations.

		Development Time Periods	
ID	**Level**	**Start**	**End**
1	252	12/08/09	20/08/09
2	252	31/07/09	12/08/09
3	227	13/11/08	25/02/09
4	259	1/10/10	15/10/10
5	259	1/10/11	31/10/11
6	242	15/09/08	08/10/08
7	255	15/05/11	03/06/11
8	252	16/05/09	15/06/09
9	262	01/06/11	31/06/11
10	262	16/02/12	15/03/12
11	255	16/04/11	15/06/11
12	262	01/06/11	21/07/11
13	242	16/04/10	15/05/10
14	248	21/12/09	31/01/10
15	227	01/12/10	07/06/11
16	252	01/04/11	31/05/11
17	262	31/02/12	15/03/12
18	227	21/04/09	15/05/11
19	224	01/03/05	15/03/05
20	233	21/03/11	23/09/11
21	245	30/03/09	01/05/09
22	255	14/01/10	31/01/10
23	262	30/03/11	15/04/11
24	230	01/02/11	15/03/11
25	252	15/11/09	15/12/09

Appendix W: Development mining approximate start and end dates for excavations associated with control populations.

		Development Time Periods	
ID	**Level**	**Start**	**End**
26	252	12/08/09	15/09/09
27	259	11/12/12	16/01/13
28	233	01/03/07	15/04/07
29	230	30/11/06	02/01/07
30	239	31/04/08	06/06/08
31	233	03/01/07	26/01/07
32	239	31/12/07	17/03/08
33	230	16/04/10	01/11/10
34	248	16/04/09	15/05/09
35	248	09/06/10	15/06/10
36	266	27/07/12	31/08/12
37	239	01/01/08	16/02/08
38	262	21/02/12	15/05/12
39	255	15/05/11	15/07/11
40	262	31/04/11	15/02/12
41	239	1/02/10	31/03/10
42	236	15/06/08	31/05/09
43	262	15/12/12	04/03/13
44	262	1/04/13	31/06/13
45	233	31/12/06	27/07/07
46	230	17/07/06	27/07/06
47	430	01/02/08	11/03/08
48	252	16/02/11	25/05/11
49	230	18/12/06	15/01/07
50	255	01/02/10	15/03/10

Appendix X: Table of all large events within test populations. Events used as central points to generate seismic populations are shown in bold.

ID	Date/Time	Local Magnitude	Apparent Stress	Proceeding ASR			During Development
				1 Week	3 Months	1 Year	
1	2012/02/11 19:10:36	0.03	4.90E+05	1	1	1.97	
	2012/09/17 00:54:46	0.23	4.72E+05	1.08	1.79	2.91	
	2013/08/04 10:03:38	1.47	1.62E+06	1	3.05	2.59	
	2013/09/16 15:06:17	1.79	8.99E+05	1	11.1	3.13	
2	**2013/08/04 10:03:38**	1.47	1.62E+06	1	1.59	1.57	
	2013/09/16 15:06:17	1.79	8.99E+05	1	1.51	1.7	
	2013/12/04 13:09:49	0.01	4.85E+05	1.2	5.99	2.62	
	2014/03/08 00:42:19	0.63	4.54E+05	1	2.02	3.12	
3	2007/08/26 21:43:36	0.53	1.25E+06	1	1	5.98	
	2009/01/24 22:03:58	1.35	2.17E+05	1	1	9.24	X
4	2013/05/01 14:25:37	0.98	3.68E+05	1	1	1.78	
	2013/10/12 11:12:24	1.34	1.52E+06	1	1.11	2.17	
5	**2013/08/01 10:28:20**	1.23	2.27E+06	3.25	4.88	4.25	
6	**2009/10/23 21:13:40**	1.22	1.73E+05	1	1.39	17.4	
	2010/07/15 17:56:45	0.30	9.40E+04	1	1.56	2.51	
7	2012/11/08 17:32:02	0.37	5.69E+05	1	3.01	2.53	
	2013/12/31 10:07:49	1.13	4.72E+05	1	4.3	3.59	
	2014/03/20 13:12:15	0.25	6.10E+05	1	1.44	3.15	
8	**2012/01/30 01:48:22**	1.11	5.94E+05	1	1.44	1.51	
	2012/11/03 07:33:11	0.62	2.51E+05	1	2.44	2.18	
	2013/11/13 22:18:34	0.44	3.68E+05	1.3	2.66	2.31	
	2014/03/31 05:30:46	0.25	1.93E+05	1.68	1.85	2.52	
9	2011/12/19 06:03:55	0.03	4.44E+05	1	1.03	2.08	
	2013/01/10 21:30:39	1.08	3.30E+05	1	3.53	1.85	
	2013/03/01 01:53:27	1.04	4.50E+05	1.9	2.71	2.48	
	2013/03/01 03:22:33	0.35	4.15E+05	2.82	2.93	2.95	
	2013/04/08 03:40:44	0.10	4.31E+05	1.87	2.87	2.81	
	2013/04/12 19:43:23	0.46	1.83E+06	1.53	3.09	3.21	
	2013/07/12 06:25:16	0.27	1.62E+05	1	3.47	2.94	
	2013/07/18 22:06:25	0.11	8.60E+04	1	2.86	2.93	
10	2012/10/30 18:27:12	0.17	2.84E+05	1	2.05	2.31	
	2012/11/08 18:33:32	1.05	2.64E+05	1	2.76	2.29	
11	**2013/03/25 16:32:24**	0.99	3.60E+05	1.18	1.25	2.23	
12	**2013/02/08 18:27:13**	0.90	1.31E+06	1	1.86	3.12	
	2013/03/30 15:10:04	0.13	2.63E+05	1.34	2.41	2.58	
	2013/07/18 22:06:25	0.11	8.60E+04	1.22	3.35	2.89	
13	2012/02/11 19:10:36	0.03	4.90E+05	1.88	3.16	1.69	
	2013/02/15 01:54:53	0.87	3.63E+05	1	1.57	2.19	
14	2013/10/25 23:16:22	0.17	8.30E+04	1	1.05	1.65	
	2014/05/23 00:56:39	0.85	2.68E+05	1	2.52	2.13	
15	**2009/08/13 11:30:36**	0.84	6.87E+05	1	1.82	3.66	
	2010/01/15 21:23:01	0.13	1.68E+05	1	2.44	3.77	
16	**2012/05/16 18:17:45**	0.84	2.80E+05	1.26	1.26	2.02	
	2014/01/02 16:57:55	0.37	2.35E+05	1	1.51	5.83	
17	2012/04/28 22:13:49	0.46	4.03E+05	1	2.21	2.2	
	2013/03/24 02:58:20	0.84	2.67E+05	1	1.41	2.37	
18	2008/08/28 20:35:48	0.55	2.79E+05	1	3	10.64	
	2009/01/05 16:26:37	0.83	1.27E+05	1	14.23	12.51	
19	**2008/04/11 20:43:39**	0.81	7.45E+05	1	4.71	3.44	
20	**2009/09/10 22:14:17**	0.80	1.99E+05	1	3.13	3.23	X
21	2011/04/19 01:13:40	0.32	1.89E+05	1	1.31	1.74	
	2011/12/27 04:54:00	0.73	1.96E+07	1	1.25	1.77	
22	2013/10/12 19:20:31	0.33	5.26E+05	1.55	1.55	1.5	
	2014/02/02 11:27:21	0.72	1.35E+06	1	2.21	1.88	
23	**2013/10/12 01:35:14**	0.71	5.93E+05	1	1.03	2.83	
	2014/05/10 16:30:24	0.45	9.85E+05	1	1.44	2.62	
24	**2011/08/03 02:04:45**	0.69	5.21E+05	1	1.28	4.47	
25	**2012/06/22 01:50:55**	0.68	1.96E+05	1	1	1.16	
	2013/01/13 17:23:07	0.58	1.69E+05	1	1.05	2.27	